

# **New Fluorine-Labelled Amino Acids as $^{19}\text{F}$ NMR Reporters for Structural Peptide Studies: Design, Synthesis, and Applications**

Zur Erlangung des akademischen Grades eines  
DOKTORS DER NATURWISSENSCHAFTEN

(Dr. rer. nat.)

der Fakultät für Chemie und Biowissenschaften der  
Universität Karlsruhe (TH)

vorgelegte  
DISSERTATION

von

Dipl.-Chem. Pavlo Mykhailiuk aus Kerch, Ukraine

Dekan:	Prof. Dr. Stefan Bräse
Referent:	Prof. Dr. Anne S. Ulrich
Korreferent:	Prof. Dr. Joachim Podlech
Tag der mündlichen Prüfung:	10. Juli 2008

## TABLE OF CONTENTS

PART 1. BACKGROUND .....	4
<b>1.1. Biological membranes and membrane-active peptides</b> .....	4
<i>1.1.1. Biological membranes</i> .....	4
<i>1.1.2. Membrane-active peptides</i> .....	6
1.1.2.1. Antimicrobial peptides.....	6
1.1.2.2. Cell-penetrating peptides .....	7
<b>1.2. Methods of structural characterization of peptides</b> .....	9
<i>1.2.1. Peptide secondary structure</i> .....	9
<i>1.2.2. Solid state <sup>19</sup>F-NMR</i> .....	11
1.2.2.1. <sup>19</sup> F nucleus in NMR .....	11
1.2.2.2. Methodology of membrane-peptide structural studies by solid state <sup>19</sup> F-NMR .....	12
<b>1.3. <sup>19</sup>F-NMR labels in solid state <sup>19</sup>F-NMR</b> .....	14
<i>1.3.1. Known <sup>19</sup>F-NMR labels, their advantages and drawbacks</i> .....	14
<i>1.3.2. Known mono-CF<sub>3</sub>-substituted analogues of Ala, Val, Leu, Ile, Met and Pro as potential <sup>19</sup>F-NMR labels</i> .....	15
PART 2. AIMS OF THE WORK.....	18
PART 3. NEW <sup>19</sup> F-NMR LABEL FOR SUBSTITUTION OF NATURAL NON-POLAR ALIPHATIC AMINO ACIDS (ALA, VAL, LEU, ILE, MET) IN PEPTIDES: (S)-3-(TRIFLUOROMETHYL)-BICYCLOPENT-[1.1.1]-1-YLGLYCINE (CF <sub>3</sub> -BPG).....	19
<b>3.1. Design of the target structure</b> .....	19
<b>3.2. Planning the synthesis of CF<sub>3</sub>-Bpg</b> .....	20
<b>3.3. Synthesis of CF<sub>3</sub>-Bpg and proof of its absolute configuration</b> .....	21
<b>3.4. Confirmation of the optical purity of CF<sub>3</sub>-Bpg</b> .....	25
<b>3.5. Synthesis of a model peptide derivative of CF<sub>3</sub>-Bpg</b> .....	27
PART 4. FIRST <sup>19</sup> F-NMR LABELS FOR PROLINE SUBSTITUTION IN PEPTIDES .....	28
<b>4.1. Design of the target compounds</b> .....	28
<b>4.2. 2-(Trifluoromethyl)-proline</b> .....	30
<i>4.2.1. Planning the synthesis of 2-(trifluoromethyl)-proline</i> .....	30
<i>4.2.2. Synthesis of 2-(trifluoromethyl), 2-(nitrile)-pyrrolidine skeleton</i> .....	31
<b>4.3. 3,4-(Trifluoromethylmethano)-prolines</b> .....	33
<i>4.3.1. Planning the synthesis of 3,4-(trifluoromethylmethano)-prolines</i> .....	33
<i>4.3.2. Photochemical addition of CF<sub>3</sub>CHN<sub>2</sub> to 3,4-dehydropoline derivative</i> ...	35
<i>4.3.3. Modification of the procedure of trifluoromethylcyclopropanation of alkenes</i> .....	35

	3
4.3.4. <i>Synthesis of 3,4-(trifluoromethylmethano)-prolines</i> .....	39
4.3.5. <i>Evaluation of stereoconfiguration of the synthesized amino acids</i> .....	41
<b>4.4. 4,5-(Trifluoromethylmethano)-prolines</b> .....	43
4.4.1. <i>Planning the synthesis of 4,5-(trifluoromethylmethano)-prolines</i> .....	43
4.4.2. <i>Synthesis of 4,5-(trifluoromethylmethano)-prolines</i> .....	45
4.4.3. <i>Evaluation of the stereoconfiguration of the synthesized compounds</i> .....	47
<b>4.5. Selection of the optimal <sup>19</sup>F-NMR label (CF<sub>3</sub>-MePro)</b> .....	50
<b>PART 5. APPLICATIONS OF THE SYNTHESIZED <sup>19</sup>F-NMR LABELS IN PEPTIDE STUDIES</b> .....	51
<b>5.1. Antimicrobial peptide GS</b> .....	51
5.1.1. <i>General information about GS</i> .....	51
5.1.2. <i>Synthesis of CF<sub>3</sub>-labelled analogue of GS</i> .....	52
5.1.3. <i>Influence of CF<sub>3</sub>-Bpg on the conformation of GS</i> .....	54
5.1.4. <i>Influence of CF<sub>3</sub>-Bpg on the orientation of GS in lipid bilayers</i> .....	54
<b>5.2. Antimicrobial peptide PGLa</b> .....	56
5.2.1. <i>General information about PGLa</i> .....	56
5.2.2. <i>Synthesis of CF<sub>3</sub>-labelled analogues of PGLa</i> .....	56
5.2.3. <i>Influence of CF<sub>3</sub>-Bpg on the conformation of PGLa</i> .....	57
5.2.4. <i>Influence of CF<sub>3</sub>-Bpg on the antimicrobial activity of PGLa</i> .....	57
5.2.5. <i>Influence of CF<sub>3</sub>-Bpg on the orientation of PGLa in lipid bilayers</i> .....	58
<b>5.3. Cell-penetrating peptide SAP</b> .....	59
5.3.1. <i>General information about SAP</i> .....	59
5.3.2. <i>Synthesis of SAP and its CF<sub>3</sub>-labelled analogues</i> .....	60
5.3.3. <i>Influence of CF<sub>3</sub>-Bpg and CF<sub>3</sub>-MePro on the conformation of SAP</i> .....	61
5.3.4. <i>Solid state <sup>19</sup>F-NMR studies of SAP in lipid bilayers</i> .....	63
<b>PART 6. EXPERIMENTAL PART</b> .....	67
<b>PART 7. SUMMARY / ZUSAMMENFASSUNG</b> .....	87
<b>PART 8. CITED LITERATURE</b> .....	89
<b>ABBREVIATIONS</b> .....	101
<b>LIST OF PUBLICATIONS</b> .....	103
<b>CURRICULUM VITAE</b> .....	105

## PART 1 BACKGROUND

This chapter introduces the necessary background information relevant for this thesis. Here biomembranes, membrane-active peptides, fluorine-labelled amino acids and solid state  $^{19}\text{F}$ -NMR are described to present the concepts and to introduce the terminology used within the thesis. The chapter also presents the motivation of this work with regard to the biological problem of membrane-peptide structural analysis.

### 1.1. Biological membranes and membrane-active peptides

#### 1.1.1. Biological membranes

All cells of all living organisms are enveloped by a membrane, which serves as a boundary between the cell interior and the extracellular environment.<sup>1,2,3</sup> Functionally the membranes do not only protect the cell from mechanical and chemical influences, but they also control transport (selective and non-selective), receive and transduce extra-cellular signals, initiate informational cascades, provide a specific environment for enzymatic catalysis, regulate recognition, adhesion and communication with other cells, provide an anchor for the extra- and intra-cellular skeleton, etc.<sup>4</sup> The same kinds of membranes enclose organelles of eukaryotic cells presenting a similar range of functions.

Biological membranes mainly consist of lipids and proteins. Minor constituents like water, various inorganic ions, small organic molecules and carbohydrates are also present, but up to few percent of total weight only. Therefore, lipids and proteins determine all the membrane functions. Protein/lipid ratios can vary greatly for membranes of different origins. The protein content can be as low as 20% of the membrane dry weight (neuronal cells), or as high as 78% (*Bacillus megaterium*).<sup>5</sup>

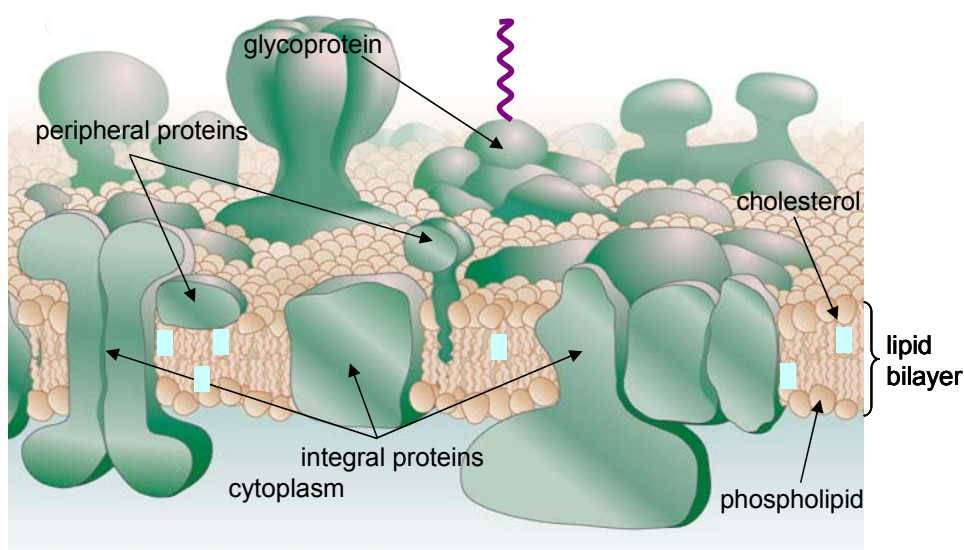


**Fig. 1.1.** “Fluid-mosaic“ model of an eukaryotic cell membrane according to Singer and Nicholson.<sup>6,7</sup>

The current understanding of biomembrane architecture is described by a model proposed in 1972 by Singer and Nicholson - the “fluid-mosaic” model (Fig. 1.1).<sup>6,7</sup> It considers a membrane as a lipid bilayer forming a two-dimensional fluid, in which the other embedded components (proteins) are freely diffusing.

The lipid composition of a membrane can differ a lot depending on the membrane origin.<sup>8</sup> The most abundant lipid classes are phospholipids, glycolipids and steroids (Fig. 1.2).<sup>9</sup> A phospholipid molecule consists of a lipophilic side chain

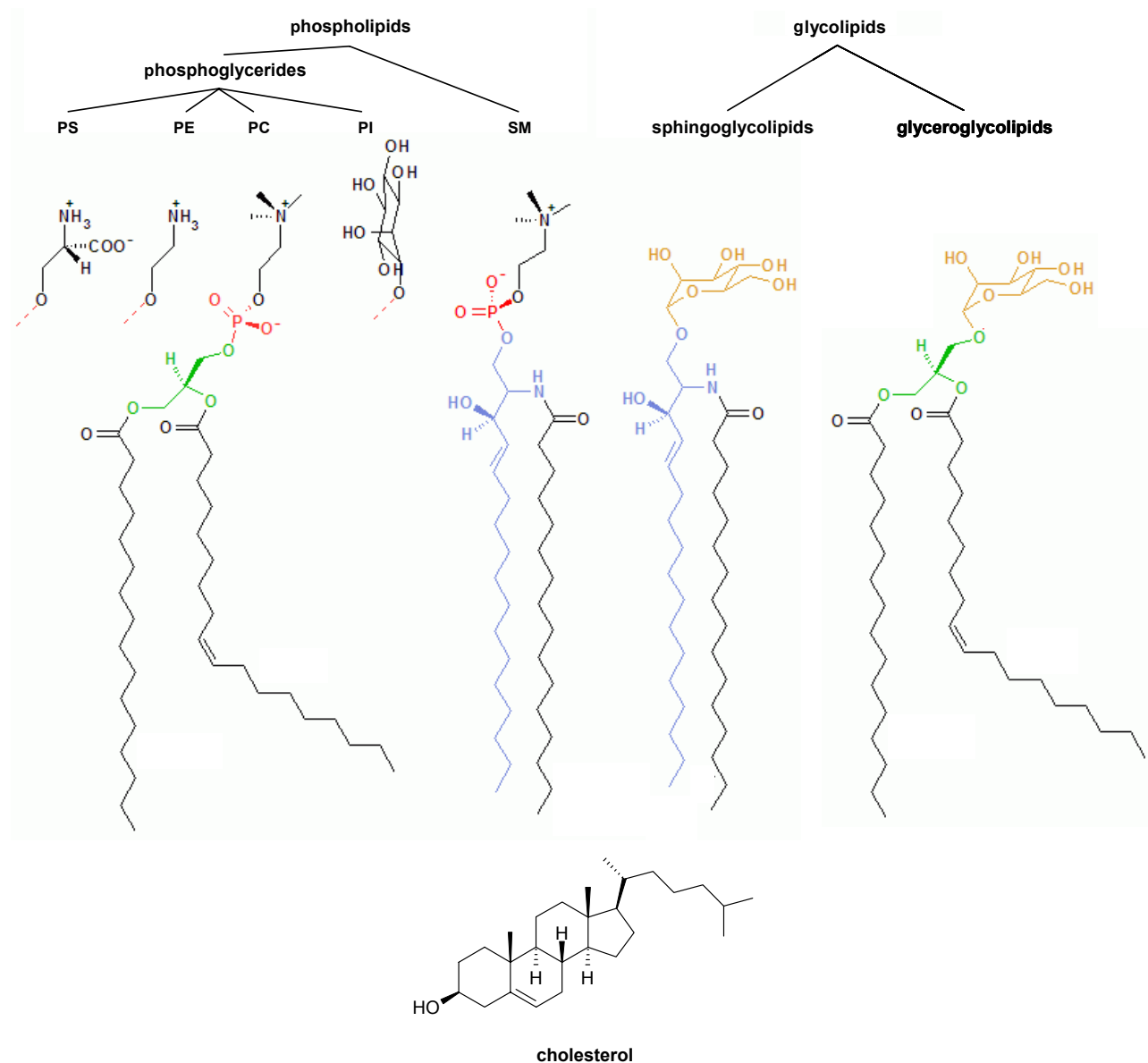


**Fig. 1.2.** Typical membrane lipids.<sup>5,8</sup> Abbreviations: PS - phosphatidylserine; PE - phosphatidylethanolamine; PC - phosphatidylcholine; PI - phosphatidylinositol, SM - sphingomyelin. The residues of phosphoric acid are highlighted in red, of glycerol - in green, of glucose - in yellow, of sphingosine - in blue.

(“tail”), glycerol residue (“neck”) and a polar hydrophilic moiety (“head”). Being arranged linearly, “tail” - “neck” - “head”, phospholipids possess an overall amphiphilic character. In an environment of uniform dielectric properties (e.g. in water) they tend, therefore, to assemble into aggregates, where energetically unfavorable contacts are minimized. The ratio between the molecular cross-sectional areas of a head group and its tail determines the overall shape of the molecule, which,

in turn, influences the molecular shape of the self-assembled aggregate.<sup>10</sup> In aqueous solution, most membrane phospholipids tend to form a lamellar phase, in which the lipid chains make up the hydrophobic core, while the headgroups are forming the interface towards the polar aqueous environment.<sup>11</sup>

### 1.1.2. Membrane-active peptides

There are many natural and synthetic peptides known, which can interact with membranes. For instance, opioid peptides ([Leu], [Met]-encephalins, dynorphin A), mastoparan X, substance P, glucagon, neurotensin, penetratin and many others.<sup>12,13,14</sup> Membrane-active peptides are very diverse functionally: they can demonstrate antimicrobial, cell-penetrating, fusogenic, amyloidogenic, signalling, anticancer, or immunomodulating activities, among others. In this work several peptides are used, which represent two important types of such functional interactions: antimicrobial peptides (AMPs) disrupt bacterial membranes, and cell-penetrating peptides (CPPs) can translocate across membranes.

#### 1.1.2.1. Antimicrobial peptides

AMPs are a group of peptides, which inhibit growth of microorganisms. These peptides are found in various living organisms and are supposed to be part of their innate immune system (Table 1.1).<sup>15-18</sup> Also many synthetic sequences and peptidomimetics show similar inhibitory effects, and therefore belong to the same functional group. Obviously, by functional definition, AMPs are antibiotics. They are active against rather wide classes of targets; among those are Gram-positive and Gram-negative bacteria, enveloped viruses, fungi, protozoa. More than 800 such peptides are reported to date.<sup>19</sup>

**Table 1.1.** Some naturally occurring AMPs.<sup>16,18</sup>

peptide	amino acid sequence	origin
magainin 2	GIGKFLHSAKKFGKAFVGEIMNS	frog
LL37	LLGDFFRKSKEKIGKEFKRIVQRIKDFLRNLVPRTES	human
bactenecin 1	RLC <sub>1</sub> RIVVIRVC <sub>1</sub> R	cow
apidaecin	GNNRPVYIPQPRPPHPRI	bee
androctonin	RSVC <sub>1</sub> RQIKIC <sub>2</sub> RRRGGC <sub>2</sub> YYKC <sub>1</sub> TNRPY	scorpion
protegrin 1	RGGRLC <sub>1</sub> YC <sub>2</sub> RRRFC <sub>2</sub> VC1VGR-NH <sub>2</sub> *	pig

\*Cysteins, which are connected by a disulfide bond are denoted by the corresponding index (C<sub>1</sub>, C<sub>2</sub>).

A uniform classification of AMPs does not exist due to the huge versatility of the group. Most often, using structural criteria, they are divided into the following classes: a) linear  $\alpha$ -helical peptides (e.g. magainin 2, pardaxin); b) cyclic and small proteins forming  $\beta$ -sheets (e.g. gramicidin S, polymixin B); c) peptides, rich in one or more specific natural amino acid (e.g. histatin, indolicidin); d) cyclic peptides with thio-ether rings (e.g. lantibiotics); e) peptaibols containing the unusual amino acid Aib (e.g. alamethicin); f) macrocyclic peptides, which contain cysteine (e.g.

circulins).<sup>20</sup> However, all AMPs are generally agreed to have some common features:<sup>21</sup>

1. short length: 10-50 amino acids;
2. overall cationic character;
3. primary or secondary amphipathic structure, which may be gained e.g. upon interaction with lipid membranes.

In contrast to conventional antibiotics, AMPs are often speculated to kill microorganisms by disruption of their biomembrane, and for many of them an action via receptor-independent mechanisms has been demonstrated.<sup>22</sup> Some models of membrane permeabilization by AMPs are shown in Fig. 1.3. In the “carpet” model,

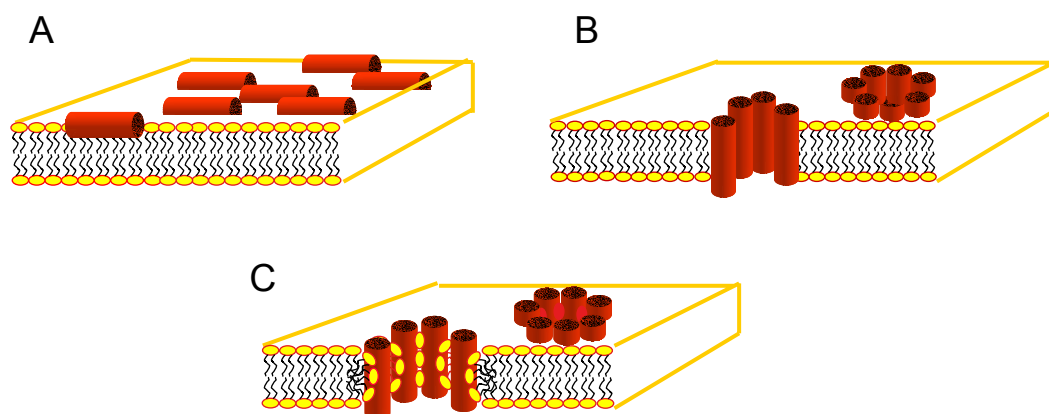


**Fig. 1.3.** Some postulated models of membrane permeabilization by antimicrobial peptides: a) “carpet” model; b) “barrel-stave” model; c) “worm-hole” model.<sup>21,22</sup>

the peptides are aligned on the outer leaflet parallel to the membrane surface and thereby induce non-specific rupture of the lipid bilayer. In the “barrel-stave” model, on the contrary, the peptides upon binding to the membrane surface arrange into aggregates and form transmembrane pores. The “worm-hole” model is similar to the “barrel-stave”, but here lipids are intercalated with peptides to line up the pore.

Since AMPs act via receptor-independent pathways, it is believed, that, on the contrary to conventional antibiotics, bacteria are not able to develop a resistance against them. Therefore, AMPs are supposed to be promising candidates as a novel generation of antibiotics.<sup>23,24</sup> Hence, any information concerning mechanisms of action of AMPs (e.g. their conformation, alignment and dynamics in biomembranes) is of exceptional importance.

#### 1.1.2.2. Cell-penetrating peptides

CPPs are a group of short peptide sequences (normally up to 40 amino acids) with the ability to gain access to the cell interior by means of different mechanisms and with the capacity to promote the intracellular delivery of covalently or non-covalently conjugated bioactive cargos.<sup>25-32</sup>

A strict classification of CPPs does not exist because of their vast variety. According to the origin, all CPPs can be roughly divided into two groups: natural (segments of natural proteins) and designer-made peptides (Table 1.2). Structurally,

CPPs are either entirely basic, or cationic and amphipathic.<sup>33,34,35</sup> Also, CPPs are shown to promote the intracellular delivery of different covalently or non-covalently attached cargoes, like DNA, RNA, peptides, proteins, liposomes, fullerenes, etc.<sup>36,37,38</sup>

**Table 1.2.** Some known CPPs.<sup>32,39</sup>

peptide	amino acid sequence	origin
Tat(48-60)	GRKKRRQRRRPPQ	human
pAntp(43-58)	RQIKIWFQNRRMKWKK	fly
pVEC	LLIILRRRIRKQAHHSK	VE cadherin
MAP	KLALKLALKALKAAKLA-NH <sub>2</sub>	designed peptide
(Arg) <sub>8</sub>	RRRRRRRR	designed peptide
MPG	GALFLGFLGAAGSTMGAWSQPKKKRKY	designed peptide
transportan	GWTLNSAGYLLGKINLKALAALAKISIL-NH <sub>2</sub>	designed peptide

The physical and chemical features of CPPs are similar to those of AMPs (amphipathic or/and cationic character, short length), but on the contrary to the latter group, CPPs have to be non-toxic compounds.

So far, no clear understanding concerning the mechanism of internalization of CPPs exists.<sup>39</sup> Until 2003 only energetically independent mechanisms were speculated to be involved. At the moment, however, it is believed that both non-endocytotic (energy-independent) and endocytotic (energy-dependent) pathways can take place. It also appears, given the complex nature of the CPP's target - the whole cell- that different mechanisms can be used simultaneously.<sup>40</sup> The issue is even more complicated in view of recent findings, that the prevailing mechanism of cell-penetration is highly dependent on the target cell line and the nature of the cargo.<sup>40</sup> Anyway, even when purely endocytotic internalization is taking place, escape from the endosome and transport across the lipid bilayer has to take place in order to reach the cytosol. Examples of mechanistic models of this essential step are outlined in Fig. 1.4.

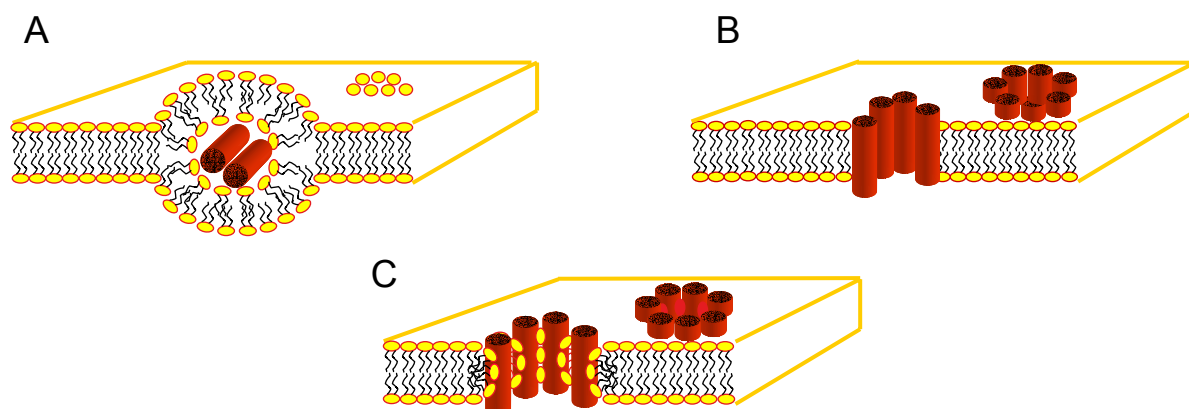


**Fig. 1.4.** Some postulated mechanisms for the translocation of CPPs through the lipid bilayer: a) “inverted micelle” model; b) “barrel-stave” model; c) “worm-hole” model.<sup>27</sup>

Since CPPs could be used as transport systems for the delivery of drugs, nanoparticles (e.g. magnetic nanoparticles) or fluorescent labels (e.g. quantum dots)



into a cell,<sup>37,39,40</sup> new technologies of chemical and/or physical manipulation of cells based on the application of CPPs are expected to emerge in the near future. Therefore, better insight into the mechanisms of action of CPPs, in particular their structure upon binding to membranes, is of great practical importance.

## 1.2. Methods of structural characterization of peptides

All methods for structural characterization of peptides can be roughly divided into those providing either partial or full structural information. The first group - for example, electron paramagnetic resonance, neutron diffraction, circular dichroism, fluorescence, or IR-spectroscopy<sup>41,42</sup> - is used mainly for the overall characterization of peptide structure. The direct methods, such as NMR in solution,<sup>43</sup> X-ray analysis<sup>44,45</sup> or electron microscopy (EM)<sup>46</sup> are, on the contrary, capable to establish fully resolved 3D peptide structures. All the latter methods, however, are not well suited to study membrane-active peptides. This is because the conformation of a peptide under the conditions imposed by the respective method (e.g. in solution, crystal, or on EM grid) and in the native environment can differ a lot. Therefore the structures determined this way, although highly accurate, may be biologically irrelevant. In the case of X-ray analysis and EM, an additional problem is due to the difficulty of getting suitable crystals (3D or 2D respectively) of peptide-membrane complexes. One of the few techniques able to resolve three-dimensional structural details of membrane-associated peptides in their quasi-native state is solid state NMR-spectroscopy.<sup>47,48</sup>

### 1.2.1. Peptide secondary structure

Since peptides are relatively small compounds, their spatial conformation is generally described in terms of secondary structure (on the contrary to proteins, which possess a more complex architecture). The secondary structure of peptides and proteins can be described by the torsion angles  $\varphi$ ,  $\psi$  and  $\omega$  (Fig. 1.5).

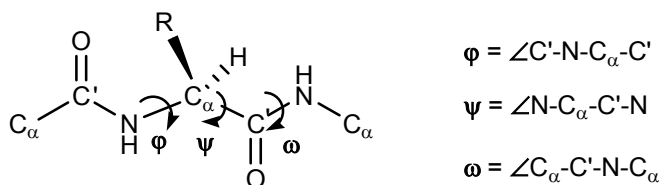


*Fig. 1.5.* Definition of torsion angles  $\varphi$ ,  $\psi$ ,  $\omega$  in peptides.

Based on the large body of structural data for peptides and proteins, and on the computational calculations, the typical (averaged) values of  $\varphi$ ,  $\psi$ ,  $\omega$  for common secondary structures are known (Table. 1.3).<sup>49,50</sup>

**Table 1.3.** Typical values of  $\phi$ ,  $\psi$ ,  $\omega$  for the most common structures of polypeptide backbone.

secondary structure element	$\phi$ ( $^{\circ}$ )	$\psi$ ( $^{\circ}$ )	$\omega$ ( $^{\circ}$ )
$3_{10}$ -helix	-60	-30	+180
$\alpha$ -helix	-57	-47	+180
$\pi$ -helix	-55	-76	+180
polyproline helix:			
type I (PP I)	-83	+158	0
type II (PP II)	-76	+146	+180
parallel $\beta$ -sheet	-119	+113	-
antiparallel $\beta$ -sheet	-139	+135	-
$\beta$ -turns*			
type I	$\phi_{i+1}$ ( $^{\circ}$ )	$\psi_{i+1}$ ( $^{\circ}$ )	$\phi_{i+2}$ ( $^{\circ}$ )
type I'	-60	-30	-90
	+60	+30	+90

\* According to the definition,  $\beta$ -turn consists of four amino acid residues. The numeration begins at the N-terminus from residue  $i$ - to  $i+3$ . Indexes at the torsion angles are shown in agreement with this numeration.

### 1.2.1. Circular dichroism spectroscopy

Circular dichroism (CD) spectroscopy is a form of the optical spectroscopy that measures the difference in absorbance of right- and left-circularly polarized light by an optically active substance. It is extensively applied to the structural characterization of peptides and proteins.<sup>51,52,53</sup> Fig. 1.6 illustrates the characteristic CD spectra of some common peptide/protein secondary structures.<sup>54</sup>

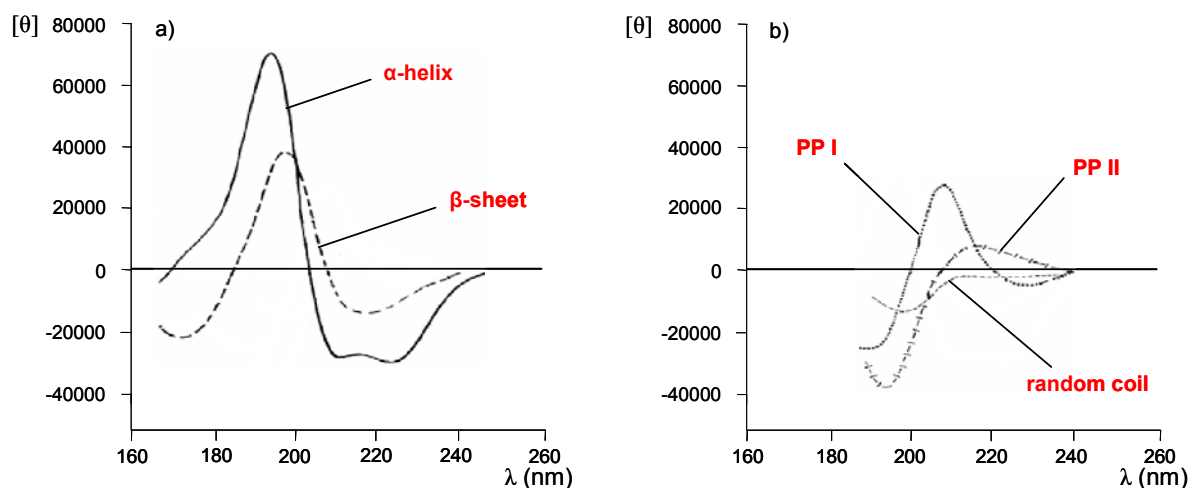


**Fig. 1.6.** CD spectra corresponding to a conformation of a)  $\alpha$ -helix, antiparallel  $\beta$ -sheet; b) polyproline type I (PP I), polyproline type II helix (PP II) and random coil.<sup>54</sup>

Normally CD spectra are measured between 260 and approximately 180 nm. If the peptide adopts more than one conformation, it is possible to extract the content of each secondary structure element (by numerical deconvolution of the CD spectrum). However, for quantification, CD data at low wavelengths (175-190 nm) are the most

critical, and given the overlap with absorbances of common solutes (salts, buffers, lipids), collection of these data can be very difficult.

### 1.2.2. Solid state $^{19}\text{F}$ -NMR

In contrast to the situation of globular proteins in solution, membrane-bound peptides are motionally restricted in the lipid bilayer, which gives rise to anisotropic (i.e. orientation dependent) NMR parameters. Today a number of methods have been established to use anisotropic interactions as a source of structural information by solid state NMR. Such studies of peptides or proteins typically rely on the use of isotope labels ( $^2\text{H}$ ,  $^{19}\text{F}$ ,  $^{15}\text{N}$ ,  $^{13}\text{C}$ ) that are either uniformly or selectively introduced into the system of interest.<sup>55</sup> These labels are used to measure structural and orientational constraints (e.g. chemical shift anisotropy (CSA), dipole-dipole, or quadrupole interactions).<sup>56,57</sup> The restraints measured on several individual labels are combined to yield the structure as well as orientation of the whole polypeptide molecule when bound to the membrane.

#### 1.2.2.1. $^{19}\text{F}$ nucleus in NMR

The  $^{19}\text{F}$  nucleus is an almost ideal NMR label for the following reasons:

1. similarity with  $^1\text{H}$  in the van der Waals radii makes substitution of  $^1\text{H}/^{19}\text{F}$  rather safe in terms of steric parameters;
2. on the contrary to  $^1\text{H}$ ,  $^2\text{H}$ ,  $^{13}\text{C}$ ,  $^{31}\text{P}$  and  $^{15}\text{N}$ , fluorine is almost absent in biological systems, thus having no natural abundance background;
3. fluorine possesses one natural isotope ( $^{19}\text{F}$ ) with the spin  $I = \frac{1}{2}$ , which is relatively simple to measure, since only CSA and dipole-dipole couplings (but not quadrupole interactions) are present for this nucleus;
4. being second only after  $^1\text{H}$  (and radioactive  $^3\text{H}$ ),  $^{19}\text{F}$  possesses the highest gyromagnetic ratio  $\gamma$  amongst all other isotopes in the periodic table, providing it with an exceptional NMR sensitivity (Table 1.4);<sup>58,59</sup>
5. the broad range of chemical shifts ( $\sim 500$  ppm) of  $^{19}\text{F}$  allows much better resolution of the signals compared with  $^1\text{H}$ ;
6. fluorine has a high sensitivity of chemical shift towards concentration, temperature, pH, etc.

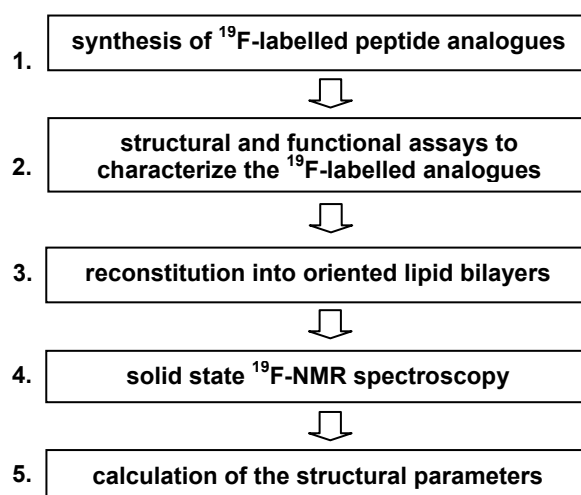
**Table 1.4.** Physical properties of  $^{19}\text{F}$  in comparison with other biologically relevant NMR-active isotopes.

isotope	$^1\text{H}$	$^2\text{H}$	$^{13}\text{C}$	$^{15}\text{N}$	$^{19}\text{F}$	$^{31}\text{P}$
electronegativity (Poling)	2.1	2.1	2.5	3.0	4.0	2.1
van der Waals radius (nm)	0.12	0.12	0.17	0.15	0.13	0.19
spin $I$	$\frac{1}{2}$	1	$\frac{1}{2}$	$\frac{1}{2}$	$\frac{1}{2}$	$\frac{1}{2}$
gyromagnetic ratio $\gamma/2\pi$ (MHz/T)	42.58	6.53	10.70	4.31	40.03	17.23
sensitivity (%) $\sim I(I+1) \gamma^3$	100	0.96	1.59	0.10	83.3	6.63
natural abundance (%)	99.985	0.015	1.1	3.7	100	100

One should always remember, however, that due to substantial differences in electronegativity (Table 1.4),  $^{19}\text{F}/^1\text{H}$  replacement can alter properties of the compound under study.<sup>60,61,62</sup> Also, technically the measurement of  $^{19}\text{F}$  is quite demanding, since it is not trivial to separate the  $^{19}\text{F}$  frequencies from that of  $^1\text{H}$  that is close by.

### 1.2.2.2. Methodology of membrane-peptide structural studies by solid state $^{19}\text{F}$ -NMR

The orientation, conformation and dynamics of membrane-bound peptides can be determined using the strategy depicted in Scheme 1.1.<sup>58</sup>



**Scheme 1.1.** General tactics to determine peptide orientation, conformation and dynamics in lipid bilayers by solid state  $^{19}\text{F}$ -NMR.

1.  $^{19}\text{F}$ -labelled peptide analogues are normally obtained by solid phase peptide synthesis (SPPS) replacing a natural amino acid by a  $^{19}\text{F}$ -labelled one.
2. In order to check whether  $^{19}\text{F}$ -labelling affects the properties of the peptide under study, the quasi-native structural (e.g. by CD, IR or NMR in solution) and functional properties (e.g. antimicrobial activity for AMPs, cell-penetration for CPPs, fusion activity for fusogenic peptides, etc.) of the  $^{19}\text{F}$ -labelled analogues have to be assayed and compared to the respective behaviour of the parent peptide (wild type peptide). For further studies only those  $^{19}\text{F}$ -labelled analogues are used, which have characteristics similar/identical to those of the wild type peptide.
3. To provide a membrane environment, the  $^{19}\text{F}$ -labelled analogues are reconstituted into the relevant mixture of lipids, where the lipid bilayers are uniaxially aligned on glass plates (oriented flat membranes). In most cases the unique orientation is assumed by the  $^{19}\text{F}$ -labelled peptides as well.
4. The peptide-lipid samples are then measured by solid state  $^{19}\text{F}$ -NMR spectroscopy. If the peptide is labelled with a single F-substituent, then the anisotropic chemical shift of fluorine is used for structural calculations. However, since the fluorine chemical shift is rather difficult to determine precisely,<sup>63</sup> the

method based on the analysis of dipole-dipole couplings in  $\text{CF}_3$ -groups is more promising.<sup>58</sup> One more advantage of  $\text{CF}_3$ -group over single F-substituent lies in its threefold higher signal intensity.

5. The dipolar coupling of a rotating  $\text{CF}_3$ -group depends on the angle  $\theta$  between the  $\text{CF}_3$  axis and the  $B_0$  (Fig. 1.7):<sup>64</sup>

$$\Delta\text{CF}_3(\theta) = \Delta^0\text{CF}_3 \langle 3\cos^2\theta - 1 \rangle / 2$$

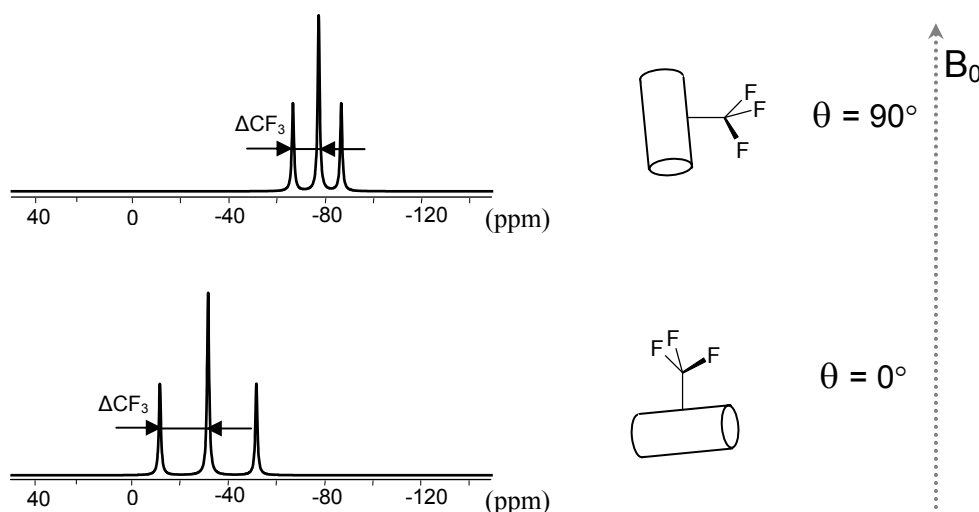


**Fig. 1.7.**  $^{19}\text{F}$ -NMR spectrum of an uniaxially aligned  $\text{CF}_3$ -group at different orientations with respect to the static magnetic field  $B_0$ . Changing the angle ( $\theta$ ) between the  $\text{C}-\text{CF}_3$  vector and  $B_0$  influences the dipole-dipole coupling in the  $\text{CF}_3$ -group.

Therefore, by measuring  $\Delta\text{CF}_3$  it is possible to calculate the orientation of a  $\text{CF}_3$ -group with respect to  $B_0$  ( $\theta$ ). If the  $\text{CF}_3$ -group is rigidly attached to the molecular framework, the orientation of the whole labelled segment can be obtained as well. The information from several individual  $\text{CF}_3$ -labels is thus used to calculate the structure as well as the orientation of the whole peptide.

An orientation of a peptide of a defined conformation in a lipid bilayer can be described by 3 parameters:  $\rho$ ,  $\tau$  and  $S_{\text{mol}}$  (Fig. 1.8).<sup>65</sup>

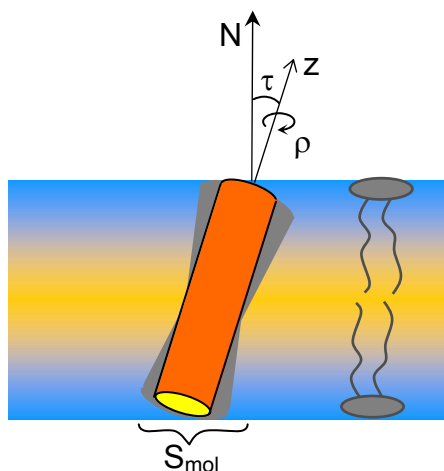


**Fig. 1.8.** Hypothetical helical peptide in an aligned lipid bilayer. Orientational parameters:  $\tau$  - angle between peptide axis  $z$  and membrane normal  $N$ ;  $\rho$  - angle, which describes the azimuthal rotation of the helix around axis  $z$ ;  $S_{\text{mol}}$  - parameter, which characterizes the mobility of the peptide as an “isotropic-wobble”.

To calculate these three parameters one must use the data from at least four individual labels.

### 1.3. $^{19}\text{F}$ -NMR labels in solid state $^{19}\text{F}$ -NMR

In this work the terms “ $^{19}\text{F}$ -NMR label” or “ $^{19}\text{F}$ -label” mean a specifically fluorinated amino acid, which has been or may potentially be used in peptide structural studies by solid state  $^{19}\text{F}$ -NMR.

#### 1.3.1. Known $^{19}\text{F}$ -NMR labels, their advantages and drawbacks

Even though a wealth of fluorine-labelled amino acids (FAAs) have been reported so far,<sup>66,67,68</sup> only few of them have been used as  $^{19}\text{F}$ -NMR labels (Fig. 1.9).

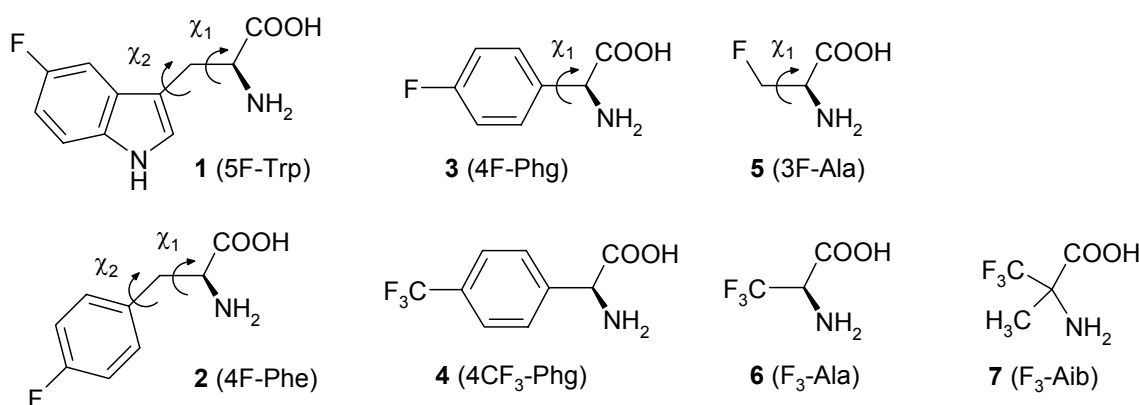


**Fig. 1.9.** Fluorine-labelled amino acids, which have been used as  $^{19}\text{F}$ -labels.

This is because not every FFA can be applied for this purpose. To be a proper  $^{19}\text{F}$ -NMR label, fluorine-labelled amino acid must meet several criteria:

1. the amino acid has to be conformationally rigid/restricted to place the  $^{19}\text{F}$ -reporter group ( $\text{CF}_3$  or single-F) in a well-defined position with regard to the peptide backbone;
2. being in place of a natural amino acid, the  $^{19}\text{F}$ -label must not disturb the structural and functional characteristics of the peptide;
3. the  $^{19}\text{F}$ -label must be chemically stable, and the amino- and carboxy-groups must be sufficiently reactive to be easily incorporated into the peptide by standard methods of SPPS;
4. the FFA possessing a  $\text{CF}_3$ -group is more promising than the corresponding analogue having a single F-substituent (Chapter 1.2.2.2).

The compatibility of the known  $^{19}\text{F}$ -NMR labels 1-7 with the abovementioned criteria is given below:

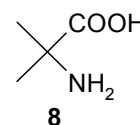
1<sup>69,70,71</sup> and 2<sup>72,73,74</sup> closely resemble the structures of Trp and Phe and are often used to substitute these natural amino acids in peptides. However, the position of the

fluorine atom in both **1** and **2** depends on the angles  $\chi_1$  and  $\chi_2$ , which makes a structural interpretation of the NMR parameters ambiguous.

**3**<sup>75-78</sup> and **4**,<sup>79,80,81</sup> being derivatives of phenylglycine, have been successfully used to substitute Ala, Val, Leu and Ile in peptides. In these labels the position of the <sup>19</sup>F reporter group is well-defined, but analysis of the chemical shift anisotropy of the single <sup>19</sup>F-substituent in **3** must still take into account the value of  $\chi_1$ . In contrast, fast rotation of the CF<sub>3</sub> group in **4** renders all <sup>19</sup>F interactions axially symmetric and collinear with the C<sub>α</sub>-C<sub>β</sub> bond, which makes this amino acid ideal for orientational analysis. The major disadvantage of this <sup>19</sup>F-NMR label, however, relies on its propensity to racemize during peptide synthesis. Thus, the target peptides, being a mixture of epimers, must be separated by HPLC, which is not always feasible.<sup>82</sup> One must always remember as well that the benzene ring is known to participate in diverse types of “weak” interactions,<sup>83</sup> hence the replacement of Ala, Val, Leu, Ile by **3** or **4** may change the properties of the peptide under investigation.<sup>84</sup>

Both **5**<sup>85,86,87</sup> and **6**<sup>88,89</sup> are structural analogues of Ala. Even though <sup>19</sup>F-label **5** has been successfully used in peptide studies, its use to obtain orientational constraints is restricted, because the position of the F-reporter depends on  $\chi_1$ . Amino acid **6**, on the contrary, has no such deficiency, since the axially symmetric CF<sub>3</sub>-group is directly attached to the aminocarboxylate moiety. However, the high propensity of its derivatives to eliminate HF under basic conditions<sup>78,90</sup> renders an application of **6** as <sup>19</sup>F-label less suitable.<sup>91</sup>

Compound **7** is an analogue of the unusual natural amino acid Aib (**8**). The CF<sub>3</sub>-group in **7** is directly attached to C<sub>α</sub>, and therefore its position is fixed. Moreover, **7**, in contrast to **6**, is stable under both acidic and basic conditions and due to the absence of proton at C<sub>α</sub> it does not racemize. This makes **7** an ideal <sup>19</sup>F-label to study Aib-rich peptides.<sup>92,93</sup> However, since the amino group is sterically hindered and electron deficient as well (due to the influence of the bulky electronegative CF<sub>3</sub>-group), an incorporation of **7** into peptides requires very long coupling times and can not be achieved by standard protocols of SPPS.<sup>94,95</sup>



From the considerations given above it is clear that all of the known <sup>19</sup>F-labels **1-7**, despite their use in peptide structural analysis, have significant disadvantages.

### 1.3.2. Known mono-CF<sub>3</sub>-substituted analogues of Ala, Val, Leu, Ile, Met and Pro as potential <sup>19</sup>F-NMR labels

In order to find proper <sup>19</sup>F-NMR labels among the already known fluorine-labelled amino acids, it makes sense to consider only those compounds, which

1. resemble the structures of natural amino acids to be substituted non-perturbingly;
2. possess single-CF<sub>3</sub>-substitution.

Let us first look into the analogues of Ala, Val, Leu, Ile, Met. A selection of candidates which resemble the structures of these amino acids is intuitive and is prevented by the absence of a strict definition of the term “structural relation”. Fig. 1.10 depicts all such CF<sub>3</sub>-substituted  $\alpha$ -amino acids with a primary amino group,

which possess saturated side chains of 2-6 carbon atoms (**9-17**). Amino acids containing another atom types in the side chain were excluded from the search, except for those having sulfur (to mimic Met).

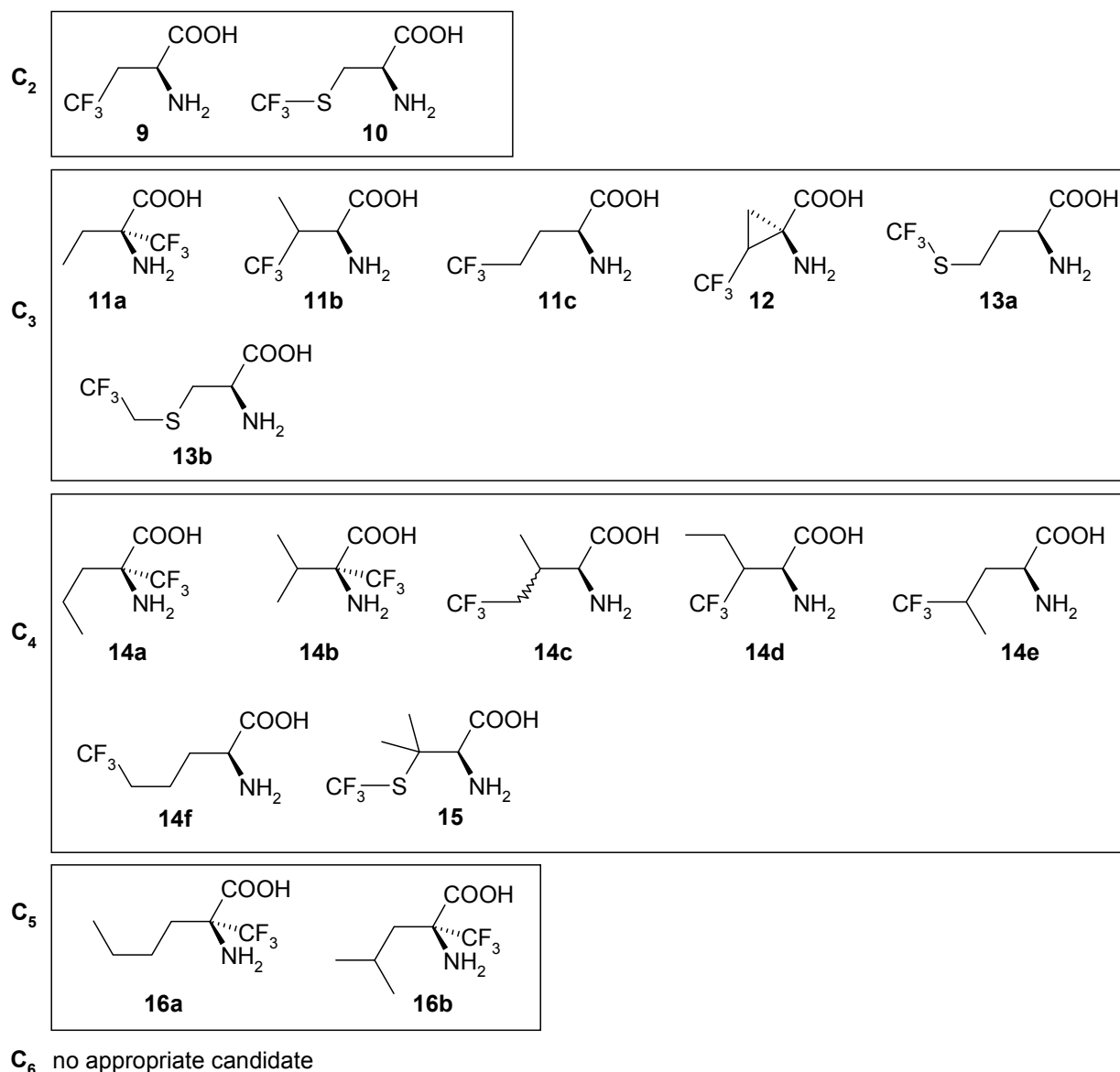


**Fig. 1.10.** Known mono- $\text{CF}_3$ -substituted analogues (**9-17**) of Ala, Val, Leu, Ile, Met (**14c** is known as a mixture of epimers; for **11b**, **12**, **14d**, **14e** both epimers are described). Symbols  $\text{C}_n$  ( $n = 2, 6$ ) correspond to the number of carbon atoms in the side chain.<sup>96-113</sup>

The flexible nature of the  $\text{CF}_3$ -group in candidates **9**,<sup>96,97,98</sup> **10**,<sup>99</sup> **11b**,<sup>100,101,102</sup> **11c**,<sup>98</sup> **13a**,<sup>103</sup> **13b**,<sup>104</sup> **14c**,<sup>105</sup> **14d**,<sup>106,107</sup> **14e**,<sup>108,109,110</sup> **14f**,<sup>111</sup> **15**<sup>99</sup> rules out their use as  $^{19}\text{F}$ -labels. Compounds **11a**,<sup>112,113</sup> **12**,<sup>114</sup> **14a**,<sup>115</sup> **14b**,<sup>112,113</sup> **16a**<sup>112,113</sup> and **16b**<sup>112,113</sup> have no such deficiency, as the  $\text{CF}_3$ -group is attached to  $\text{C}_\alpha$  (or to  $\text{C}_\beta$  of the rigid cyclopropane ring in **12**). Still, the presence of the bulky electron-withdrawing  $\text{CF}_3$ -group in close spatial proximity to the aminocarboxylate part could severely alter the steric and electronic environment of the peptide backbone. It will also reduce the chemical reactivity of the amino acids, thereby making their use in SPPS difficult.



In the case of Pro, it is worth to consider the mono- $\text{CF}_3$ -substituted analogues of proline and its nearest structural homologues - pipercolic and azetidinic acids. Amino acids possessing atoms other than carbon in the side chain were not considered here. Amongst the wealth of theoretically possible variants, only compounds **17(a,b)**<sup>116-119</sup> and **18**<sup>120</sup> are described in the literature (Fig. 1.11).

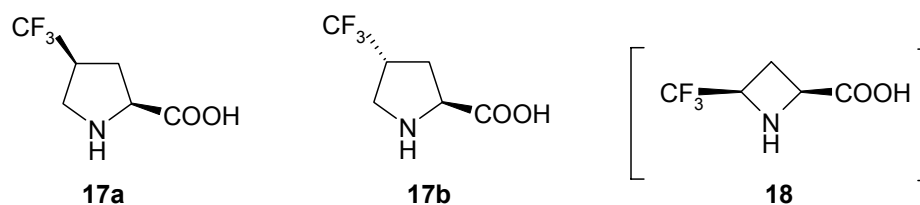
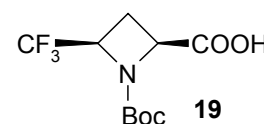


*Fig. 1.11.* Known mono- $\text{CF}_3$ -substituted analogues of Pro, pipercolic and azetidinic acid (**17-18**).<sup>116-120</sup>

Amino acids **17(a,b)** resemble the structure of Pro very closely. Moreover, the conformational mobility of the pyrrolidine ring in **17(a,b)** might be substantially reduced by the “pucker effect” of the bulky electronegative  $\text{CF}_3$ -group.<sup>121</sup> However, since the position of the  $\text{CF}_3$ -group is not rigidly fixed, isomers **17(a,b)** are not suitable as  $^{19}\text{F}$ -labels. In the  $\text{CF}_3$ -substituted derivative of azetidinic acid, compound **18**, the conformation of the side chain, and therefore the location of  $\text{CF}_3$ -group, is highly restricted by the four-membered ring. Still, the presence of the bulky electron-withdrawing  $\text{CF}_3$ -moiety in the spatial proximity to the aminocarboxylate part will diminish the chemical reactivity of the amino acid and can influence the peptide conformation.<sup>92-95</sup> Moreover, this compound is only known in the Boc-protected form (**19**). Therefore, amino acid **18** cannot be considered as a proper  $^{19}\text{F}$ -label.



## PART 2

### AIMS OF THE WORK

The aims of this dissertation were as follows:

- Design and synthesis of an optimized  $^{19}\text{F}$ -NMR label (label 1) as a substituent for non-polar aliphatic amino acids (Ala, Val, Leu, Ile, Met) for solid state NMR structural studies of membrane-active peptides.
- Design and synthesis of further structural  $^{19}\text{F}$ -NMR labels (labels 2) as potential substituents for proline in biologically active peptides.
- Incorporation of label 1 into the structurally and functionally well characterized antimicrobial peptides GS (gramicidin S) and PGLa (peptidyl-glycylleucine-carboxamide), to check of the compatibility of label 1 with solid state peptide synthesis (SPPS).
- Study of the  $^{19}\text{F}$ -labelled analogues of GS and PGLa by established functional (antimicrobial assays) and structural (circular dichroism) methods in order to confirm the compatibility of label 1 with the structure and function of these peptides.
- Proof-of-principle solid state  $^{19}\text{F}$ -NMR studies utilizing the novel label 1 on PGLa and GS.
- Incorporation of the new labels (labels 1 and 2) into the novel cell-penetrating peptide SAP (Sweet Arrow Peptide) to check the compatibility of label 2 with SPPS, and to examine any possible influence of label 2 (when substituted for Pro) on the conformation of SAP.
- Combined use of labels 1 and 2 to study the structure and orientation of SAP in lipid bilayers by solid state  $^{19}\text{F}$ -NMR analysis.

## PART 3

NEW  $^{19}\text{F}$ -NMR LABEL FOR SUBSTITUTION OF NATURAL NON-POLAR ALIPHATIC AMINO ACIDS (ALA, VAL, LEU, ILE, MET) IN PEPTIDES:  
 (*S*)-3-(TRIFLUOROMETHYL)-BICYCLOPENT-[1.1.1]-1-YLGLYCINE  
 ( $\text{CF}_3$ -BPG)

This chapter describes the stereoselective synthesis of the novel  $\text{CF}_3$ -substituted conformationally rigid amino acid (*S*)-3-(trifluoromethyl)-bicyclopent-[1.1.1]-ylglycine ( $\text{CF}_3$ -Bpg). The compound was designed as a proper  $^{19}\text{F}$ -NMR label for substitution of Ala, Val, Leu, Ile and Met in membrane-bound peptides.

The results described in this chapter have been recently published in *Mykhailiuk P. K., Afonin S., Chernega A. N., Rusanov E. B., Platonov M. O., Dubinina G. G., Berditsch M., Ulrich A. S., Komarov I. V.* Conformationally rigid trifluoromethyl-substituted  $\alpha$ -amino acid designed for peptide structure analysis by solid state  $^{19}\text{F}$ -NMR spectroscopy // *Angew. Chem.* - 2006. - Vol. 118. - P. 5787-5789; *Angew. Chem. Int. Ed.* - 2006. - Vol. 45. - P. 5659-5661.

### 3.1. Design of the target structure

The principles of design were based on the known advantages and disadvantages of the previously used  $^{19}\text{F}$ -labels (Chapter 1.3.2). In search of a rigid *L*-amino acid that would fulfil all criteria for a proper  $^{19}\text{F}$ -label, the bicyclo-[1.1.1]pentane system was chosen. Placing the  $\text{CF}_3$  and aminocarboxylate moieties at the bridgehead positions of this skeleton yields the  $^{19}\text{F}$ -labelled amino acid **20** ( $\text{CF}_3$ -Bpg) as the target (Fig. 3.1). The  $\text{C}_\alpha$ - $\text{C}_\beta$  and  $\text{C}$ - $\text{CF}_3$  bonds in **20** are collinear; the side chain can rotate only around these bonds. In contrast to **3** and **4**, in **20** the  $\text{CF}_3$  group and the  $\text{C}_\alpha$  are separated by a saturated bicyclic cage. This should make **20** less prone to racemization, since the transmission of electronic effects across the bicyclo-[1.1.1]pentane cage is far less pronounced than through an aromatic ring.<sup>122</sup> Neither degradation by the loss of HF (as in **6**) nor an unusually low reactivity of the aminocarboxylate moiety as a result of steric hindrance (as in **7**) are expected for **20** under SPPS conditions.

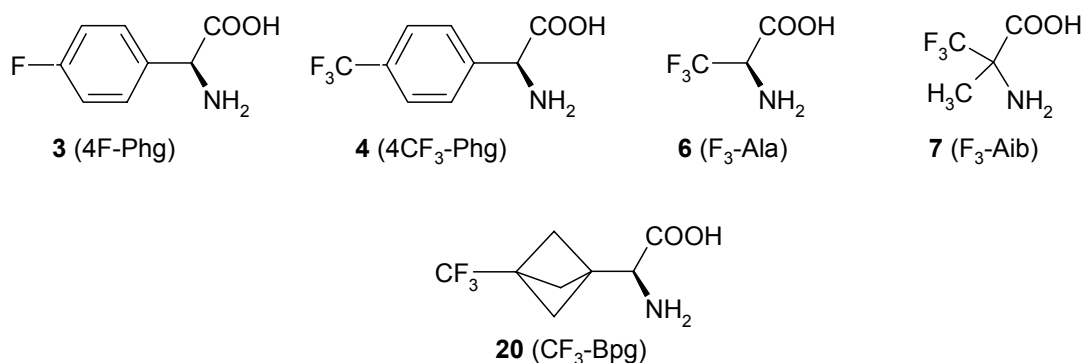


Fig. 3.1. Known (**3**, **4**, **6**, **7**) and proposed (**20**)  $^{19}\text{F}$ -labels.

To examine the suitability of **20** for substitution of non-polar amino acids, its calculated properties<sup>123</sup> were compared with those of the non-polar proteinogenic amino acids and the aforementioned <sup>19</sup>F-labels **3**, **4**, **6**, **7** (Table 3.1). The shape and steric volume of **20** resemble closely the corresponding values of Leu, Ile, Met, Trp, and Phe. The similarity to Pro, Val, and Ala is poorer. The non-aromatic character of **20** constitutes its main difference to Trp and Phe. If one considers the values of octanol/water partition coefficients, a substitution of Leu, Ile, or Met by **20** would cause minimal changes in the mean hydrophobicity, which is an important prerequisite for the proper folding of a polypeptide.<sup>124</sup> According to all parameters from Table 3.1. **20** is closer to the natural non-polar amino acids than any of the previously used phenylglycine derivatives (**3**, **4**).

**Table 3.1.** Calculated physical properties of <sup>19</sup>F-labels **3**, **4**, **6**, **7**, **20** and natural amino acids Met, Ile, Leu, Val, Ala, Pro, Phe, Trp.<sup>123</sup>

molecule	SASA [ $\text{\AA}^2$ ] <sup>a</sup>	FOSA [ $\text{\AA}^2$ ] <sup>b</sup>	volume [ $\text{\AA}^3$ ] <sup>c</sup>	QlogP <sub>o/w</sub> <sup>d</sup>
CF <sub>3</sub> -Bpg( <b>20</b> )	384.8	136.2	624.9	-0.72
4F-Phg ( <b>3</b> )	359.7	15.6	561.4	-1.73
4CF <sub>3</sub> -Phg ( <b>4</b> )	405.3	15.7	647.0	-0.53
F <sub>3</sub> -Ala ( <b>6</b> )	276.9	20.1	407.7	-2.0
F <sub>3</sub> -Aib ( <b>7</b> )	301.3	69.4	454.1	-1.73
Met	357.8	167.4	549.5	-1.63
Ile	338.6	204.5	527.5	-1.65
Leu	334.5	205.7	522.9	-1.64
Val	311.8	176.1	474.0	-1.96
Ala	260.8	105.3	368.5	-2.63
Pro	301.6	175.8	449.0	-2.04
Phe	364.9	60.7	592.3	-1.06
Trp	416.3	43.3	683.8	-0.92

a) solvent-accessible surface area; b) hydrophobic component of SASA; c) total solvent accessible volume; d) predicted octanol/water partition coefficient.

### 3.2. Planning the synthesis of CF<sub>3</sub>-Bpg

Retrosynthetic analysis of **20** was based on a comparison with synthetic approaches to amino acids with similar structure. At the time this work was started, there were two such compounds described in the literature: **21**<sup>125</sup> and **22**<sup>126</sup> (Fig. 3.2).

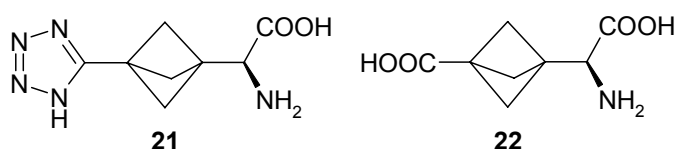
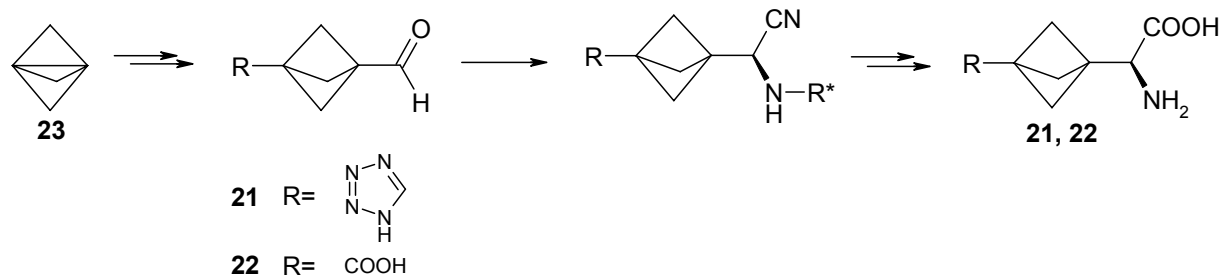


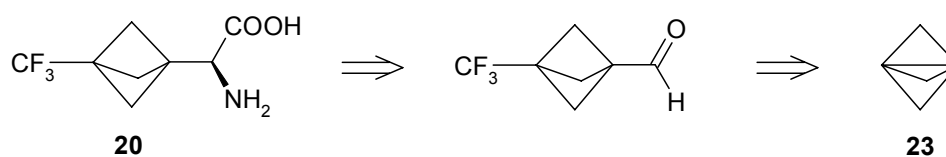
**Fig. 3.2.** Known amino acids with the bicyclopent-[1.1.1]-1-yl skeleton.<sup>125-126</sup>

The key step in the synthesis of both **21** and **22** is the asymmetric Strecker reaction of aldehydes obtained from propellane **23** (Scheme 3.1).



**Scheme 3.1.** Known syntheses of **21** and **22** (R\* - chiral auxiliary).<sup>125-126</sup>

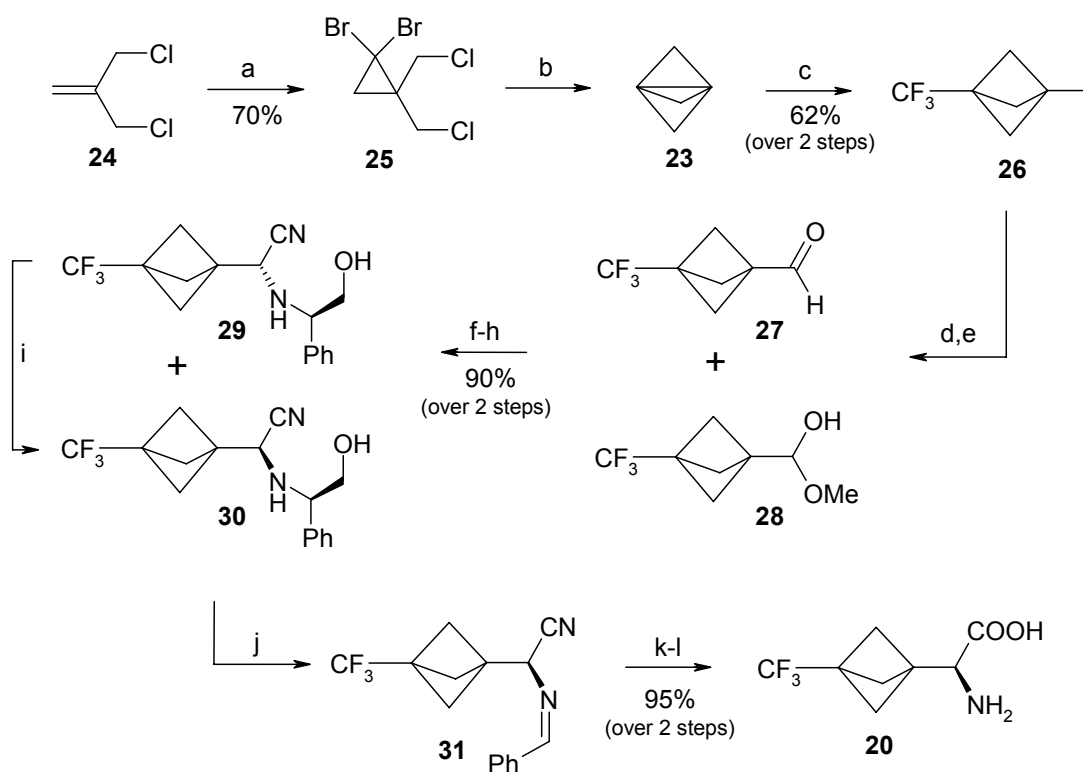
The transformations depicted above were taken as a basis for the retrosynthetic analysis of **20** (Scheme 3.2).



**Scheme 3.2.** Retrosynthetic scheme of **20**.

### 3.3. Synthesis of CF<sub>3</sub>-Bpg and proof of its absolute configuration

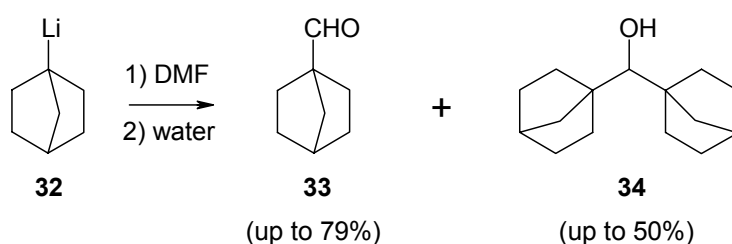
The proposed strategy was successfully realized (Scheme 3.3).



**Scheme 3.3.** Synthesis of **20**. Reagents and conditions: a) 40% aq. NaOH, CHBr<sub>3</sub>; b) MeLi, pentane, -78 °C, 0.5 h; c) CF<sub>3</sub>I, pentane, RT, 20 h; d) *t*-BuLi, Et<sub>2</sub>O, -78 °C, 1 h; e) HCO<sub>2</sub>Me, Et<sub>2</sub>O, -78 °C, RT, 3 h; f) (*R*)- $\alpha$ -phenylglycinol, CH<sub>2</sub>Cl<sub>2</sub>, RT, 2 h; g) Me<sub>3</sub>SiCN, RT, 10 h; h) chromatographic separation; i) MeOH, reflux, 3 h; j) Pb(OAc)<sub>4</sub>, CH<sub>2</sub>Cl<sub>2</sub>, 0 °C, 5 min; k) 20% HCl, reflux, 2 h; l) chromatography on Dowex-50.

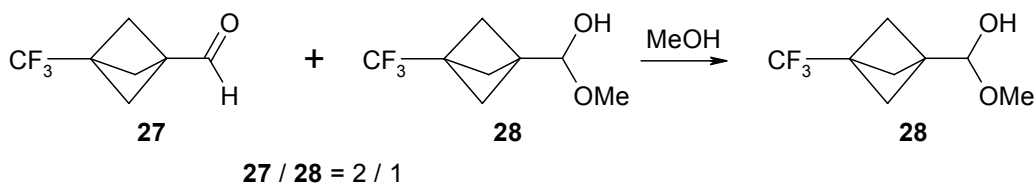
The first three synthetic steps were performed according to literature procedures. Dibromocyclopropanation of dichloroisobutene **24**<sup>127</sup> over NaOH/CHBr<sub>3</sub> gave the corresponding dibromocyclopropane **25**. The key intermediate of the whole synthesis - propellane **23**<sup>128-132</sup> - was obtained by treating **25** with MeLi. Addition of CF<sub>3</sub>I at the “inverted” carbon atoms of propellane led to iodide **26**. According to the literature procedure, iodide **26** must be purified by crystallization, which leads to a loss of material.<sup>133</sup> Here, however, crude **26** was obtained with a purity of > 95% and therefore no purification was needed at all (yield 62% calculated on **25**).

The incorporation of the -CHO moiety into the bicyclopentyl skeleton was inspired by an analogous formylation of 1-norbornyllithium **32** to produce aldehyde **33** (Scheme 3.4).<sup>134</sup> Similarly, iodide **26** was converted to the corresponding lithium



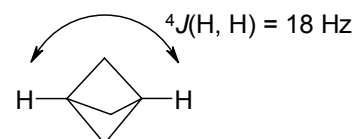
**Scheme 3.4.** The known synthesis of **33**. Depending on the reaction conditions the side product **34** formed in 0-50% yield. The highest yield of **33** was 79%.<sup>124</sup>

salt by reaction with *t*-BuLi, and treated afterwards with an excess of formylating reagent. Taking into account an expected high volatility of **27**, DMF (b.p. = 154 °C) was replaced by the more volatile HCO<sub>2</sub>Me (b.p. = 31 °C). To inhibit formation of side product **35**, the reaction was carried out at -78 °C. Surprisingly, together with the target aldehyde **27**, the hemiacetal **28** formed as well. The ratio **27/28** in the mixture was ~2/1. As expected, after addition of excess of MeOH to **27/28**, in both <sup>1</sup>H- and <sup>19</sup>F-NMR spectra the signals of **27** disappeared, while the signals of **28** remained (Scheme 3.5).



**Scheme 3.5.** Conversion of aldehyde **27** into hemiacetal **28** by dissolving in MeOH.

The formation of **28** in the synthesis of **27** is a quite unexpected observation, since acyclic aliphatic hemiacetals without electron-withdrawing substituents in direct proximity to the carbonyl group are supposed to be unstable.<sup>135</sup> On the other hand, while the standard values of the <sup>4</sup>*J*(H, H)-constants are in a range of 0-3 Hz,<sup>136</sup> the <sup>4</sup>*J*(H, H) between the bridgehead protons in the bicyclo[1.1.1]pentane skeleton is known to be as high as 18 Hz.<sup>137</sup> This suggests the



transmission of electronic effects across the bicyclopentane cage to be efficient, which may stabilize **28** via the electron-withdrawing effect of the CF<sub>3</sub>-group.

Assuming the transformation acetal  $\leftrightarrow$  aldehyde to be reversible,<sup>135</sup> the unseparated mixture **27/28** was used in the next step, the asymmetric Strecker reaction with (*R*)- $\alpha$ -phenylglycinol as a chiral inductor.<sup>138-145</sup> Here, the isomers **29/30** were formed in  $\sim$ 1/1 ratio, which means that the chiral induction did not happen (Fig. 3.3). Separation of **29/30** was performed by flash column chromatography

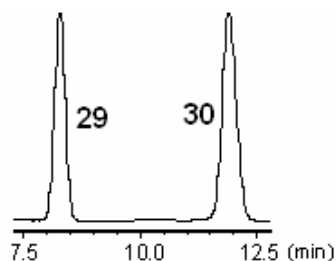


Fig. 3.3. Fragment of HPLC chromatogram of the reaction mixture **29/30**.

and the absolute configuration of the obtained isomers was established by X-ray analysis of **30** (Fig. 3.4).<sup>146</sup>

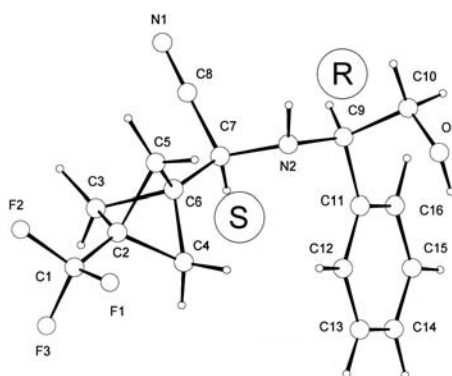
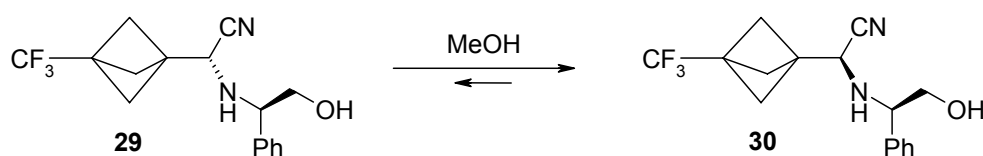


Fig. 3.4. Molecular structure of **30**.

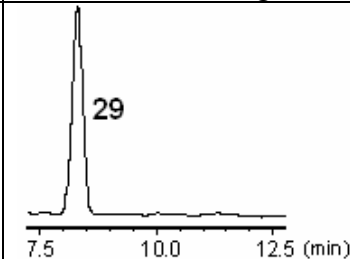
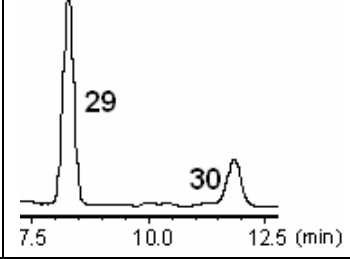
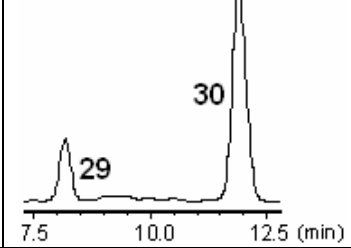
Quite useful for the synthesis was the observation that in methanolic solution of **29** the isomer **30** appeared with time (Scheme 3.6). This process was proven by



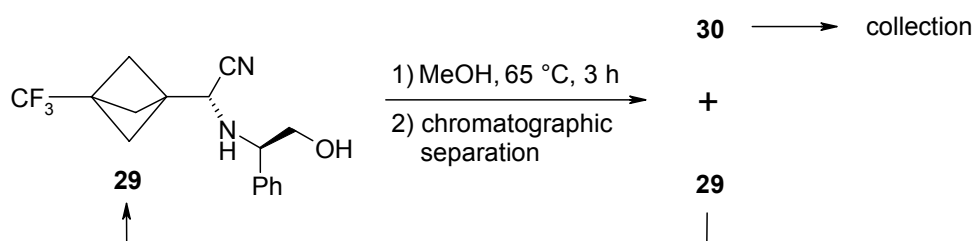
Scheme 3.6. Isomerization of **29** in MeOH.

<sup>1</sup>H- and <sup>19</sup>F-NMR and analytical HPLC (Table 3.2). In 36 h at 20 °C, about 20% of **29** dissolved in MeOH was converted into **30**. At 65 °C the process occurred faster, and the state of equilibrium **29/30** = 1/4 was reached in 3 h.

**Table 3.2.** Fragments of HPLC chromatograms of **29** under various incubation conditions.

isomerization conditions	HPLC chromatogram
a) MeOH, 20 °C, 5 min	
b) MeOH, 20 °C, 36 h	
c) MeOH, 65 °C, 3 h	

The observed isomerization allowed to convert the isomer **29** completely into the target compound **30** (Scheme 3.7), hence the yield of **30** was raised from 53% to 90% (calculated on **26**).

**Scheme 3.7.** The process of converting of isomer **29** into **30**.

Later, upon scale-up, the synthesis of **30** was optimized even further. The problem was in the inapplicability of flash chromatographic separation of **29/30** (difference in  $R_f < 0.05$ ) when working on a large scale. For instance, to separate 5 g of **29/30** entirely, a column with a length of 1 m and width 10 cm was used. Obviously, to separate 100 g of this mixture, a more convenient procedure had to be applied. Therefore, conditions for separation of **29/30** by crystallization were found (see Experimental Part).



The last synthetic steps were rather trivial. The isomer **30** was oxidized by  $\text{Pb}(\text{OAc})_4$ , and subsequent hydrolysis of the Schiff base **31** in 20%  $\text{HCl}_{\text{aq}}$  accomplished the synthesis of **20**.

Noteworthy, in the  $^{13}\text{C}$ -NMR spectrum of **20** (as well as in **29-30**), the signal of  $\text{C}_\alpha$  is a quartet ( $J(\text{C}, \text{F}) = 2 \text{ Hz}$ ). No doubt, this is the result of coupling to fluorine atoms, the interaction occurring over 5 bonds (Fig. 3.5).

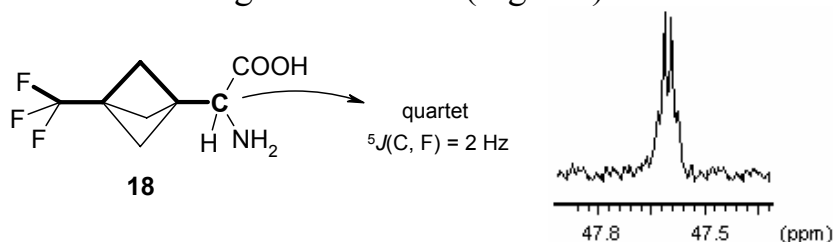


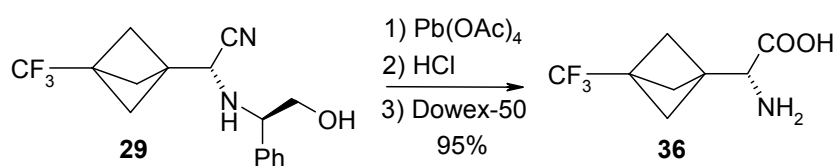
Fig. 3.5. Signal of  $\text{C}_\alpha$  in  $^{13}\text{C}$ -NMR spectrum of **20**.

### 3.4. Confirmation of the optical purity of $\text{CF}_3$ -Bpg

It is generally known that amino acids possessing electron-withdrawing substituents are prone to racemization.<sup>147</sup> Since the stability of the hemiacetal **28** could be caused by an electron-withdrawing effect of the  $\text{CF}_3$ -group, the amino acid **20** could have an increased propensity to racemization as well. Taking into account the relatively harsh hydrolysis conditions used for **30** (120 °C, 2 h, 20%  $\text{HCl}$ ) during the last step of the synthesis, one might have doubts concerning the optical purity of **20**.

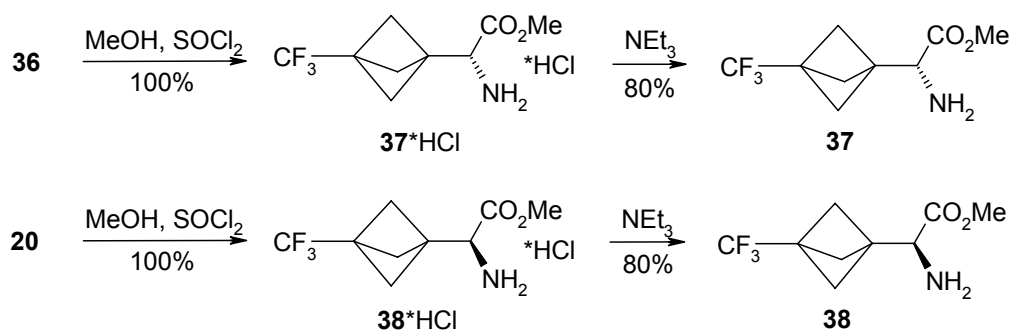
One method, among others,<sup>148,149</sup> to determine the optical purity of amino acids is the use of lanthanide shift reagents (LSRs).<sup>150</sup> The technique is based on the ability of  $\text{Eu}$ ,  $\text{Pr}$  and  $\text{Yb}$  derivatives to shift the NMR signals of a bound substrate without substantially broadening them (in contrast to other lanthanides). This effect is due to the formation of a “pseudo-contact” complex between the lanthanide metal and the functional groups of the substrate (most often  $\text{NH}_2$  or  $\text{OH}$ ). Provided that the LSR is a chiral compound (possessing a chiral ligand), it can be used to determine the enantiomeric excess ( $ee$ ) of the substrate, since the chemical shifts of the diastereomeric complexes of the LSR with different enantiomers are not equal. The  $ee$  of amino acids can be revealed by converting them first into the corresponding methyl esters, which are subsequently analyzed by LSR. Determination of  $ee$  is performed by integrating the signals of the  $\text{CO}_2\text{Me}$ -groups of the methyl ester in the  $^1\text{H}$ -NMR spectrum.

Since the analysis requires both enantiomers, (*R*)- $\alpha$ -amino acid **36** was synthesized first (Scheme 3.8).



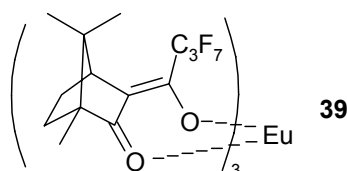
Scheme 3.8. Synthesis of **36**.

Next, **36** and **20** were converted into the hydrochlorides **37**\*HCl/**38**\*HCl by standard MeOH/SOCl<sub>2</sub> treatment. The target methyl esters **37** and **38** were obtained from the corresponding hydrochlorides by treating with NEt<sub>3</sub> (Scheme 3.9).



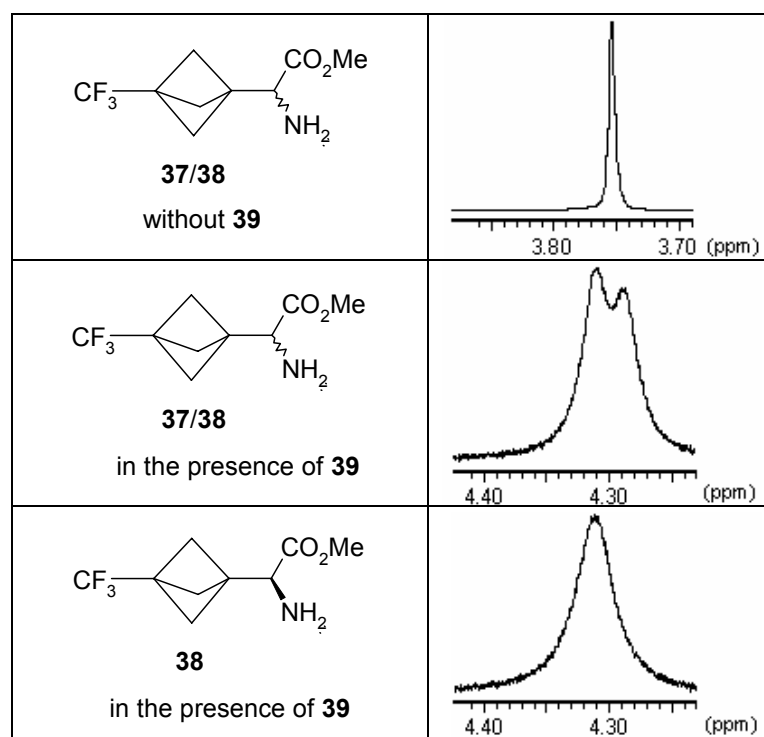
**Scheme 3.9.** Syntheses of **37** and **38**.

As LSR the compound **39** was used:



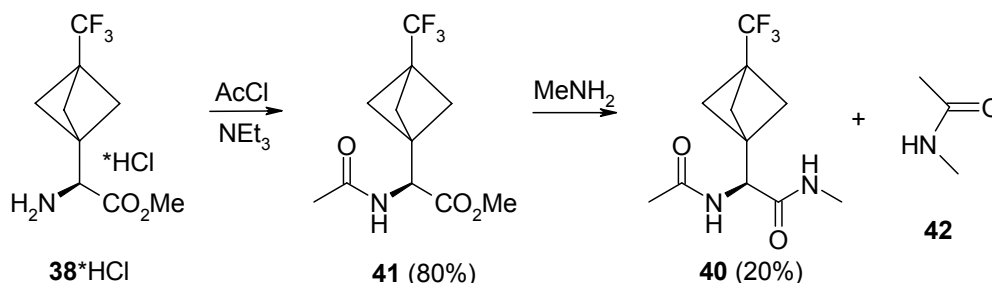
The results of the LSR assisted purity check of **38** are summarized in Table 3.3. They undoubtedly prove **38**, and hence amino acid **20**, to be pure (*S*)-enantiomers.

**Table 3.3.** Signal of CO<sub>2</sub>Me group in a <sup>1</sup>H-NMR spectrum (CDCl<sub>3</sub>) of a) mixture **37/38**; b) mixture **37/38** (0.05M/0.05M) in the presence of **39** (0.05M); c) **38** (0.1M) in the presence of **39** (0.05M).



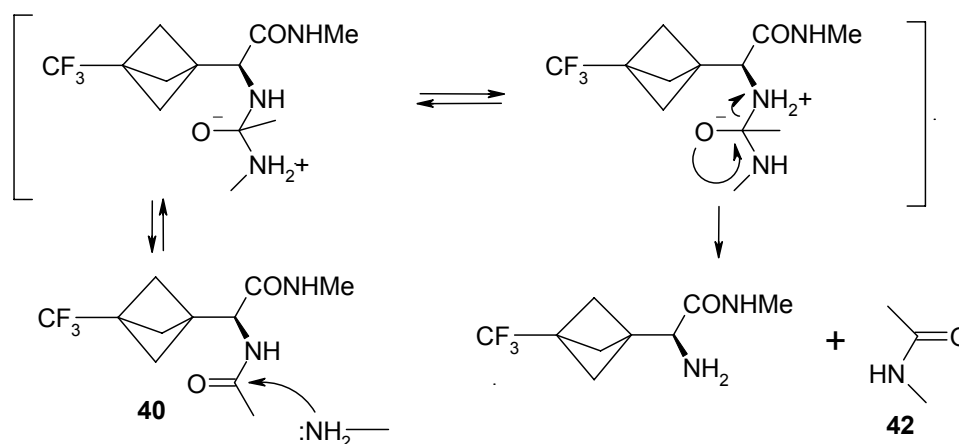
### 3.5. Synthesis of a model peptide derivative of CF<sub>3</sub>-Bpg

To confirm the possibility of incorporating **20** into the peptide backbone, the simplest peptide model - diamide **40** - was synthesized (Scheme 3.10). The obtaining of monoamide **41** by reaction of **38**\*HCl with AcCl/NEt<sub>3</sub> was performed without troubles. In the next step, however, the target diamide **40** was obtained with an unexpectedly low yield of ~20%.



*Scheme 3.10.* Synthesis of **40**.

The amide **42** was also identified among the reaction products, and its presence suggested an explanation of the poor yield of **40**. Since the reaction was carried out under rather drastic conditions (100 °C) using excess of MeNH<sub>2</sub>, the compound **40**, after being formed, reacted further with methylamine (Scheme 3.11).



*Scheme 3.11.* Suggested mechanism of amide **42** formation in the reaction of **40** with excess of methylamine at 100 °C.

The synthesis of diamide **40** proved that it is possible to incorporate **20** into polypeptides.

## PART 4

FIRST  $^{19}\text{F}$ -NMR LABELS FOR PROLINE SUBSTITUTION IN PEPTIDES

In the following chapter the syntheses of 3,4- and 4,5-(trifluoromethylmethano)-prolines and precursors to 2-(trifluoromethyl)-proline are described. These conformationally restricted amino acids were designed as  $^{19}\text{F}$ -NMR labels for Pro substitution in membrane-bound peptides.

The results described in this chapter have been published in the following manuscripts:

*Grygorenko O. O., Kopylova N. A., Mykhailiuk P. K., Meißner A., Komarov I. V.* An approach to 2-cyanopyrrolidines bearing a chiral auxiliary // *Tetrahedron: Asymmetry*. - 2007. - Vol. 20. - P. 290-297;

*Mykhailiuk P. K., Afonin S., Palamarchuk G. V., Shishkin O. V., Ulrich A. S., Komarov I. V.* Synthesis of trifluoromethyl-substituted proline analogues - new  $^{19}\text{F}$ -NMR labels for peptides in polyproline II conformation // *Angew. Chem.* - 2008. - in press;

*Mykhailiuk P. K., Afonin S., Ulrich A. S., Komarov I. V.* A convenient route to trifluoromethyl-substituted cyclopropane derivatives // *Synthesis*. - 2008. - in press.

#### 4.1. Design of the target compounds

The location of proline residues in proteins is peculiar: they are most frequently found in loops and in flanking positions of stable secondary structure elements ( $\alpha$ -helices,  $\beta$ -strands), as well as in various turns.<sup>151,152</sup> This location is a consequence of two major structural properties of Pro: first, the lack of hydrogen on the  $\alpha$ -amino group prevents hydrogen-bonding within a polypeptide, and second, the cyclic nature of the side chain reduces the conformational freedom and typically restricts the torsion angle  $\varphi$  to  $-63^\circ (\pm 15^\circ)$ .<sup>153</sup> Pro-rich peptides (PRPs) in aqueous solvents often exist in a left-handed "poly-*L*-proline II" (PPII) conformation, with  $\varphi \sim -75^\circ$ ,  $\psi \sim 150^\circ$  and  $\omega = 180^\circ$ .<sup>154</sup> Stable PPII sequences reflect the functional dichotomy of PRP: they either act as structural building blocks or they are constituents of specific peptide-peptide and peptide-ligand recognition sites.<sup>155</sup> Taking into account the importance of PRPs, and the absence of the promising  $^{19}\text{F}$ -labels for Pro substitution in the literature (Chapter 1.3.2), the design of such compounds is of special importance.

In the case of Pro, however, it is not trivial to design such label with a fixed  $\text{CF}_3$ -group, that would not perturb the peptide conformation. The hypothetical  $^{19}\text{F}$ -labels **43** and **44** (Fig. 4.1), for instance, are conformationally rigid amino acids and therefore possess fixed  $\text{CF}_3$ -groups. However, one can state that **43-44** will influence

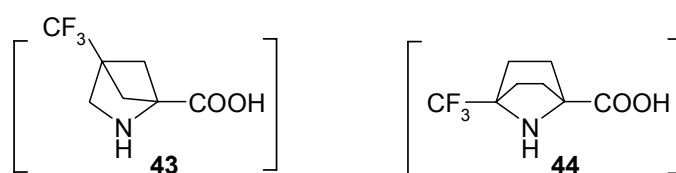


**Fig. 4.1.** Hypothetical conformationally rigid  $^{19}\text{F}$ -labels **43** and **44** with fixed  $\text{CF}_3$ -group.

the native peptide conformation, since in their known non-substituted analogues **45**<sup>156,157</sup>-**46**<sup>158,159</sup> the angle  $\varphi$  adopts values of either  $\pm 29^\circ$  (**45**), or  $\pm 36 \sim \pm 51^\circ$  (**46**), which is far away from the normal range around  $-63^\circ$  ( $\pm 15^\circ$ ) for Pro.<sup>153</sup> Thus, **43-44** are not suitable <sup>19</sup>F-labels. In other hypothetical <sup>19</sup>F-NMR labels, conformationally non-rigid amino acids **47(a,b)** the angle  $\varphi$ , on the contrary to **45-46**, is not fixed (Fig. 4.2). However, the position of the CF<sub>3</sub>-group is not fixed either. Hence, **47(a,b)** are also not proper <sup>19</sup>F-labels.

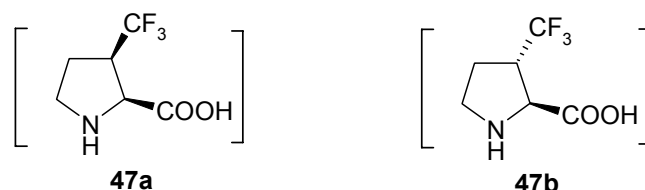
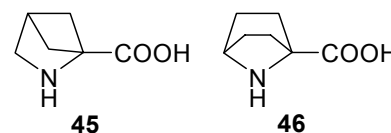


*Fig. 4.2.* Hypothetical <sup>19</sup>F-labels **47(a,b)** with flexible CF<sub>3</sub>-group.

In this thesis a library of CF<sub>3</sub>-substituted conformationally restricted Pro analogues **48-50** was proposed (Fig. 4.3) to produce potential <sup>19</sup>F-labels for Pro substitution.

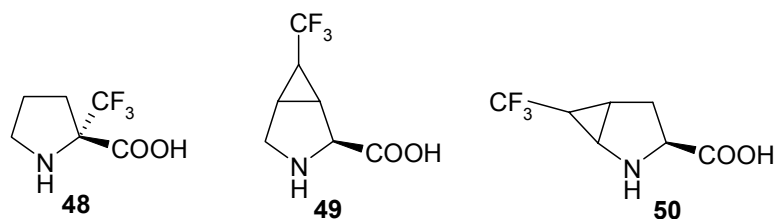


*Fig. 4.3.* Designed <sup>19</sup>F-NMR labels for substitution of Pro in peptides.

In amino acid **48** the position of the CF<sub>3</sub>-group is well defined with respect to the molecular backbone, since it is directly attached to C<sub>α</sub>. However, a spatial proximity of the bulky electron-withdrawing CF<sub>3</sub>-group to the aminocarboxylate moiety reduces the reactivity of the amino group in **48** and could alter the steric and electronic environment of the peptide backbone.<sup>160,161,162</sup> The isomers **49-50**, on the contrary to **48**, possess a CF<sub>3</sub>-group which is sufficiently distant from the peptide backbone to prevent its perturbation and influence the reactivity of the aminocarboxylate moiety. The angle  $\varphi$  in these compounds, in contrast to **43-44**, is not fixed. Moreover, since the conformational mobility of **49-50** is restricted by the presence of the rigid three-membered ring, the position of the CF<sub>3</sub>-group is better fixed than in **47(a,b)**. However, it may still turn out that the partially flexible non-rigid location of the CF<sub>3</sub>-group in **49-50** may cause some ambiguities in the interpretation of the <sup>19</sup>F-NMR spectra.

## 4.2. 2-(Trifluoromethyl)-proline

### 4.2.1. Planning the synthesis of 2-(trifluoromethyl)-proline

At the time this work was started, there were three compounds **51**,<sup>163</sup> **52**,<sup>164</sup> **53**<sup>165,166</sup> described in the literature, which are structurally similar to **48** (Fig. 4.4).

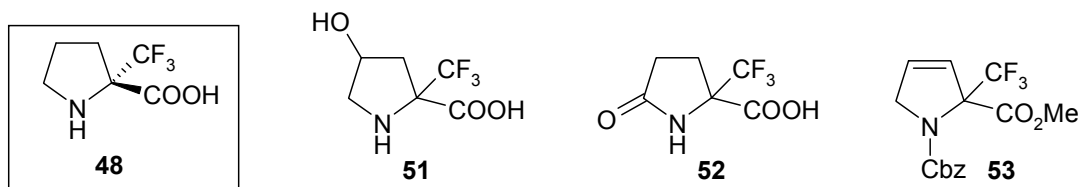
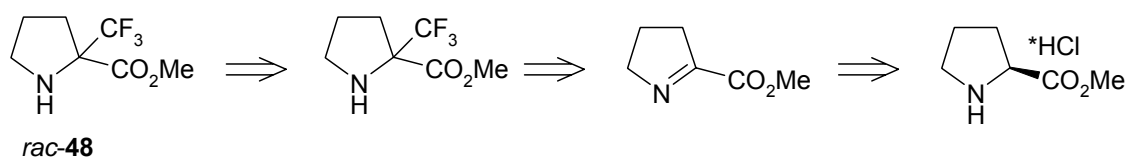


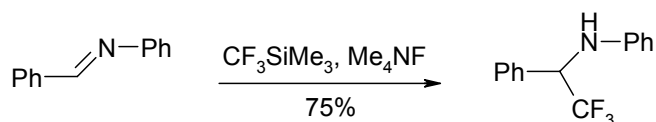
Fig. 4.4. 2-Trifluoromethylproline (**48**) and known structure-related compounds (**51**, **52**, **53**).<sup>163-166</sup>

Synthesis of **51**, **52** and **53** included 4-5 steps from commercially available materials, and all three compounds were known in racemic form only. Therefore, the fundamentally different strategies to obtain **48** were proposed.

The first approach allowed obtaining *rac*-**48** in only 3 steps from the commercially available proline methyl ester hydrochloride (Scheme 4.1). This method was based on the known addition of CF<sub>3</sub>SiMe<sub>3</sub> to imines (Scheme 4.2).<sup>167,168</sup>

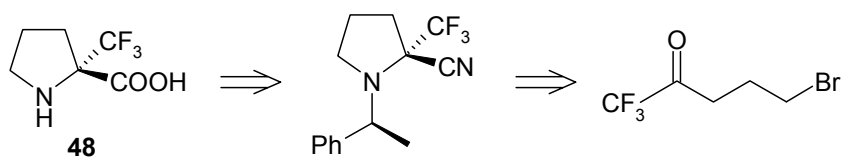


Scheme 4.1. Approach 1: retrosynthetic analysis of **48** in racemic form.

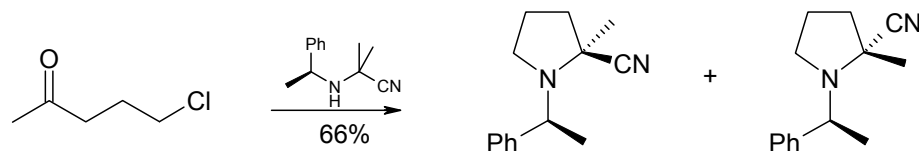


Scheme 4.2. An example of the reaction between CF<sub>3</sub>SiMe<sub>3</sub> and non-activated imines in the presence of fluoride-anion.<sup>167,168</sup>

For synthesis of optically pure **48**, an approach (Scheme 4.3) based on the known cyclization of  $\gamma$ -halogenketones into the corresponding diastereomeric aminonitriles (Scheme 4.4)<sup>169</sup> was proposed.



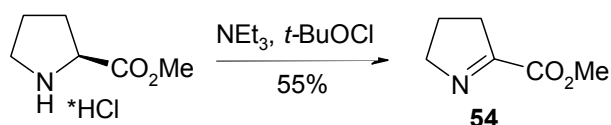
Scheme 4.3. Approach 2: retrosynthetic analysis of (*S*)-**48**.



**Scheme 4.4.** An example of converting of the  $\gamma$ -halogenketone into the corresponding cyclic aminonitriles.<sup>169</sup>

#### 4.2.2. Synthesis of 2-(trifluoromethyl), 2-(nitrile)-pyrrolidine skeleton

Approach 1: The compound **54** was easily synthesized from proline methyl ester in one step according to the literature procedure (Scheme 4.5).<sup>170</sup>



**Scheme 4.5.** Synthesis of **54**.<sup>170</sup>

In the following reaction, - addition of  $\text{CF}_3\text{SiMe}_3$  to the double  $\text{C}=\text{N}$  bond of **54** - however, a mixture of products was obtained. Notably, in the  $^1\text{H-NMR}$  spectrum there were no signals of  $\text{CO}_2\text{Me}$ -group detected. At the same time GC-MS analysis revealed the presence of two peaks having molecular masses of 165 and 254 ( $m/z$ ) respectively. The interpretation of these products is illustrated in Fig. 4.5.

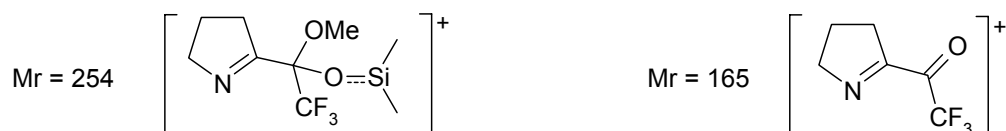
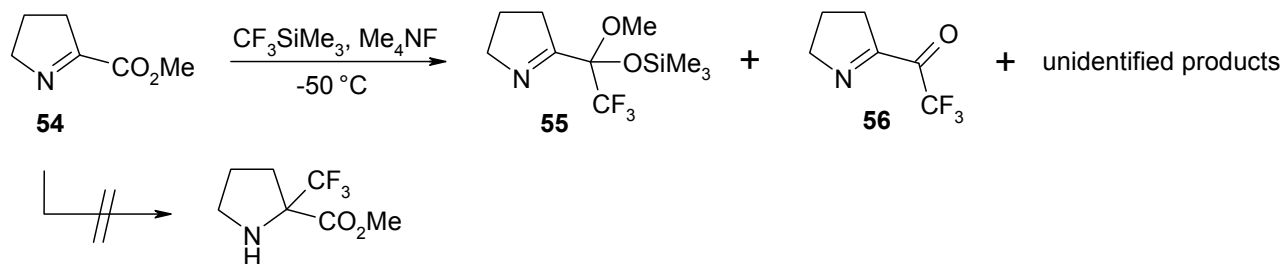


**Fig. 4.5.** Structural interpretation of signals with  $m/z$  of 165 and 254, seen in GC-MS analysis of the mixture obtained after addition of  $\text{CF}_3\text{SiMe}_3$  to **54**.

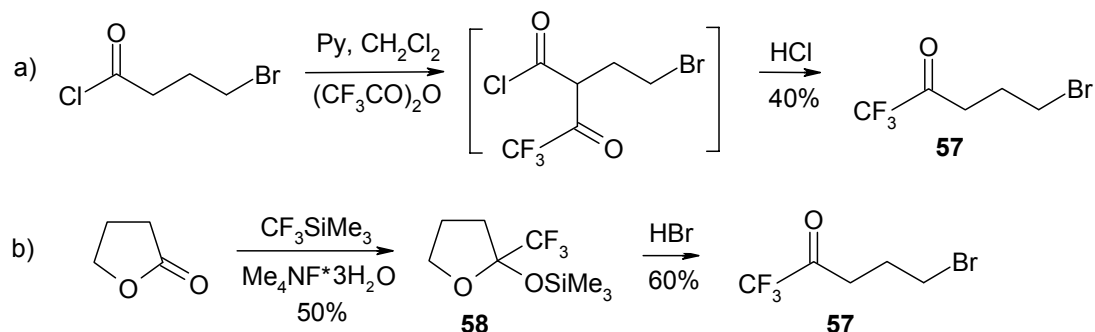
This result suggested that in **54** the  $\text{CO}_2\text{Me}$ -group was more reactive than the  $\text{C}=\text{N}$  bond towards  $\text{CF}_3\text{SiMe}_3$  (Scheme 4.6).



**Scheme 4.6.** Reaction between  $\text{CF}_3\text{SiMe}_3$  and **54** at  $-50\text{ }^\circ\text{C}$  catalyzed by  $\text{Me}_4\text{NF}$ .

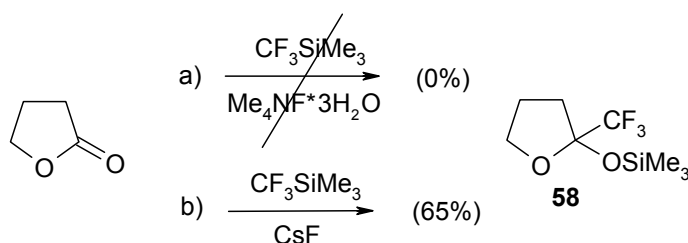
Formation of the mixture **55/56** is a rather strange result, because normally a reaction between  $\text{CF}_3\text{SiMe}_3$  and a carboxymethyl group requires at least room temperature.<sup>171</sup>

Approach 2: For the starting  $\gamma$ -halogenketone **57** two synthetic roots are described in the literature (Scheme 4.7).<sup>172,173</sup>



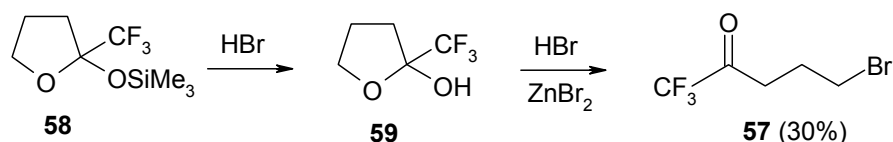
**Scheme 4.7.** Known syntheses of **57**.<sup>172,173</sup>

The first method is based on trifluoroacetylation of 4-bromobutyryl chloride, followed by subsequent hydrolysis of the corresponding intermediate (Scheme 4.7, a). However, this reaction was not reproducible, since complex mixtures were obtained every time. An alternative way to synthesize **57** (Scheme 4.7, b) was not reproducible either. Under conditions described in the literature,<sup>173,174</sup> an addition of  $\text{CF}_3\text{SiMe}_3$  to  $\gamma$ -butyrolactone in the presence of  $\text{Me}_4\text{NF}\cdot 3\text{H}_2\text{O}$  did not happen. Therefore, another catalyst was used - anhydrous  $\text{CsF}$ , - which allowed to obtain **58** in 65% yield (Scheme 4.8).



**Scheme 4.8.** Synthesis of **58** according to a) literature procedure<sup>174</sup>; b) modified procedure.

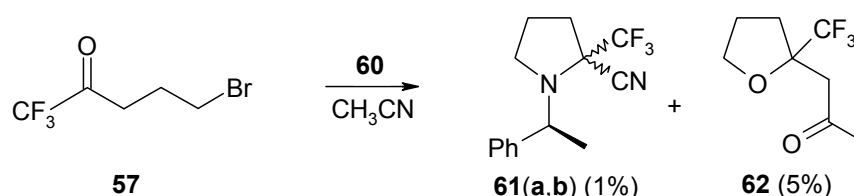
The next step - opening of the tetrahydrofuran ring of **58** - was problematic as well. Even after refluxing of **58** with 48% aq. HBr over 60 h the reaction did not proceed at all (however, according to the literature procedure it had to be finished in 24 h). The reaction stopped at the stage of formation of alcohol **59**, whose relative stability might be caused by an electron-withdrawing effect of the  $\text{CF}_3$ -group. Addition of catalytic amounts of  $\text{ZnBr}_2$  accelerated the reaction and allowed to obtain **57** in 30% yield (Scheme 4.9).



**Scheme 4.9.** Synthesis of **57**.



The key step of the synthesis - cyclization of **57** with aminonitrile **60** to produce the corresponding 2-trifluoromethyl-pyrrolidines - was not productive. Although the target compounds **61(a,b)** were detected in the reaction mixture by NMR and GC-MS, the isolated yield was too low (1%). This might be caused by the high reactivity of the carbonyl group in **57**, therefore reaction takes place with any of the nucleophiles present in the reaction mixture. The present hypothesis was proven by isolation of **62** along with **61(a,b)** (Scheme 4.10).



*Scheme 4.10.* Synthesis of **61(a,b)** and **62**.

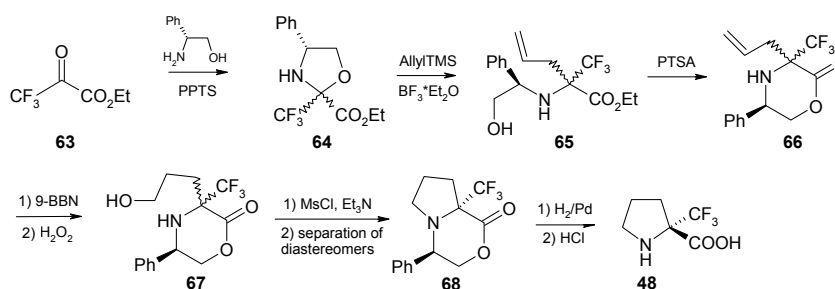
Unfortunately, the proposed synthetic strategies to **48** (Scheme 4.1, Scheme 4.3) could not be realized, since the selected key reactions either led to unexpected products or produced low yields of the target compounds.\*

### 4.3. 3,4-(Trifluoromethylmethano)-prolines

#### 4.3.1. Planning the synthesis of 3,4-(trifluoromethylmethano)-prolines

To design the synthesis of **49** rationally, the synthetic methods to already known compounds **69**,<sup>175,176</sup> **70**,<sup>177</sup> **71**,<sup>178,179</sup> resembling the structure of **49** closely, (Fig. 4.6) were analyzed.

\* While this work was in progress, the publication “Chaume G., Van Severen M. C., Marinkovich S., Brigaud T. Straightforward synthesis of (*S*)- and (*R*)- $\alpha$ -trifluoromethyl proline from chiral oxazolidines derived from ethyl trifluoropyruvate // *Org. Lett.* - 2006. - V. 8. - P. 6123-6126” appeared.



The authors reported the synthesis of (*S*)-**48** in 6 steps from ethyl 3,3,3-trifluoropyruvate **63**. Notably, compounds **64-67** were mixtures of diastereomers, which were separated only at the stage of the product **68**.

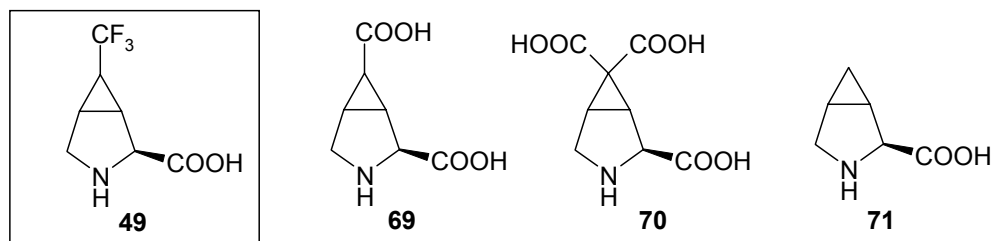
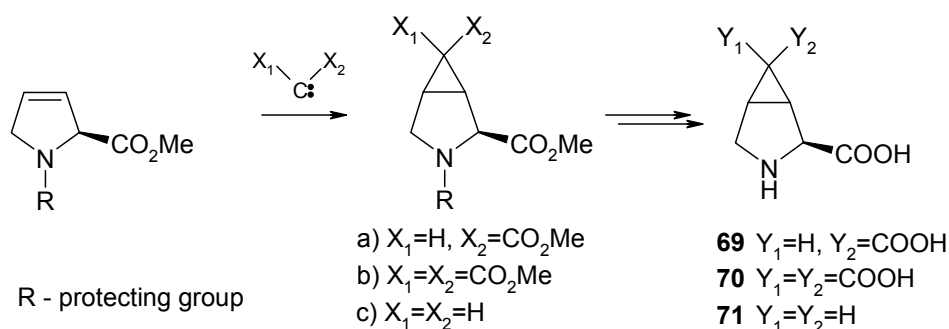


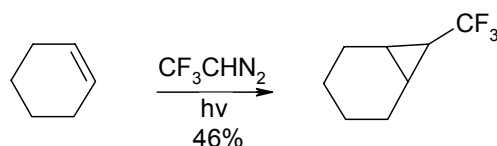
**Fig. 4.6.** 3,4-(Trifluoromethylmethano)-proline (**49**) and known compounds with related structures (**69**, **70**, **71**).<sup>175-179</sup>

There are different strategies to **69**, **70**, **71** reported in the literature, but one approach, among others, is the same for all compounds. It relies on the addition of the corresponding carbenes to protected derivatives of 3,4-dehydroproline (Scheme 4.11).

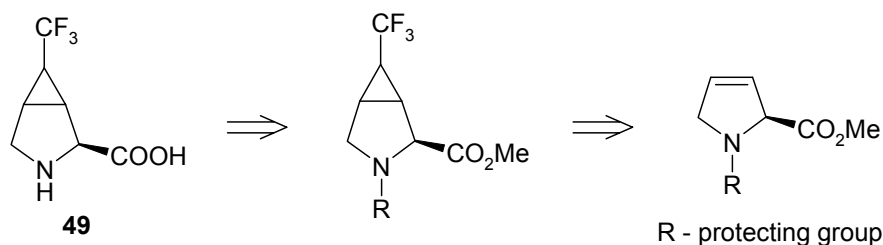


**Scheme 4.11.** Known syntheses of **69-71**.<sup>176-177</sup>

Knowing that the photolytic addition of  $CF_3CHN_2$  to alkenes is feasible (Scheme 4.12),<sup>180,181,182</sup> a key step in the retrosynthetic scheme of **49** was suggested to be based on photochemical trifluoromethylcyclopropanation of protected 3,4-dehydroproline (Scheme 4.13).



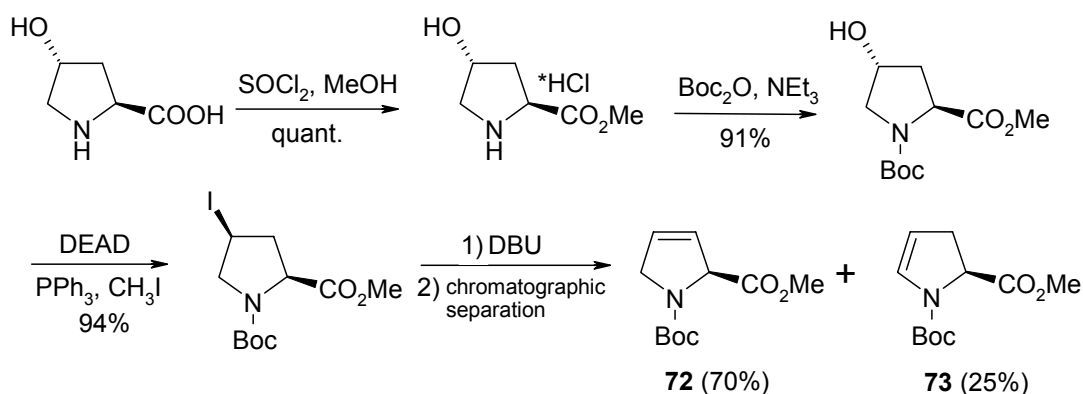
**Scheme 4.12.** Known example of the photolytic reaction between  $CF_3CHN_2$  and alkenes.<sup>180</sup>



**Scheme 4.13.** Retrosynthetic analysis of **49**.

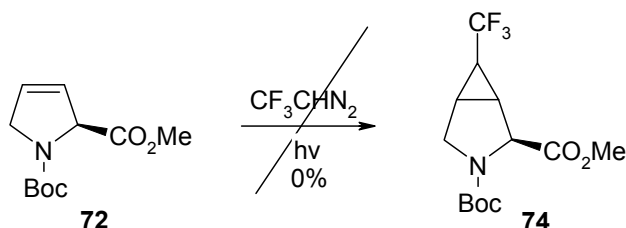
### 4.3.2. Photochemical addition of $CF_3CHN_2$ to 3,4-dehydroproline derivative

The starting alkene **72** was synthesized from commercially available 4-hydroxyproline according to the literature procedure (Scheme 4.14).<sup>183</sup>



**Scheme 4.14.** Synthesis of **72**.<sup>183</sup>

The crucial step in the synthesis of **49** - photochemical decomposition of  $CF_3CHN_2$  and subsequent addition of  $CF_3CH:$  to the C=C double bond of **72** - was not productive. Even after irradiation of the reaction mixture during 1 month, the formation of **74** was not observed (Scheme 4.15).

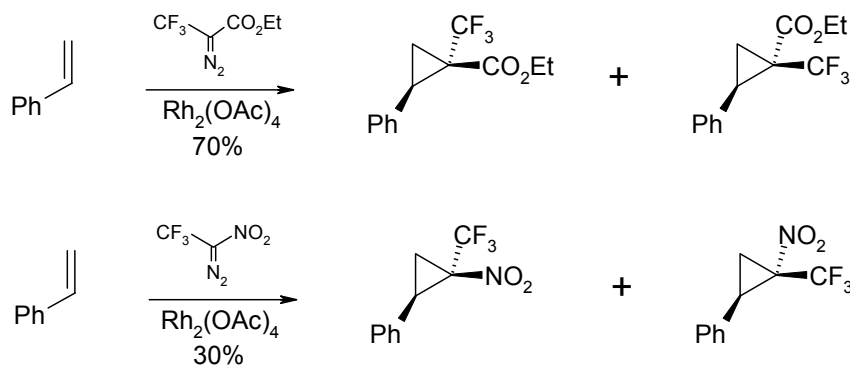


**Scheme 4.15.** Photolytic reaction between  $CF_3CHN_2$  and **72** does not lead to **74**.

Due to zero yield of **74**, the procedure of trifluoromethylcyclopropanation of alkenes was modified.

### 4.3.3. Modification of the procedure of trifluoromethylcyclopropanation of alkenes

Often, cyclopropanation of C=C double bonds utilizes metallocatalysis.<sup>184,185</sup> The most common catalyst in these reactions is  $Rh_2(OAc)_4$ ,<sup>186</sup> although for asymmetric cyclopropanation rhodium catalysts bearing chiral ligands can be used.<sup>187,188</sup> Syntheses of  $CF_3$ -substituted cyclopropane derivatives by addition of the corresponding  $CF_3$ -substituted carbenes to double C=C bonds are also known (Scheme 4.16).<sup>189-194</sup>



**Scheme 4.16.** Some known examples of trifluoromethylcyclopropanation of alkenes catalyzed by  $\text{Rh}_2(\text{OAc})_4$ .<sup>189,193</sup>

Surprisingly, there was no information in the literature concerning the use of metallocatalysts while working with  $\text{CF}_3\text{CHN}_2$ . Therefore, to test the feasibility of this method, a set of alkenes with different types of  $\text{C}=\text{C}$  double bonds was systematically examined (Fig. 4.7).

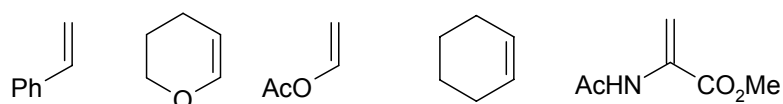
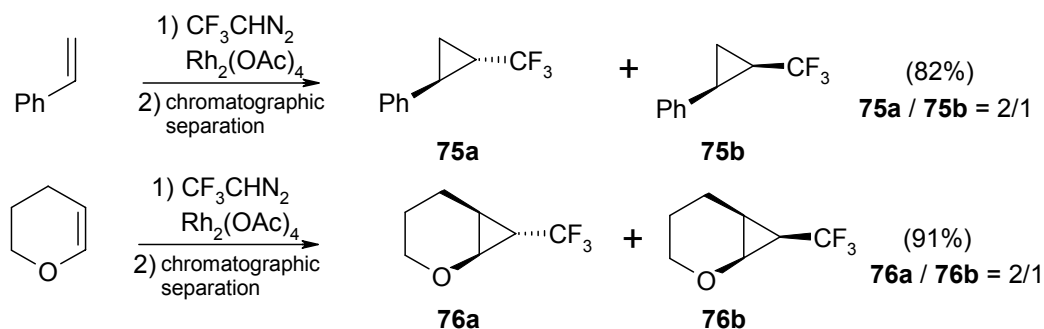


**Fig. 4.7.** Model alkenes selected for trifluoromethylcyclopropanation by  $\text{CF}_3\text{CHN}_2$  in the presence of metal catalysts.

Styrene and 3,4-dihydropyran, possessing activated  $\text{C}=\text{C}$  bonds, indeed reacted with  $\text{CF}_3\text{CHN}_2$  in the presence of  $\text{Rh}_2(\text{OAc})_4$ . The products ( $\pm$ )**75(a,b)** and ( $\pm$ )**76(a,b)** were isolated by distillation, isomers *cis*-(**75b**, **76b**) and *trans*-(**75a**, **76a**) being separated by flash column chromatography (Scheme 4.17).



**Scheme 4.17.** Syntheses of ( $\pm$ )**75(a,b)** and ( $\pm$ )**76(a,b)**.

The determination of the relative configuration of separated isomers was based on the rule that in cyclopropane derivatives the  $^3J_{\text{cis}}(\text{H}, \text{H})$ -constant is always larger than the  $^3J_{\text{trans}}(\text{H}, \text{H})$ -constant.<sup>195</sup> In the  $^1\text{H-NMR}$  spectrum of ( $\pm$ )**75a**, the benzylic proton has one  $^3J_{\text{cis}}(\text{H}, \text{H}) = 9.3$  Hz and two  $^3J_{\text{trans}}(\text{H}, \text{H}) = 5.6$  Hz constants, therefore the configuration of ( $\pm$ )**75a** is *trans* (Fig. 4.8). The benzylic proton of the *cis*-isomer ( $\pm$ )**75b** has, on the contrary, one  $^3J_{\text{trans}}(\text{H}, \text{H}) = 8.0$  Hz and two  $^3J_{\text{cis}}(\text{H}, \text{H}) = 8.4$  Hz constants (Fig. 4.8).

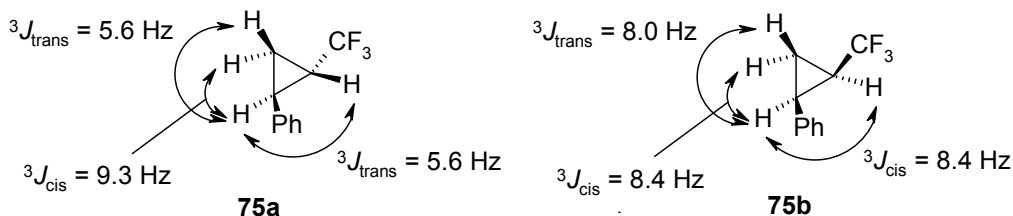


**Fig. 4.8.** Analysis of the  $^3J(\text{H}, \text{H})$ -constants in cyclopropane fragments of **75a** and **75b**.

The same is true for ( $\pm$ )**76(a,b)**. The  $^1\text{H}$ -NMR spectrum of ( $\pm$ )**76a** shows for the proton at C(1)  $^3J_{\text{cis}}(\text{H}, \text{H}) = 7.6 \text{ Hz}$  and  $^3J_{\text{trans}}(\text{H}, \text{H}) = 2.0 \text{ Hz}$ , which undoubtedly assigns this isomer to be *trans*. Obviously, **76b** is in this case the *cis*-isomer.

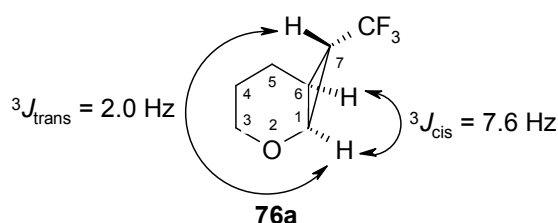
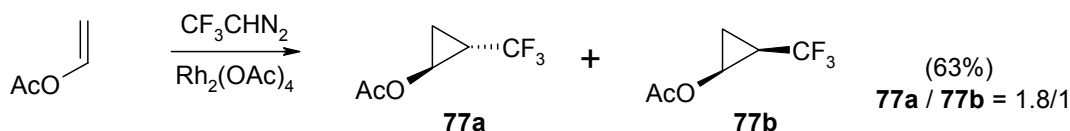


**Fig. 4.9.** Analysis of the  $^3J(\text{H}, \text{H})$ -constants in the cyclopropane fragment of **76a**.

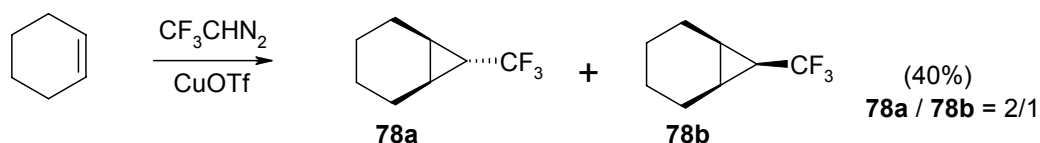
The evaluation of the relative configurations of ( $\pm$ )**75(a,b)** and ( $\pm$ )**76(a,b)** was in full accordance with the formation of the less sterically constrained *trans*-isomers as the major reaction products: **75a/75b** = 2/1 and **76a/76b** = 2/1.

In the case of vinylacetate the reaction proceeded as well, however, the products ( $\pm$ )**77(a,b)** could not be separated due to their high volatility (Scheme 4.18).



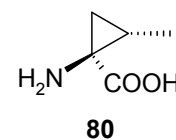
**Scheme 4.18.** Synthesis of ( $\pm$ )**77(a,b)**.

The cyclopropanation of cyclohexene was not productive with  $\text{Rh}_2(\text{OAc})_4$ , but the cyclopropanes ( $\pm$ )**78(a,b)** were obtained with a moderate yield (40%) using  $\text{CuOTf}^{196,197}$  as a catalyst (Scheme 4.19). The high volatility of isomers ( $\pm$ )**78(a,b)** hindered their separation, like in ( $\pm$ )**77(a,b)**.

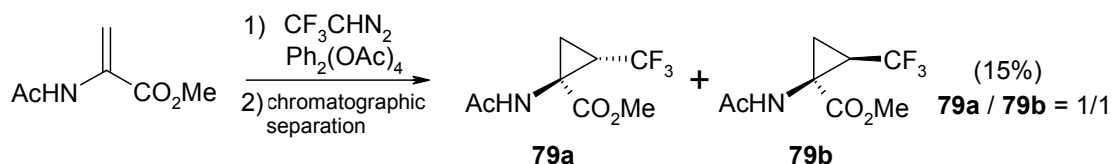


**Scheme 4.19.** Synthesis of ( $\pm$ )**78(a,b)**.

To demonstrate the practical suitability of the present approach, both diastereoisomers of trifluoronorcoronamic acid - analogues of naturally occurring norcoronamic acid **80**, which is a building block of the toxin norcoronatine from *Pseudomonas syringae*, were synthesized.<sup>198</sup>

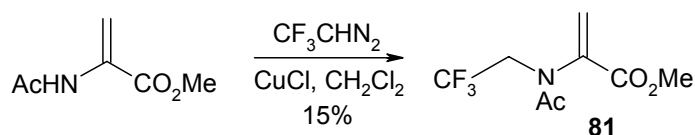


Cyclopropanation of the corresponding derivative of methyl acrylate<sup>199</sup> in the presence of  $\text{Rh}_2(\text{OAc})_4$  led to the desired products ( $\pm$ )**79(a,b)** (Scheme 4.20).



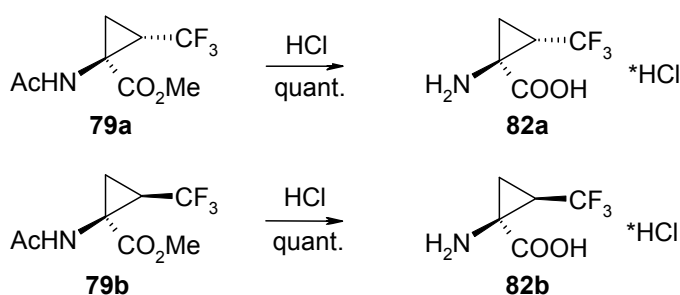
**Scheme 4.20.** Synthesis of ( $\pm$ )**79(a,b)**.

Notably, the choice of catalyst was crucial in this transformation, as the use of  $\text{CuCl}$  yielded compound **81** as the major reaction product (Scheme 4.21).



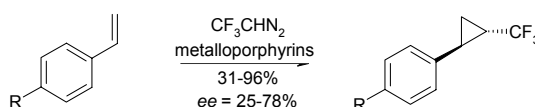
**Scheme 4.21.** Synthesis of **81**.

Treating ( $\pm$ )**79a** in 20%  $\text{HCl}$  at 80 °C for 30 h afforded the amino acid ( $\pm$ )**82a**, with spectral characteristics identical to those described previously for the *trans*-trifluoronorcoronamic acid.<sup>200</sup> The *cis*-trifluoronorcoronamic acid ( $\pm$ )**82b** was obtained from ( $\pm$ )**79b** following the same procedure (Scheme 4.22).\*



**Scheme 4.22.** Synthesis of ( $\pm$ )**82(a,b)**.

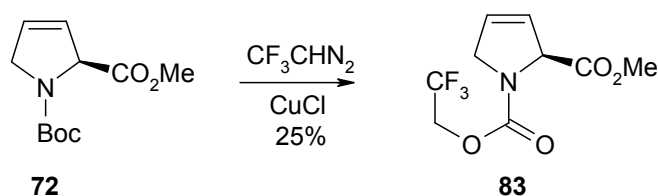
\* As the present work was in progress the publication describing first example of catalytic trifluoromethylcarbene generation and its stereoselective addition to styrene derivatives appeared: *Le Maux P., Juillard S., Simonneaux G.* Asymmetric synthesis of trifluoromethylphenyl cyclopropanes catalyzed by chiral metalloporphyrins // *Synthesis*. - 2006. - Vol. 10. - P. 1701-1704.



Notably, the authors observed a formation of exclusively *trans*-cyclopropane products.

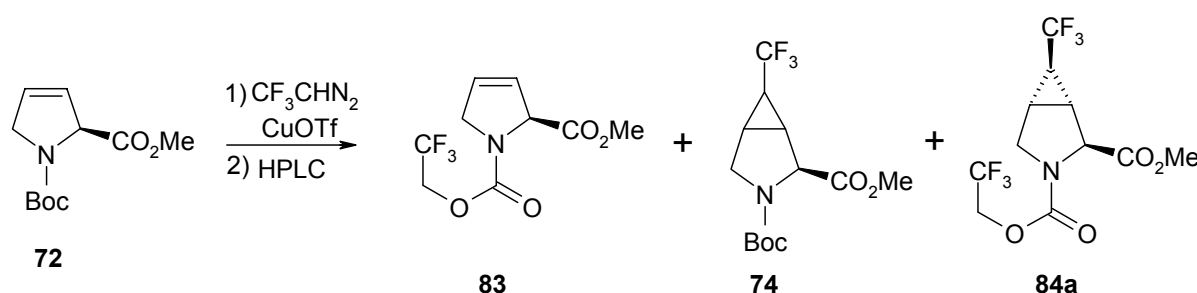
#### 4.3.4. Synthesis of 3,4-(trifluoromethylmethano)-prolines

Since the procedure of CF<sub>3</sub>-cyclopropanation of alkenes was demonstrated to be successful, this reaction was applied for the synthesis of **49(a,b)**. However, the transformation of **72** was found to be rather dependent on the catalyst nature. For example, in the presence of CuCl or Rh<sub>2</sub>(OAc)<sub>4</sub>, compound **83** was the main reaction product (Scheme 4.23).



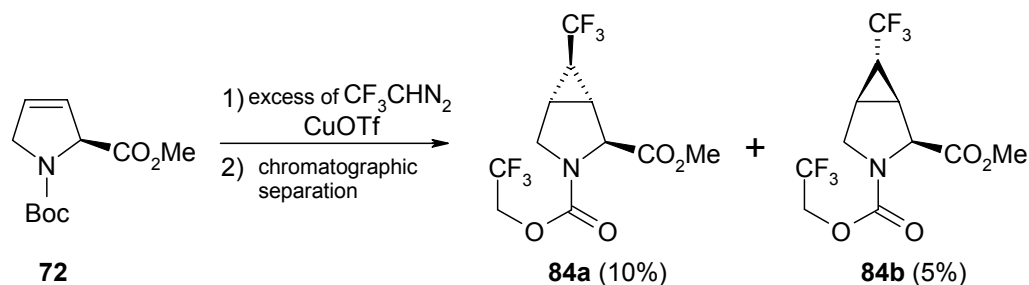
**Scheme 4.23.** Synthesis of **83**.

In the presence of CuOTf, however, a complex mixture was observed, from which compounds **74**, **83** and **84a** were isolated by HPLC (Scheme 4.24). Obviously,



**Scheme 4.24.** Reaction between **72** and CF<sub>3</sub>CHN<sub>2</sub> catalyzed by CuOTf.

in contrast to CuCl and Rh<sub>2</sub>(OAc)<sub>4</sub>, the use of CuOTf increased the reactivity of the C=C bond towards CF<sub>3</sub>CH<sub>2</sub>·, however, the reaction with Boc-group still took place. To circumvent this problem an excess of CF<sub>3</sub>CHN<sub>2</sub> was used, which allowed to obtain the target products **84(a,b)** in 15% yield (Scheme 4.25).

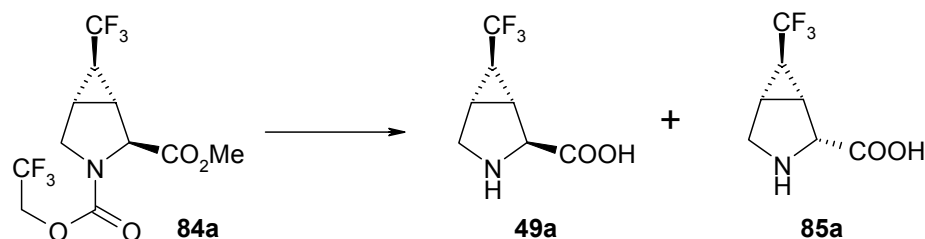


**Scheme 4.25.** Synthesis of **84(a,b)**.

Since the cleavage of the CF<sub>3</sub>CH<sub>2</sub>OCO-group from a nitrogen atom has not yet been described in the literature, a lot of experimentation was needed to find optimal conditions for this transformation. Hydrolysis under basic conditions was tried first.

Unfortunately, together with the cleavage of CF<sub>3</sub>CH<sub>2</sub>OCO-group, an extensive epimerization at C<sub>α</sub> occurred as well (Table 4.1).

**Table 4.1.** Cleavage of the carbamate group of **84a** under basic conditions.



N <sup>o</sup>	reagent	quantity (eq.)	t (°C)	time (h)	conversion (%)*	49a/85a
1.	NaOH (H <sub>2</sub> O-THF)	4	25	20	0	-
2.	NaOH (H <sub>2</sub> O-THF)	4	80	10	80	5/1
3.	NaOH (H <sub>2</sub> O-THF)	4	80	20	100	4/1
4.	NaOH (H <sub>2</sub> O-THF)	3	80	10	60	6/1
5.	NaOH (H <sub>2</sub> O-MeOH)	4	80	10	70	3/1/1( <b>86</b> )

\* according to <sup>19</sup>F-NMR.

Notably, while carrying out the hydrolysis of **84a** in an H<sub>2</sub>O-MeOH mixture together with **49a/85a**, a considerable amount of **86** formed as well (Table 3.1, N<sup>o</sup> 5). In order to reduce formation of the epimerized product **85a**, while retaining a high reaction conversion, an acidic hydrolysis was tried next (Table 4.2).

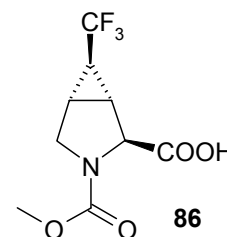


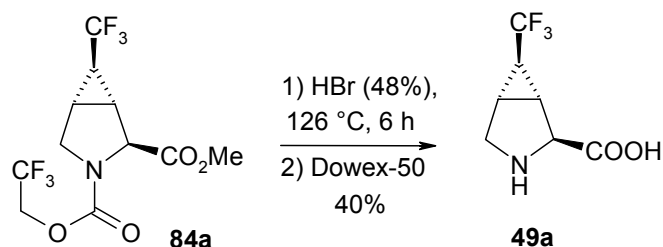
**Table 4.2.** Cleavage of carbamate group of **84a** under acidic conditions.

N <sup>o</sup>	reagent	quantity (eq.)	t (°C)	time (h)	conversion (%)*	49a/85a
1.	HCl (36 %, H <sub>2</sub> O)	excess	25	20	0	-
2.	HCl (36 %, H <sub>2</sub> O)	excess	110	20	0	-
3.	HBr (48 %, H <sub>2</sub> O)	excess	25	20	0	-
4.	HBr (48 %, H <sub>2</sub> O)	excess	126	10	95	5/1
5.	HBr (48 %, H <sub>2</sub> O)	excess	126	8	93	7/1
6.	HBr (48 %, H <sub>2</sub> O)	excess	126	6	90	9/1
7.	HBr (48 %, H <sub>2</sub> O)	excess	126	4	70	11/1

\* according to <sup>19</sup>F-NMR.

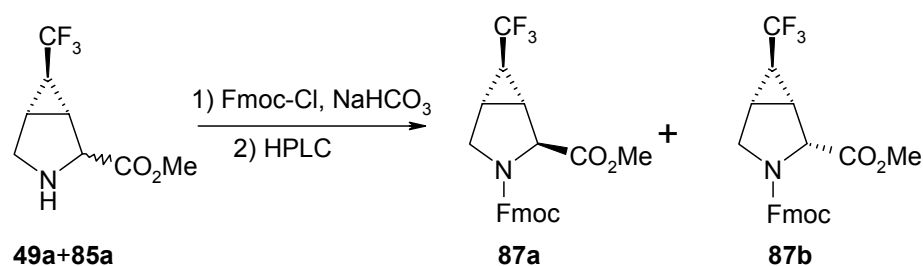
The best result was observed while performing hydrolysis in 48% aq. HBr for 6 h (Table 3.2, N<sup>o</sup> 6). After purification of the reaction mixture on Dowex-50, two fractions were obtained. Amino acid **49a** was isolated from the first one with a yield of 40% and purity of 90% (Scheme 4.26). The second fraction, containing a





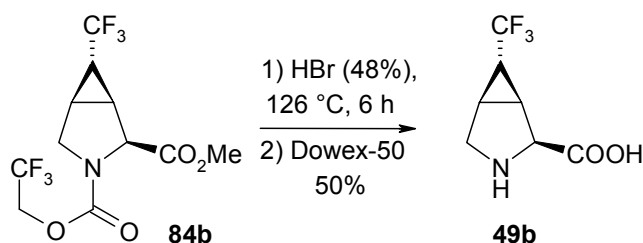
**Scheme 4.26.** Synthesis of **49a**.

considerable amount of **85a**, was converted into the corresponding Fmoc-derivatives **87(a,b)**, which were separated by HPLC (Scheme 4.27).



**Scheme 4.27.** Synthesis of **87(a,b)**.

Interestingly, under the conditions identical to those used for hydrolysis of **84a**, isomer **84b** afforded pure **49b** (Scheme 4.28).



**Scheme 4.28.** Synthesis of **49b**.

#### 4.3.5. Evaluation of stereoconfiguration of the synthesized amino acids

The formation of four stereoisomers of **49**, possessing an (*S*)-configuration at the aminocarboxylate moiety, is theoretically possible (Fig. 4.10).

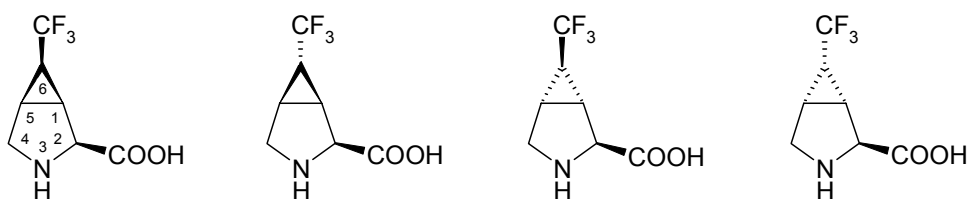


**Fig. 4.10.** Theoretically possible isomers of **49** with (*S*)-configuration at C(2).

First, the configuration at the C(1) and C(5) atoms in the cyclopropane rings of **49(a,b)** was established. For this the  $^1\text{H-NMR}$  spectra of **49(a,b)** and the known structurally related amino acids **88**, **89**, **71a**, **71b** (Fig. 4.11) were compared.<sup>176,178,179</sup>

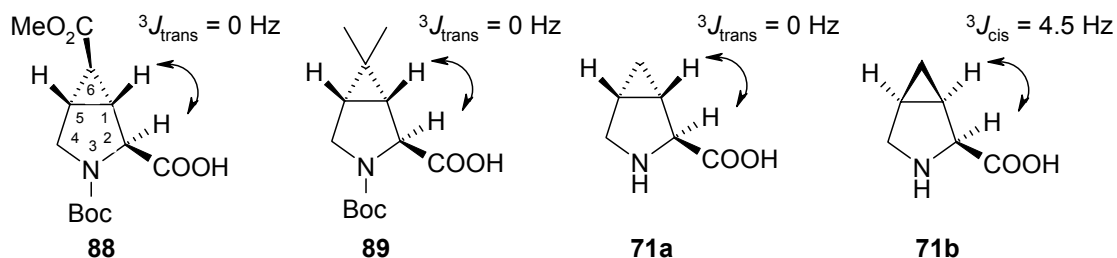


**Fig. 4.11.** Compounds **88**, **89**, **71(a,b)** and corresponding  $^3J(\text{H}, \text{H})$ -constants between protons at C(2) and C(1).<sup>176,178,179</sup>

In the  $^1\text{H-NMR}$  spectra of three *trans*-methanoprolines **88**, **89**, **71a** the signal of the proton at C(2) is either singlet (**71a**) or pair of singlets (two rotamers are observed for **88**, **89**). In contrast, in the  $^1\text{H-NMR}$  spectrum of the *cis*-isomer **71b** the same proton is a doublet ( $^3J(\text{H}, \text{H}) = 4.5 \text{ Hz}$ ). In the  $^1\text{H-NMR}$  spectrum of **49a** the proton at C(2) is a singlet, but in **49b** a doublet with  $^3J(\text{H}, \text{H}) = 4.4 \text{ Hz}$ . This confirms that **49a** possesses the cyclopropane fragment in *trans*-configuration with respect to the COOH-group, while **49b** in *cis*-configuration (Fig. 4.12).

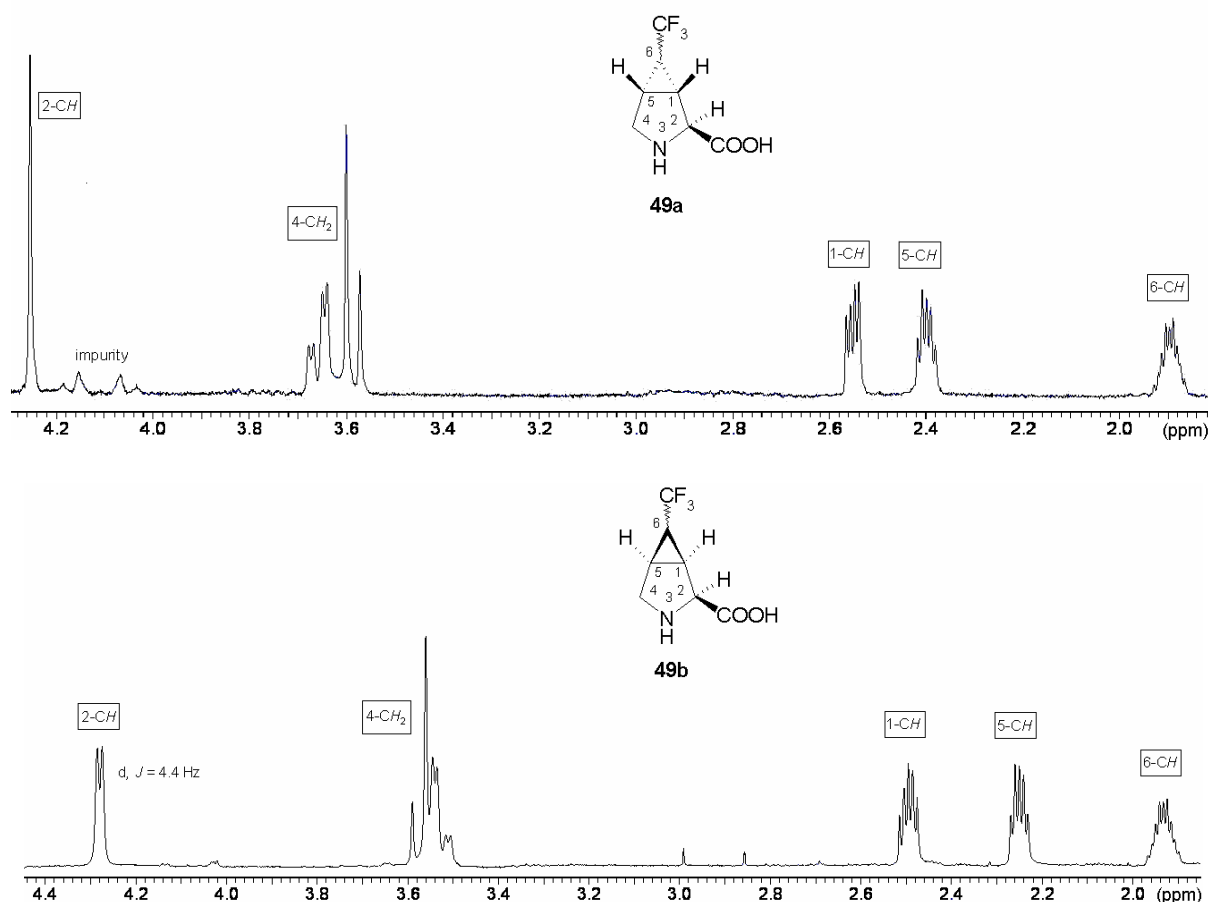


**Fig. 4.12.**  $^1\text{H-NMR}$  spectra of **49a** and **49b** and assignment of the observed signals.

Next question to be answered was the configuration at C(6) in **49(a,b)**. As it was mentioned earlier (Chapter 4.3.3) in cyclopropane derivatives  ${}^3J_{cis}(\text{H}, \text{H})$ -constant is larger than the corresponding  ${}^3J_{trans}(\text{H}, \text{H})$ -constant. For both isomers **49(a,b)** two types of coupling constants are seen (Fig. 4.13).

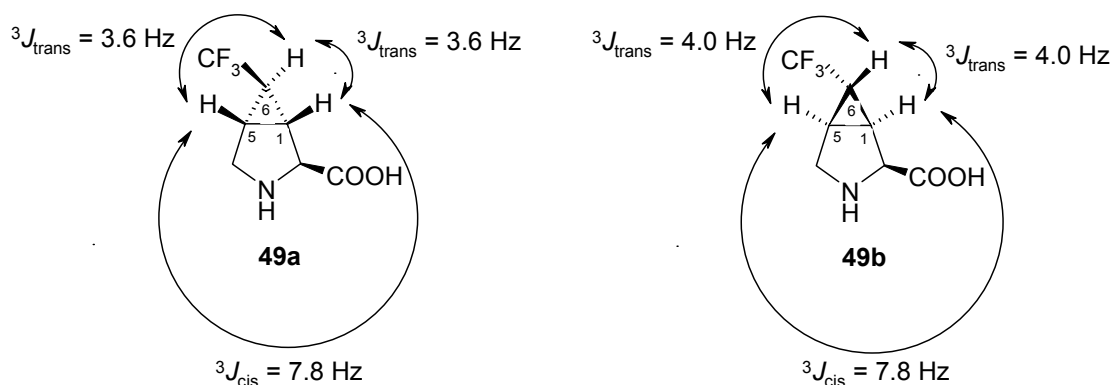


**Fig. 4.13.** Analysis of the  ${}^3J(\text{H}, \text{H})$ -constants in the cyclopropane ring of both **49a** and **49b**.

This observation suggests that in **49(a,b)** the proton at C(6) has an *anti*-orientation relative to the protons at C(1) and C(5). For the isomer **49b** this assumption was readily confirmed by an NOE between the protons at C(4) and C(6) (Fig. 4.14). Although in **49a** the analogous correlations were not detected, they were found in the NOESY-spectrum of **87a** (Fig. 4.14).

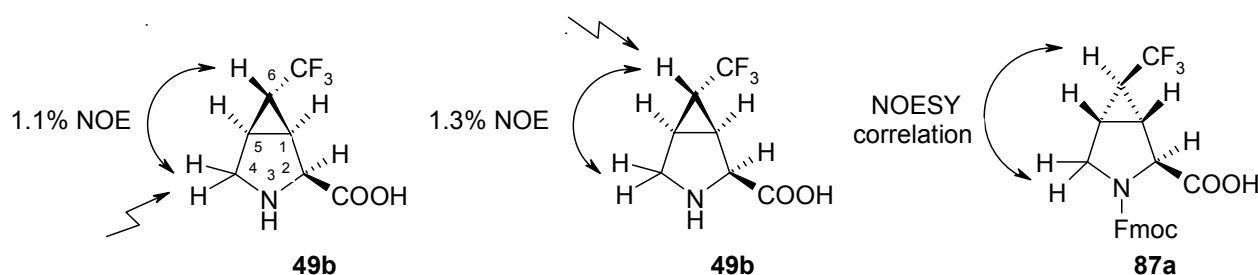


**Fig. 4.14.** The Nuclear Overhauser Effect (NOE) between protons at C(4) and C(6) in **49b**, and the NOESY correlation between protons at C(6) and C(4) in **87a** confirm the stereoconfiguration of these compounds.

#### 4.4. 4,5-(Trifluoromethylmethano)-prolines

##### 4.4.1. Planning the synthesis of 4,5-(trifluoromethylmethano)-prolines

To plan the synthesis of **50** rationally, synthetic methods to the known structurally related amino acids **90**<sup>201,202</sup> and **91a, 91b**<sup>203,204</sup> (Fig. 4.15) were analyzed first.

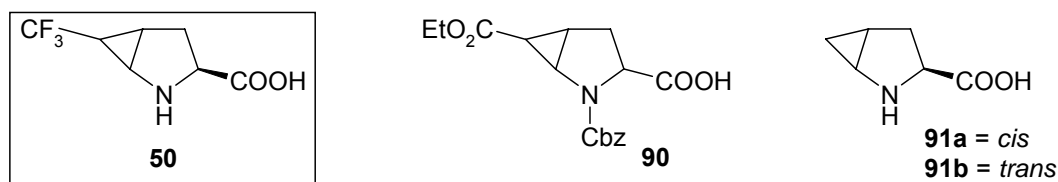
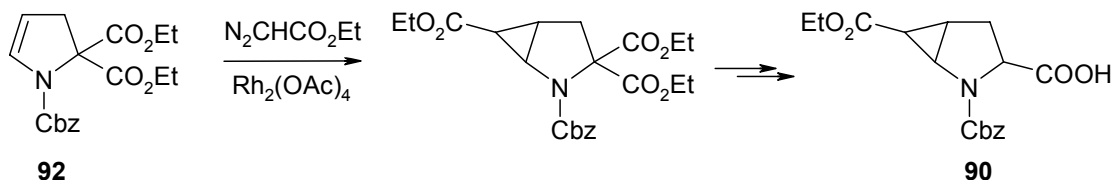


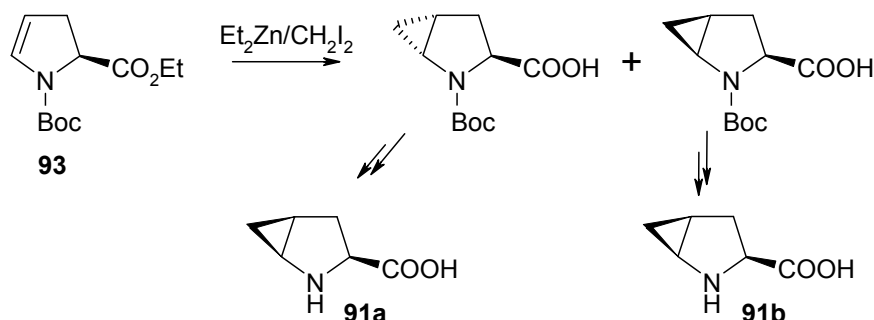
**Fig. 4.15.** 4,5-(Trifluoromethylmethano)-proline (**50**) and known compounds with similar structure (**90**, **91a**, **91b**).<sup>201-204</sup>

The key step in the synthesis of **90** is cyclopropanation of **92** with ethyldiazoacetate in the presence of  $\text{Rh}_2(\text{OAc})_4$  (Scheme 4.29).



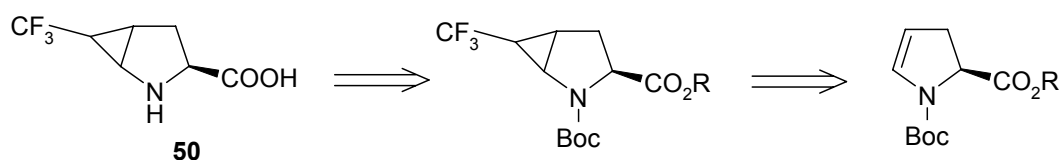
**Scheme 4.29.** Synthesis of the known compound **90**.<sup>201,202</sup>

Concerning the synthesis of 4,5-methanoprolines **91(a,b)**, one approach among others relies on the cyclopropanation of the unsaturated substrate **93** using Simmons-Smith reaction (Scheme 4.30).<sup>203</sup>



**Scheme 4.30.** Known synthesis of the compounds **91(a,b)**.<sup>203</sup>

Both transformations described above are based on cyclopropanation; following them in the synthesis of **50** it was decided to use trifluoromethylcyclopropanation as well (Scheme 4.31).

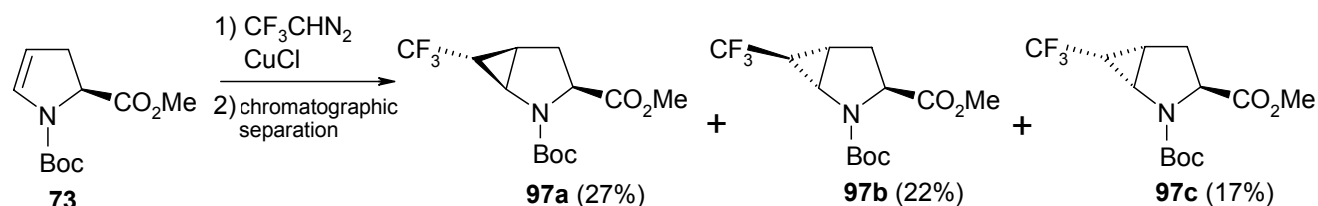


**Scheme 4.31.** Retrosynthetic analysis of **50**.

#### 4.4.2. Synthesis of 4,5-(trifluoromethylmethano)-prolines

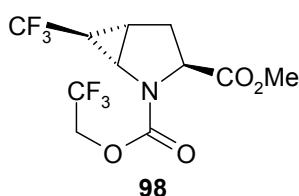
The starting compound **73** was obtained as a side product in the synthesis of **49(a,b)** (Scheme 4.14). Addition of  $\text{CF}_3\text{CH}:$  to the  $\text{C}=\text{C}$  double bond in **73** occurred rather fast, independently on the catalyst ( $\text{CuCl}$ ,  $\text{Rh}_2(\text{OAc})_4$  or  $\text{CuOTf}$ ), in contrast to the analogous reaction of **72** (Chapter 4.3.4). Apparently, this difference is a consequence of the presence of the N-Boc group directly at the double bond in **73**.

The best results were obtained using the less active catalyst  $\text{CuCl}$ , since in the presence of  $\text{Rh}_2(\text{OAc})_4$  or  $\text{CuOTf}$  an extensive formation of unidentified side products was observed. Using  $^1\text{H}$ - and  $^{19}\text{F}$ -NMR for reaction monitoring, the process was stopped after the disappearance of the signals from the starting material **73**, which allowed to obtain only the target products **97(a,b,c)** (Scheme 4.32).

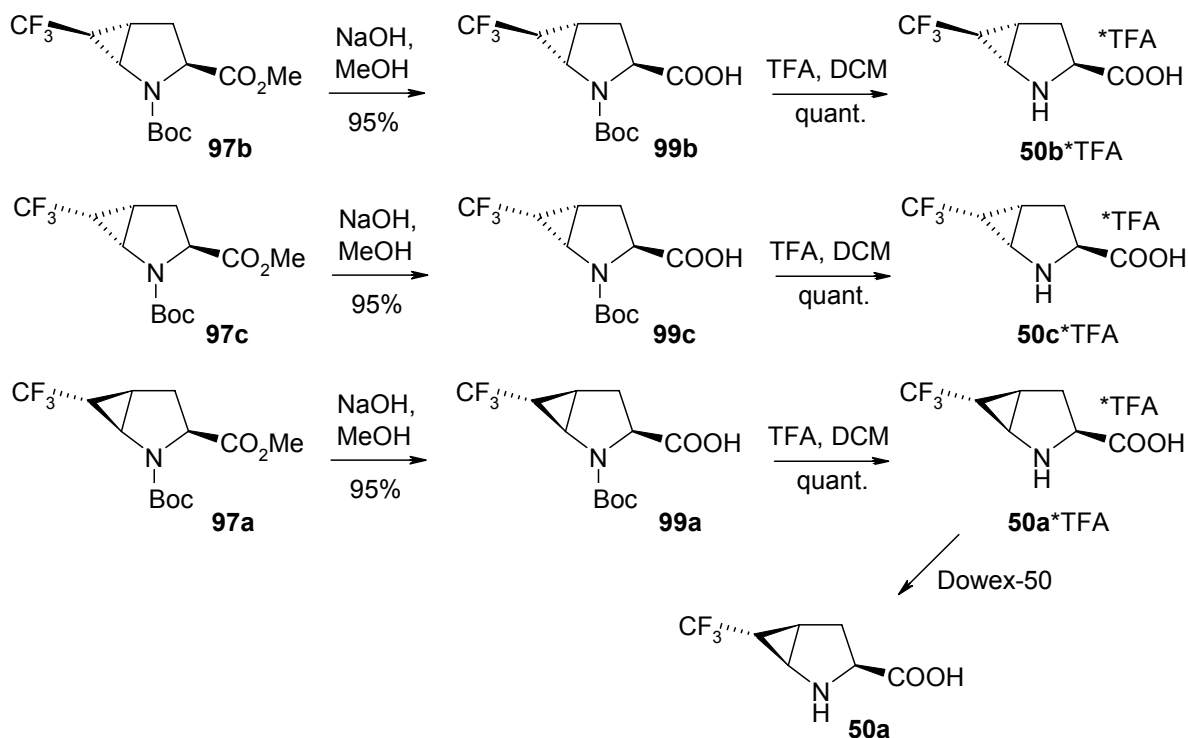


*Scheme 4.32.* Synthesis of **97(a,b,c)**.

By using an excess of  $\text{CF}_3\text{CHN}_2$ , however, the formation of a rather complex mixture was observed, from which, along with **97(a,b,c)**, compound **98** was isolated as well:

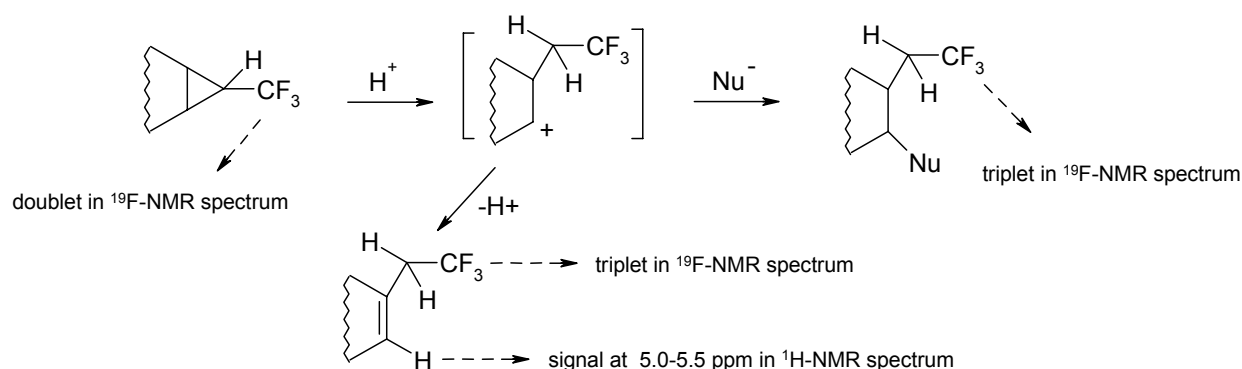


The last steps of the synthesis were rather trivial: basic hydrolysis of  $\text{CO}_2\text{Me}$ -groups followed by cleavage of Boc-groups ( $\text{TFA}/\text{CH}_2\text{Cl}_2$ ) led to the formation of the target amino acids **50 (a,b,c)\*TFA** (Scheme 4.33).



**Scheme 4.33.** Synthesis of **50(b,c)\*TFA** and **50a**.

Notably, while **50a\*TFA** was converted into its zwitterionic form **50a** by cation-exchange chromatography on Dowex-50 resin, two other isomers under the same conditions partially (**50b\*TFA**) or completely (**50c\*TFA**) decomposed. Unfortunately, the products of decomposition were not isolated, however, typical triplets in  $^{19}\text{F}$ -NMR spectra and signals at 5.0-5.5 ppm in  $^1\text{H}$ -NMR spectra indicated that cleavage of the cyclopropane ring may have happened (Scheme 4.34).



**Scheme 4.34.** Suggested mechanism and NMR evidence for cleavage of the cyclopropane ring in **50(b,c)** under acidic conditions.

Interestingly, while in the  $^{13}\text{C}$ -NMR spectra of both **50(a,b)\*TFA** the signal of  $\text{C}_\alpha$  is a singlet, in **50c\*TFA** the same carbon produces a quadruplet. This is a result of coupling to fluorine atoms, the interaction occurring through five bonds with  $^5J(\text{C}, \text{F}) = 4 \text{ Hz}$  (Fig. 4.16).

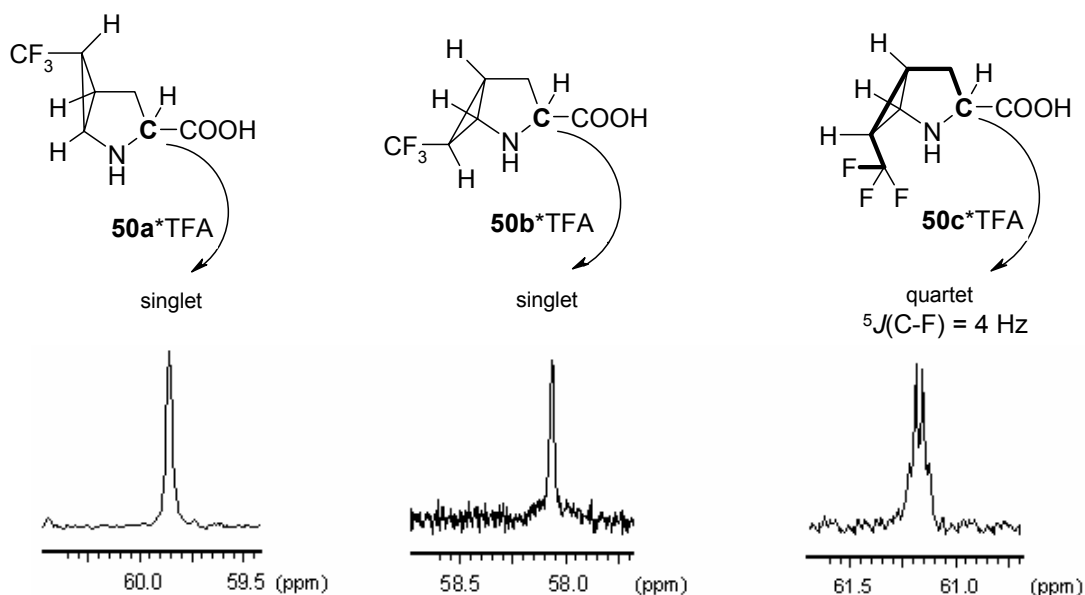


**Fig. 4.16.** Signal of  $C_\alpha$  in the  $^{13}\text{C}$ -NMR spectra of **50(a,b,c)**\*TFA.

#### 4.4.3. Evaluation of the stereoconfiguration of the synthesized compounds

The formation of four stereoisomers of **50**, possessing the (*S*)-configuration at the aminocarboxylate moiety, is theoretically possible (Fig. 4.17).

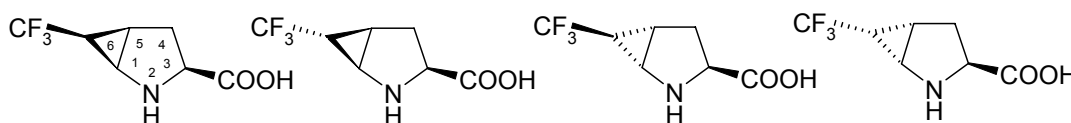


**Fig. 4.17.** Theoretically possible isomers **50** with (*S*)-configuration at C(3).

The major experimental evidence proving a configuration of the stereocenters in **50a** is the presence of a cross-peak between 6-H and 4- $H_a$  in the NOESY spectrum. These protons can be in spatial proximity in only one case out of four (Fig. 4.18).

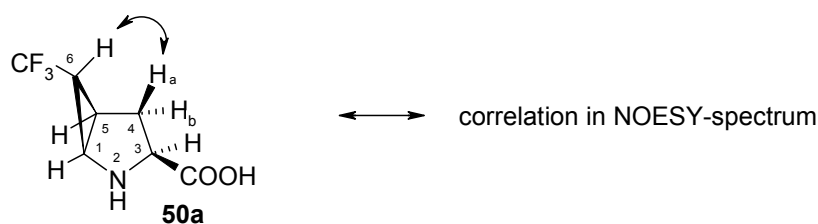


**Fig. 4.18.** NOESY correlation between protons 4- $H_a$  and 6-H in **50a** determines the stereoconfiguration of this compound.

Structure assignment of **50b** was carried out on its precursor **99b**. The NOESY correlations in **99b** undoubtedly prove its structure (Fig. 4.19).

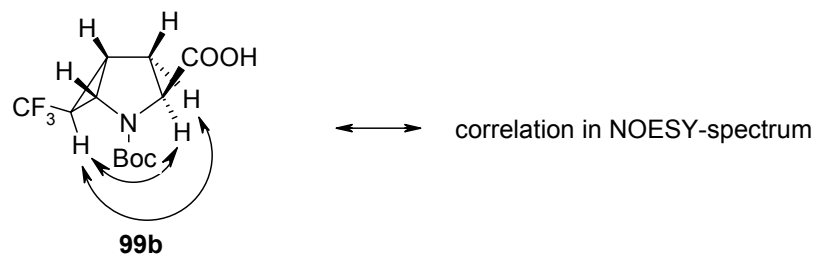


Fig. 4.19. Key NOESY correlations in **99b**.

The established structure was additionally confirmed by X-ray analysis of the precursor **97b** (Fig. 4.20).<sup>205</sup>

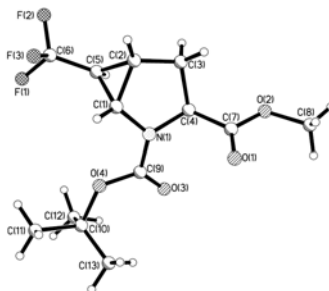


Fig. 4.20. Molecular structure of **97b**.

Determination of the relative configuration of the stereocenters in **50c** was also performed on its precursor **99c**. In the NOESY spectrum of **99c** the area of correlation peak between 4-H<sub>a</sub> and 5-H is larger than that of the correlation between 4-H<sub>b</sub> and 5-H (Fig. 4.21). This proves that the protons 5-H and 4-H<sub>a</sub> are in a *syn*-orientation. Thus, **99c** possesses the same configuration of the cyclopropane ring with regard to the COOH group as its isomer **99b**. Apparently, **99c** differs from **99b** only by the configuration at C(6).

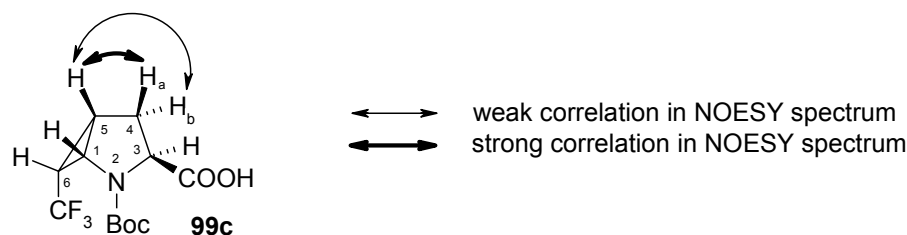


Fig. 4.21. Key NOESY correlations in **99c**.

The established structures of **50a** and **99(b,c)** are in full accordance with the observed NOESY-correlations of protons in their cyclopropane moieties (Fig. 4.22). In both **50a** and **99b**, the correlation peak between 1-H and 5-H (*syn*-protons) is larger than that between 1-H and 6-H (*anti*-protons). In contrast, in **99c** both correlations are of the same strength, due to the *syn*-arrangement of all three protons:



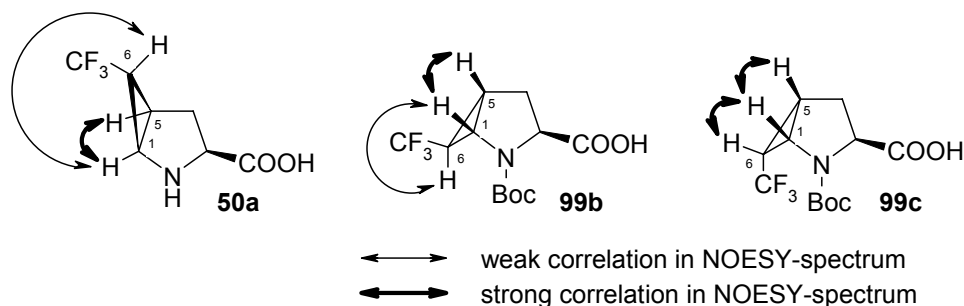


Fig. 4.22. NOESY correlations of protons in the cyclopropane rings of **50a**, **99b** and **99c**.

The proposed structures were additionally confirmed by the multiplicity of the proton at the respective C(1) in the  $^1\text{H-NMR}$  spectra of **50(a,b,c)\*TFA** (Fig. 4.23). In

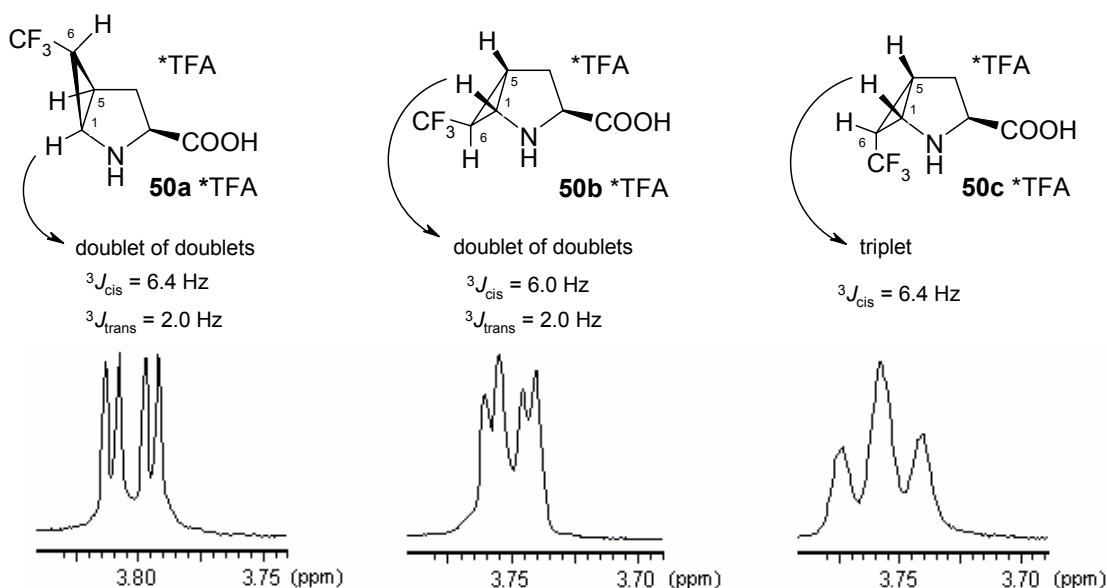


Fig. 4.23. Multiplicities of proton at C(1) and respective coupling constants in **50(a,b,c)\*TFA** are in full accordance with the established structures of these isomers.

**50a\*TFA**, the signal of the 1-H proton is a doublet of doublets ( $^3J_{\text{cis}} = 6.4 \text{ Hz}$ ,  $^3J_{\text{trans}} = 2.0 \text{ Hz}$ ), which is in accordance with an *anti*-orientation of 6-H with regard to 1-H and 5-H. In **50b\*TFA** the same situation is observed, the 1-H proton signal is a doublet of doublets ( $^3J_{\text{cis}} = 6.0 \text{ Hz}$ ,  $^3J_{\text{trans}} = 2.0 \text{ Hz}$ ). In contrast to **50(a,b)\*TFA**, in **50c\*TFA** the 1-H proton peak is a triplet with a characteristic constant  $^3J_{\text{cis}} = 6.0 \text{ Hz}$ , which again confirms that all the three cyclopropane protons are in a *syn*-configuration.

The structure of **98** was determined based on the correlations between protons 6-H and 3-H; 6-H and 4-H<sub>b</sub> in the NOESY spectrum (Fig. 4.24).

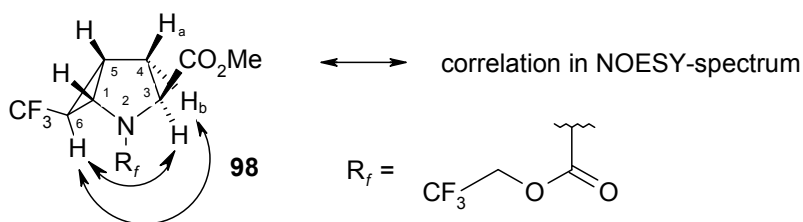


Fig. 4.24. Key NOESY correlations in **98**.

Later, the established structure was confirmed by X-ray analysis of **98** (Fig. 4.25).<sup>206</sup>

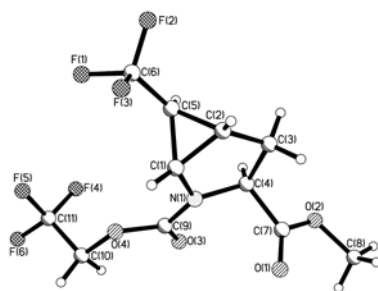


Fig. 4.25. Molecular structure of **98**.

#### 4.5. Selection of the optimal $^{19}\text{F}$ -NMR label ( $\text{CF}_3$ -MePro)

In principle, each isomer of the synthesized compounds **49** and **50** could be used as a  $^{19}\text{F}$ -label (Fig. 4.26). However, the amino acids **49(a,b)** are not that

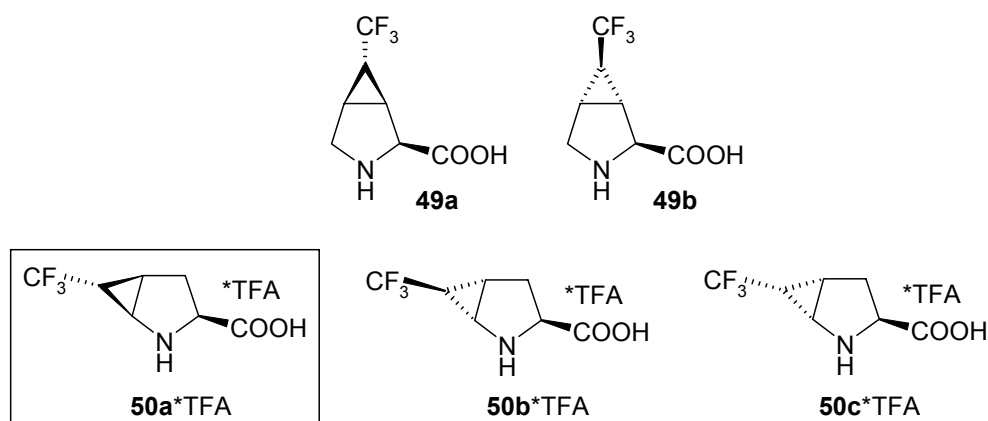


Fig. 4.26. Synthesized amino acids **49(a,b)** and **50(a,b,c)\*TFA** and the selected  $^{19}\text{F}$ -label **50a\*TFA**.

preferable, because of the poor total yield of their synthesis. The isomers **50(b,c)\*TFA** are not stable at low pH (as it became apparent during chromatography on Dowex-50), which may cause problems at the stage of peptide synthesis. In contrast, **50a\*TFA** ( $\text{CF}_3$ -MePro) is stable at both low and high pH, and was therefore selected as a  $^{19}\text{F}$ -label for substitution of Pro in peptides.

## PART 5

### APPLICATIONS OF THE SYNTHESIZED $^{19}\text{F}$ -NMR LABELS IN PEPTIDE STUDIES

In this part the practical application of the new  $^{19}\text{F}$ -labels **20** and **50a** is highlighted. First, to address the question about the utility of **20** in peptide studies, this label was incorporated into the structurally and functionally well characterized antimicrobial peptides: gramicidin S (GS) and peptidyl-glycylleucine-carboxyamide (PGLa). The synthesized  $^{19}\text{F}$ -labelled analogues of GS and PGLa were analyzed by antimicrobial assays, circular dichroism, and solid state  $^{19}\text{F}$ -NMR to assess the functional and structural influence of Val/**20**, Leu/**20**, Ile/**20**, Ala/**20** substitutions. It was demonstrated that **20** fulfills all the requirements for a proper label for solid state  $^{19}\text{F}$ -NMR of polypeptides. Initial structural studies of the cell-penetrating peptide “Sweet Arrow Peptide” (SAP) with an as yet unknown structure in the membrane bound state were then carried out using **20** and **51a** to validate the use of **51a** as a  $^{19}\text{F}$ -NMR label as well. Indeed, the potential of **51a** for being a proper structural label for substitution of Pro in polyproline type II helices (PP II) was shown.

The results described in this chapter have been described in the following manuscripts:

*Afonin S., Mykhailiuk P. K., Komarov I. V., Ulrich A. S.* Evaluating the use of  $\text{CF}_3$ -bicyclopentylglycine as a label for  $^{19}\text{F}$ -NMR structure analysis of membrane-bound peptides // *J. Pept. Sci.* - 2007. - Vol. 13. - P. 614-623;

*Mykhailiuk P. K., Afonin S., Palamarchuk G. V., Shishkin O. V., Ulrich A. S., Komarov I. V.* Synthesis of trifluoromethyl-substituted proline analogues - new  $^{19}\text{F}$ -NMR labels for peptides in polyproline II conformation // *Angew. Chem.* - 2008. - in press.

## 5.1. Antimicrobial peptide GS

### 5.1.1. General information about GS

GS is a natural cyclic decapeptide, containing the unusual amino acid ornithine (Orn) and the D-enantiomer of phenylalanine ( $^{\text{D}}\text{Phe}$ ) (Fig. 5.1).

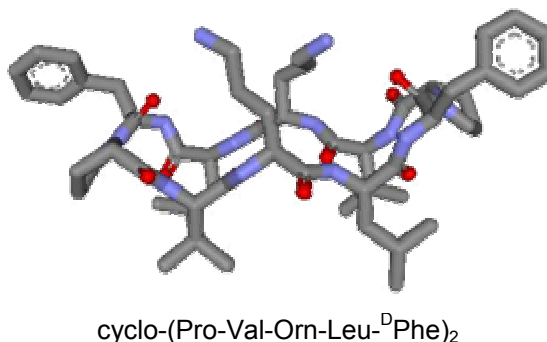


**Fig. 5.1.** Structural model and amino acid sequence of GS.

GS is produced by *A. migulanus* (formerly *B. brevis*) among other antimicrobial peptides via a non-ribosomal biosynthetic pathway.<sup>207,208</sup> The peptide exhibits a broad spectrum of antibiotic activity against both Gram-positive and Gram-negative bacteria, as well as against some fungi.<sup>209</sup> It also shows significant levels of hemolytic activity, which limits its medical use to topical applications.<sup>210</sup>

Structurally GS may be regarded as an anti-parallel  $\beta$ -sheet, flanked by two nearly ideal type-II  $\beta$ -turns, and stabilized by 4 intramolecular hydrogen bonds.<sup>211</sup> The positively charged Orn side-chains are positioned on one side of the cyclic plane, while the hydrophobic Val and Leu are on the opposite side, which gives rise to an amphipatic nature of GS.<sup>212</sup> The amphipaticity is considered to be a major feature responsible for the strong interaction of GS with lipid membranes. It should be mentioned that GS is a typical antimicrobial peptide in a sense that it does not require a specific receptor for its interaction with the target (i.e. with the bacterial membrane).<sup>213</sup>

### 5.1.2. Synthesis of $CF_3$ -labelled analogue of GS

GS contains two amino acids which potentially could be substituted by  $^{19}F$ -label **20** - Leu and Val. As **20** more closely resembles Leu than Val according to lipophilicity (Chapter 3.1), and since Leu was previously shown to be successfully substituted by both 4F-Phg (**3**) and 4 $CF_3$ -Phg (**4**) without major alterations in the GS structure and function,<sup>77,80</sup> this amino acid was chosen as a position to test the substitution (Fig. 5.2).

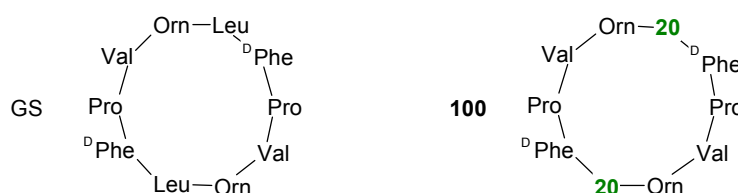
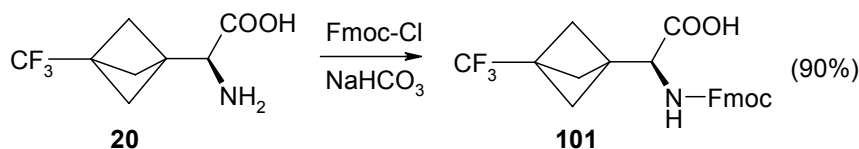


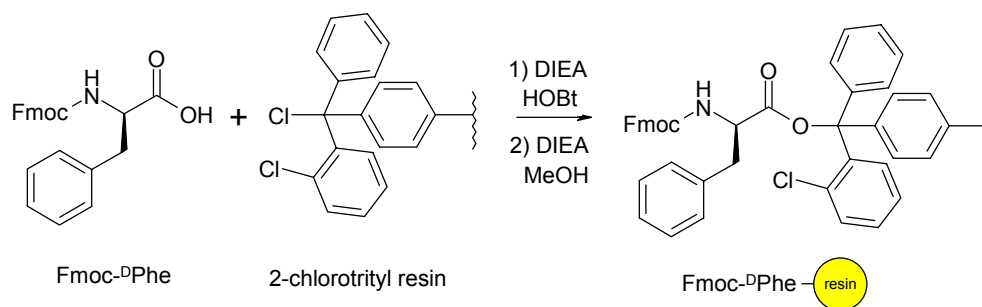
**Fig. 5.2.** Amino acid sequences of GS and its  $CF_3$ -labelled analogue **100** with two equivalent Leu/**20** substitutions.

First, compound **20** was Fmoc-protected using standard procedures (Scheme 5.1).<sup>214</sup>



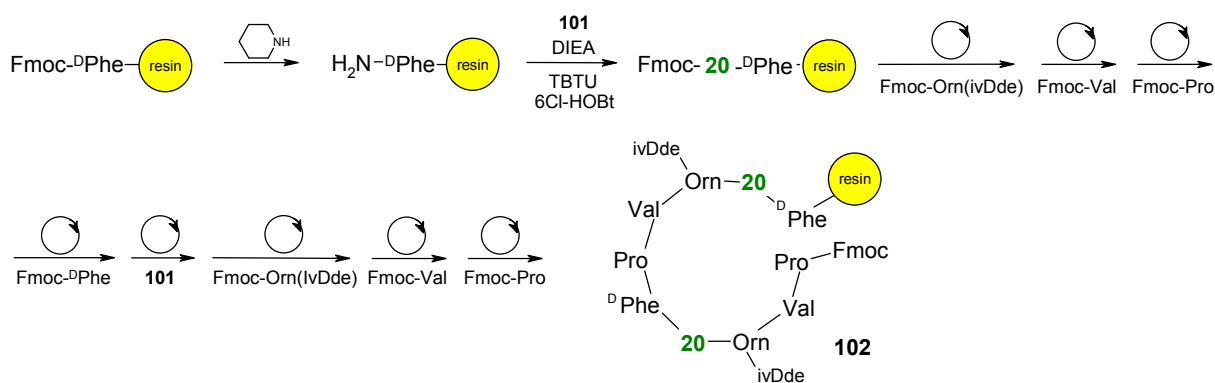
**Scheme 5.1.** Synthesis of **101**.

The synthesis of peptide **100** was carried out on 2-chlorotrityl resin, starting from Fmoc- $^{19}F$ -Phe (Scheme 5.2).<sup>215</sup>



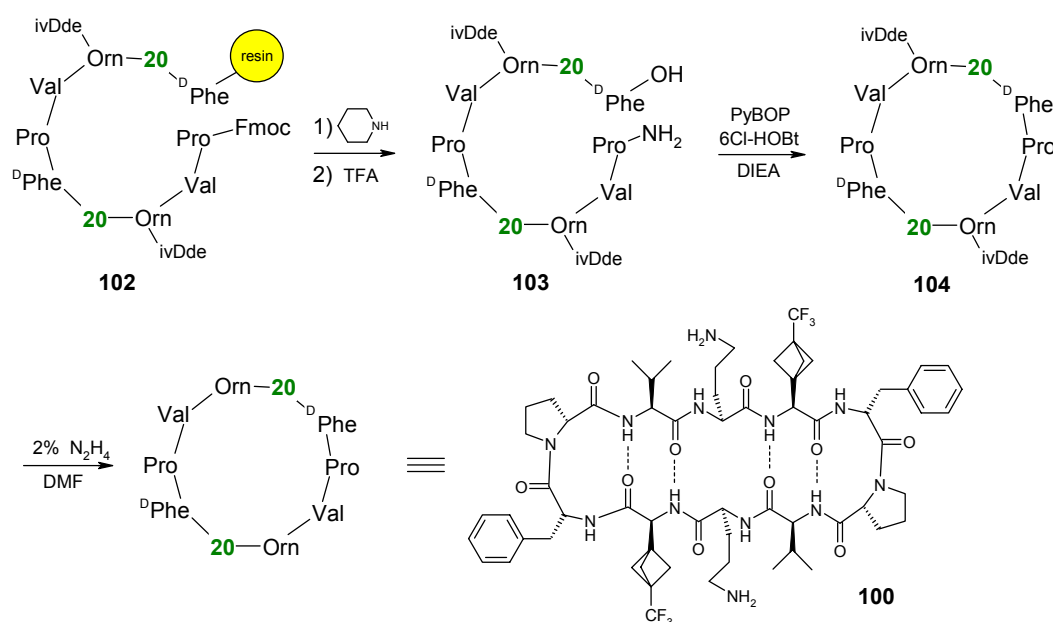
**Scheme 5.2.** Attachment of the first amino acid (<sup>D</sup>Phe) to 2-chlorotrityl resin in the synthesis of **100**.

<sup>19</sup>F-label **20** was successfully incorporated into the peptide in the form of the Fmoc-derivative **101**, using standard activators TBTU/6Cl-HOBt. The following amino acids were incorporated analogously (Scheme 5.3).



**Scheme 5.3.** Synthesis of the linear precursor of **100**, the decapeptide **102**.

Removal of the Fmoc-group from **102** was followed by cleavage from the resin, to give the linear decapeptide **103**. The target peptide **100** was obtained by cyclization of **103** in solution (**104**) and subsequent cleavage of the ivDde-protecting groups from Orn (Scheme 5.4).



**Scheme 5.4.** Synthesis of **100**.

During the synthesis, neither degradation nor racemization of **20** was observed, and the target **100** was formed as a single diastereomer. Thus, the new  $^{19}\text{F}$ -label **20** was fully compatible with standard protocols of SPPS. Moreover, **20** increased the yield of the  $\text{CF}_3$ -labelled GS analogue 4-fold compared to the racemically prone Phg-based labels **3** and **4**.<sup>77,80</sup>

### 5.1.3. Influence of $\text{CF}_3$ -Bpg on the conformation of GS

To examine the conformational preferences of GS and **100**, CD spectra of both peptides were measured under identical conditions. As can be seen from the Fig. 5.3, the CD spectra of GS and **100** are almost identical; hence the  $^{19}\text{F}$ -label **20** did not perturb the conformation of GS.

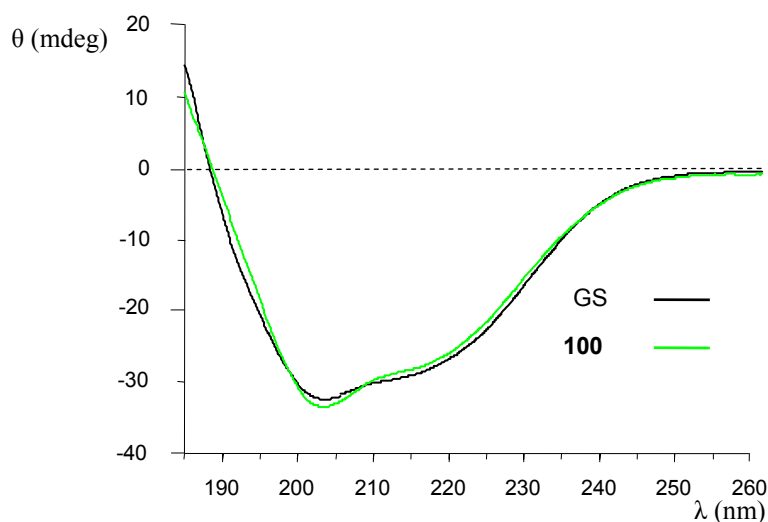


**Fig. 5.3.** CD spectra of GS and **100** in water-ethanol solution (1/1) at 20 °C, with a peptide concentration of 90  $\mu\text{M}$ .

### 5.1.4. Influence of $\text{CF}_3$ -Bpg on the orientation of GS in lipid bilayers

To evaluate the applicability of  $\text{CF}_3$ -Bpg (**20**) for structural peptide studies, solid state  $^{19}\text{F}$ -NMR spectroscopy was used. To do so, a macroscopically oriented sample of **100**, reconstituted in DMPC bilayers, was measured at different temperatures. The spectra acquired here were compared with  $^{19}\text{F}$ -NMR data obtained from an analogue of GS that had been previously labelled with 4F-Phg (**3**) at the very same positions of the peptide, as shown in Fig. 5.4.<sup>216</sup>

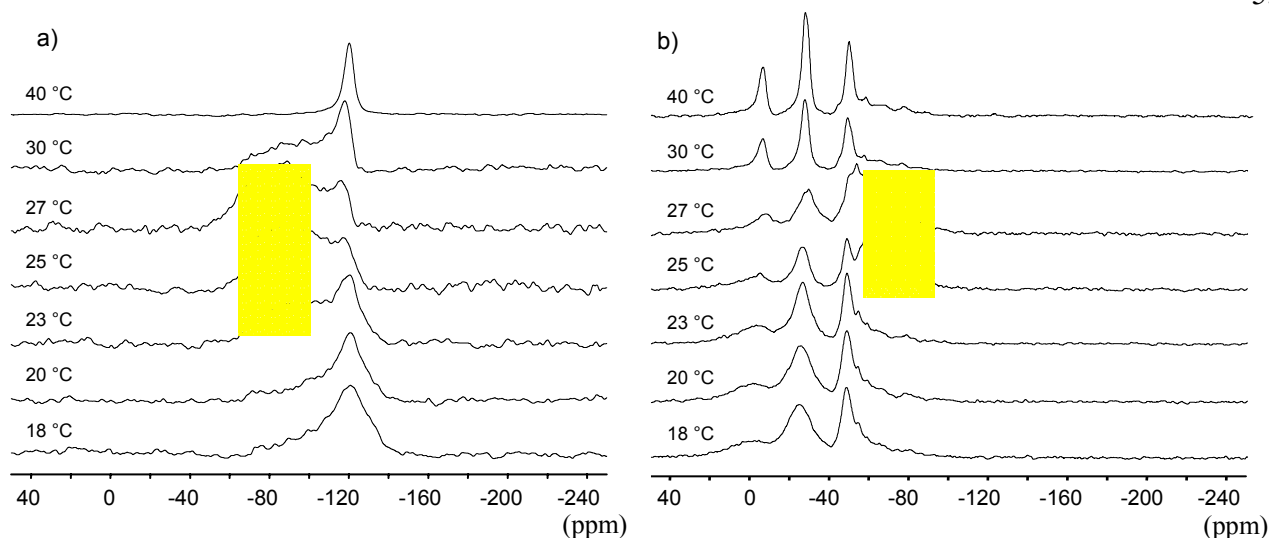


**Fig. 5.4.** Solid state  $^{19}\text{F}$ -NMR spectra of GS analogues with a) Leu/4F-Phg (**3**) substitutions; b) Leu/ $\text{CF}_3$ -Bpg (**20**) substitutions (**100**). Both peptides were reconstituted into macroscopically oriented DMPC bilayers at a peptide/lipid ratio of 1/40 (mol/mol). Spectra were measured with the membrane normal aligned parallel to the magnetic field. Resonances corresponding to the flipped peptide alignment are highlighted in yellow.

Spectra of GS-analogue labelled with 4F-Phg (**3**) at both low (18-20 °C) and high (30-40 °C) temperatures contained predominantly a single peak (Fig. 5.4,a), which corresponds to a flat alignment of GS on the bilayer surface (Fig. 5.5, a). In the range of 23-27 °C, however, new signals had been previously found to appear due to re-alignment of GS into an upright transmembrane state (Fig. 5.5, b).<sup>216</sup> The solid state  $^{19}\text{F}$ -NMR spectra acquired here for **100** (Fig. 5.4, b) are in full accordance with the abovementioned re-alignment of GS, which is induced by the lipid phase transition from the gel to the liquid crystalline state. At the temperature intervals of 18-23 °C and 30-40 °C a single well-resolved triplet signal is seen in the spectra, while in the temperature range of 25-27 °C same new broad signal appears, suggesting an orientational flip of up to 50% GS molecules. The results obtained here, thus prove the suitability of  $\text{CF}_3$ -Bpg (**20**) for peptide structural studies.

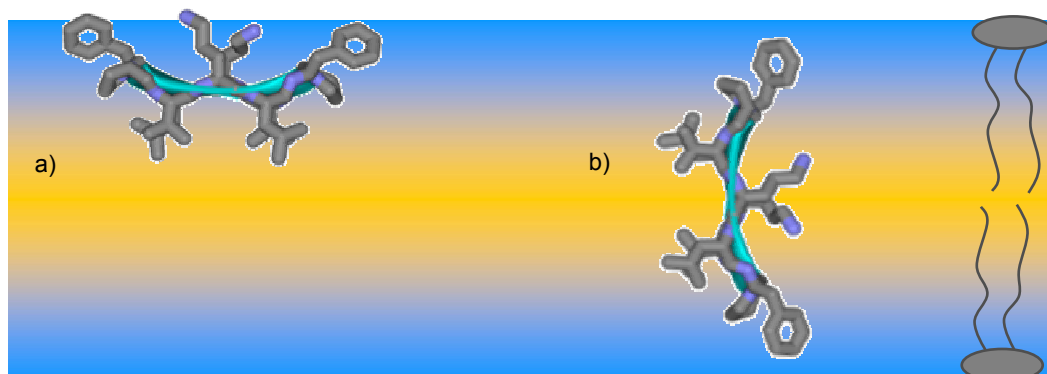
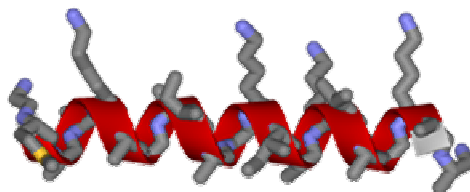


**Fig. 5.5.** Different orientations of GS embedded in a DMPC bilayer: a) flat alignment on the membrane surface; b) upright transmembrane alignment.<sup>216</sup>

## 5.2. Antimicrobial peptide PGLa

### 5.2.1. General information about PGLa

PGLa belongs to the magainin family of antimicrobial peptides, and it is found in the skin secretions of the frog *Xenopus laevis*.<sup>217,218,219</sup> This cationic peptide possesses high affinity to bacterial membranes and is able to permeabilize them. It is supposed that specific receptors are not involved in the process of antimicrobial action of PGLa.<sup>220</sup> Upon binding to biomembranes PGLa adopts an amphipatic  $\alpha$ -helix conformation as illustrated in Fig. 5.6.<sup>221</sup>



Gly-Met-Ala-Ser-Lys-Ala-Gly-Ala-Ile-Ala-Gly-Lys-Ile-Ala-Lys-Val-Ala-Leu-Lys-Ala-Leu-NH<sub>2</sub>

**Fig. 5.6.** Structural model of PGLa in ideal  $\alpha$ -helix conformation and amino acid sequence of PGLa.

### 5.2.2. Synthesis of CF<sub>3</sub>-labelled analogues of PGLa

PGLa was labelled with **20** at the positions 9 (Ile), 10 (Ala), 13 (Ile) and 14 (Ala), as the behaviour of the previously used <sup>19</sup>F-label 4CF<sub>3</sub>-Phg (**4**) at these positions had been comprehensively described.<sup>80</sup> The corresponding labelled peptides **106-109** (Fig. 5.7) were synthesized using standard protocols of SPPS on Rink-amide resin.

- 106:** Gly-Met-Ala-Ser-Lys-Ala-Gly-Ala-**20**-Ala-Gly-Lys-Ile-Ala-Lys-Val-Ala-Leu-Lys-Ala-Leu-NH<sub>2</sub>  
**107:** Gly-Met-Ala-Ser-Lys-Ala-Gly-Ala-Ile- **20**-Gly-Lys-Ile-Ala-Lys-Val-Ala-Leu-Lys-Ala-Leu-NH<sub>2</sub>  
**108:** Gly-Met-Ala-Ser-Lys-Ala-Gly-Ala-Ile-Ala-Gly-Lys-**20**-Ala-Lys-Val-Ala-Leu-Lys-Ala-Leu-NH<sub>2</sub>  
**109:** Gly-Met-Ala-Ser-Lys-Ala-Gly-Ala-Ile-Ala-Gly-Lys-Ile- **20**-Lys-Val-Ala-Leu-Lys-Ala-Leu-NH<sub>2</sub>

**Fig. 5.7.** Amino acid sequences of CF<sub>3</sub>-labelled analogues of PGLa, **106-109**.

The amino acid **20** was easily incorporated into the peptides by using the standard activators HCTU/HOBt. Moreover, this process effectively occurred with the use of only a double excess of Fmoc-derivative **101**.<sup>\*</sup> The amino acids next to the <sup>19</sup>F-label **20** were incorporated without difficulties as well. All HPLC chromatograms of crude **106-109** mixtures contained only one major peak, thus indicating that **20** did not racemize during the synthesis.<sup>†</sup> Here again, similar to the synthesis of **100**, the new <sup>19</sup>F-label **20** appeared to be completely compatible with the standard techniques of SPPS.

<sup>\*</sup> Incorporation of the natural amino acids was performed using a fourfold excess of the corresponding Fmoc-derivatives.

<sup>†</sup> Analysis of minor peaks by MALDI-TOF revealed that they had masses different from that of the target peptide.



### 5.2.3. Influence of $CF_3$ -Bpg on the conformation of PGLa

To evaluate the potential influence of the  $^{19}F$ -label **20** on the PGLa conformation, CD spectra of **106-109** and PGLa were measured in detergent micelles and compared.

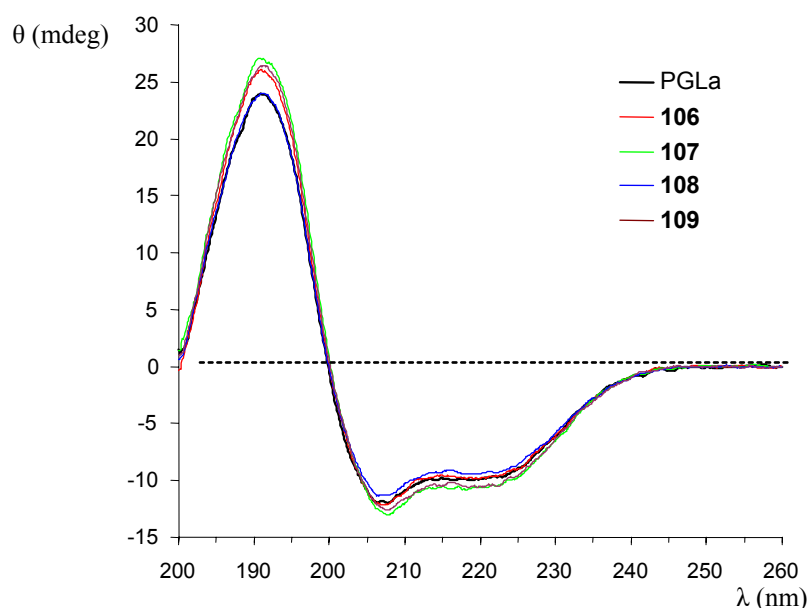


**Fig. 5.8.** CD spectra of PGLa and **106-109** (30  $\mu$ M) in water sodium dodecyl sulfate micelles (5 mM) at 20  $^{\circ}$ C.

Fig. 5.8 demonstrates that the CD spectra of all peptides in water in the presence of SDS micelles are similar and correspond to an  $\alpha$ -helical conformation. This means that incorporation of the  $^{19}F$ -label **20** into PGLa did not influence the membrane-bound conformation of PGLa.

### 5.2.4. Influence of $CF_3$ -Bpg on the antimicrobial activity of PGLa

After the synthesis of the PGLa analogues **106-109** and comparison of their conformational preferences, the antimicrobial activity of these peptides against several strains of Gram-positive and Gram-negative bacteria was evaluated (Table 5.1).

**Table 5.1.** Minimal inhibitory concentration (MIC, mg/ml) values\* of PGLa and its analogues **106-109**.

strain	peptide	PGLa	<b>106</b>	<b>107</b>	<b>108</b>	<b>109</b>
<i>E.coli</i> ATCC 25922		8	8	8	8	8
<i>E.coli</i> DH5		4	4	4	4	4
<i>Acinetobacter sp.</i> ATCC 33304		4	4	4	8	8
<i>S. aureus</i> ATCC 25923		8	8	4	8	4
<i>B. subtilis</i> ATCC 6633		4	4	2	4	4
<i>M. luteus</i> ATCC10240		16	4	2	4	2
<i>K. rhizophila</i> ATCC 9341		8	8	4	8	4

\* peptide concentration, at which bacterial growth is suppressed by 50%.

Since the MIC values were similar for all peptides, the assay proved that the presence of the  $^{19}\text{F}$ -label **20** did not influence the antimicrobial activity of PGLa.<sup>222</sup>

### 5.2.5 Influence of $\text{CF}_3$ -Bpg on the orientation of PGLa in lipid bilayers

To evaluate further the potential of  $\text{CF}_3$ -Bpg (**20**) as a  $^{19}\text{F}$ -label, solid state  $^{19}\text{F}$ -NMR spectra of oriented samples containing **106-109**, embedded in DMPC bilayers, were measured (Fig. 5.9). Two peptide/lipid (P/L) ratios of 1/200 and 1/50 were used, because under these conditions PGLa is known to adopt different orientations: a surface-aligned “S-state” at P/L = 1/200 (Fig. 5.10, a) and an obliquely tilted “T-state” at P/L = 1/50 (Fig. 5.10, b).<sup>80,223,224</sup>

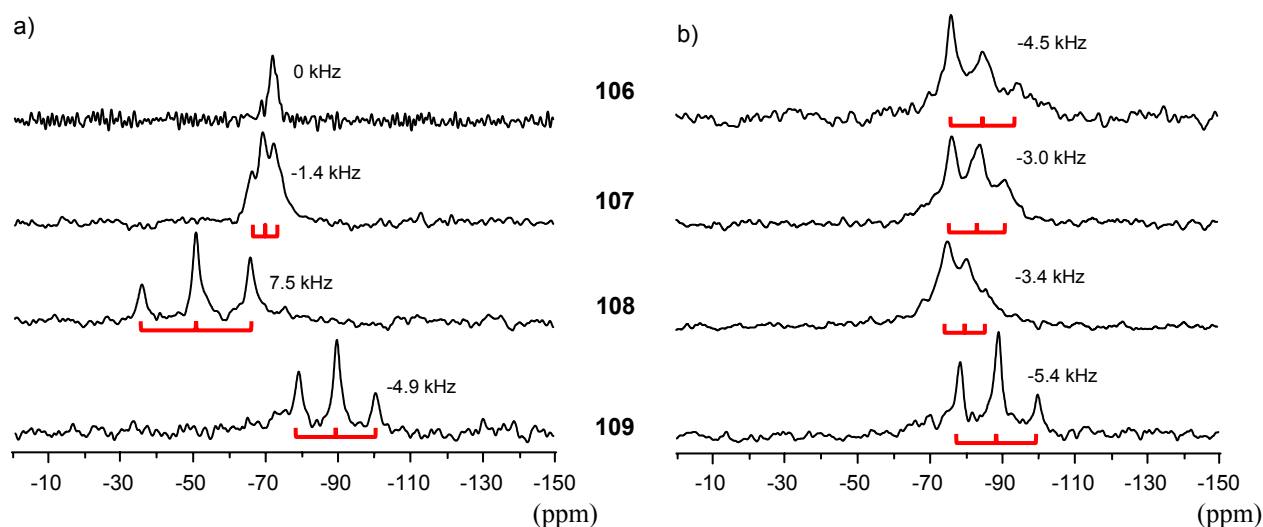


**Fig. 5.9.** Solid state  $^{19}\text{F}$ -NMR spectra of **106-109**, reconstituted into macroscopically oriented DMPC bilayers. Two peptide/lipid (mol/mol) ratios are compared: a) 1/200, corresponding to the surface-bound S-state; b) 1/50, corresponding to the tilted T-state. All samples were measured at 35 °C with the membrane normal parallel to the magnetic field. The measured dipole-dipole splittings are depicted in red and the corresponding coupling values are given.

All peptides were well aligned, as there were no powder lineshapes seen, and the individually labelled positions obviously produced different spectra. Differences were also seen for the two peptide/lipid ratios, suggesting that the alignment of PGLa indeed differs in the two concentration regimes addressed here.

From the collected four sets of orientational constraints (dipolar splittings) for each P/L ratio, the orientational parameters ( $\rho$ ,  $\tau$  and  $S_{\text{mol}}$ ) of PGLa were calculated. The results obtained here are compared with previous data acquired from four  $4\text{CF}_3$ -Phg (**4**) labels attached to the very same positions in the peptide (Table 5.2).

**Table 5.2.** Numerical best-fit solutions for the structure and dynamics of PGLa in DMPC, obtained using the established label 4CF<sub>3</sub>-Phg (**4**) and the new CF<sub>3</sub>-Bpg (**20**). The number of constraints used and their positions in PGLa are indicated (RMSD: root mean square deviation between the experimental and calculated values of the spectral splittings).

labels used	labelled positions	RMSD (kHz)	S <sub>mol</sub>	ρ (°)	τ (°)
<i>P/L = 1/200 (S-state)</i>					
4 × CF <sub>3</sub> -Bpg ( <b>20</b> )	Ile9, Ala10, Ile13, Ala14	0.2	0.68	116	98
4 × 4CF <sub>3</sub> -Phg ( <b>4</b> )	Ile9, Ala10, Ile13, Ala14	0.5	0.60	112	97
<i>P/L = 1/50 (T-state)</i>					
4 × CF <sub>3</sub> -Bpg ( <b>20</b> )	Ile9, Ala10, Ile13, Ala14	0.3	0.63	89	134
4 × 4CF <sub>3</sub> -Phg ( <b>4</b> )	Ile9, Ala10, Ile13, Ala14	0.2	0.63	91	134

As can be seen from Table 5.2, the values of τ, ρ and S<sub>mol</sub> obtained at both peptide concentrations are essentially the same, irrespective of which NMR labels are analyzed. At P/L = 1/200 the peptide possesses a surface-bound “S-state” (Fig. 5.10, a). Upon increasing the peptide concentration to 1/50, the change in tilt angle (τ) by over ~30° demonstrated that PGLa is flipped into the tilted “T-state” (Fig. 5.10, b).

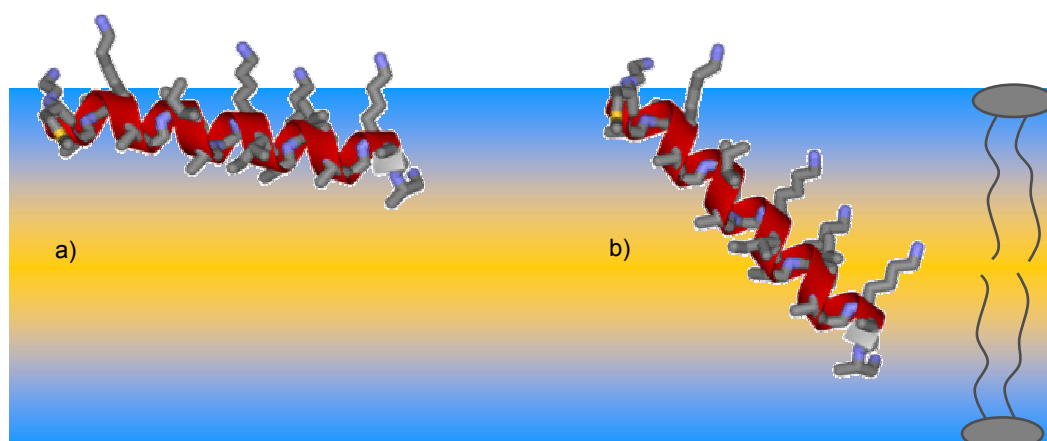


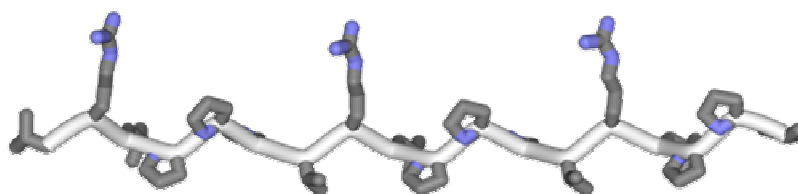
**Fig. 5.10.** Different orientations of PGLa embedded in a lipid bilayer: a) “S-state”; b) “T-state”.<sup>80,223,224</sup>

The results, obtained here on PGLa confirm the conclusions drawn in the previous section (Chapter 5.1), expand the range of experimentally tested substitution positions (Leu/**20**, Ile/**20**, Ala/**20**) and prove the full equivalency of the structural data obtained with the use of **20** compared to those acquired using the established <sup>19</sup>F-label 4CF<sub>3</sub>-Phg (**4**).

### 5.3. Cell-penetrating peptide SAP

#### 5.3.1. General information about SAP

SAP is a new synthetic cell-penetrating peptide developed in 2004 (Fig. 5.11).<sup>225-229</sup>

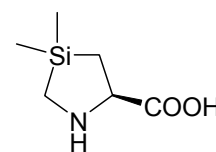


Val-Arg-Leu-Pro-Pro-Pro-Val-Arg-Leu-Pro-Pro-Pro-Val-Arg-Leu-Pro-Pro-Pro

**Fig. 5.11.** Structural model of SAP in an ideal PP II conformation, and amino acid sequence of SAP.

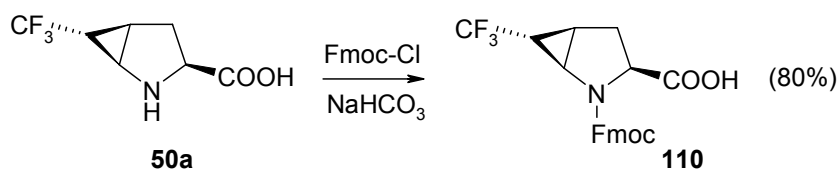
SAP is a peptide prone to aggregation: in aqueous solution at concentrations above 50  $\mu\text{M}$  it forms fibrils. The main conformation of SAP in water solution is a PP II helix.<sup>230</sup>

Concerning the mechanism of cell penetration by SAP, it is postulated that, at least in HeLa cells, it occurs via receptor-independent endocytosis.<sup>231,232</sup> Interestingly, a substitution of Pro by more hydrophilic silano-Pro has been shown to cause a 20-fold increase in the cellular uptake of SAP.<sup>233</sup> It is also important that, on the contrary to many other CPPs, SAP demonstrates very low toxicity to HeLa cells. The structure of SAP upon binding to biomembranes and during the process of cell-penetration is unknown.



### 5.3.2. Synthesis of SAP and its $\text{CF}_3$ -labelled analogues

For structural studies of SAP the new  $^{19}\text{F}$ -labels **20** and **51a** were used. First, the Pro-derived amino acid **51a** was converted into its Fmoc-derivative **110** (Scheme 5.5).



**Scheme 5.5.** Synthesis of **110**.

The  $^{19}\text{F}$ -label  $\text{CF}_3\text{Bpg}$  (**20**) was incorporated into SAP at the positions 3 (Leu), 7 (Val), 9 (Leu), 13 (Val) or 15 (Leu).  $^{19}\text{F}$ -label **51a** was introduced instead of Pro at 11 position of SAP (Fig. 5.12).

- 111:** Val-Arg-**20**-Pro-Pro-Pro-Val-Arg-Leu-Pro-Pro-Pro-Val-Arg-Leu-Pro-Pro-Pro  
**112:** Val-Arg-Leu-Pro-Pro-Pro-**20**-Arg-Leu-Pro-Pro-Pro-Val-Arg-Leu-Pro-Pro-Pro  
**113:** Val-Arg-Leu-Pro-Pro-Pro-Val-Arg-**20**-Pro-Pro-Pro-Val-Arg-Leu-Pro-Pro-Pro  
**114:** Val-Arg-Leu-Pro-Pro-Pro-Val-Arg-Leu-Pro-**51a**-Pro-Val-Arg-Leu-Pro-Pro-Pro  
**115:** Val-Arg-Leu-Pro-Pro-Pro-Val-Arg-Leu-Pro-Pro-Pro-**20**-Arg-Leu-Pro-Pro-Pro  
**116:** Val-Arg-Leu-Pro-Pro-Pro-Val-Arg-Leu-Pro-Pro-Pro-Val-Arg-**20**-Pro-Pro-Pro

**Fig. 5.12.** Amino acid sequences of  $\text{CF}_3$ -labelled SAP analogues of SAP **111-116**.

The synthesis of SAP was carried out manually, controlling each coupling step by MALDI-TOF and analytical HPLC. This monitoring revealed that incorporation of Arg and the amino acid following the Arg (Val) into the peptide was not complete. However, after double coupling had been applied during the incorporation of Arg and Val, the crude SAP was obtained with a purity of > 95% (Fig. 5.13).

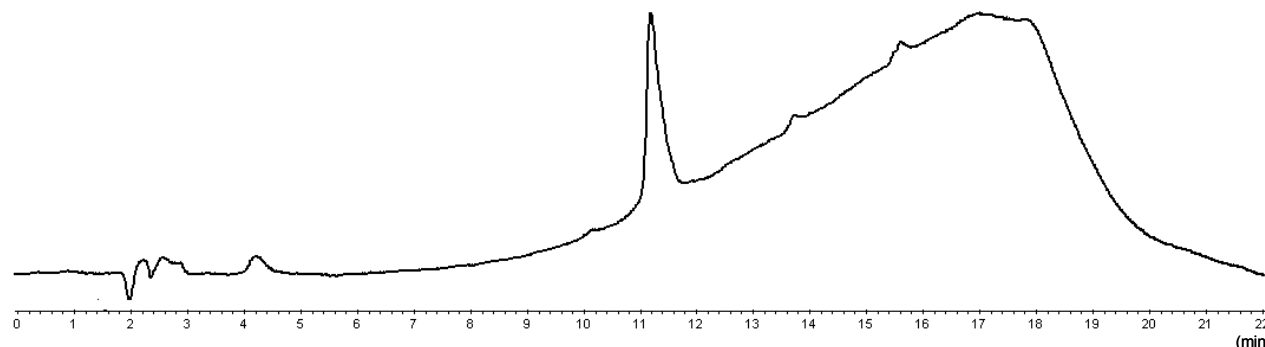


**Fig. 5.13.** HPLC chromatogram of manually synthesized SAP. Arg and Val were incorporated by using double coupling.

Synthesis of the  $\text{CF}_3$ -labelled SAP analogues **111-116** was performed analogously to SAP. During the synthesis of **114** it was found that amino group of **51a**, when incorporated in the peptide, had a reduced reactivity. However, by increasing the reaction time, coupling of the next amino acid (Pro) occurred completely. HPLC of all reaction mixtures **111-116** showed a single peak, thus suggesting that neither **20** nor **51a** had racemized during synthesis.

### 5.3.3. Influence of $\text{CF}_3$ -Bpg and $\text{CF}_3$ -MePro on the conformation of SAP

In order to clarify whether incorporation of the new  $^{19}\text{F}$ -labels **20** and **51a** influences the conformation of SAP, CD spectra of **111-116** were acquired and compared with those of native SAP (Fig. 5.14).

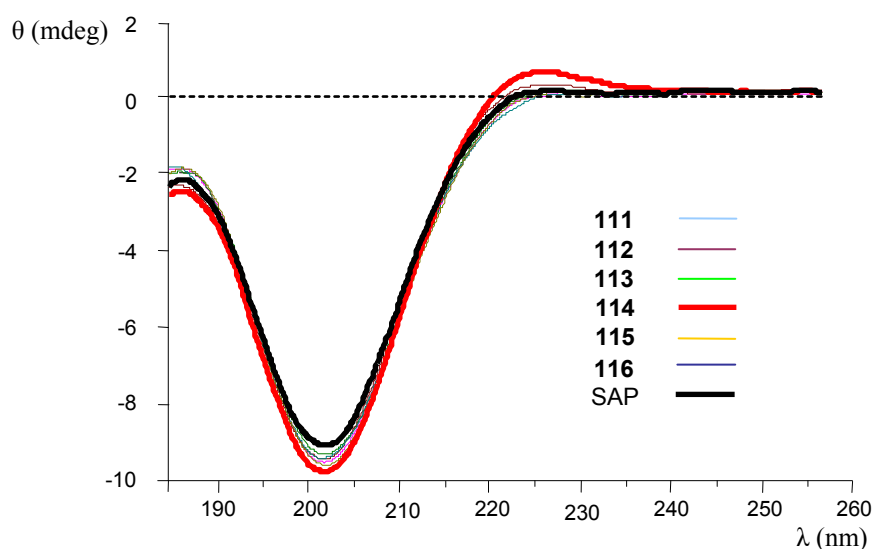


**Fig. 5.14.** CD spectra of SAP and **111-116** (10  $\mu\text{M}$ ) in 10 mM buffer  $\text{NaH}_2\text{PO}_4/\text{Na}_2\text{HPO}_4$  at 20  $^\circ\text{C}$ .

As can be seen from the Fig. 5.14,  $^{19}\text{F}$ -label **20** did not perturb the PP II conformation of SAP, since CD spectra of **111-113**, **115**, **116** and SAP are almost identical.  $^{19}\text{F}$ -label **51a**, on the contrary to **20**, appears to stabilize the PP II conformation, since the bands at 203 and 223 nm in the spectrum of **114** have significantly higher intensity than the corresponding signals in all other peptides.

A major obstacle in quantifying the formation of PP II helix by CD is its close resemblance to the random coil conformation. To properly quantify the PP II contribution, spectral data has to be acquired down to 178 nm,<sup>53</sup> which is experimentally a challenging task. However, semiquantitative data for a random coil/PP II equilibrium can be obtained from temperature dependent measurements. The results of such temperature series for SAP, **113** and **114** are shown in Fig. 5.15. Since the CD spectra of each peptide at different temperatures have only one isodichroic point, the equilibrium between the two conformations (random coil and PP II) exists for all tested peptides. Interestingly, **114** reveals a higher amount of PP II assembled molecules, since the positive intensity of the signal at 223 nm persists even at 50 °C.

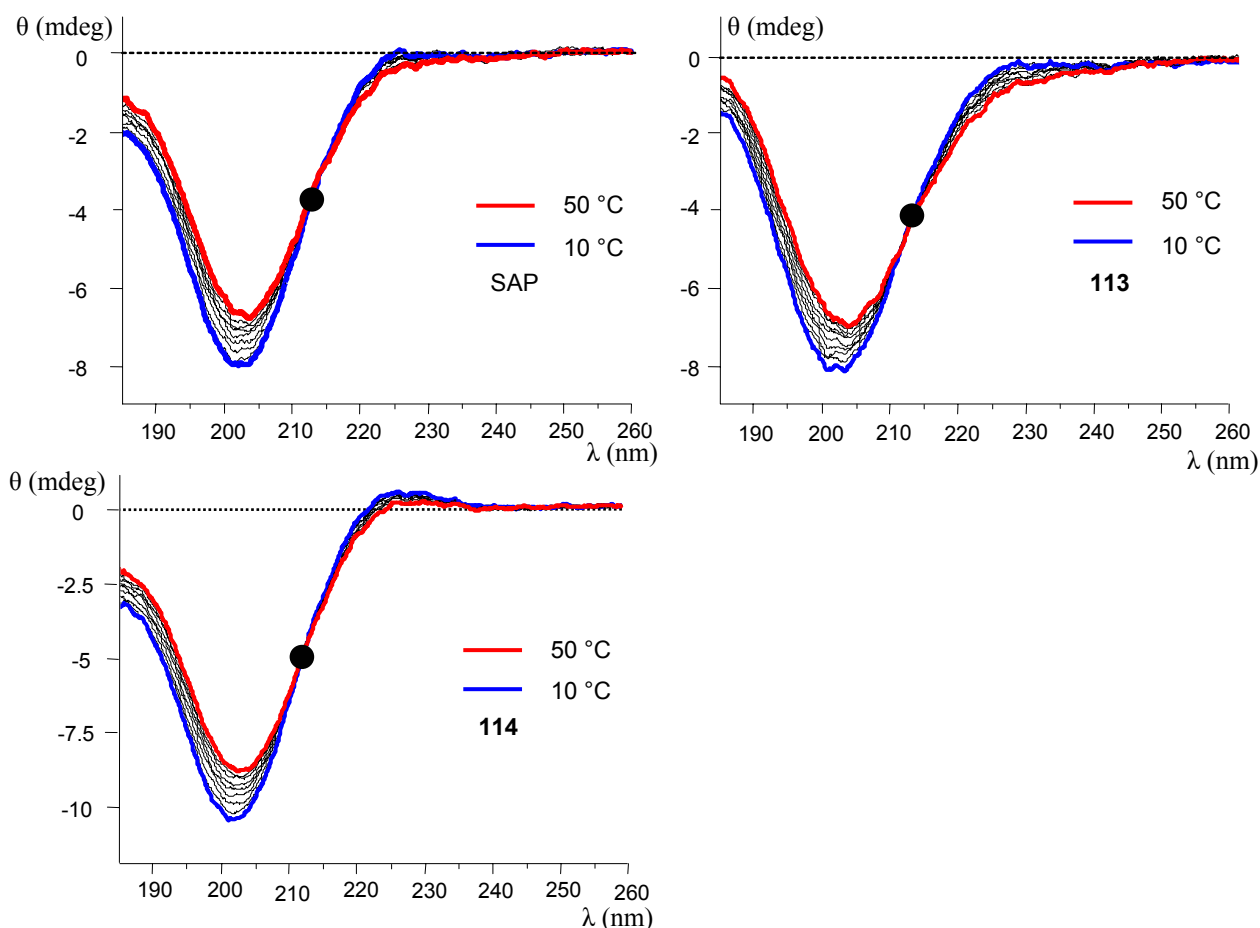


**Fig. 5.15.** CD spectra of SAP, **113** and **114** (10  $\mu\text{M}$ ) in 10 mM buffer  $\text{NaH}_2\text{PO}_4/\text{Na}_2\text{HPO}_4$  (pH = 7.4) at temperatures 10-50 °C (changed in steps of 5 °C). For each peptide the isodichroic point is indicated by a black dot.

To examine the propensity of SAP, **113** and **114** to self-assemble into aggregates, the CD spectra were measured over a concentration range of 5-150  $\mu\text{M}$ . SAP and **113** exhibit spectral changes up to 50  $\mu\text{M}$ , which for SAP was shown in the literature to reflect oligomerization (fibril formation)<sup>230</sup> beyond this point (Fig. 5.16).

In contrast, **114** oligomerized only at a concentration twice as high (100  $\mu\text{M}$ ), which might be a result of an increased PP II population.

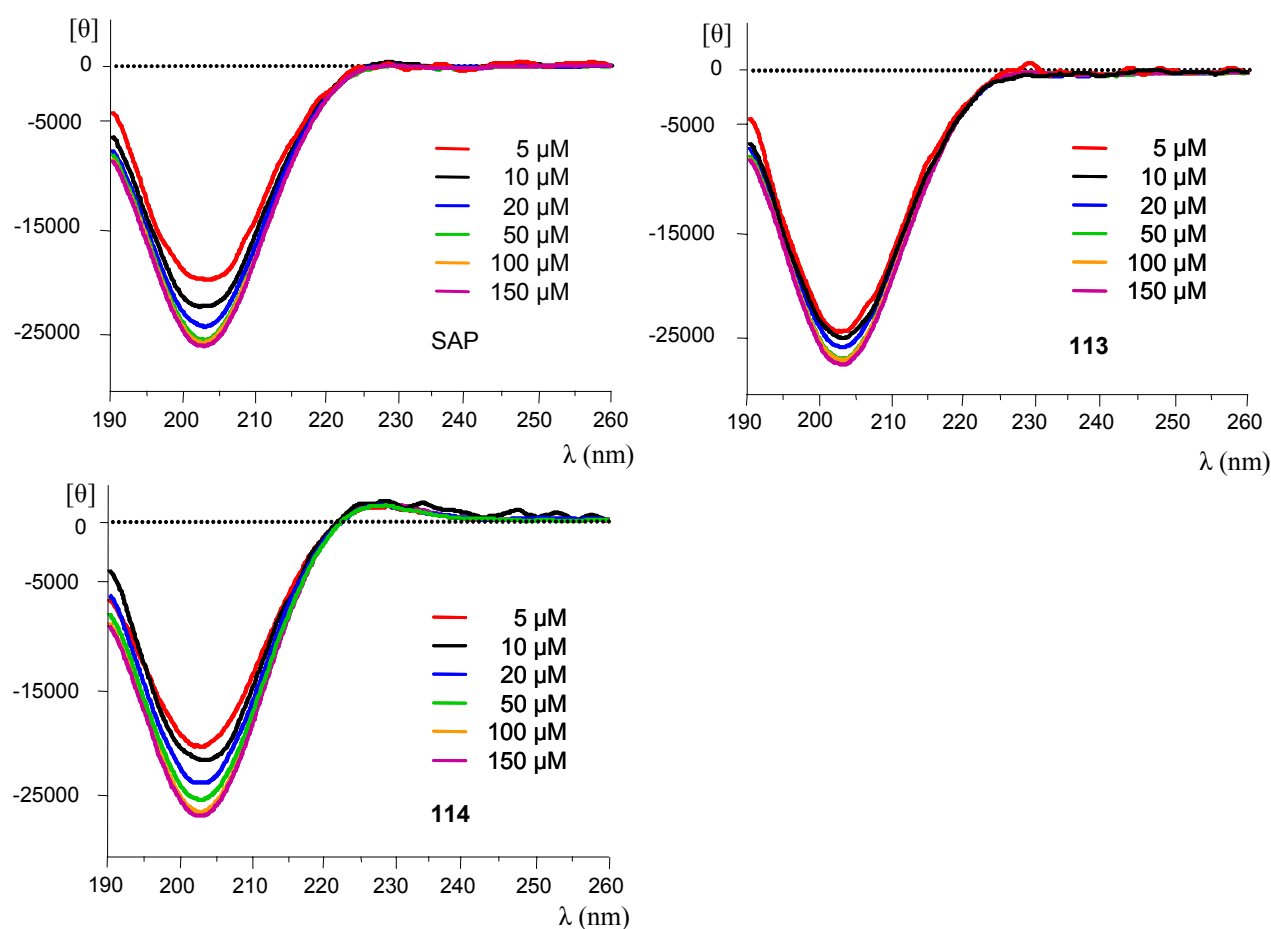


**Fig. 5.16.** CD spectra of SAP, **113** and **114** over a concentration range (5-150  $\mu\text{M}$ ) where oligomerization is expected. The spectra were measured in 10 mM  $\text{NaH}_2\text{PO}_4/\text{Na}_2\text{HPO}_4$  buffer at 20  $^\circ\text{C}$ .

All the CD data confirmed that **20** does not change the conformational behaviour of SAP, whereas **51a** seems to stabilize the PP II conformation of SAP.

#### 5.3.4. Solid state $^{19}\text{F}$ -NMR studies of SAP in lipid bilayers

To study the structure of SAP upon binding to biomembrane, solid state  $^{19}\text{F}$ -NMR spectra of **111-116** in lipid bilayers were measured. The lipid DMPC was used first, as it is known to orient well and is one of the most popular biomembrane models. It has a lipid phase transition temperature of  $T_c = 24$   $^\circ\text{C}$  and therefore provides a convenient system to access both gel and liquid crystalline states.<sup>234</sup> All  $^{19}\text{F}$ -labelled SAP-analogues were reconstituted and measured in the temperature range of 15-55  $^\circ\text{C}$ . Fig. 5.17 shows a representative temperature series from the sample containing **116** at P/L of 1/50. All other peptides, including **114**, showed virtually the same temperature dependent spectral changes at both P/L = 1/50 and 1/200 (and are therefore not shown). At low temperatures (gel state of lipids) the solid state  $^{19}\text{F}$ -NMR spectra predominantly contained quasi-isotropic singlets. At

higher temperatures (above  $T_c$  of DMPC), additional signals appeared reversibly at the cost of the quasi-isotropic signals (liquid crystalline state of lipids). Therefore, SAP seems to have different modes of interaction (orientation and/or structure) with the zwitterionic DMPC bilayers below (“isotropic” state of SAP) and above  $T_c$  (“ordered” state of SAP).

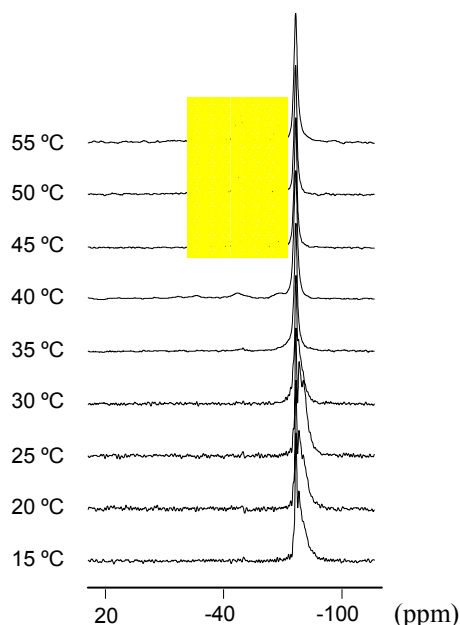


**Fig. 5.17.** Solid state  $^{19}\text{F}$ -NMR spectra of **116** over a temperature range 15–55 °C (changed in steps of 5 °C). Peptide/DMPC = 1/50 (mol/mol).

Both “isotropic” and “ordered” states were observed for all peptides also in POPC and DMPC/DMPG (3/1, mol/mol) bilayers (data not shown), suggesting neither the type of lipid chain nor the presence of negatively charged lipids affects this general behaviour of the cationic peptide. It should be noted that the kinetics of the transition between the two SAP states appear to be rather slow, since different equilibration times (10 min, 0.5 h, 4 h, 12 h, 24 h) produced different proportions of the molecules in the different states. At high temperature (55 °C) using a prolonged equilibration time (12 h), a pure “ordered” state was observed (Fig. 5.18). In all cases, however, the spectral appearance was rather complex and the coexistence of 2–3 triplets was evident (Fig. 5.18). This means that under the abovementioned conditions SAP possesses several orientations (assuming that one splitting corresponds to one particular orientation or conformation). The calculation of all these structures is a considerable challenge, since the signals are significantly overlapped and therefore an extraction of the corresponding dipole-dipole constants is hindered. An experimental solution of this problem is currently in progress (i.e. different multipulse experiments to separate and assign the individual splittings).



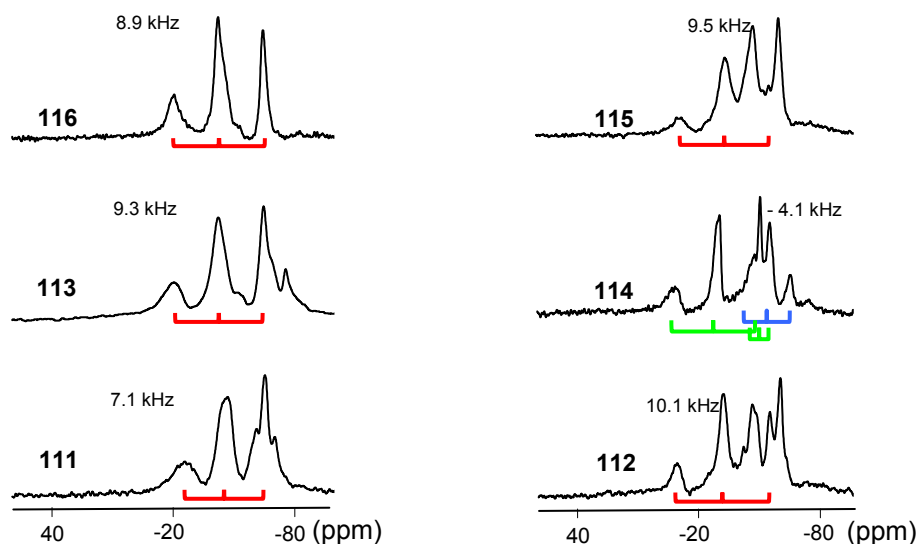


**Fig. 5.18.** Solid state  $^{19}\text{F}$ -NMR spectra of **111-116** at 55 °C. Peptide/lipid = 1/50. Lipids: DMPC/DMPG = 3/1. Before measurement each sample was pre-equilibrated at the corresponding temperature for 12 h. Dominant dipole-dipole splittings are depicted in red, the corresponding values of dipole-dipole constants being given above the signals. For the peptide **114** all the constants are shown (depicted in blue and green).

In the extensively equilibrated “ordered state”, nevertheless, all peptides labelled with  $\text{CF}_3$ -Bpg (**111**, **112**, **113**, **115**, **116**) show one predominant splitting among others (Fig. 5.18). Therefore, from the collected sets of orientational constraints, the compatibility of SAP structure with various helical conformations (PP II,  $3_{10}$ -helix,  $\pi$ -helix,  $\alpha$ -helix) was tested (Table 5.3).

**Table 5.3.** Numerical best-fit solutions for the structure of SAP modeled as a PP II helix,  $3_{10}$ -helix,  $\pi$ -helix or an  $\alpha$ -helix. The dipole-dipole splittings from the dominant triplets in the peptides **111**, **112**, **113**, **115**, **116** were used for calculations. (RMSD: root mean square deviation between the experimental and calculated values of the spectral splittings).

conformation	RMSD (kHz)	$S_{\text{mol}}$	$\tau$ (°)	$\rho$ (°)
PP II	0.77	1.0	83	139
$3_{10}$ -helix	1.94	1.0	91	35
$\pi$ -helix	> 4.8	-	-	-
$\alpha$ -helix	> 7.3	-	-	-

From the Table 5.3 it can be seen that the minimal RMSD value is observed for the PP II conformation, with  $\rho = \sim 139^\circ$ ,  $\tau = \sim 83^\circ$  and  $S_{\text{mol}} = \sim 1.0$ . In order to clarify whether the peptide **114** with the as yet unexplored Pro-derived  $^{19}\text{F}$ -label (**51a**) meets this solution as well, all splittings present in solid state  $^{19}\text{F}$ -NMR spectrum of **114** (Fig. 5.18) were included one by one in this calculation. The calculation confirmed that one constant (-4.1 kHz) among the three possibilities does indeed fit to the obtained solution.

Thus, one state of SAP (among others) in the model membranes corresponds to the PP II conformation under the experimental conditions tested (55 °C;

DMPC/DMPG = 3/1, P/L = 1/50). The peptide is aligned parallel to the lipid bilayer surface ( $\tau = 83^\circ$ ), the lipophilic residues of Val and Leu are pointing towards the interior and the hydrophilic residues of Arg out of the lipid bilayer ( $\rho = 139^\circ$ ) (Fig. 5.19). The observation that there is no wobbling ( $S_{\text{mol}} = 1.0$ ) suggests that the peptide is in an oligomeric state.

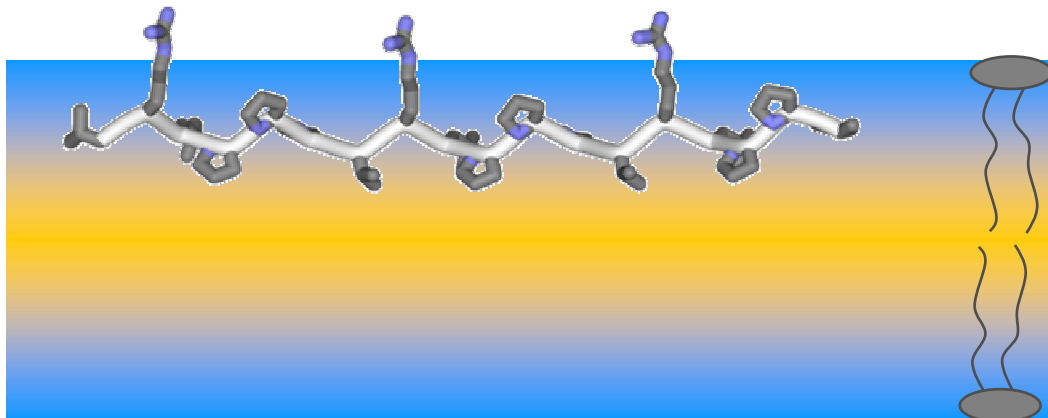


**Fig. 5.19.** SAP orientation in a lipid bilayer (SAP/lipid = 1/50; DMPC/DMPG = 3/1) at 55 °C.

PART 6  
EXPERIMENTAL PART

All air- and moisture-sensitive reactions were performed under an argon atmosphere using standard Schlenk technique. Solvents were purified according to standard procedures.<sup>235</sup> All starting materials, which are not described in the experimental part, were purchased from Acros, Merck, Enamine and Fluka. Melting points are uncorrected. Analytical TLC was performed using Polychrom SiF<sub>254</sub> plates. <sup>1</sup>H-, <sup>13</sup>C- and <sup>19</sup>F-NMR spectra were recorded either on a Varian Unity Plus 400 spectrometer (at 400, 101 and 377 MHz respectively) or on a Bruker Avance 500 spectrometer (at 500 MHz, 125 and 470 MHz). Chemical shifts are reported in ppm downfield from TMS (<sup>1</sup>H, <sup>13</sup>C) or C<sub>6</sub>F<sub>6</sub> (<sup>19</sup>F) as internal standards. IR spectra were obtained on a Hewlett Packard UR 20 spectrometer. The  $\nu_{\max}$  (cm<sup>-1</sup>) values of the IR spectra are given for the main absorption bands. Mass spectra were recorded either on an Agilent 1100 LCMSD SL instrument by chemical ionization (CI), or on a Bruker Biflex IV instrument (MALDI-TOF). MALDI samples were co-crystallized with a matrix of 3,5-dihydroxy-benzoic acid from acetonitrile/water solutions onto a stainless steel target. Elemental analysis: Microanalytic Laboratory, Institute of Organic Chemistry, University of Karlsruhe. Optical rotation values were measured on a PerkinElmer 341 polarimeter.

**1-Iodo-3-(trifluoromethyl)-bicyclo[1.1.1]pentane, 26**

16.53 g (55.7 mmol) **25** and 40 ml of absolute pentane were placed in a Favorsky flask. To this suspension cooled to -78 °C 1.6M solution of MeLi in Et<sub>2</sub>O (99 ml) was added dropwise over 20 min. The cooling was stopped; the mixture was allowed to warm to 0 °C and stirred for 1 h at this temperature. Thereafter, mixture of Et<sub>2</sub>O, pentane and propellane was distilled under reduced pressure into an ampule cooled by liquid nitrogen. Favorsky flask was disconnected and 10.9 g (55.7 mmol) CF<sub>3</sub>I was froze into the ampule. The ampule was closed and leaved in a safety place for 3 days. Evaporation of the solvent at 0 °C (the product is very volatile) gave **26** (9.05 g, 34.5 mmol, 62%) as a white crystals.

<sup>1</sup>H-NMR (400 MHz, DMSO-D<sub>6</sub>): 2.52 (s).

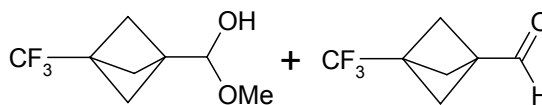
<sup>19</sup>F-NMR (377 MHz, DMSO-D<sub>6</sub>): 95.87 (s).

The obtained product has to be immediately used in the next step, otherwise it must be purified by sublimation prior to the use (at 0 °C under an argon atmosphere decomposition of **26** occurs completely in one week).

**3-(Trifluoromethyl)bicyclo[1.1.1]pentane-1-carbaldehyde, 27**

**Methoxy[3-(trifluoromethyl)bicyclo[1.1.1]pent-1-yl]methanol, 28**

A solution of *t*-BuLi in Et<sub>2</sub>O (2.0 ml of 1.6 M, 3.2 mmol) was added dropwise to a stirred solution of **26** (424 mg, 1.6 mmol) in Et<sub>2</sub>O (10 ml) at -78 °C. The addition was completed in 10 min, and the mixture was stirred for additional 30 min at -78 °C. This mixture, cooled to -78 °C, was added dropwise to a stirred solution of HCO<sub>2</sub>Me (0.40 ml, 6.8 mmol) in Et<sub>2</sub>O (15 ml) at -78



°C over 10 min. Once the addition had been completed, the stirred mixture was allowed to warm to room temperature. After extraction with H<sub>2</sub>O (3 × 10 ml) the water phase was discarded. The organic layer was separated, dried over MgSO<sub>4</sub> and concentrated in vacuum at 0 °C to ~10 ml (the products are very volatile!). The resulting solution of **27** and **28** in Et<sub>2</sub>O was used in the next step without further purification.

For the synthesis of individual compounds the obtained solution was evaporated at 0 °C under reduced pressure. Yellowish oil. Ratio **27/28** is ~2/1.

<sup>1</sup>H-NMR (400 MHz, CDCl<sub>3</sub>): 9.61 (s, 1H, CHO from **27**); 4.51 (s, 1H, CH from **28**); 3.41 (s, 3H, OCH<sub>3</sub> from **28**); 2.25 (s, 6H, CH<sub>2</sub> from **27**); 1.90 (s, 6H, CH<sub>2</sub> from **28**).

<sup>19</sup>F-NMR (377 MHz, CDCl<sub>3</sub>): 88.24 (s, CF<sub>3</sub> from **27**); 88.48 (s, CF<sub>3</sub> from **28**).

After addition of several drops of MeOH into NMR-tube, both <sup>1</sup>H- and <sup>19</sup>F-NMR spectra contained only signals of hemiacetale **28**.

**2(S)-{[(1R)-2-Hydroxy-1-phenylethyl]amino}-2-[3-(trifluoromethyl)bicyclo [1.1.1]pent-1-yl]acetonitriles, 30**

**2(R)-{[(1R)-2-Hydroxy-1-phenylethyl]amino}-2-[3-(trifluoromethyl)bicyclo [1.1.1]pent-1-yl]acetonitriles, 29**

A solution of (*R*)-2-phenylglycinol (222 mg, 1.6 mmol) in MeOH (20 ml) was added to the solution of **27** and **28** in Et<sub>2</sub>O (10 ml), obtained in the previous step, and the resulting mixture was stirred for 2 h at room temperature. After cooling to 0 °C, Me<sub>3</sub>SiCN (634 mg, 6.4 mmol) was added, and the resulting mixture was stirred at room temperature for 10 h. Evaporation of the solvent in vacuum gave a residue, which was submitted to column chromatography. Elution with hexane/EtOAc = 3/2 afforded **30** first (244 mg, 0.78 mmol, 53%) as a colorless solid. R<sub>f</sub> = 0.7. Crystals for X-ray analysis were obtained by crystallization from hexane. M.p. = 99-100 °C.

[α]<sub>D</sub><sup>20</sup> = -133.1 (*c* = 0.26 mg/ml, MeOH).

<sup>1</sup>H-NMR (400 MHz, CDCl<sub>3</sub>): 7.38-7.30 (m, 5H, Ph); 4.80 (dd, <sup>3</sup>J(H, H) = 9.6, 4.0 Hz, 1H, CHCH<sub>2</sub>); 3.80 (dd, <sup>2,3</sup>J(H, H) = 10.4, 4.0 Hz, 1H, CHCH<sub>2</sub>); 3.58 (dd, <sup>2,3</sup>J(H, H) = 10.4, 9.6 Hz, 1H, CHCH<sub>2</sub>); 3.42 (s, 1H, CHCN); 2.35 (bs, 2H, OH+NH); 2.06-2.00 (2 d, <sup>2</sup>J(H, H) = 9.6 Hz, 6H, CH<sub>2</sub>).

<sup>19</sup>F-NMR (377 MHz, CDCl<sub>3</sub>): 88.66 (s, CF<sub>3</sub>).

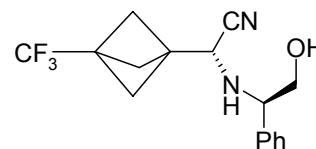
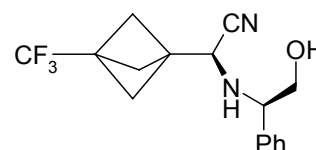
<sup>13</sup>C-NMR (101 MHz, CDCl<sub>3</sub>): 137.97 (s, ipso-C, Ph); 129.21 (s, CH, Ph); 128.73 (s, CH, Ph); 127.27 (s, CH, Ph); 122.65 (q, CF<sub>3</sub>, <sup>1</sup>J(C, F) = 274 Hz); 117.86 (s, CN); 67.53 (s, CHPh); 63.19 (s, CH<sub>2</sub>OH); 48.67 (bs, CH<sub>2</sub>); 47.52 (q, CHCN, <sup>5</sup>J(C, F) = 2 Hz); 38.87 (s, CH<sub>2</sub>CCH); 37.40 (q, CF<sub>3</sub>C, <sup>2</sup>J(C, F) = 40 Hz).

IR (KBr): 2232 (ν C≡N), 1175 (ν C-O) cm<sup>-1</sup>.

MS (*m/z*): 311.2 (M)<sup>+</sup>.

Further elution with the same solvent yielded **29** (202 mg, 0.62 mmol, 40%) as a colorless solid. R<sub>f</sub> = 0.65. Analytically pure sample was obtained by crystallization from hexane. M.p. =

101-102 °C. [α]<sub>D</sub><sup>20</sup> = -21.4 (*c* = 0.25 mg/ml, MeOH).



$^1\text{H-NMR}$  (400 MHz,  $\text{CDCl}_3$ ): 7.34-7.26 (m, 5H, Ph); 4.00 (s, 1H,  $\text{CHCN}$ ); 3.92 (dd,  $^3J(\text{H}, \text{H}) = 8.0, 4.0$  Hz, 1H,  $\text{CHCH}_2$ ); 3.72 ( $^{2,3}J(\text{H}, \text{H}) = 11.2, 4.0$  Hz, 1H,  $\text{CHCH}_2$ ); 3.63 (dd,  $^{2,3}J(\text{H}, \text{H}) = 11.2, 8.0$  Hz, 1H,  $\text{CHCH}_2$ ); 3.2-2.3 (bs, 2H,  $\text{OH}+\text{NH}$ ); 2.00-1.95 (2 d,  $^2J(\text{H}, \text{H}) = 9.6$  Hz, 6H,  $\text{CH}_2$ ).

$^{19}\text{F-NMR}$  (377 MHz,  $\text{CDCl}_3$ ): 88.64 (s,  $\text{CF}_3$ ).

$^{13}\text{C-NMR}$  (101 MHz,  $\text{DMSO-D}_6$ ): 141.64 (s, ipso-C, Ph); 128.71 (s, CH, Ph); 128.22 (s, CH, Ph); 127.87 (s, CH, Ph); 122.83 (q,  $\text{CF}_3$ ,  $^1J(\text{C}, \text{F}) = 274$  Hz); 119.07 (s, CN); 66.55 (s,  $\text{CHPh}$ ); 63.75 (s,  $\text{CH}_2$ ); 49.19 (bs,  $\text{CH}_2\text{OH}$ ); 47.61 (q,  $\text{CH}(\text{CN})\text{N}$ ,  $^5J(\text{C}, \text{F}) = 2$  Hz); signal  $\text{CH}_2\text{-C-CH}$  is hidden by the residual peak of  $\text{DMSO-D}_6$ ; 36.76 (q,  $\text{CF}_3\text{C}$ ,  $^2J(\text{C}, \text{F}) = 38$  Hz).

IR (KBr): 2240 ( $\nu\text{C}\equiv\text{N}$ ), 1172 ( $\nu\text{C-O}$ )  $\text{cm}^{-1}$ .

MS ( $m/z$ ): 311.2 ( $\text{M}^+$ ), 284.4 ( $\text{M} - \text{CH}_2\text{OH}^+$ ), 282 ( $\text{M} - \text{HCN}^+$ ).

### Isomerization of 2(R)-{[(1R)-2-hydroxy-1-phenylethyl]amino}-2-[3-(trifluoromethyl)bicyclo[1.1.1]pent-1-yl]acetonitrile, **29**

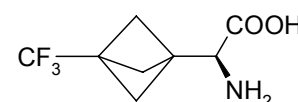
Isomer **29** was refluxed in MeOH (~10 ml MeOH per 1 g of **29**) for ~3 h. Evaporation of the solvent gave solid mixture of **29/30** (~1/4), which was separated by either column chromatography or crystallization:

Separation of **29/30** by crystallization:

- 1) Isomerized mixture **29/30** (~1/4) was crystallized from cyclohexane.
- 2) The obtained mixture **29/30** (~1/5) was crystallized from  $\text{CCl}_4$  (6 ml  $\text{CCl}_4$  per 1 g of **29/30**) to give pure **30**.
- 3) The mother liquids were collected, evaporated, isomerized in MeOH, and the formed mixture was separated by crystallization again.

### (2S)-2-Amino-2-[3-(trifluoromethyl)bicyclo[1.1.1]pent-1-yl]ethanoic acid, **20**

$\text{Pb}(\text{OAc})_4$  (0.200 mg, 0.45 mmol) was added to a solution of **30** (100 mg, 0.32 mmol) in  $\text{CH}_2\text{Cl}_2/\text{MeOH}$  (20 ml, 1/1) stirred at 0 °C. After being stirred at this temperature for 5 min, the reaction was quenched with saturated aq. solution of  $\text{NaHCO}_3$  (5 ml). The resulting insoluble material was removed by filtration and washed with  $\text{CH}_2\text{Cl}_2$  (10 ml). Organic layer was separated, and the aqueous layer was extracted with  $\text{CH}_2\text{Cl}_2$  ( $2 \times 15$  ml). The combined organic phases were evaporated in vacuum to give the Schiff base **31** as yellow oil. It was dissolved in aq. HCl (6M, 20 ml) and refluxed for 2 h. After cooling, the reaction mixture was washed with  $\text{Et}_2\text{O}$  ( $3 \times 5$  ml) and the aqueous layer was evaporated to produce a white solid. Afterwards, the residue was dissolved in  $\text{H}_2\text{O}$  (~5 ml), neutralized with aq. NaOH (0.3M) and submitted to ion exchange resin chromatography (Dowex 50  $\times$  400, cation-exchange). Elution with water followed by aq.  $\text{NH}_3$  (10%) afforded **20** (63 mg, 0.30 mmol, 95%) as a white solid. M.p. = 210-212 °C.  $[\alpha]_D^{20} = +14.0$  ( $c = 0.84$  mg/ml,  $\text{H}_2\text{O}$ ).



$^1\text{H-NMR}$  (400 MHz,  $\text{D}_2\text{O}$ ): 3.70 (s, 1H, CH); 1.94 (s, 6H,  $\text{CH}_2$ ).

$^{19}\text{F-NMR}$  (377 MHz,  $\text{D}_2\text{O}$ ): 87.66 (s,  $\text{CF}_3$ ).

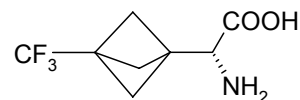
$^{13}\text{C}$ -NMR (101 MHz,  $\text{D}_2\text{O}$ ): 171.64 (s, COOH); 122.61 (q,  $\text{CF}_3$ ,  $^1J(\text{C}, \text{F}) = 274$  Hz); 54.71 (s,  $\text{CH}_2$ ); 47.75 (q, CH,  $^5J(\text{C}, \text{F}) = 2$  Hz); 37.35 (q,  $\text{CH}_2\text{CCH}$ ,  $^4J(\text{C}, \text{F}) = 2$  Hz); 36.05 (q,  $\text{CF}_3\text{C}$ ,  $^2J(\text{C}, \text{F}) = 40$  Hz).

MS (m/z): 210 ( $\text{M}^+$ ),

Elemental analysis, calculated for  $\text{C}_8\text{H}_{10}\text{F}_3\text{NO}_2$ : C, 45.94; H, 4.82; N, 6.70. Found: C, 45.78; H, 4.53; N, 6.59.

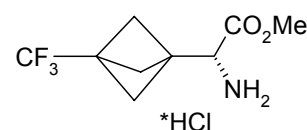
**(2R)-2-Amino-2-[3-(trifluoromethyl)bicyclo[1.1.1]pent-1-yl]ethanoic acid, 36**

**36** was synthesized from **29** analogous to **20**.



**(1R)-Bicyclo[1.1.1]pentane-1-methanaminium,  $\alpha$ -(methoxycarbonyl)-3-(trifluoromethyl), chloride, 37\*HCl**

A solution of **36** (35 mg, 0.17 mmol) in 0.25 ml MeOH was cooled to  $-20$  °C and treated with  $\text{SOCl}_2$  (27  $\mu\text{l}$ ). Cooling was stopped and the mixture was left to stir for 3 days at room temperature. Evaporation of the solvent gave **37\*HCl** as a white solid (43 mg, 0.17 mmol, 100%).

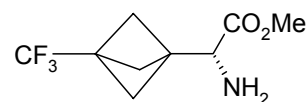


$^1\text{H}$ -NMR (400 MHz,  $\text{CD}_3\text{OD}$ ): 4.31 (s, 1H, CH); 3.87 (s, 1H,  $\text{OCH}_3$ ); 2.15-2.09 (2 d, 6H,  $\text{CH}_2$ ).

$^{19}\text{F}$ -NMR (377 MHz,  $\text{CD}_3\text{OD}$ ): 90.89 (s,  $\text{CF}_3$ ).

**(1R)-Bicyclo[1.1.1]pentane-1-acetic acid,  $\alpha$ -amino-3-(trifluoromethyl)-, methyl ester, 37**

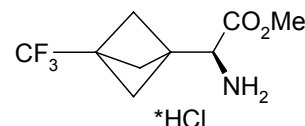
$\text{NEt}_3$  (15 mg) was added to a solution of **37\*HCl** (43 mg, 0.17 mmol) in MeOH (0.5 ml). The suspension was diluted with  $\text{Et}_2\text{O}$  (5 ml) and the formed  $\text{NEt}_3\text{*HCl}$  was removed by filtration. Evaporation of the solvent from the mother liquid gave **37** as colorless oil (29 mg, 0.14 mmol, 80%).



$^1\text{H}$ -NMR (400 MHz,  $\text{CDCl}_3$ ): 3.74 (s, 1H,  $\text{OCH}_3$ ); 3.63 (s, 1H, CH); 1.93 (s, 6H,  $\text{CH}_2$ ).

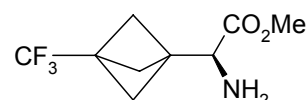
**(1S)-Bicyclo[1.1.1]pentane-1-methanaminium,  $\alpha$ -(methoxycarbonyl)-3-(trifluoromethyl), chloride, 38\*HCl**

**38\*HCl** was synthesized from **20** analogous to **37\*HCl**.



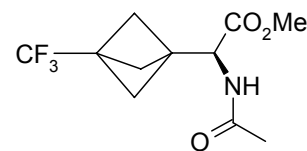
**(1S)-Bicyclo[1.1.1]pentane-1-acetic acid,  $\alpha$ -amino-3-(trifluoromethyl)-, methyl ester, 38**

**38** was synthesized from **38\*HCl** analogous to **37**.



**Methyl (2S)-2-(acetamino)-2-[3-(trifluoromethyl)bicyclo[1.1.1]pent-1-yl]acetate, 41**

NEt<sub>3</sub> (39 mg, 0.39 mmol) and CH<sub>3</sub>COCl (17 mg, 0.22 mmol) were added to a suspension of **38**\*HCl (50 mg, 0.19 mmol) in dioxane (3 ml) at once. The mixture was stirred for 15 min, diluted with water (2 ml) and extracted with CH<sub>2</sub>Cl<sub>2</sub> (3 × 10 ml). Organic phase was dried over MgSO<sub>4</sub> and evaporated. Colorless solid (40 mg, 0.15 mmol, 80%).

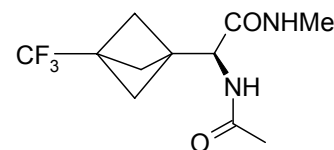


<sup>1</sup>H-NMR (400 MHz, CD<sub>3</sub>OD): 4.60 (s, 1H, CH); 3.74 (s, 3H, OCH<sub>3</sub>); 2.00-1.94 (m, 9H, CH<sub>2</sub> + CH<sub>3</sub>CO).

<sup>19</sup>F-NMR (101 MHz, CD<sub>3</sub>OD): 87.29 (s, CF<sub>3</sub>).

### (2*S*)-2-(Acetylamino)-*N*-methyl-2-[3-(trifluoromethyl)bicyclo [1.1.1]pent-1-yl]acetamide, **40**

A solution of **41** (40 mg, 0.15 mmol) in MeOH (3 ml) and 40% aq. MeNH<sub>2</sub> (1 ml) was placed into a sealed tube and heated at 100 °C for 5 h. After evaporation of the solvent the residue was purified by flash column chromatography. Elution with CH<sub>2</sub>Cl<sub>2</sub>/MeOH = 9/1 produced **40** (8 mg, 0.03 mmol, 20%) first as a colorless solid. R<sub>f</sub> = 0.7.



<sup>1</sup>H-NMR (400 MHz, CD<sub>3</sub>OD): 4.45 (s, 1H, CH); 2.73 (s, 3H, CH<sub>3</sub>NH); 2.00 (s, 3H, CH<sub>3</sub>CO); 1.94 (s, 6H, CH<sub>2</sub>).

<sup>19</sup>F-NMR (377 MHz, CD<sub>3</sub>OD): 90.85 (s, CF<sub>3</sub>).

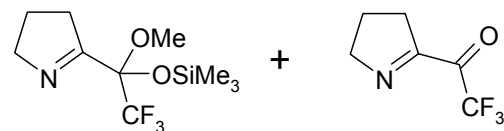
Further elution afforded CH<sub>3</sub>CONHCH<sub>3</sub> as a colorless solid. R<sub>f</sub> = 0.6.

<sup>1</sup>H-NMR (400 MHz, CD<sub>3</sub>OD): 2.69 (s, 3H, CH<sub>3</sub>NH); 1.91 (s, 3H, CH<sub>3</sub>CO).

### 3,4-Dihydro-5-[2,2,2-trifluoro-1-methoxy-1-[(trimethylsilyl)oxy]ethyl]-2*H*-pyrrole, **55**

#### 1-(3,4-Dihydro-2*H*-pyrrol-5-yl)-2,2,2-trifluoro-1-ethanone, **56**

NH<sub>4</sub>F (430 mg, 4.8 mmol) was activated at 120-130 °C in vacuum over 2 h. After cooling to room temperature a solution of **54** (600 mg, 4.8 mmol) in THF (40 ml) was added. Thereafter, to the formed suspension CF<sub>3</sub>SiMe<sub>3</sub> (738 mg, 5.4 mmol) was added dropwise at -60 °C and the reaction was stirred at this temperature for additional 2 h. After warming to room temperature the mixture was diluted with water (40 ml), extracted with CH<sub>2</sub>Cl<sub>2</sub> (3 × 50 ml) and dried over MgSO<sub>4</sub>. Evaporation of the solvent afforded 720 mg of oily material.



In GC-MS chromatogram of the obtained mixture 3 peaks were visible:

1 peak, **56**: 165 (M)<sup>+</sup>, 137 (M-CH<sub>2</sub>N)<sup>+</sup>, 96 (M-CF<sub>3</sub>)<sup>+</sup>, 69 (CF<sub>3</sub>)<sup>+</sup>, 68 (M-CF<sub>3</sub>CO)<sup>+</sup>.

2 peak, **55**: 254 (M-Me)<sup>+</sup>, 254 (M-CF<sub>3</sub>)<sup>+</sup>, 96, 73 (SiMe<sub>3</sub>)<sup>+</sup>.

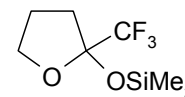
3 peak, unidentified compound: 195, 163, 128, 96.

If the reaction mixture was quenched with 1M HCl (instead of H<sub>2</sub>O) <sup>1</sup>H-NMR spectrum became significantly simpler and contained predominantly signals of **57**.

<sup>1</sup>H-NMR (400 MHz, CD<sub>3</sub>OD): 4.33-4.25 (m, 2H); 2.98-2.90 (m, 2H); 2.47-2.38 (m, 2H).

**Trimethyl[[tetrahydro-2-(trifluoromethyl)-2-furanyl]oxy]-silane, 58**

CsF (2.63 g, 17,3 mmol) was activated at 120-130 °C in vacuum over 2 h. After cooling to room temperature a solution of  $\gamma$ -butyrolactone (20.8 g, 220 mmol) in THF (80 ml) was added. The resulting suspension was cooled to -10 °C, and  $\text{CF}_3\text{SiMe}_3$  (37.5 g, 264 mmol) was added dropwise afterwards. The cooling was stopped and the mixture was stirred for 20 h at room temperature. CsF was filtered off, solvent was evaporated and the residue was distilled (20 mm, 55-65 °C) to produce **57** (36.7 g, 74%).

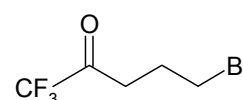


$^1\text{H-NMR}$  (400 MHz,  $\text{CDCl}_3$ ): 4.17-4.11 (m, 1H, 4- $\text{CH}_2$ ); 3.94-3.86 (m, 1H, 4- $\text{CH}_2$ ); 2.28-2.20 (m, 1H, 3- $\text{CH}_2$ ); 2.11-1.93 (m, 1H from 3- $\text{CH}_2$  and 2H from 4- $\text{CH}_2$ ); 0.14 (s, 9H,  $\text{Si}(\text{CH}_3)_3$ ).

$^{19}\text{F-NMR}$  (377 MHz,  $\text{CDCl}_3$ ): 78.52 (s,  $\text{CF}_3$ ).

**1-Bromo-5,5,5-reifluoropentane-4-on, 57**

To the solution, obtained after dissolving Zn (27 mg, 0,4 mmol) in 48% aq. HBr (10 ml), **58** (4.5 g, 20 mmol) was added. The mixture was refluxed over 78 h, cooled, diluted with water and extracted with EtOAc. Organic phase was dried over  $\text{MgSO}_4$ , concentrated and redistilled in vacuum (20 mm, 65-75 °C). Colorless liquid (1.7 g, 3 mmol, 15%).

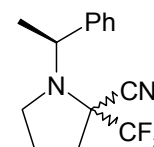


$^1\text{H-NMR}$  (400 MHz,  $\text{CDCl}_3$ ): 3.46 (t,  $^3J(\text{H}, \text{H}) = 6.0$  Hz, 2H,  $\text{CH}_2\text{Br}$ ); 2.94 (t,  $^3J(\text{H}, \text{H}) = 6.8$  Hz, 2H,  $\text{C}(\text{O})\text{CH}_2$ ); 2.23 (m, 2H,  $\text{CH}_2\text{CH}_2\text{Br}$ ).

$^{19}\text{F-NMR}$  (377 MHz,  $\text{CDCl}_3$ ): 82.64 (s,  $\text{CF}_3$ ).

**(2RS)-1-[(1S)-1-Phenylethyl]-2-(trifluoromethyl)pirrolidine-carbonitrile, 61(a,b)****1-[2-(Trifluoromethyl)tetrahydrofuran-2-yl]acetone, 62**

Aminonitrile **60** (0.62 g, 3.3 mmol) was added to a solution of **57** (0,65 g, 3.0 mmol) in  $\text{CH}_3\text{CN}$  (5 ml). The mixture obtained was refluxed for 12 h, then poured into excess of 10% sodium hydroxide solution and extracted with dichloromethane. The combined extracts were dried ( $\text{MgSO}_4$ ) and evaporated under reduced pressure. The residue was purified (eluent - hexane/EtOAc = 20/1) by flash column chromatography to produce **61a** (7 mg, 0.03 mmol, 1%) first (configuration is not confirmed).  $R_f = 0.60$ .



$^1\text{H-NMR}$  (400 MHz,  $\text{CDCl}_3$ ): 7.13-7.24 (m, 5H, Ph); 4.44 (q,  $^3J(\text{H}, \text{H}) = 6.8$  Hz, 1H,  $\text{CHCH}_3$ ); 2.89 (q,  $^3J(\text{H}, \text{H}) = 7.2$  Hz, 1H, 5- $\text{CH}_2$ ); 2.75 (m, 1H, 5- $\text{CH}_2$ ); 2.39 and 2.32 (m, 2H, 3- $\text{CH}_2$ ); 1.78 (m, 2H, 4- $\text{CH}_2$ ); 1.49 (d,  $^3J(\text{H}, \text{H}) = 6.8$  Hz, 3H,  $\text{CHCH}_3$ ).

$^{19}\text{F-NMR}$  (377 MHz,  $\text{CDCl}_3$ ): 84.6 (s,  $\text{CF}_3$ ).

$^{13}\text{C-NMR}$  (101 MHz,  $\text{CDCl}_3$ ): 143.2 (s, ipso-C, Ph); 131.0 (q,  $^1J(\text{C}, \text{F}) = 252$  Hz,  $\text{CF}_3$ ); 128.3 (s, CH, Ph); 126.9 (s, CH, Ph); 126.5 (s, CH, Ph); 117.2 (s, CN); 68.2 (s, 2-C); 55.5 (s,  $\text{CHCH}_3$ ); 45.3 (s, 5- $\text{CH}_2$ ); 35.7 (s, 3- $\text{CH}_2$ ); 23.0 ( $\text{CH}_3$ ); 14.7 (s, 4- $\text{CH}_2$ ).

IR (neat): 2232 ( $\nu \text{C}\equiv\text{N}$ )  $\text{cm}^{-1}$ .

MS ( $m/z$ ): 268 ( $\text{M}^+$ ), 105 ( $\text{PhCHCH}_3^+$ ).

Next fraction was a mixture of **61a/61b** = 0.8/1.  $R_f = 0.57$ .

$^1\text{H-NMR}$  (400 MHz,  $\text{CDCl}_3$ ): 7.24-7.13 (m, 5H, Ph from **61a** and 5H, Ph from **61b**); 4.44  $^3J(\text{H}, \text{H}) = 6.8$  Hz, 1H,  $\text{CHCH}_3$  from **61a**); 4.30 (q,  $^3J(\text{H}, \text{H}) = 6.8$  Hz, 1H,

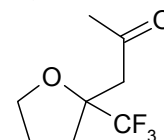


CHCH<sub>3</sub> from 61b); 3.31 (m, 1H, 5-CH<sub>2</sub>, from 61b); 2.89 (m, 1H, 5-CH<sub>2</sub> from 61a and 1H, 5-CH<sub>2</sub> from 61b); 2.75 (m, 1H, 5-CH<sub>2</sub> from 61a); 2.31-2.39 (m, 2H, 3-CH<sub>2</sub> from 61a and 2H, 3-CH<sub>2</sub> from 61b); 1.90 (m, 1H, 4-CH<sub>2</sub> from 61b); 1.78-1.65 (m, 2H, 4-CH<sub>2</sub> from 61a and 1H, 4-CH<sub>2</sub> from 61b); 1.49 (d, <sup>3</sup>J(H, H) = 6.8 Hz, 3H, CHCH<sub>3</sub> from 61a); 1.37 (d, <sup>3</sup>J(H, H) = 6.8 Hz, 3H, CHCH<sub>3</sub> from 61b).

<sup>19</sup>F-NMR (377 MHz, CDCl<sub>3</sub>): 85.1 (s, CF<sub>3</sub> from 61b); 84.6 (s, CF<sub>3</sub> from 61a).

Third fraction: **62** (20 mg, 0.15 mmol, 5%). R<sub>f</sub> = 0.30.

<sup>1</sup>H-NMR (400 MHz, CDCl<sub>3</sub>): 3.85 (d, *J* = 7.2 Hz, 2H, OCH<sub>2</sub>); 2.88 (d, <sup>2</sup>J(H, H) = 14.4 Hz, 1H, CH<sub>2</sub>CO); 2.41 (d, <sup>2</sup>J(H, H) = 14.4 Hz, 1H, CH<sub>2</sub>CO); 2.34 (m, 1H); 2.11 (s, 3H, CH<sub>3</sub>); 2.05 (m, 1H); 1.94 (m, 2H).



<sup>19</sup>F-NMR (377 MHz, CDCl<sub>3</sub>): 84.7 (s, CF<sub>3</sub>).

<sup>13</sup>C-NMR (101 MHz, CDCl<sub>3</sub>): 201.2 (s, C=O); 124.6 (q, <sup>1</sup>J(C, F) = 281.5 Hz, CF<sub>3</sub>); 81.9 (q, <sup>2</sup>J(C, F) = 27.6 Hz, CCF<sub>3</sub>); 69.2 (OCH<sub>2</sub>); 43.2 (s, CH<sub>2</sub>); 31.1 (CH<sub>3</sub>); 28.5 (s, CH<sub>2</sub>); 24.6 (s, CH<sub>2</sub>).

IR (neat): 1716 (ν C=O) cm<sup>-1</sup>.

MS (m/z): 127 (M-CF<sub>3</sub>)<sup>+</sup>, 69 (CF<sub>3</sub>)<sup>+</sup>, 43 (CH<sub>3</sub>CO)<sup>+</sup>.

### Cyclopropanation of 75-79. General procedure

Diazotrifluoroethane, obtained in a generator flask by reaction of CF<sub>3</sub>CH<sub>2</sub>NH<sub>2</sub>\*HCl (1 eq) with NaNO<sub>2</sub> (1 eq), was gradually blown off by an inert gas through a drying tube (MgSO<sub>4</sub>) into a vessel equipped with a condenser. The vessel contained a stirring mixture of alkene and the catalyst (10 mol %) (in the case of **79**, CH<sub>2</sub>Cl<sub>2</sub> was used as a solvent). The mixture Ar/CF<sub>3</sub>CHN<sub>2</sub> was blowing through an inlet in such a way, that it passed through the stirring mixture. To achieve a full reaction conversion a large excess of CF<sub>3</sub>CHN<sub>2</sub> was used. Otherwise, the starting material could be removed by treating the mixture with acidic (pH ~5) 5% aq. KMnO<sub>4</sub> solution and subsequent extraction of the cyclopropane derivatives with CH<sub>2</sub>Cl<sub>2</sub>.

The products **75-78(a,b)** were isolated by distillation, and afterwards isomers **75(a,b)** and **76(a,b)** were separated by flash column chromatography. High volatility of **77(a,b)** and **78(a,b)** hindered their preparative separation. Products **79(a,b)** were isolated chromatographically.

#### 1-[(1*SR*,2*SR*)-2-(Trifluoromethyl)cyclopropyl]benzene, (±)**75a**

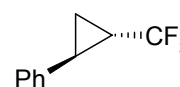
#### 1-[(1*RS*,2*SR*)-2-(Trifluoromethyl)cyclopropyl]benzene, (±)**75b**

Catalyst - Rh<sub>2</sub>(OAc)<sub>4</sub>. B.p. of the mixture (±)**75(a,b)** = 75-80 °C (20 mm).

**75a/75b** = 2/1.

(±)**75a**: R<sub>f</sub> = 0.7 in pentane/Et<sub>2</sub>O = 2/1.

<sup>1</sup>H-NMR (400 MHz, CDCl<sub>3</sub>): 7.32 (t, <sup>3</sup>J(H, H) = 7.6 Hz, 2H, Ph); 7.25 (t, <sup>3</sup>J(H, H) = 7.6 Hz, 1H, Ph); 7.16 (d, <sup>3</sup>J(H, H) = 7.6 Hz, 2H, Ph); 2.44 (dt, <sup>3</sup>J(H, H) = 9.2 Hz, 1H, PhCH); 1.87 (m, 1H, CF<sub>3</sub>CH); 1.46 (dt, <sup>2,3</sup>J(H, H) = 9.6, 5.6 Hz, 1H, CH<sub>2</sub>); 1.25 (m, 1H, CH<sub>2</sub>).



<sup>19</sup>F-NMR (377 MHz, CDCl<sub>3</sub>): 94.92 (d, <sup>3</sup>J(H, F) = 7.5 Hz, CF<sub>3</sub>).

$^{13}\text{C}$ -NMR (101 MHz,  $\text{CDCl}_3$ ): 139.24 (s, ipso-C, Ph); 129.64 (s, CH, Ph); 128.82 (s, CH, Ph); 128.35 (s, CH, Ph); 123.68 (q,  $^1J(\text{C}, \text{F}) = 220.5$  Hz,  $\text{CF}_3$ ); 23.14 (q,  $^2J(\text{C}, \text{F}) = 37.3$  Hz,  $\text{CF}_3\text{CH}$ ); 19.78 (q,  $^3J(\text{C}, \text{F}) = 3.2$  Hz, PhCH); 11.06 (q,  $^3J(\text{C}, \text{F}) = 3.2$  Hz,  $\text{CH}_2$ ).

MS (m/z): 206 ( $\text{M}$ )<sup>+</sup>.

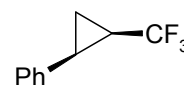
(±)**75b**:  $R_f = 0.5$  (pentane/ $\text{Et}_2\text{O} = 2/1$ ).

$^1\text{H}$ -NMR (400 MHz,  $\text{CDCl}_3$ ): 7.33 (d,  $^3J(\text{H}, \text{H}) = 4.4$  Hz, 4H, Ph); 7.27 (m, 1H, Ph); 2.54 (dt,  $^3J(\text{H}, \text{H}) = 8.4, 8.0$  Hz, 1H, PhCH); 1.91 (m, 1H,  $\text{CF}_3\text{CH}$ ); 1.51 (dd,  $^{2,3}J(\text{H}, \text{H}) = 7.2, 5.6$  Hz, 1H,  $\text{CH}_2$ ); 1.35 (m, 1H,  $\text{CH}_2$ ).

$^{19}\text{F}$ -NMR (377 MHz,  $\text{CDCl}_3$ ): 100.59 (d,  $^3J(\text{H}, \text{F}) = 7.5$  Hz,  $\text{CF}_3$ ).

$^{13}\text{C}$ -NMR (101 MHz,  $\text{CDCl}_3$ ): 135.49 (s, Ph); 133.10 (q,  $^1J(\text{C}, \text{F}) = 221.5$  Hz,  $\text{CF}_3$ ); 127.14 (s, Ph); 126.99 (s, Ph); 126.71 (s, Ph); 20.71 (q,  $^3J(\text{C}, \text{F}) = 3.2$  Hz, Ph-CH); 20.45 (q,  $^2J(\text{C}, \text{F}) = 35.2$  Hz,  $\text{CF}_3\text{CH}$ ); 6.63 (q,  $^3J(\text{C}, \text{F}) = 3.2$  Hz,  $\text{CH}_2$ ).

MS (m/z): 206 ( $\text{M}$ )<sup>+</sup>.



**(1RS,6RS,7RS)-7-(Trifluoromethyl)-2-oxabicyclo[4.1.0]heptane, (±)76a**

**(1SR,6SR,7RS)-7-(Trifluoromethyl)-2-oxabicyclo[4.1.0]heptane, (±)76b**

Catalyst -  $\text{Rh}_2(\text{OAc})_4$ . B.p. of the mixture (±)**76(a,b)** = 50-55 °C (20 mm).

**76a/76b** = 2/1.

(±)**76a**:  $R_f = 0.8$  in pentane/ $\text{Et}_2\text{O} = 2/1$ .

$^1\text{H}$ -NMR (400 MHz,  $\text{CDCl}_3$ ): 3.72 (dd,  $^3J(\text{H}, \text{H}) = 7.6, 2.0$  Hz, 1H, 1-CH); 3.57 (dtd,  $^{2,3}J(\text{H}, \text{H}) = 11.2, 3.2, 1.2$  Hz, 1H, 3- $\text{CH}_2$ ); 3.28 (td,  $^{2,3}J(\text{H}, \text{H}) = 11.2, 1.6$  Hz, 1H, 3- $\text{CH}_2$ ); 2.06 (dd,  $^{2,3}J(\text{H}, \text{H}) = 14.0, 4.8$  Hz, 1H, 5- $\text{CH}_2$ ); 1.98 (m, 1H, 5- $\text{CH}_2$ ); 1.55 (m, 2H, 4- $\text{CH}_2$  and 6-CH); 1.44 (m, 2H, 4- $\text{CH}_2$  and 7-CH).

$^{19}\text{F}$ -NMR (377 MHz,  $\text{CDCl}_3$ ): 96.61 (d,  $^3J(\text{H}, \text{F}) = 7.5$  Hz,  $\text{CF}_3$ ).

$^{13}\text{C}$ -NMR (101 MHz,  $\text{CDCl}_3$ ): 125.20 (q,  $^1J(\text{C}, \text{F}) = 270.4$  Hz,  $\text{CF}_3$ ); 64.08 (s, 3- $\text{CH}_2$ ); 53.02 (q,  $^3J(\text{C}, \text{F}) = 2.5$  Hz, 1-CH); 25.24 (q,  $^2J(\text{C}, \text{F}) = 35.2$  Hz, 7-CH); 21.83 (s, 5- $\text{CH}_2$ ); 20.32 (s, 4- $\text{CH}_2$ ); 14.89 (s, 6-CH).

MS (m/z): 166 ( $\text{M}$ )<sup>+</sup>.

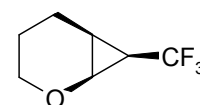
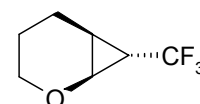
(±)**76b**:  $R_f = 0.6$  pentane/ $\text{Et}_2\text{O} = 2/1$ .

$^1\text{H}$ -NMR (400 MHz,  $\text{CDCl}_3$ ): 3.70 (m, 2H, 1-CH and 3- $\text{CH}_2$ ); 3.29 (td,  $^{2,3}J(\text{H}, \text{H}) = 11.4, 2.0$  Hz, 1H, 3- $\text{CH}_2$ ); 2.06 (m, 2H, 5- $\text{CH}_2$ ); 1.73 (m, 1H, 4- $\text{CH}_2$ ); 1.46 (m, 1H, 4- $\text{CH}_2$ ); 1.28 (m, 2H, 6-CH and 7-CH).

$^{19}\text{F}$ -NMR (377 MHz,  $\text{CDCl}_3$ ): 106.27 (d,  $^3J(\text{H}, \text{F}) = 7.5$  Hz,  $\text{CF}_3$ ).

$^{13}\text{C}$ -NMR (101 MHz,  $\text{CDCl}_3$ ): 126.00 (q,  $^1J(\text{C}, \text{F}) = 270.4$  Hz,  $\text{CF}_3$ ); 64.19 (s, 3- $\text{CH}_2$ ); 51.91 (bs, 1-CH); 22.40 (q,  $^2J(\text{C}, \text{F}) = 35.2$  Hz, 7-CH); 20.25 (s, 5- $\text{CH}_2$ ); 14.17 (s, 4- $\text{CH}_2$ ); 12.49 (s, 6-CH).

MS (m/z): 166 ( $\text{M}$ )<sup>+</sup>.

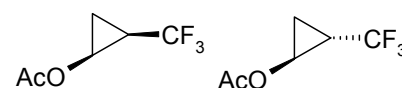


**2-(Trifluoromethyl)cyclopropylacetate, (±)77(a,b)**

Catalyst -  $\text{Rh}_2(\text{OAc})_4$ . B.p. of the mixture (±)**77(a,b)** = 60-70 °C (200 mm).

**77a/77b** = 1.8/1.0.

$^1\text{H}$ -NMR (400 MHz,  $\text{CDCl}_3$ ): 4.40 (m, 1H, 1-CH from 77a and 1H, 1-CH from 77b); 2.13 (s, 3H,  $\text{CH}_3$  from



77b); 2.10 (s, 3H,  $CH_3$  from 77a); 1.90 (m, 1H, 2- $CH$  from 77a); 1.76 (m, 1H, 2- $CH$  from 77b); 1.45-1.20 (m, 2H, 3- $CH_2$  from 77a and 2H, 3- $CH_2$  from 77b).

$^{19}F$ -NMR (377 MHz,  $CDCl_3$ ): 100.84 (d,  $^3J(H, F) = 7.5$  Hz,  $CF_3$  from 77b); 95.84 (d,  $^3J(H, F) = 7.5$  Hz,  $CF_3$  from 77a).

$^{13}C$ -NMR (101 MHz,  $CDCl_3$ ): 170.09 (s,  $CH_3COO$  from 77b); 169.59 (s,  $CH_3COO$  from 77a); 125.12 (q,  $^1J(C, F) = 271.1$  Hz,  $CF_3$  from 77b); 124.76 (q,  $^1J(C, F) = 270.1$  Hz,  $CF_3$  from 77a); 49.07-48.96 (2 overlapped q,  $^3J(C, F) = 4.0$  Hz, O- $CH$ ); 20.10 (s,  $CH_3$  from 77a); 20.09 (s,  $CH_3$  from 77b); 19.95 (q,  $^2J(C, F) = 37.1$  Hz,  $CCF_3$  from 77a); 20.37 (q,  $^2J(C, F) = 36.1$  Hz,  $CCF_3$  from 77b); 9.06 (q,  $^3J(C, F) = 3.1$  Hz,  $CH_2$  from 77a); 8.07 (q,  $^3J(C, F) = 3.1$  Hz,  $CH_2$  from 77b).

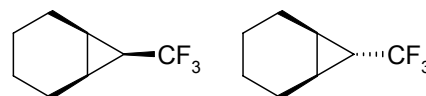
MS (m/z): 168 (M) $^+$ .

### 7-(Trifluoromethyl)bicyclo [4.1.0]heptane, ( $\pm$ )78(a,b)

Catalyst -  $CuOTf \cdot 0.5C_6H_6$ . B.p. of the mixture ( $\pm$ )78(a,b) = 60-70 °C (100 mm). 78a/78b = 2/1.

$^1H$ -NMR (400 MHz,  $CDCl_3$ ): 2.05-1.97 (m, 4H,  $CH_2$ ); 1.65-1.33 (m, 6H,  $CH_2+CH$ ); 1.42-1.30 (m, 2H, 7- $CH$ ).

$^{19}F$ -NMR (377 MHz,  $CDCl_3$ ): 100.57 (d,  $^3J(H, F) = 7.5$  Hz,  $CF_3$  from 78b); 95.59 (d,  $^3J(H, F) = 7.5$  Hz,  $CF_3$  from 78a).



MS (m/z): 164 (M) $^+$ .

**Methyl (1*RS*,2*RS*)-1-(acetylamino)-2-(trifluoro-methyl)cyclopropane-carboxylate, ( $\pm$ )79a**

**Methyl (1*RS*,2*SR*)-1-(acetylamino)-2-(trifluoro-methyl)cyclopropane-carboxylate, ( $\pm$ )79b**

The reaction was carried out in  $CH_2Cl_2$ . Catalyst  $Rh_2(OAc)_4$ .

79a/79b = 1/1.

( $\pm$ )79a:  $R_f = 0.4$  in  $CH_2Cl_2/MeOH = 5/1$ .

$^1H$ -NMR (400 MHz,  $CDCl_3$ , rotamers): 6.31 (2 bs, 1H,  $NH$ ); 3.70 (2 s, 3H,  $OCH_3$ ); 2.12 (m, 1H,  $CF_3CH$ ); 1.92 (2 s, 3H,  $CH_3CO$ ); 1.61 (m, 1H,  $CH_2$ ); 1.42 (m, 1H,  $CH_2$ ).

$^{19}F$ -NMR (377 MHz,  $CDCl_3$ ): 101.41 (d,  $^3J(H, F) = 7.5$  Hz,  $CF_3$ ).

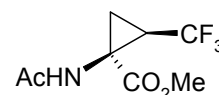
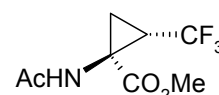
MS (m/z): 204 (M+1) $^+$ .

( $\pm$ )79b:  $R_f = 0.35$  ( $CH_2Cl_2/MeOH = 5/1$ ).

$^1H$ -NMR (400 MHz,  $CDCl_3$ ): 5.86 (bs, 1H,  $NH$ ); 3.68 (s, 3H,  $OCH_3$ ); 2.40 (m, 1H,  $CF_3CH$ ); 1.97 (bs, 4H,  $CH_3CO$  and  $CH_2$ ); 1.68 (t,  $^{2,3}J(H, H) = 6.8$  Hz, 1H,  $CH_2$ ).

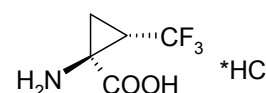
$^{19}F$ -NMR (377 MHz,  $CDCl_3$ ): 100.07 (d,  $^3J(H, F) = 7.5$  Hz,  $CF_3$ ).

MS (m/z): 204 (M+1) $^+$ .



### ( $\pm$ )-Trifluoronorcoronamic acid hydrochloride, ( $\pm$ )82a

A solution of ( $\pm$ )79a in 6M HCl was heated to 80 °C over 30 h ( $^{19}F$ -NMR control). Evaporation of the solvent gave ( $\pm$ )82a as a white solid (quant.).



$^1\text{H-NMR}$  (400 MHz,  $\text{D}_2\text{O}$ ): 2.35 (m, 1H,  $\text{CF}_3\text{CH}$ ); 2.92 (bs, 1H,  $\text{CH}_2$ ); 1.61 (bs, 1H,  $\text{CH}_2$ ).

$^{19}\text{F-NMR}$  (377 MHz,  $\text{CD}_3\text{OD}$ ): 104.56 (d,  $^3J(\text{H}, \text{F}) = 7.5$  Hz,  $\text{CF}_3$ ).

MS ( $m/z$ ): 170 ( $\text{M-Cl}$ ) $^+$ .

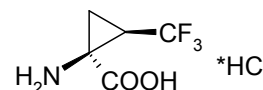
**(±)-Trifluoro-*allo*-norcoronamic acid hydrochloride, (±)82b**

Compound (±)**82b** was synthesized from (±)**79b** analogous to (±)**82a**.

$^1\text{H-NMR}$  (400 MHz,  $\text{D}_2\text{O}$ ): 2.75 (m, 1H,  $\text{CF}_3\text{CH}$ ); 1.93 (t,  $^{2,3}J(\text{H}, \text{H}) = 9.2$  Hz, 1H,  $\text{CH}_2$ ); 1.87 (t,  $^{2,3}J(\text{H}, \text{H}) = 9.2$  Hz, 1H,  $\text{CH}_2$ ).

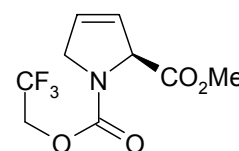
$^{19}\text{F-NMR}$  (377 MHz,  $\text{CD}_3\text{OD}$ ): 102.33 (d,  $^3J(\text{H}, \text{F}) = 7.5$  Hz,  $\text{CF}_3$ ).

MS ( $m/z$ ): 170 ( $\text{M-Cl}$ ) $^+$ .



**2-Methyl 1-(2,2,2-trifluoroethyl) 2,5-dihydro-1*H*-pyrrole-1,2-dicarboxylate, 83**

An excess of trifluoromethyldiazomethane, obtained in a generator flask by reaction of  $\text{CF}_3\text{CH}_2\text{NH}_2 \cdot \text{HCl}$  with  $\text{NaNO}_2$  was gradually blown off by an inert gas through a drying tube ( $\text{MgSO}_4$ ) into a vessel, equipped with a condenser. The vessel contained a stirring solution of **72** (1.00 g, 4.41 mmol) and anhydrous  $\text{CuCl}$  (500 mg) in hexane. The mixture  $\text{Ar}/\text{CF}_3\text{CHN}_2$  was blowing through an inlet such a way, that it passed through a stirring solution. After 5 eq of  $\text{CF}_3\text{CH}_2\text{NH}_2 \cdot \text{HCl}$  had been used, the reaction was stopped; the conversion of **72** was 30%. The mixture was diluted with  $\text{CH}_2\text{Cl}_2$  and filtered. The filtrate was concentrated in vacuum and the residue was purified by flash chromatography. Elution with hexane/ $\text{EtOAc} = 10/1$  afforded starting material **72** first ( $R_f = 0.4$  in hexane/ $\text{EtOAc} = 4/1$ ) and then **83** (0.29 g, 1.15 mmol, 26%) as a colorless viscous oil ( $R_f = 0.35$  in hexane/ $\text{EtOAc} = 4/1$ ).



$^1\text{H-NMR}$  (400 MHz,  $\text{CDCl}_3$ , rotamers): 6.02 (m, 1H, 3- $\text{CH}$ ); 5.79 (m, 1H, 4- $\text{CH}$ ); 5.03 (m, 1H, 2- $\text{CH}$ ); 4.60 (m, 1H,  $\text{OCH}_2\text{CF}_3$ ); 4.37 (m, 3H,  $\text{OCH}_2\text{CF}_3 + 5\text{-CH}_2$ ); 3.77, 3.74 (2 s, 3H,  $\text{OCH}_3$ ).

$^{19}\text{F-NMR}$  (377 MHz,  $\text{CDCl}_3$ , rotamers): 87.70, 87.52 (2 t,  $^3J(\text{F}, \text{H}) = 7.5$  Hz,  $\text{CF}_3$ ).

$^{13}\text{C-NMR}$  (126 MHz,  $\text{CDCl}_3$ , rotamers): 170.02, 169.81 (2 s,  $\text{COOCH}_3$ ); 152.52, 152.01 (2 s,  $\text{NCO}$ ), 129.00, 128.78 (2 s, 3- $\text{CH}$ ); 125.22, 125.05 (2 s, 4- $\text{CH}$ ); 130.8 (q,  $^1J(\text{C}, \text{F}) = 267.1$  Hz,  $\text{CF}_3$ ); 66.74, 66.22 (2 s, 2- $\text{CH}$ ); 61.49, 61.36 (2 q,  $^2J(\text{C}, \text{F}) = 37.8$  and  $35.2$  Hz,  $\text{OCH}_2\text{CF}_3$ ); 54.42, 53.53 (2 s, 5- $\text{CH}_2$ ); 52.35 (s,  $\text{OCH}_3$ ).

IR (neat): 1735 ( $\nu\text{C=O}$ )  $\text{cm}^{-1}$ .

MS ( $m/z$ ): 254 ( $\text{M}+1$ ) $^+$ .

**2-Methyl 3-(2,2,2-trifluoroethyl) (1*R*,2*S*,5*S*,6*R*)-6-(trifluoromethyl)-3-azabicyclo[3.1.0]hexane-2,3-dicarboxylate, 84a**

**2-Methyl 3-(2,2,2-trifluoroethyl) (1*S*,2*S*,5*R*,6*S*)-6-(trifluoromethyl)-3-azabicyclo[3.1.0]hexane-2,3-dicarboxylate, 84b**

An excess of  $\text{CF}_3\text{CHN}_2$  (obtained as described above) was gradually blown off by an inert gas and passed through a drying tube ( $\text{MgSO}_4$ ) into a vessel containing a stirring mixture of **72** (4.00 g, 17.62 mmol) and  $\text{CuOTf} \cdot 0.5\text{C}_6\text{H}_6$  (500 mg). The formed black tarry oil, consisted of **84a**, **84b** and side products, was dissolved in

CH<sub>2</sub>Cl<sub>2</sub> and triturated with acidic (pH ~5) 5% aq. solution of KMnO<sub>4</sub> (to remove compounds possessing C=C double bond). Water phase was separated and washed twice with CH<sub>2</sub>Cl<sub>2</sub>. Organic phases were combined, dried over MgSO<sub>4</sub>, and evaporated. The residue was dissolved in CH<sub>2</sub>Cl<sub>2</sub>/TFA (1/4) mixture and stirred for 2 h (to remove compounds possessing Boc-groups). Finally, the solution was evaporated and the residue was purified by flash chromatography. Elution with hexane/EtOAc = 20/1 afforded **84a** first (590 mg, 1.76 mmol, 10%) as a yellowish oil. R<sub>f</sub> = 0.5 in hexane/EtOAc = 5/1.

<sup>1</sup>H-NMR (400 MHz, CDCl<sub>3</sub>, rotamers): 4.46 (m, 1H, OCH<sub>2</sub>CF<sub>3</sub>); 4.43, 4.42 (2 s, 1H, 2-CH); 4.30 (m, 1H, OCH<sub>2</sub>CF<sub>3</sub>); 3.76 (m, 1H, 4-CH<sub>2</sub>); 3.74-3.72 (2 s, 3H, OCH<sub>3</sub>); 3.71, 3.68 (2 d, <sup>3</sup>J(H, H) = 4.0 Hz, 1H, 4-CH<sub>2</sub>); 2.13 (td, <sup>3</sup>J(H, H) = 8.0, 3.2 Hz, 1H, 1-CH); 2.02 (m, 1H, 5-CH); 1.52 (m, 1H, 6-CH).

<sup>19</sup>F-NMR (377 MHz, CDCl<sub>3</sub>, rotamers): 96.54, 96.50 (2 d, <sup>3</sup>J(F, H) = 7.5 Hz, 3F, CHCF<sub>3</sub>); 87.54, 87.45 (2 t, <sup>3</sup>J(F, H) = 7.5 Hz, 3F, OCH<sub>2</sub>CF<sub>3</sub>).

IR (neat): 1758 (ν C=O in COOMe), 1741 (ν C=O in NCOOCH<sub>2</sub>CF<sub>3</sub>) cm<sup>-1</sup>.

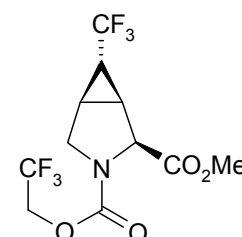
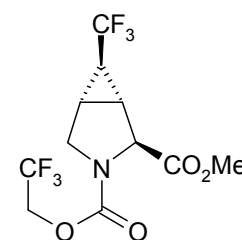
MS (m/z): 336 (M+1)<sup>+</sup>.

Further elution gave the isomer **84b** (240 mg, 0.88 mmol, 5%) as a yellowish oil. R<sub>f</sub> = 0.4 in hexane/EtOAc = 5/1.

<sup>1</sup>H-NMR (400 MHz, CDCl<sub>3</sub>, rotamers): 4.53 (m, 1H, OCH<sub>2</sub>CF<sub>3</sub>); 4.43, 4.40 (2 d, <sup>3</sup>J(H, H) = 4.8 Hz, 1H, 2-CH); 4.30 (m, 1H, OCH<sub>2</sub>CF<sub>3</sub>); 3.81 (m, 1H, 4-CH<sub>2</sub>); 3.77, 3.75 (2 s, 3H, OCH<sub>3</sub>); 3.69 (m, 1H, 4-CH<sub>2</sub>); 2.26 (m, 1H, 1-CH); 2.07 (m, 1H, 5-CH); 2.20 (m, 1H, 6-CH).

<sup>19</sup>F-NMR (377 MHz, CDCl<sub>3</sub>, rotamers): 96.02 (d, <sup>3</sup>J(F, H) = 7.5 Hz, 3F, CHCF<sub>3</sub>), 87.67, 87.57 (2 t, <sup>3</sup>J(F, H) = 7.5 Hz, 3F, OCH<sub>2</sub>CF<sub>3</sub>).

MS (m/z): 336 (M+1)<sup>+</sup>.



### (1R,2S,5S,6R)-6-(Trifluoromethyl)-3-azabicyclo[3.1.0]hexane-2-carboxylic acid, **49a**

A solution of **84a** (500 mg, 1.49 mmol) in aq. HBr (36%, 10 ml) was refluxed for 6 h and evaporated. The black tarry residue was redissolved in H<sub>2</sub>O (~1 ml), neutralized with aq. NaOH (0.3M) to pH ~9 and submitted to an ion exchange column chromatography (Dowex 50 × 400). Elution with water followed by aq. pyridine (10%) afforded **49a** (145 mg, 0.75 mmol, 50%) first as a yellowish amorphous solid (116 mg, 0.60 mmol, yield 40%, purity 90%). [α]<sub>D</sub><sup>20</sup> = -23.3 (c = 0.167 mg/ml, MeOH).

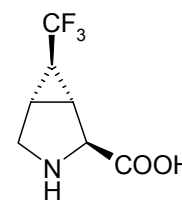
<sup>1</sup>H-NMR (400 MHz, D<sub>2</sub>O): 4.32 (s, 1H, 2-CH); 3.69 (dd, <sup>2,3</sup>J(H, H) = 12.0, 3.6 Hz, 1H, 4-CH<sub>2</sub>); 3.53 (d, <sup>2</sup>J(H, H) = 12.0, 1H, 4-CH<sub>2</sub>); 2.51 (dd, 1H, <sup>3</sup>J(H, H) = 7.8, 3.6 Hz, 1-CH); 2.35 (dt, 1H, <sup>3</sup>J(H, H) = 7.8, 3.6 Hz, 5-CH); 1.81 (m, 1H, 6-CH).

<sup>19</sup>F-NMR (377 MHz, CD<sub>3</sub>OD): 95.48 (d, <sup>3</sup>J(H, F) = 3.8 Hz, CF<sub>3</sub>).

IR (KBr): 1617 (ν<sub>as</sub> COO<sup>-</sup>), 1386 (ν<sub>s</sub> COO<sup>-</sup>) cm<sup>-1</sup>.

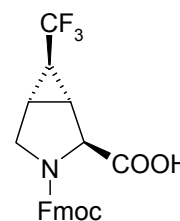
MS (m/z): 196 (M+1)<sup>+</sup>.

Second fraction (50 mg, 17%) was mixture of **49a** and **85a**.



**(1*R*,2*S*,5*S*,6*R*)-3-[(9*H*-Fluoren-9-ylmethoxy)carbonyl]-6-(trifluoromethyl)-3-azabicyclo [3.1.0]hexane-2-carboxylic acid, 89a**

A solution of Fmoc-Cl (73 mg, 0.28 mmol) in dioxane (2 ml) was added dropwise over 15 min to a solution of **49a+85a** (50 mg, 0.26 mmol) and Na<sub>2</sub>CO<sub>3</sub> (100 mg) in dioxane-water (25 ml, 2/3) at 0 °C (ice bath). After being stirred at this temperature for 30 min, the reaction was left overnight at room temperature. Water (50 ml) was added and the formed solution was extracted with Et<sub>2</sub>O (3 × 5 ml). Organic layer was discarded; water phase was acidified with aq. HCl to pH ~1 and extracted with EtOAc (3 × 10 ml). After drying over (MgSO<sub>4</sub>) the solution was evaporated to give oily residue which was purified by HPLC (column: Vydac C20, 4.6 × 250 mm). 10 mg (0.02 mmol, 9%). White solid.



<sup>1</sup>H-NMR (400 MHz, CDCl<sub>3</sub>, rotamers): 7.80 (pseudo t, 2H, <sup>3</sup>J(H, H) = 8.5, 7.0 Hz); 7.63 (m, 2H); 7.40 (pseudo t, 2H, *J* = 9.5, 9.0 Hz); 7.32 (m, 2H); 4.54-4.13 (m, 4H, CHCH<sub>2</sub>O + 2-CH); 3.71, 3.62 (2 m, 2H, 4-CH<sub>2</sub>); 2.46, 2.37 (2 m, 1H, 1-CH); 2.19 (m, 1H, 5-CH); 1.93 (m, 1H, 6-CH).

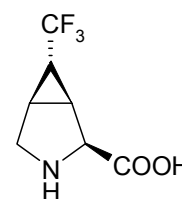
<sup>19</sup>F-NMR (377 MHz, CD<sub>3</sub>OD): 94.21, 94.21 (2 bs, CF<sub>3</sub>).

MS (*m/z*): 420 (M+1)<sup>+</sup>.

**(1*S*,2*S*,5*R*,6*S*)-6-(Trifluoromethyl)-3-azabicyclo[3.1.0]hexane-2-carboxylic acid, 49b**

Amino acid **49b** was purified synthesized from **84b** analogous to **49a**. Yellowish amorphous solid (yield 50%).

<sup>1</sup>H-NMR (400 MHz, D<sub>2</sub>O): 4.28 (d, <sup>3</sup>J(H, H) = 4.0 Hz, 1H, 2-CH); 3.58 (d, <sup>2</sup>J(H, H) = 12.0 Hz, 1H, 4-CH<sub>2</sub>); 3.53 (dd, <sup>2,3</sup>J(H, H) = 12.0, 4.0 Hz, 1H, 4-CH<sub>2</sub>); 2.50 (dt, 1H, <sup>3</sup>J(H, H) = 7.8, 4.0 Hz, 1-CH); 2.25 (dt, 1H, <sup>3</sup>J(H, H) = 7.8, 4.0 Hz, 5-CH); 1.93 (m, 1H, 6-CH).



<sup>19</sup>F-NMR (377 MHz, CD<sub>3</sub>OD): 95.49 (d, <sup>3</sup>J(H, F) = 3.8 Hz, CF<sub>3</sub>).

<sup>13</sup>C-NMR (126 MHz, CD<sub>3</sub>OD): 169.60 (s, COOH); 124.94 (q, <sup>1</sup>J(C, F) = 270.4 Hz, CF<sub>3</sub>); 61.94 (s, 2-CH); 46.50 (s, 4-CH<sub>2</sub>); 22.79 (s, 1-CH); 19.57 (s, 5-CH); 19.03 (q, <sup>2</sup>J(C, F) = 36.5 Hz, 6-CH).

IR (KBr): 1620 (ν<sub>as</sub> COO<sup>-</sup>), 1391 (ν<sub>s</sub> COO<sup>-</sup>) cm<sup>-1</sup>.

MS (*m/z*): 196 (M+1)<sup>+</sup>.

**2-*tert*-Butyl 3-methyl (1*S*,3*S*,5*R*,6*R*)-6-(trifluoromethyl)-2-azabicyclo[3.1.0]hexane-2,3-dicarboxylate, 97a**

**2-*tert*-Butyl 3-methyl (1*S*,3*S*,5*S*,6*S*)-6-(trifluoromethyl)-2-azabicyclo[3.1.0]hexane-2,3-dicarboxylate, 97b**

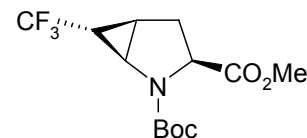
**2-*tert*-Butyl 3-methyl (1*S*,3*S*,5*S*,6*R*)-6-(trifluoromethyl)-2-azabicyclo[3.1.0]hexane-2,3-dicarboxylate, 97c**

**3-Methyl 2-(2,2,2-trifluoroethyl) (1*S*,3*S*,5*S*,6*S*)-6-(trifluoromethyl)-2-azabicyclo[3.1.0]hexane-2,3-dicarboxylate, 98**

CF<sub>3</sub>CHN<sub>2</sub> (obtained as described above) was gradually blown off by an inert gas from the generator flask and passed through a drying tube (MgSO<sub>4</sub>) into a vessel containing a stirring mixture of **93** (4.00 g, 17.62 mmol) and anhydrous CuCl (500

mg). The reaction was monitored by  $^1\text{H}$ -,  $^{19}\text{F}$ -NMR and HPLC. After the starting material had been disappeared, the trifluoromethyldiazomethane bubbling was immediately stopped. The reaction mixture was diluted with  $\text{CH}_2\text{Cl}_2$ , filtered, and evaporated. The oily residue was submitted to flash chromatography. Elution with hexane/EtOAc = 20/1 produced **97a** (1.46 g, 4.75 mmol, 27%) first as a colorless viscous oil.  $R_f = 0.5$  in hexane/EtOAc = 5/1.  $[\alpha]_D^{20} = +11.2$  ( $c = 0.67$  mg/ml, MeOH).

$^1\text{H}$ -NMR (400 MHz,  $\text{CDCl}_3$ , rotamers): 4.42 (2 dd,  $^3J(\text{H}, \text{H}) = 11.6, 3.2$  Hz, 1H, 3-CH); 3.78, 3.62 (2 dd,  $^3J(\text{H}, \text{H}) = 7.2, 1.6$  Hz, 1H, 1-CH); 3.72, 3.71 (2 s,  $\text{OCH}_3$ ); 2.64 (m, 1H, 4- $\text{CH}_2$ ); 2.23-2.08 (m, 2H, 4- $\text{CH}_2$ , 6-CH); 1.90 (m, 1H, 5-CH); 1.47, 1.38 (2 s, 9H,  $\text{C}(\text{CH}_3)_3$ ).



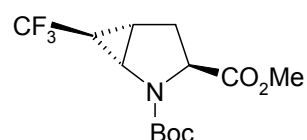
$^{19}\text{F}$ -NMR (377 MHz,  $\text{CDCl}_3$ , rotamers): 97.04, 96.73 (2 d,  $^3J(\text{H}, \text{F}) = 7.5$  Hz,  $\text{CF}_3$ ).

$^{13}\text{C}$ -NMR (126 MHz,  $\text{CDCl}_3$ , rotamers): 173.65, 173.51 (2 s,  $\text{COOCH}_3$ ); 153.99, 153.38 (2 s, NCO); 124.22 (2 q,  $^1J(\text{C}, \text{F}) = 270.4$  Hz,  $\text{CF}_3$ ); 81.14, 81.03 (2 s,  $\text{OC}(\text{CH}_3)_3$ ); 59.53, 59.20 (2 s, 3-CH); 52.50, 52.36 (2 s,  $\text{OCH}_3$ ); 39.72 (2 overlapped q,  $^3J(\text{C}, \text{F}) = 3.8$  Hz, 1-CH), 30.82, 29.84 (2 s,  $\text{CH}_2$ ); 28.29, 28.20 (2 s,  $\text{C}(\text{CH}_3)_3$ ); 25.95 (2 overlapped q,  $^2J(\text{C}, \text{F}) = 36.5$  Hz, 6-CH); 19.38-20.29 (2 overlapped q,  $^3J(\text{C}, \text{F}) = 3.8$  Hz, 5-CH).

IR (neat): 1744 ( $\nu\text{C}=\text{O}$  in  $\text{COOMe}$ ), 1711 ( $\nu\text{C}=\text{O}$  in Boc)  $\text{cm}^{-1}$ .

MS ( $m/z$ ): 210 ( $\text{M-Boc}+2$ ) $^+$  (the sample was prepared by dissolving **97a** in TFA, therefore the Boc group was cleaved).

Further elution afforded **97b** (1.31 g, 4.23 mmol, 22 %) as a white solid. Crystallization from cyclohexane gave crystals suitable for an X-ray analysis.  $R_f = 0.4$  in hexane/EtOAc = 5/1.



M.p. = 86-87  $^\circ\text{C}$ .  $[\alpha]_D^{20} = -135.2$  ( $c = 0.55$  mg/ml, MeOH).

$^1\text{H}$ -NMR (400 MHz,  $\text{CDCl}_3$ , rotamers): 4.03 (bs, 1H, 3-CH); 3.72 (bs, 4H, 1-CH +  $\text{OCH}_3$ ); 2.42 (m, 1H, 4- $\text{CH}_2$ ); 2.32 (m, 1H, 4- $\text{CH}_2$ ); 2.03 (bs, 1H, 5-CH); 1.47 (bs, 10H, 6-CH +  $\text{C}(\text{CH}_3)_3$ ).

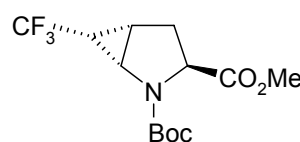
$^{19}\text{F}$ -NMR (377 MHz,  $\text{CDCl}_3$ , rotamers): 96.96, 96.54 (2 bs,  $\text{CF}_3$ ).

$^{13}\text{C}$ -NMR (126 MHz,  $\text{CDCl}_3$ , rotamers): 171.78 (s,  $\text{COOCH}_3$ ); 154.91 (bs, NCO); 124.01 (q,  $^1J(\text{C}, \text{F}) = 271.6$  Hz,  $\text{CF}_3$ ); 81.27 (s,  $\text{OC}(\text{CH}_3)_3$ ); 60.30 (s, 3-CH); 52.43 (s,  $\text{OCH}_3$ ); 39.72 (q,  $^3J(\text{C}, \text{F}) = 2.52$  Hz, 1-CH); 31.34 (bs,  $\text{CH}_2$ ); 29.27 (bs, 6-CH); 28.21 (s,  $\text{C}(\text{CH}_3)_3$ ); 19.92 (s, 5-CH).

IR (KBr): 1758 ( $\nu\text{C}=\text{O}$  in  $\text{COOMe}$ ), 1711 ( $\nu\text{C}=\text{O}$  in Boc)  $\text{cm}^{-1}$ .

MS ( $m/z$ ): 210 ( $\text{M-Boc}+2$ ) $^+$ .

The isomer **97c** (0.93 g, 3.00 mmol, 17%) was eluted from the column immediately after **97b** as a colorless viscous oil.  $R_f = 0.35$  in hexane/EtOAc = 5/1.



$^1\text{H}$ -NMR (400 MHz,  $\text{CDCl}_3$ , rotamers): 4.38, 4.22 (2 dd,  $^3J(\text{H}, \text{H}) = 10.0, 4.4$  Hz, 1H, 3-CH); 3.82 (m, 1H, 1-CH); 3.75, 3.74 (2 s, 3H,  $\text{OCH}_3$ ); 2.65 (m, 1H, 4- $\text{CH}_2$ ); 2.30 (m, 1H, 4- $\text{CH}_2$ ); 2.07 (m, 1H, 5-CH); 1.58 (m, 1H, 6-CH); 1.47, 1.45 (2 s, 9H,  $\text{C}(\text{CH}_3)_3$ ).

$^{19}\text{F}$ -NMR (377 MHz,  $\text{CDCl}_3$ ): 103.65 (d,  $^3J(\text{H}, \text{F}) = 7.5$  Hz,  $\text{CF}_3$ ).

$^{13}\text{C}$ -NMR (126 MHz,  $\text{CDCl}_3$ , rotamers): 172.60 (s,  $\text{COOCH}_3$ ); 154.57, 154.05 (2 s, NCO); 126.16 (2 q,  $^1J(\text{C}, \text{F}) = 275.4$  Hz,  $\text{CF}_3$ ); 80.96, 80.91 (2 s,  $\text{OC}(\text{CH}_3)_3$ ); 63.48, 62.94 (2 q,  $^5J(\text{H}, \text{F}) = 1.3$  Hz, 3-CH); 52.39, 52.21 (2 s,  $\text{OCH}_3$ ); 41.02, 40.92 (2 q,  $^3J(\text{C}, \text{F}) = 1.3$  Hz, 1-CH); 28.98, 27.88 (2 s,  $\text{CH}_2$ ); 28.17, 28.11 (2 s,  $\text{C}(\text{CH}_3)_3$ ); 27.41 (2 overlapped q,  $^2J(\text{C}, \text{F}) = 35.2$  Hz, 6-CH); 21.26, 19.92 (2 q,  $^3J(\text{C}, \text{F}) = 1.3$  Hz, 5-CH).

IR (neat): 1752 ( $\nu\text{C}=\text{O}$  in  $\text{COOMe}$ ), 1706 ( $\nu\text{C}=\text{O}$  in Boc).

MS (m/z): 210 ( $\text{M-Boc}+2$ ) $^+$ .

In a case the reaction was not stopped after the starting material **73** had been disappeared, a replacement of  $\text{COOC}(\text{CH}_3)_3$ -group into  $\text{COOCH}_2\text{CF}_3$ -group occurred. Compound **98** was isolated from the complex reaction mixture by flash column chromatography with the purity of ~80% (containing ~20% of **97b**). Crystals of **98** suitable for an X-ray structure analysis were obtained by crystallization from cyclohexane.  $R_f = 0.38$  in hexane/EtOAc = 5/1. White solid. M.p. = 56-57  $^\circ\text{C}$ .

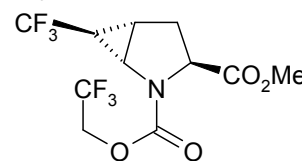
$^1\text{H}$ -NMR (400 MHz,  $\text{CDCl}_3$ , rotamers): 4.48 (bs, 1H,  $\text{OCH}_2\text{CF}_3$ ); 4.27 (bs, 1H,  $\text{OCH}_2\text{CF}_3$ ); 4.08 (bs, 1H, 3-CH); 3.81, 3.68 (2 bs, 1H, 1-CH); 3.62 (s, 3H,  $\text{OCH}_3$ ); 2.36 (bs, 1H, 4- $\text{CH}_2$ ); 2.30 (bs, 1H, 4- $\text{CH}_2$ ); 1.99 (bs, 1H, 5-CH); 1.46 (bs, 1H, 6-CH).

$^{19}\text{F}$ -NMR (377 MHz,  $\text{CDCl}_3$ , rotamers): 96.53, 96.15 (2 bs, 3F,  $\text{CHCF}_3$ ), 87.36, 87.28 (2 bs, 3F,  $\text{OCH}_2\text{CF}_3$ ).

$^{13}\text{C}$ -NMR (126 MHz,  $\text{CDCl}_3$ , rotamers): 170.91 (s,  $\text{COOCH}_3$ ); 153.44, 152.97 (2 s, NCO); 123.62 (q,  $^1J(\text{C}, \text{F}) = 271.6$  Hz,  $\text{CF}_3$ ); 122.80 (q,  $^1J(\text{C}, \text{F}) = 276.8$  Hz,  $\text{CF}_3$ ); 61.73 (q,  $^2J(\text{C}, \text{F}) = 37.8$  Hz,  $\text{OCH}_2\text{CF}_3$ ); 61.58, 60.83 (2 bs, 3-CH); 52.74 (s,  $\text{OCH}_3$ ); 40.80, 39.75 (2 bs, 1-CH); 32.30, 31.19 (2 s,  $\text{CH}_2$ ); 30.25 (q,  $^2J(\text{C}, \text{F}) = 34.0$  Hz, 6-CH); 20.05, 20.64 (2 s, 5-CH).

IR (KBr): 1752 ( $\nu\text{C}=\text{O}$  in  $\text{COOMe}$ ), 1731 ( $\nu\text{C}=\text{O}$  in  $\text{NCOOCH}_2\text{CF}_3$ ).

MS (m/z): 336 ( $\text{M}+1$ ) $^+$ .

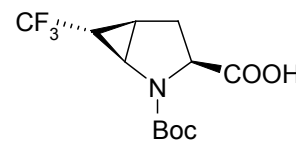


### (1*R*,3*S*,5*R*,6*R*)-2-(*tert*-Butoxycarbonyl)-6-(trifluoromethyl)-2-azabicyclo[3.1.0]hexane-3-carboxylic acid, **99a**

An aqueous solution of NaOH (13.8 ml, 0.93M, 12.8 mmol) was slowly added to a stirring solution of **97a** (1.0 g, 3.23 mmol) in MeOH (10 ml) and the resulting suspension was stirred for 2 h. The transparent solution was evaporated (to remove MeOH), redissolved in  $\text{H}_2\text{O}$  (10 ml) and extracted with  $\text{CH}_2\text{Cl}_2$  ( $2 \times 3$  ml). The organic layer was discarded; water phase was acidified to pH ~2 with aq. HCl and extracted again with  $\text{CH}_2\text{Cl}_2$  ( $3 \times 5$  ml). After being dried ( $\text{MgSO}_4$ ), the solvent was evaporated to produce **99a** (905 mg, 3.06 mmol, 95%) as a white solid. M.p. = 121-122  $^\circ\text{C}$ .

$^1\text{H}$ -NMR (400 MHz,  $\text{CDCl}_3$ , rotamers): 8.13 (bs, 1H,  $\text{COOH}$ ); 4.61, 4.34 (2 dd,  $^3J(\text{H}, \text{H}) = 11.2$ ; 2.0 Hz, 1H, 3-CH); 3.88, 3.74 (2 dd,  $^3J(\text{H}, \text{H}) = 6.8$ ; 1.2 Hz, 1H, 1-CH); 2.81-2.61 (m, 1H, 4- $\text{CH}_2$ ); 2.30-2.22 (2 dd,  $^{2,3}J(\text{H}, \text{H}) = 14.0$ ; 2.4 Hz, 1H, 4- $\text{CH}_2$ ); 2.08 (bs, 1H, 5-CH); 1.98 (m, 1H, 6-CH); 1.49-1.41 (2 s, 9H,  $\text{C}(\text{CH}_3)_3$ ).

$^{19}\text{F}$ -NMR (377 MHz,  $\text{CDCl}_3$ , rotamers): 96.81, 96.50 (2 d,  $^3J(\text{H}, \text{F}) = 7.5$  Hz,  $\text{CF}_3$ ).





IR (KBr): 1752 ( $\nu$ C=O in COOH), 1650 ( $\nu$ C=O in Boc)  $\text{cm}^{-1}$ .

MS ( $m/z$ ): 296 ( $M+1$ )<sup>+</sup>.

**(1*S*,3*S*,5*S*,6*S*)-2-(*tert*-Butoxycarbonyl)-6-(trifluoromethyl)-2-azabicyclo[3.1.0]hexane-3-carboxylic acid, **99b****

Amino acid **99b** (95% yield) was obtained from **97b** analogous to **99a**. White solid. M.p. = 121-122 °C.

<sup>1</sup>H-NMR (400 MHz, CD<sub>3</sub>OD, rotamers): 4.10 (bs, 1H, 3-CH);

3.76, 3.66 (2 bs, 1H, 1-CH); 2.55 (2 d,  $J = 9.6$  Hz, 1H, 4-CH<sub>2</sub>);

2.34 (m, 1H, 4-CH<sub>2</sub>); 2.11 (bs, 1H, 5-CH); 1.89 (m, 1H, 6-CH); 1.46, 1.44 (2 s, 9H,

C(CH<sub>3</sub>)<sub>3</sub>).

<sup>19</sup>F-NMR (377 MHz, CD<sub>3</sub>OD, rotamers): 95.87, 95.62 (2 bs, CF<sub>3</sub>).

<sup>13</sup>C-NMR (101 MHz, CD<sub>3</sub>OD, rotamers): 173.56 (bs, COOH); 155.20, 154.78 (2 bs,

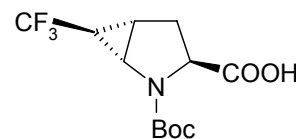
NCO); 124.30 (q,  $^1J(\text{C}, \text{F}) = 270.6$  Hz, CF<sub>3</sub>); 81.23, 80.65 (bs, OC(CH<sub>3</sub>)<sub>3</sub>); 60.22 (m,

3-CH); 39.69 (s, 1-CH); 31.35, 30.77 (2 q,  $^3J(\text{C}, \text{F}) = 2.8$  Hz, CH<sub>2</sub>); 27.95 (bs, 6-

CH); 26.97 (s, C(CH<sub>3</sub>)<sub>3</sub>); 19.49, 20.02 (2 bs, 5-CH).

IR (KBr): 1756 ( $\nu$ C=O in COOH), 1654 ( $\nu$ C=O in Boc)  $\text{cm}^{-1}$ .

MS ( $m/z$ ): 296 ( $M+1$ )<sup>+</sup>.



**(1*S*,3*S*,5*S*,6*R*)-2-(*tert*-Butoxycarbonyl)-6-(trifluoromethyl)-2-azabicyclo[3.1.0]hexane-3-carboxylic acid, **99c****

Amino acid **99c** (95% yield) was obtained from **97c** analogous to **99a**. White solid. M.p. = 120-121 °C.

<sup>1</sup>H-NMR (400 MHz, CD<sub>3</sub>OD, rotamers): 4.20 (2 dd,  $^3J(\text{H}, \text{H}) =$

10.0, 3.6 Hz, 1H, 3-CH); 3.73 (m, 1H, 1-CH); 2.64 (q,  $^2J(\text{H}, \text{H})$

= 10.0 Hz, 1H, 4-CH<sub>2</sub>); 2.35 (m, 1H, 4-CH<sub>2</sub>); 2.20 (m, 1H, 5-CH); 1.77 (m, 1H, 6-

CH); 1.47, 1.42 (2 s, 9H, C(CH<sub>3</sub>)<sub>3</sub>).

<sup>19</sup>F-NMR (377 MHz, CD<sub>3</sub>OD, rotamers): 103.17, 103.09 (2 d,  $^3J(\text{H}, \text{F}) = 7.5$  Hz,

CF<sub>3</sub>).

<sup>13</sup>C-NMR (101 MHz, CD<sub>3</sub>OD, rotamers): 173.73, 173.58 (2 s, COOCH<sub>3</sub>); 156.73,

156.39 (2 s, NCO); 128.21 (q,  $^1J(\text{C}, \text{F}) = 272.9$  Hz, CF<sub>3</sub>); 82.57, 82.27 (2 s,

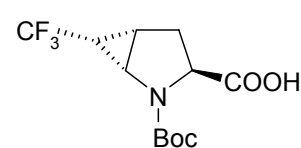
OC(CH<sub>3</sub>)<sub>3</sub>); 65.27, 65.05 (2 q,  $^5J(\text{C}, \text{F}) = 2.0$  Hz, 3-CH); 42.24, 42.01 (2 q,  $^3J(\text{C}, \text{F}) =$

2.0 Hz, 1-CH); 30.03, 29.14 (2 s, CH<sub>2</sub>); 28.71, 28.62 (2 s, C(CH<sub>3</sub>)<sub>3</sub>); 22.31 (2

overlapped q,  $^2J(\text{C}, \text{F}) = 34.2$  Hz, 6-CH), 22.46, 21.17 (2 q,  $^3J(\text{C}, \text{F}) = 2.0$  Hz, 5-CH).

IR (KBr): 1720 ( $\nu$ C=O in COOH), 1694 ( $\nu$ C=O in Boc).

MS ( $m/z$ ): 296 ( $M+1$ )<sup>+</sup>.



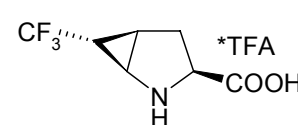
**(1*R*,3*S*,5*R*,6*R*)-3-Carboxy-6-(trifluoromethyl)-2-azoniabicyclo[3.1.0]hexane trifluoroacetate, **97a**\*TFA**

**99a** (500 mg, 1.69 mmol) was dissolved in 5 ml of TFA/CH<sub>2</sub>Cl<sub>2</sub> (1/4), and the mixture was stirred for 2 h.

Evaporation of the solvent afforded **97**\*TFA (523 mg, 1.69 mmol, quant.) as a white solid. M.p. = 145-146 °C.

<sup>1</sup>H-NMR (400 MHz, CD<sub>3</sub>OD): 4.68 (dd,  $^3J(\text{H}, \text{H}) = 10.8, 3.2$  Hz, 1H, 3-CH), 3.82

(dd,  $^3J(\text{H}, \text{H}) = 6.4, 2.0$  Hz, 1H, 1-CH), 2.82 (m, 1H, 4-CH<sub>2</sub>), 2.53 (dd,  $^{2,3}J(\text{H}, \text{H}) =$



14.0; 2.8 Hz, 1H, 4-CH<sub>2</sub>), 2.38 (dd, <sup>3</sup>J(H, H) = 10.8; 5.6 Hz, 1H, 5-CH), 2.10 (m, 1H, 6-CH).

<sup>19</sup>F-NMR (377 MHz, CD<sub>3</sub>OD): 95.31 (d, <sup>3</sup>J(H, F) = 3.8 Hz, CF<sub>3</sub>); 85.43 (s, CF<sub>3</sub>COO<sup>-</sup>).

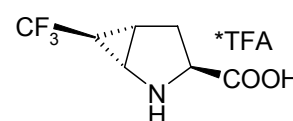
<sup>13</sup>C-NMR (126 MHz, CD<sub>3</sub>OD): 171.12 (s, COOH); 161.15 (q, <sup>2</sup>J(C, F) = 36.5 Hz, COOH in CF<sub>3</sub>COO<sup>-</sup>); 123.72 (q, <sup>1</sup>J(C, F) = 270.4 Hz, CF<sub>3</sub>); 116.48 (q, <sup>1</sup>J(C, F) = 292.3 Hz, CF<sub>3</sub> in CF<sub>3</sub>COO<sup>-</sup>); 59.85 (s, 3-CH); 38.17 (q, <sup>3</sup>J(C, F) = 3.8 Hz, 1-CH); 29.58 (s, CH<sub>2</sub>); 23.08 (q, <sup>2</sup>J(C, F) = 36.5 Hz, 6-CH); 20.81 (q, <sup>3</sup>J(C, F) = 3.8 Hz, 5-CH).

IR (KBr): 1730 (ν C=O in COOH), 1683 (ν<sub>as</sub> COO<sup>-</sup>), 1632 (ν<sub>s</sub> COO<sup>-</sup>).

MS (m/z): 196 (M-CF<sub>3</sub>COO<sup>-</sup>)<sup>+</sup>.

**(1*S*,3*S*,5*S*,6*S*)-3-Carboxy-6-(trifluoromethyl)-2-azoniabicyclo[3.1.0]hexane trifluoroacetate, 97b\*TFA**

**97b**\*TFA was synthesized from **99b** analogous to **97a**\*TFA (quant. yield). White solid. M.p. = 143-144 °C.



[α]<sub>D</sub><sup>20</sup> = -25.0 (c = 0.207 mg/ml, MeOH).

<sup>1</sup>H-NMR (400 MHz, CD<sub>3</sub>OD): 4.21 (t, <sup>3</sup>J(H, H) = 8.0 Hz, 1H, 3-CH); 3.75 (dd, <sup>3</sup>J(H, H) = 6.0, 2.0 Hz, 1H, 1-CH); 2.66 (dd, <sup>2,3</sup>J(H, H) = 12.8, 8.0 Hz, 1H, 4-CH<sub>2</sub>); 2.56 (m, 1H, 4-CH<sub>2</sub>); 2.38 (m, 2H, 5-CH and 6-CH).

<sup>19</sup>F-NMR (377 MHz, CD<sub>3</sub>OD): 104.13 (d, <sup>3</sup>J(H, F) = 7.5 Hz, CF<sub>3</sub>CH); 85.37 (s, CF<sub>3</sub>COO<sup>-</sup>).

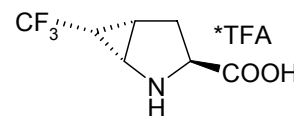
<sup>13</sup>C-NMR (101 MHz, CD<sub>3</sub>OD): 169.71 (s, COOH); 161.15 (q, <sup>2</sup>J(C, F) = 35.2 Hz, COO<sup>-</sup> in CF<sub>3</sub>COO<sup>-</sup>); 125.52 (q, <sup>1</sup>J(C, F) = 270.9 Hz, CHCF<sub>3</sub>); 116.49 (q, <sup>1</sup>J(C, F) = 289.2 Hz, CF<sub>3</sub> in CF<sub>3</sub>COO<sup>-</sup>); 58.06 (s, 3-CH), 37.67 (q, <sup>3</sup>J(C, F) = 4.0 Hz, 1-CH); 29.76 (s, 4-CH<sub>2</sub>), 21.22 (q, <sup>2</sup>J(C, F) = 37.3 Hz, 6-CH); 20.53 (q, <sup>3</sup>J(C, F) = 2.0 Hz, 5-CH).

IR (KBr): 1733 (ν C=O in COOH), 1679 (ν<sub>as</sub> COO<sup>-</sup>), 1636 (ν<sub>s</sub> COO<sup>-</sup>) cm<sup>-1</sup>.

MS (m/z): 196 (M-CF<sub>3</sub>COO<sup>-</sup>)<sup>+</sup>.

**(1*S*,3*S*,5*S*,6*R*)-3-Carboxy-6-(trifluoromethyl)-2-azobicyclo[3.1.0]hexane trifluoroacetate, 97c\*TFA**

**97c**\*TFA was synthesized from **99c** analogous to **97a**\*TFA (quant. yield). White solid. M.p. = 143-144 °C.



<sup>1</sup>H-NMR (400 MHz, CD<sub>3</sub>OD): 4.39 (t, <sup>3</sup>J(H, H) = 8.8 Hz, 1H, 3-CH); 3.76 (t, <sup>3</sup>J(H, H) = 6.4 Hz, 1H, 1-CH); 2.69 (m, 2H, 4-CH<sub>2</sub>); 2.44 (m, 1H, 5-CH); 2.21 (m, 1H, 6-CH).

<sup>19</sup>F-NMR (377 MHz, CD<sub>3</sub>OD): 104.13 (d, <sup>3</sup>J(H, F) = 7.5 Hz, CF<sub>3</sub>CH); 85.37 (s, CF<sub>3</sub>COO<sup>-</sup>).

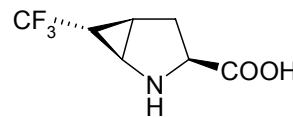
<sup>13</sup>C-NMR (101 MHz, CD<sub>3</sub>OD): 169.19 (s, COOH); 160.20 (q, <sup>2</sup>J(C, F) = 36.2 Hz, COO<sup>-</sup> in CF<sub>3</sub>COO<sup>-</sup>); 125.54 (q, <sup>1</sup>J(C, F) = 273.6 Hz, CHCF<sub>3</sub>); 116.00 (q, <sup>1</sup>J(C, F) = 292.6 Hz, CF<sub>3</sub> in CF<sub>3</sub>COO<sup>-</sup>); 61.11 (q, <sup>5</sup>J(C, F) = 4.0 Hz, 3-CH); 39.81 (q, <sup>3</sup>J(C, F) = 2.0 Hz, 1-CH); 27.24 (s, 4-CH<sub>2</sub>); 21.46 (q, <sup>2</sup>J(C, F) = 39.2 Hz, 6-CH); 22.02 (q, <sup>3</sup>J(C, F) = 2.0 Hz, 5-CH).

IR (KBr): 1731 (ν C=O in COOH), 1680 (ν<sub>as</sub> COO<sup>-</sup>), 1635 (ν<sub>s</sub> COO<sup>-</sup>) cm<sup>-1</sup>.

MS ( $m/z$ ): 196 ( $M-CF_3COO$ )<sup>+</sup>.

**(1*R*,3*S*,5*R*,6*R*)-6-(Trifluoromethyl)-2-azabicyclo[3.1.0]hexane-3-carboxylic acid, 97a**

An aqueous solution of **97a**\*TFA was neutralized with aq. NaOH (0.3M) and submitted to an ion exchange chromatography (Dowex 50 × 400). Elution with water and then with aq. pyridine (10%) afforded **97a** in quant. yield. White solid (yield 100%). M.p. > 200 °C.  $[\alpha]_D^{20} = -37.0$  ( $c = 0.544$  mg/ml, H<sub>2</sub>O).



<sup>1</sup>H-NMR (400 MHz, D<sub>2</sub>O): 4.39 (dd, <sup>3</sup> $J(H, H) = 11.2, 2.8$  Hz, 1H, 3-CH); 3.80 (dd, <sup>3</sup> $J(H, H) = 6.8, 2.4$  Hz, 1H, 3-CH); 2.72 (m, 1H, 4-CH<sub>2</sub>); 2.48 (dd, <sup>2,3</sup> $J(H, H) = 14.0, 2.8$  Hz, 1H, 4-CH); 2.38 (dd, <sup>3</sup> $J(H, H) = 10.8, 6.4$  Hz, 1H, 5-CH); 2.05 (m, 1H, 6-CH).

<sup>19</sup>F-NMR (377 MHz, D<sub>2</sub>O): 95.81 (d, <sup>3</sup> $J(H, F) = 3.8$  Hz, CF<sub>3</sub>).

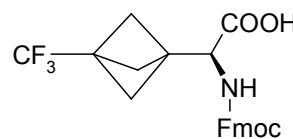
MS ( $m/z$ ): 196 ( $M+1$ )<sup>+</sup>.

IR (KBr): 1636 ( $\nu_{as}$  COO<sup>-</sup>), 1569 ( $\delta$  NH<sub>2</sub><sup>+</sup>), 1388 ( $\nu_s$  COO<sup>-</sup>) cm<sup>-1</sup>.

Under the same purification conditions the isomers **97(b,c)**\*TFA decomposed, partially (**97b**\*TFA) or completely (**97c**\*TFA).

**(2*S*)-2-{{[9*H*-Fluoren-9-ylmethoxy]carbonyl}amino}-2-[3-(trifluoromethyl)bicyclo[1.1.1]pent-1-yl]carboxylic acid, 101**

A solution of Fmoc-Cl (1.30 g, 5.01 mmol) in dioxane (5 ml) was added dropwise over 15 min to a solution of **20** (1.00 g, 4.77 mmol) and Na<sub>2</sub>CO<sub>3</sub> (2 g) in dioxane-water (50 ml, 2/3) at 0 °C. After being stirred at this temperature for 30 min, the reaction was left overnight at room temperature. Water (500 ml) was added and the formed mixture was extracted with Et<sub>2</sub>O (3 × 50 ml). The organic layer was discarded; water phase was acidified with aq. HCl to pH ~1 and extracted with EtOAc (3 × 50 ml). The organic phase was dried (MgSO<sub>4</sub>) and evaporated to give **101** (1.87 g, 4.29 mmol, 90%) as a white solid. An analytically pure sample was obtained by crystallization from hexane-EtOAc mixture. M.p. = 203-204 °C.



<sup>1</sup>H-NMR (400 MHz, CD<sub>3</sub>OD, rotamers): 7.71 (d, <sup>3</sup> $J(H, H) = 7.6, 2H$ ); 7.64, 7.57 (2 t, <sup>3</sup> $J(H, H) = 6.8$  Hz, 2H); 7.34 (t, <sup>3</sup> $J(H, H) = 7.6$  Hz, 2H); 7.27 (t, <sup>3</sup> $J(H, H) = 7.2$  Hz, 2H); 4.50, 4.36 (2 m, 1H, OCH<sub>2</sub>CH); 4.37 (dd,  $J = 11.5, 6.5$  Hz, 1H, OCH<sub>2</sub>CH); 4.30 (s, 1H, CHCOOH); 4.20 (t, <sup>3</sup> $J(H, H) = 6.8$  Hz, 1H, OCH<sub>2</sub>CH); 1.94, 1.89 (2 d, <sup>2</sup> $J(H, H) = 9.2$  Hz, 6H, CH<sub>2</sub>); 1.68 (s, 1H, COOH).

<sup>19</sup>F-NMR (377 MHz, CD<sub>3</sub>OD, rotamers): 87.95, 87.82 (2 s, CF<sub>3</sub>).

<sup>13</sup>C-NMR (101 MHz, CD<sub>3</sub>OD, rotamers): 171.85(s, COOH); 157.73 (s, NCO); 144.54, 144.34 (2 s, *tert*-C in Fmoc-group); 141.84 (s, *tert*-C in Fmoc-group); 127.49 (s, CH); 126.80 (s, CH); 124.81, 124.73 (2 s, CH); 124.42 (q, <sup>1</sup> $J(C, F) = 215.2$  Hz, CF<sub>3</sub>); 119.57 (s, CH); 67.96, 67.83 (2 s, OCH<sub>2</sub>CH); 59.34, 58.69 (2 s, CCOOH); 39.79, 39.22 (2 s, OCH<sub>2</sub>CH); 30.46, 30.35 (2 s); 25.31, 24.76 (2 q, <sup>2</sup> $J(C, F) = 27.3$  Hz, CCF<sub>3</sub>); 19.35, 20.20 (2 s).

**(1*R*,3*S*,5*R*,6*R*)-2-[(9*H*-Fluoren-9-ylmethoxy)carbonyl]-6-(trifluoromethyl)-2-azabicyclo[3.1.0]hexane-3-carboxylic acid, **110****

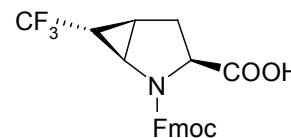
**110** was synthesized from **50a** analogous to **101**. White solid (80% yield). M.p. = 193-194 °C.

<sup>1</sup>H-NMR (500 MHz, CD<sub>3</sub>OD, rotamers): 7.82 (t, <sup>3</sup>*J*(H, H) = 8.0 Hz, 2H); 7.69 (t, <sup>3</sup>*J*(H, H) = 7.0 Hz, 1.2H); 7.61 (dd, <sup>3</sup>*J*(H, H) = 7.0, 3.5 Hz, 0.8 H); 7.42 (pseudo q, <sup>3</sup>*J*(H, H) = 7.0 Hz, 2H); 7.33 (t, <sup>3</sup>*J*(H, H) = 7.0 Hz, 2H); 4.61-4.47 (2 overlapped dd, *J* = 8.5, 3.0 Hz, 1H, 3-CH); 4.51 (dd, *J* = 10.0, 6.5 Hz, 0.6H); 4.38 (m, 2H); 4.19 (t, *J* = 6.5 Hz, 0.4H); 3.92, 3.82 (2 dd, <sup>3</sup>*J*(H, H) = 7.0, 1.5 Hz, 1H, 1-CH); 2.82 (m, 1H, 4-CH<sub>2</sub>); 2.27-2.07 (m, 3H, 4-CH<sub>2</sub>, 5-CH and 6-CH).

<sup>19</sup>F-NMR (377 MHz, CD<sub>3</sub>OD, rotamers): 96.61, 96.41 (2 bs, CF<sub>3</sub>).

<sup>13</sup>C-NMR (125 MHz, CD<sub>3</sub>OD, rotamers): 174.65, 174.33 (2 s, COOH); 155.03, 154.71 (2 s, NCO); 143.84, 143.77, 143.65, 143.56 (4 s, *tert*-C in Fmoc-group); 141.26, 141.20, 141.10 (3 s, 2 *tert*-C in Fmoc-group); 127.49 (s, CH); 126.87, 126.81 (2 s, CH); 124.82, 124.74 (2 s, CH); 124.42 (2 q, <sup>1</sup>*J*(C, F) = 270.4 Hz, CF<sub>3</sub>); 119.58 (s, CH); 67.98, 67.85 (2 s, OCH<sub>2</sub>); 59.36, 58.71 (2 s, 3-CH); 46.97, 46.86 (2 s, OCH<sub>2</sub>CH); 39.79, 39.22 (2 q, <sup>3</sup>*J*(C, F) = 3.8 Hz, 1-CH); 30.48, 29.36 (2 s, 4-CH<sub>2</sub>); 28.28, 24.87 (2 overlapped q, <sup>2</sup>*J*(C, F) = 36.3 Hz, 6-CH); 19.36, 20.22 (2 s, 5-CH).

MS (m/z): 420 (M+1)<sup>+</sup>.



**Cyclo-(Pro-Val-Orn-20-<sup>D</sup>Phe)<sub>2</sub>, **100****

**100** was synthesized manually using standard Fmoc-protocol of SPPS. 2-chlorotrityl resin. The synthesis was started from <sup>D</sup>Phe using 2-chlorotrityl resin. While incorporating Orn into the peptide sequence, side chain protected Fmoc-(ivDde)Orn was used. Incorporation of natural amino acids: Fmoc-amino acid (4 eq) / TCTU (4 eq) / 6Cl-HOBt (4 eq) and DIEA (8 eq) for 2 h. Incorporation of **20**: **101** (2 eq) / TCTU (2 eq) / 6Cl-HOBt (2 eq) / DIEA (4 eq) for 2 h. The coupling efficiency was monitored by Kaiser test.<sup>236</sup> Deprotection was carried out with 20% piperidine in DMF for 20 min. The peptides were cleaved from the resin at room temperature by treatment with a cocktail of TFA (95%), water (2.5%) and TIS (2.5%) for 4 h with occasional shaking. The resin was filtered off and washed with pure TFA twice. The combined filtrates were evaporated under a gentle stream of nitrogen. The formed oily residue was redissolved in H<sub>2</sub>O and lyophilized to produce linear decapeptide **103**. To the solution of **103** in CH<sub>2</sub>Cl<sub>2</sub> (~ 1mg/ml) activators (3 eq. PyBop, 3 eq. 6Cl-HOBt in minimum DMF) were added and the mixture was stirred for 30 min. After addition of 6 eq. DIEA the mixture was leaved to stirr for 24 h. Evaporation of the solvent afforded the residue, which was partitioned in H<sub>2</sub>O-EtOAc mixture. After being dried (MgSO<sub>4</sub>) the organic phase was evaporated to obtain a colorless oil (**104**), which was dissolved in 20 ml 2% N<sub>2</sub>H<sub>4</sub> in DMF and stirred for 2 h. Evaporation of the solvent gave the residue which was purified further by HPLC. Analytical RP-HPLC was done on an Agilent 1100 HPLC device using Zorbax Eclipse<sup>®</sup> XDB-C<sub>8</sub> column (4.6 mm × 150 mm). Peptide was purified by semipreparative RP-HPLC (Jasco, Japan; 10 × 250 mm Vydac C18-column). The crude peptide was loaded on the column as 5 mg/ml solution in MeOH. 5 mM HCl was used as ion-pairing agent

instead of conventional TFA. After the purification, the peptide was of > 95% purity according to analytical HPLC and it was stored as lyophilized powder at -40 °C until use.

MALDI-TOF (m/z): 1297.7 [M+1]<sup>+</sup>, calculated 1296.5.

### CF<sub>3</sub>-labelled PGLa analogues, 106-109

Peptides were synthesized automatically using standard Fmoc-protocol of SPPS. Rink-amide resin. While incorporating Lys or Ser into the peptide sequence, side chain protected Fmoc-(Boc)Lys and Fmoc-(*t*Bu)Ser were used. Incorporation of natural amino acids: Fmoc-amino acid (4 eq) / TBTU (4 eq) / 6Cl-HOBt (4 eq) and DIEA (8 eq) for 2 h. Incorporation of **20**: **101** (2 eq) / TBTU (2 eq) / 6Cl-HOBt (2 eq) / DIEA (4 eq) for 2 h. Deprotection was carried out with 20% piperidine in DMF for 20 min. The peptides were cleaved from the resin at room temperature by treatment with a cocktail of TFA (95%), water (2.5%) and TIS (2.5%) for 4 h with occasional shaking. The resin was filtered off and washed with pure TFA twice. The combined filtrates were evaporated under a gentle stream of nitrogen and the products were precipitated with cold diethyl ether. After centrifugation the supernatant (diethyl ether) was decanted. The solid precipitate was redissolved in H<sub>2</sub>O and lyophilized. Peptides were purified by semi-preparative RP-HPLC (Jasco, Japan; 10 × 250 mm Vydac C18-column). The crude peptides were loaded on the column as 7 mg/ml solution in MeOH. The H<sub>2</sub>O/MeCN gradients were individually optimized for each peptide at 30-40 °C. 5 mM HCl was used as ion-pairing agent instead of conventional TFA. After purification, all peptides were of > 95% purity according to analytical HPLC, and they were stored as lyophilized powders at -40 °C until use.

**106**, MALDI-TOF (m/z): 2045.9 [M]<sup>+</sup>, calculated 2046.5.

**107**, MALDI-TOF (m/z): 2088.3 [M]<sup>+</sup>, calculated 2088.6.

**108**, MALDI-TOF (m/z): 2046.1 [M]<sup>+</sup>, calculated 2046.5.

**109**, MALDI-TOF (m/z): 2088.2 [M]<sup>+</sup>, calculated 2088.6.

### SAP and its CF<sub>3</sub>-labelled analogues, 111-116

All peptides (SAP and **111-116**) have been synthesized manually using standard solid phase Fmoc-protocols. 2-Chlorotrityl resin. While incorporating Arg into the peptide sequence, side chain protected Fmoc-(Pbf)Arg was used. Incorporation of natural amino acids: Fmoc-amino acids (4 eq) / TBTU (4 eq) / 6-Cl-HOBT (4 eq) and DIEA (8 eq) for 2 h. **51a** was incorporated by utilizing **110** (2 eq) / DIC (6 eq) / 6-Cl-HOBt (2 eq) for 2 h. The incorporation of **20** was achieved by using **101** (2 eq) / TBTU (2 eq) / 6-Cl-HOBt / DIEA (4 eq) for 2 h. While incorporating 12-Pro (next to **51a**), Val and Arg double couplings were used. Second couplings were done by using Fmoc-amino acid (4 eq) / PyBop (4 eq) / DIEA (8 eq). The coupling efficiency was monitored by Kaiser test. Deprotection was carried out with 20% piperidine in DMF for 20 min. The peptides were cleaved from the resin at room temperature by treatment with a cocktail of TFA (95%), water (2.5%) and TIS (2.5%) for 12 h with occasional shaking. The resin was filtered off and washed with pure TFA twice. The combined filtrates were evaporated under a gentle stream of nitrogen and the products were precipitated with cold diethyl ether. After

centrifugation the supernatant (diethyl ether) was decanted. The solid precipitate was redissolved in H<sub>2</sub>O and lyophilized. Analytical RP-HPLC was done on an Agilent 1100 HPLC device using Zorbax Eclipse<sup>®</sup> XDB-C<sub>8</sub> column (4.6 × 150 mm). Peptides were purified by preparative RP-HPLC (Jasco, Japan; 25 × 250 mm Vydac C20-column). The H<sub>2</sub>O/MeOH gradients were individually optimized for each peptide at 40 °C. The crude peptides were loaded on the column as 50 mg/ml solution in MeOH. 5 mM HCl was used as ion-pairing agent instead of conventional TFA.

After the purification, all peptides were of > 95% purity according to analytical HPLC and they were stored as lyophilized powders at -40 °C until use.

SAP, MALDI-TOF (m/z): 1998.7 [M+1]<sup>+</sup>, calculated 1997.5.

111, MALDI-TOF (m/z): 2076.4 [M+1]<sup>+</sup>, calculated 2075.5.

112, MALDI-TOF (m/z): 2089.7 [M]<sup>+</sup>, calculated 2089.5.

113, MALDI-TOF (m/z): 2075.9 [M]<sup>+</sup>, calculated 2075.5.

114, MALDI-TOF (m/z): 2077.7 [M]<sup>+</sup>, calculated 2077.5.

115, MALDI-TOF (m/z): 2090.8 [M+1]<sup>+</sup>, calculated 2089.5.

116, MALDI-TOF (m/z): 2089.5 [M]<sup>+</sup>, calculated 2089.5.

### Preparation of macroscopically aligned NMR samples

Oriented samples of system peptide/lipid were prepared according to standard procedures described in details in recent reviews.<sup>58,65,237</sup>

### NMR Spectroscopy

All solid state NMR measurements were carried out on a Bruker Avance 500 MHz spectrometer (Bruker BioSpin, Rheinstetten, Germany). <sup>19</sup>F-NMR was performed at 470 MHz with a <sup>19</sup>F/<sup>1</sup>H double-tuned, flat-coil probe (Doty Scientific, Columbia, SC, USA) that could be manually tilted. Simple 1-pulse experiments with a 90° pulse width of 1.8 μs and 10-15 kHz TPPM 1H-decoupling were used to acquire regular <sup>19</sup>F-NMR spectra. All samples were measured with the membrane normal parallel to the magnetic field.

### Calculation of PGLa and SAP structures

The homonuclear <sup>19</sup>F-<sup>19</sup>F dipolar couplings of <sup>19</sup>F-NMR label **20** in five different positions of SAP and four positions of PGLa were collected and used to calculate the orientation of the peptides in the lipid bilayer. The backbone of SAP was modeled as an ideal α-, 3<sub>10</sub>-, π-helices and PP II; the PGLa - as α-helix. The alignment of such ideal model structures in the lipid bilayer are described by a tilt angle τ with respect to the membrane normal and by an azimuthal rotation ρ around the helix axis. To determine these two values together with the order parameter S<sub>mol</sub>, all three parameters were systematically varied in a grid search. The minimal RMSD-values (root mean square deviation between the experimental and calculated <sup>19</sup>F-<sup>19</sup>F dipolar couplings) found were taken as a basis for ρ, τ and S<sub>mol</sub>. The method is described in detail in a number of recent reviews<sup>58,65,238</sup>

## PART 7. SUMMARY

A new trifluoromethyl-substituted conformationally rigid *L*- $\alpha$ -amino acid ((*S*)-3-trifluoromethyl-bicyclo[1.1.1]-1-ylglycine, CF<sub>3</sub>-Bpg) was synthesized. This compound was specifically designed to serve as a proper <sup>19</sup>F-label for substituting natural non-polar amino acids (Ala, Val, Leu, Ile, Met) in peptides, in order to study them by solid state <sup>19</sup>F-NMR. The stereochemistry of the final product was determined by X-ray analysis, and its optical purity was confirmed using a lanthanide shift reagent. With the aim of scaling up the synthetic protocol, separation conditions of two key intermediates by crystallization were found. Thus, the scale of the synthesis could be successfully increased from milligrams to hundred grams.

The new <sup>19</sup>F-label CF<sub>3</sub>-Bpg was incorporated into the two antimicrobial peptides GS and PGLa, which are well structurally and functionally characterized, in order to demonstrate its compatibility with structural peptide studies by solid state <sup>19</sup>F-NMR. Four analogues of PGLa and one GS analogue were synthesized. The <sup>19</sup>F-labelled peptides were thoroughly analyzed by means of CD, solid state <sup>19</sup>F-NMR, and antimicrobial tests. The new amino acid was shown to fully meet all requirements to serve as an ideal structural <sup>19</sup>F-NMR label.

As a basis for the design of further labels, a method for the construction of trifluoromethyl-substituted cyclopropane derivatives from alkenes and trifluoromethyldiazomethane was developed. The key feature of this transformation was the use of metallocatalysis. By using a modified Gaspar-Roth procedure, the optimized synthetic scheme allowed to obtain the target compounds on a gram scale. Proline and norcoronamic acid were used as examples to demonstrate the applicability of this strategy for synthesizing trifluoromethyl-substituted analogues of natural amino acids, being a fundamentally new approach for constructing of compounds of this class.

Using this approach a library of new <sup>19</sup>F-labels, trifluoromethyl-substituted conformationally restricted *L*- $\alpha$ -amino acids, was thus designed to replace proline in peptides. All compounds, except for 2-(trifluoromethyl)-proline, were successfully synthesized. The stereoconfiguration of the different isomeric products was established by NMR and X-ray structural analysis. One isomer among the five synthesized, namely (1*R*,3*S*,5*R*,6*R*)-6-(trifluoromethyl)-2-azabicyclo[3.1.0]hexane-3-carboxylic acid (CF<sub>3</sub>-MePro) was used for further studies.

The new <sup>19</sup>F-labels CF<sub>3</sub>-Bpg and CF<sub>3</sub>-MePro were incorporated into a novel cell-penetrating peptide SAP and six <sup>19</sup>F-labelled analogues were synthesized. Their conformational behaviour was investigated, showing that the label CF<sub>3</sub>-MePro stabilizes the helical PP II conformation of SAP, while CF<sub>3</sub>-Bpg has no influence. The structure, dynamics and orientation of SAP in lipid membranes were then studied by solid state <sup>19</sup>F-NMR, showing that the peptide prefers a surface-bound PP II helix under certain conditions.

## ZUSAMMENFASSUNG

Eine neue Fluor-markierte konformationell starre *L*- $\alpha$ -Aminosäure ((*S*)-3-Trifluormethyl-bicyclo-pent-[1.1.1]-1-ylglycine, CF<sub>3</sub>-Bpg) wurde synthetisiert. Diese Verbindung wurde als eine ideale Markierung für die Substitution von in der Natur vorkommenden, unpolaren Aminosäuren (Ala, Val, Leu, Ile, Met) in Peptiden konzipiert, um sie für Festkörper <sup>19</sup>F-NMR Untersuchungen einzusetzen. Die Stereokonfiguration des Produkts wurde mittels Röntgenbeugungsanalyse ermittelt, und die optische Reinheit wurde mit Hilfe von „Lanthanide-shift“ Reagenzien bestätigt. Um die Synthese zu optimieren, wurden Bedingungen für die Trennung von zwei Schlüsselintermediaten durch Kristallisation gefunden. Damit ließ sich der synthetische Maßstab erfolgreich von einigen Milligramm auf ca. hundert Gramm erhöhen.

Die neue <sup>19</sup>F-Markierung CF<sub>3</sub>-Bpg wurde in die antimikrobiellen Peptide GS und PGLa eingebaut, die strukturell und funktionell bereits gut untersucht worden sind. Vier PGLa-Analoga und ein GS-Analog wurden synthetisiert. Diese <sup>19</sup>F-markierten Peptide wurden umfassend mittels CD, Festkörper <sup>19</sup>F-NMR und antimikrobiellen Tests charakterisiert. Es konnte gezeigt werden, dass CF<sub>3</sub>-Bpg alle Voraussetzungen einer idealen strukturellen <sup>19</sup>F-Markierung erfüllt.

Als Grundlage zur Darstellung weiterer <sup>19</sup>F-Markierungen wurde eine neue Methode für die Herstellung von Trifluormethyl-substituierten Cyclopropan-Derivaten aus Alkenen und trifluormethyldiazomethan entwickelt. Der Schlüssel zum Erfolg dieser Transformation war die Anwendung einer Metallkatalyse. Mit Hilfe einer optimierten Gaspar-Roth Methode wurden die gewünschten Produkte im Gramm-Maßstab synthetisiert. Am Beispiel von Prolin und Norkoronamin-Säure wurde gezeigt, dass sich diese neue Strategie für die Synthese der Trifluormethyl-substituierten Analoga von natürlichen Aminosäuren eignet.

Auf diese Weise wurde eine Bibliothek mit neuen <sup>19</sup>F-Markierungen, bestehend aus Trifluormethyl-substituierten konformationell beschränkten *L*- $\alpha$ -Aminosäuren, für die Substitution von Prolin in Peptiden entworfen. Alle Verbindungen, außer 2-(Trifluormethyl)-prolin, wurden erfolgreich synthetisiert. Die Stereokonfiguration der hergestellten, isomeren Aminosäuren wurde mit Hilfe von NMR und Röntgenbeugungsanalyse bestimmt. Eines der sechs synthetisierten Isomere, (1*R*,3*S*,5*R*,6*R*)-6-(Trifluormethyl)-2-azabicyclo[3.1.0]hexan-3-carbonsäure (CF<sub>3</sub>-MePro), wurde für die weiteren Untersuchungen ausgewählt.

Die neuen <sup>19</sup>F-Markierungen CF<sub>3</sub>-Bpg und CF<sub>3</sub>-MePro wurden in das neue Zell-penetrierende Peptid SAP eingebaut, und fünf Fluor-markierte Analoga wurden synthetisiert. Das konformationelle Verhalten aller Peptide wurde untersucht. Es konnte gezeigt werden, dass die Aminosäure CF<sub>3</sub>-MePro die PP II-Konformation von SAP stabilisiert, während die Markierung CF<sub>3</sub>-Bpg sie hingegen nicht beeinflusste. Die Struktur, Dynamik und Orientierung von SAP in Lipidmembranen wurden mittels Festkörper <sup>19</sup>F-NMR analysiert und zeigte, dass das Peptid unter bestimmten Bedingungen eine oberflächlich gebundene PP II Helix ausbildet.



PART 8.  
CITED LITERATURE

- 
- <sup>1</sup> *Stryer L.* Biochemie. - 1990. - Spektrum der Wissenschaft Verlagsgesellschaft mbH, Heidelberg. - P. 295-325.
- <sup>2</sup> *Alberts B., Bray D., Lewis J., Raff M., Roberts K., Watson J. D.* Molecular biology of the cell. - 1994. - Garland Publishing Inc., New York.
- <sup>3</sup> *Lodish H., Berk A., Zipursky L., Matsudaira P., Baltimore D., Darnell J.* Molecular Cell Biology. - 2000. - W. H. Freeman Company, New York.
- <sup>4</sup> *Kotyk A., Yanachek K.* Membrane transport. - 1980. - Mir, Moscow [russ].
- <sup>5</sup> *Ivkov V. G., Berestovsky G. N.* Lipid bilayer of biological membranes. - 1984. - Nauka, Moscow [russ].
- <sup>6</sup> *Singer S. J., Nicolson G. L.* The fluid mosaic model of the structure of cell membranes // Science. - 1972. - Vol. 175. - P. 720-731.
- <sup>7</sup> *Jacobson K., Sheets E. D., Simson R.* Revisiting the fluid mosaic model of membranes // Science. - 1995. - Vol. 268. - P. 1441-1442.
- <sup>8</sup> *Dowhan W.* Molecular basic for membrane phospholipids diversity: Why are there so many lipids? // Ann. Rev. Biochem. - 1997. - Vol. 66. - P. 199-232.
- <sup>9</sup> *Ivkov V. G., Berestovsky G. N.* Dynamic structure of lipid bilayer. - 1987. - Nauka, Moscow [russ].
- <sup>10</sup> *de Kruijff B.* Polymorphic regulation of membrane lipid composition // Nature. - 1987. - Vol. 329. - P. 587-588.
- <sup>11</sup> *Small D. M.* Handbook of lipid research: The physical chemistry of lipids, from alkanes to phospholipids. - 1986. - Plenum Press, New York.
- <sup>12</sup> *Picone D., D'Ursi A., Motta A., Tancredi T., Temussi P. A.* Conformational preferences of [Leu5]enkephalin in biomimetic media. Investigation by <sup>1</sup>H-NMR // Eur. J. Biochem. - 1990. - Vol. 192. - P. 433-439.
- <sup>13</sup> *Behnam B. A., Deber C. M.* Evidence for a folded conformation of methionine- and leucine-enkephalin in a membrane environment // J. Biol. Chem. - 1984. - Vol. 259. - P. 14935-14940.
- <sup>14</sup> *Pervushin K. V., Arsen'ev A. S.* NMR spectroscopy in the study of the spatial structure of membrane peptides and proteins // Bioorg. Khim. - 1995. - Vol. 21. - P. 83-111 [russ].
- <sup>15</sup> *Durr M., Peschel A.* Chemokines meet defensins: the merging concepts of chemoattractants and antimicrobial peptides in host defense // Infect. Immun. - 2002. - Vol. 70. - P. 6515-6517.
- <sup>16</sup> *Hancock R. E., Diamond G.* The role of cationic antimicrobial peptides in innate host defences // Trends Microbiol. - 2000. - Vol. 8. - P. 402-410.
- <sup>17</sup> *Zasloff M.* Antimicrobial peptides of multicellular organisms // Nature. - 2002. - Vol. 415. - P. 389-395.
- <sup>18</sup> *Hancock R. E. W., Chapple D. S.* Peptide antibiotics // Antimicrobial agents and chemotherapy. - 1999. - Vol. 43. - P. 1317-1323.
- <sup>19</sup> <http://aps.unmc.edu/AP/main.php>.
- <sup>20</sup> *Epand R. M., Vogel H. J.* Diversity of antimicrobial peptides and their mechanisms of action // Biochim. Biophys. Acta. - 1999. - Vol. 1462. - P. 11-28.
- <sup>21</sup> *Hof W., Veerman E. C. I., Helmerhorst E. J., Amerongen A. V. N.* Antimicrobial peptides: properties and applicability // J. Biol. Chem. - 2001. - Vol. 382. - P. 597-619.
- <sup>22</sup> *Yeaman M. R., Yount N. Y.* Mechanisms of antimicrobial peptide action and resistance // Pharmacol. Rev. - 2003. - Vol. 55. - P. 27-55.
- <sup>23</sup> *Hancock R. E. W.* Peptide antibiotics // The Lancet. - 1997. - Vol. 349. - P. 418-422.
- <sup>24</sup> *Stallmann H. P., Faber C., Nieuw Amerongen A. V., Wuisman P. I. J. M.* Antimicrobial peptides: review of their application in musculoskeletal infections // Injury Int. J. Care Injured. - 2006. - Vol. 37. - P. 34-40.
- <sup>25</sup> *Vives E., Brodin P., Lebleu B.* A truncated HIV-1 Tat protein basic domain rapidly translocates through the plasma membrane and accumulates in the cell nucleus // J. Biol. Chem. - 1997. - Vol. 272. - P. 16010-16017.

- <sup>26</sup> *Derossi D., Joliot A. H., Chassaing G., Prochiantz A.* Cell internalization of the third helix of the antennapedia homeodomain is receptor-independent // *J. Biol. Chem.* - 1996. - Vol. 271. - P. 18188-18193.
- <sup>27</sup> *Lundberg P., Langel Ü.* A brief introduction to cell-penetrating peptides // *J. Mol. Recognit.* - 2003. - Vol. 16. - P. 227-233.
- <sup>28</sup> *Deshayes S., Morris M. C., Divita G., Heitz F.* Cell-penetrating peptides: tools for intracellular delivery of therapeutics // *Cell. Mol. Life Sci.* - 2005. - Vol. 62. - P. 2039-2049.
- <sup>29</sup> *Fernandez-Carneado J., Kogan M. J., Pujals S., Giralt E.* Amphipathic peptides and drug delivery // *Biopolymers.* - 2004. - Vol. 76. - P. 196-203.
- <sup>30</sup> *Richard J. P., Melikov K., Vives E., Ramos C., Verbeure B., Gait M. J., Chernomordik L. V., Lebleu B.* Cell-penetrating peptides. A reevaluation of the mechanism of cellular uptake // *J. Biol. Chem.* - 2003. - Vol. 278. - P. 585-590.
- <sup>31</sup> *Kerkis A., Hayashi M. A. F., Yamane T., Kerkis I.* Properties of cell penetrating peptides (CPPs) // *IUBMB Life.* - 2006. - Vol. 58. - P. 7-13.
- <sup>32</sup> *Henriques S. T., Melo M. N., Castanho M. A. R. B.* Cell-penetrating peptides and antimicrobial peptides: how different are they? // *Biochem. J.* - 2006. - Vol. 399. - P. 1-7.
- <sup>33</sup> *Melikov K., Chernomordik L. V.* Arginine-rich cell penetrating peptides: from endosomal uptake to nuclear delivery // *Cell. Mol. Life Sci.* - 2005. - Vol. 62. - P. 2739-2749.
- <sup>34</sup> *Tung C., Weissleider R.* Arginine containing peptides as delivery vectors // *Adv. Drug. Deliv. Rev.* - 2003. - Vol. 55. - P. 281-294.
- <sup>35</sup> *Mitchel D. J., Kim D. T., Steinmann L., Fathman C. G., Rothbard J. B.* Polyarginine enters cells more efficiently than other polycationic homopolymers // *J. Pept. Res.* - 2000. - Vol. 56. - P. 320-325.
- <sup>36</sup> *Fawell S., Serry J., Daikh Y., Moore C., Chen L. L., Pepinsky B., Barsoum J.* Tat-mediated delivery of heterologous proteins into cells // *Proc. Natl. Acad. Sci. USA.* - 1994. - Vol. 91. - P. 664-668.
- <sup>37</sup> *Grupta B., Levchenko T. S., Torchilin T. S.* Intracellular delivery of large molecules and small particles by cell-penetrating proteins and peptides // *Adv. Drug Deliv. Rev.* - 2005. - Vol. 57. - P. 637-651.
- <sup>38</sup> *Dietz G. P., Bdeh M.* Delivery of bioactive molecules into the cell: the Trojan horse approach // *Mol. Cell Neurosci.* - 2004. - Vol. 27. - P. 85-131.
- <sup>39</sup> *Zorko M., Langel Ü.* Cell-penetrating peptides: mechanism and kinetics of cargo delivery // *Adv. Drug Deliv. Rev.* - 2005. - Vol. 57. - P. 529-545.
- <sup>40</sup> *Patel L. N., Zaro J. L., Shen W.* Cell-penetrating peptides: intracellular pathways and pharmaceutical perspectives // *Pharm. Res.* - 2007. - Vol. 24. - P. 1977-1992.
- <sup>41</sup> *Torres J., Kukol A., Arkin I. T.* Use of a single glycine residue to determine the tilt and orientation of a transmembrane helix. A novel structural label for Infrared spectroscopy // *Biophys. J.* - 2000. - Vol. 79. - P. 3139-3143.
- <sup>42</sup> *Bradshaw J. P., Darkes M. J., Harroun T. A., Katsaras J., Epand R. M.* Oblique membrane insertion of viral fusion peptide probed by neutron diffraction *Biochem.* - 2000. - Vol. 39. - P. 6581-6585.
- <sup>43</sup> *Evans N. S. J.* *Biomolecular NMR spectroscopy* -1995. - Oxford University Press Inc., New York.
- <sup>44</sup> *Michel H.* Crystallization of membrane proteins // *Trends Bioch. Sci.* - 1983. - Vol. 8. - P. 56-59.
- <sup>45</sup> *Ostermeier C., Iwata S., Ludwig B., Michel H.* Fv Fragment-mediated crystallization of the membrane protein bacterial cytochrome C oxidase // *Nature Struct. Biol.* - 1995. - Vol. 2. - P. 842-846.
- <sup>46</sup> *McVitie S., McComb W. D.* *Electron Microscopy and Analysis* 2003. - 2004. - CRC Press.
- <sup>47</sup> *Torres J., Kukol A., Arkin I. T.* A new structural label for infrared spectroscopy // *Biophys. J.* - 2000. - Vol. 79. - P. 3139-3143.

- <sup>48</sup> Houbiers M. C., Wolfs C. J., Spruijt R. B., Bollen Y. J., Hemminga M. A., Goormaghtigh E. Conformation and orientation of the gene 9 minor coat protein of bacteriophage M13 in phospholipid bilayers // *Biochem. Biophys. Acta.* - 2001. - Vol. 1511. - P. 224-235.
- <sup>49</sup> Komarov I. V., Grigorenko A. O., Turov A. V., Khilya V. P. Conformationally rigid cyclic  $\alpha$ -amino acids in the design of peptidomimetics, peptide models and biologically active compounds // *Russ. Chem. Rev.* - 2004. - Vol. 73. - P. 785-810.
- <sup>50</sup> Rose G. D., Gierasch L. M., Smith J. A. Turns in peptides and proteins. *Advances in protein chemistry.* - 1985. - Academic Press, New York.
- <sup>51</sup> Johnson W. C. Protein secondary structure and circular dichroism: a practical guide // *Proteins.* - 1990. - Vol. 7. - P. 205-214.
- <sup>52</sup> Greenfield N., Fasman G. D. Computed circular dichroism spectra for the evaluation of protein conformation // *Biochemistry.* - 1969. - Vol. 8. - P. 4108-4116.
- <sup>53</sup> Alder A. J., Greenfield N. J., Fasman G. D. Circular dichroism and optical rotary dispersion of proteins and polypeptides // *Meth. Enzymology.* - 1973. - Vol. 27. - P. 675.
- <sup>54</sup> Brahms S., Brahms J. Determination of protein secondary structure in solution by vacuum ultraviolet circular dichroism // *J. Mol. Biol.* - 1980. - Vol. 138. - P. 149-178.
- <sup>55</sup> Strandberg E., Ulrich A. S. NMR methods for studying membrane-active antimicrobial peptides // *Concepts in Magnetic Resonance Part A.* - 2004. - Vol. 23. - P. 89-120.
- <sup>56</sup> Salgado J., Grage S. L., Kondejewski L. H., Hodges R. S., McElhaney R. N., Ulrich A. S. Alignment of the antimicrobial  $\beta$ -sheet peptide gramicidin S in membranes: a solid state  $^{19}\text{F}$ -NMR study in oriented lipid bilayers // *J. Biomol. NMR.* - 2001. - Vol. 21. - P. 191-208.
- <sup>57</sup> Grage S. L., Ulrich A. S. Structural parameters from  $^{19}\text{F}$  homonuclear dipolar couplings, obtained by multipulse solid state NMR in static oriented systems // *J. Magn. Reson.* - 1999. - Vol. 138. - P. 98-106.
- <sup>58</sup> Ulrich A. S. Solid state  $^{19}\text{F}$ -NMR methods for studying biomembranes // *Prog. NMR Spectr.* - 2005. - Vol. 46. - P. 1-21.
- <sup>59</sup> [www.biophysics.org/education/gerig.pdf](http://www.biophysics.org/education/gerig.pdf).
- <sup>60</sup> Ruzza P., Siligardi G., Donella-Deana A., Calderan A., Hussain R., Rubini C., Cesaro L., Osler A., Guiotto A., Pinna L. A., Borin G. 4-Fluoroproline derivative peptides: effect on PPII conformation and SH3 affinity // *J. Pept. Sci.* - 2006. - Vol. 12. - P. 462-471.
- <sup>61</sup> Wang R., Ksebati M. B., Corbett T. H., Kern E. R., Drach J. C., Zemlicka J. Methylene-gem-difluorocyclopropane analogues of nucleosides: synthesis, cyclopropene-methylenecyclopropane rearrangement, and biological activity // *J. Med. Chem.* - 2001. - Vol. 44. - P. 4019-4022.
- <sup>62</sup> Welch J., Eswarakrishnan S. *Fluorine in Bioorganic Chemistry.* - 1991. - Wiley, New York.
- <sup>63</sup> Glaser R. W., Ulrich A. S. Susceptibility corrections in solid state NMR experiments with oriented membrane samples. Part I: applications. - *J. Magn. Reson.* - 2003; Vol. 164. - P. 104-114.
- <sup>64</sup> Grage S. L., Ulrich A. S. Orientation-dependent  $^{19}\text{F}$  dipolar couplings within a trifluoromethyl-group are revealed by multipulse solid state NMR // *J. Magn. Res.* - 2000. - Vol. 146. - P. 81-88.
- <sup>65</sup> Ulrich A. S., Wadhvani P., Dürr U. H. N., Afonin S., Glaser R. W., Strandberg E., Tremouilhac P., Sachse C., Berditchevskaia M., Grage S. *NMR Spectroscopy of Biological Solids.* - 2004. - Ed. A. Ramamoorthy. Taylor & Francis. - P. 215-236.
- <sup>66</sup> Kukhar V. P., Soloshonok V. A. *Fluorine-containing amino acids synthesis and properties.* - 1994. - John Wiley & Sons, New York.
- <sup>67</sup> Sutherland A., Willis C. L. Synthesis of fluorinated amino acids // *Nat. Prod. Rep.* - 2000. - Vol. 17. - P. 621-631.
- <sup>68</sup> Qiu X., Meng W., Qin F. Synthesis of fluorinated amino acids // *Tetrahedron.* - 2004. - Vol. 60. - P. 6711-6745.
- <sup>69</sup> Goss R. J. M., Newill P. L. A. A convenient and environmentally friendly synthesis of *L*-halotryptophans // *Chem. Commun.* - 2006. - Vol. 47. - P. 4924-4925.
- <sup>70</sup> Grage S. L., Wang J., Cross T. A., Ulrich A. S. Structure analysis of fluorine-labelled tryptophan side-chains in gramicidin A by solid state  $^{19}\text{F}$ -NMR // *Biophys. J.* - 2002. - Vol. 83. - P. 3336-3350.

- <sup>71</sup> Cotton M., Tian C., Busath D. D., Shirts R. B., Cross T. A. Modulating Dipoles for Structure-Function Correlations in the Gramicidin A Channel // *Biochemistry*. - 1999. - Vol. 38. - P. 9197-9205.
- <sup>72</sup> Saghiyan A. S., Dadayan S. A., Petrosyan S. G., Manasyan L. L., Geolchanyan A. V., Djamgaryan S. M., Andreasyan S. A., Maleev V. I., Khrustalev V. N. New chiral Ni<sup>II</sup> complexes of Schiff's bases of glycine and alanine for efficient asymmetric synthesis of  $\alpha$ -amino acids // *Tetrahedron: Asymmetry*. - 2006. - Vol. 17. - P. 455-467.
- <sup>73</sup> Buffy J. J., Waring A. J., Hong M. Determination of peptide oligomerization in lipid bilayers using <sup>19</sup>F spin diffusion NMR // *J. Am. Chem. Soc.* - 2005. - Vol. 127. - P. 4477-4483.
- <sup>74</sup> Kukhar V. P., Belokon Y. N., Soloshonok V. A., Svistunova N. Y., Rozhenko A. B., Kuzmina N. General method for the asymmetric synthesis of fluorine-containing phenylalanines and  $\alpha$ -methylphenylalanines via alkylation of the chiral nickel(II) schiff's base complexes of glycine and alanine // *Synthesis*. - 1993. - Vol. 1. - P. 117-120.
- <sup>75</sup> Inaba T., Kozono I., Fujita M., Ogura K. An efficient and practical synthesis of *L*- $\alpha$ -amino acids using (*R*)-phenylglycinol as a chiral auxiliary // *Bull. Chem. Soc. Jpn.* - 1992. - Vol. 65. - P. 2359-2365.
- <sup>76</sup> Mellin-Morliere C., Aitken D. J., Bull S. D., Davies S. G., Husson H. P. A practical asymmetric synthesis of homochiral  $\alpha$ -arylglycines // *Tetrahedron: Asymmetry*. - 2001. - Vol. 12. - P. 149-155.
- <sup>77</sup> Afonin S., Glaser R. W., Berditchevskaia M., Wadhwani P., Guhrs K. H., Mollmann U., Perner A., Ulrich A. S. 4-Fluorophenylglycine as a label for <sup>19</sup>F-NMR structure analysis of membrane-associated peptides // *ChemBioChem*. - 2003. - Vol. 4. - P. 1151-1163.
- <sup>78</sup> Afonin S., Dürr U. H. N., Glaser R. W., Ulrich A. S. "Boomerang"-like insertion of a fusogenic peptide in a lipid membrane revealed by solid state <sup>19</sup>F-NMR // *Magn. Reson. Chem.* - 2004. - Vol. 42. - P. 195-203.
- <sup>79</sup> Morgan J., Pinhey J. T., Sherry C. J. Reaction of organolead triacetates with 4-ethoxycarbonyl-2-methyl-4,5-dihydro-1,3-oxazol-5-one. The synthesis of  $\alpha$ -aryl- and  $\alpha$ -vinyl-N-acetylglycines and their ethyl esters and their enzymatic resolution // *J. Chem. Soc., Perkin Trans. 1*. - 1997. - Vol. 5. - P. 613-619.
- <sup>80</sup> Gläzer R. S. W., Sachse C., Dürr U. H. N., Wadhwani P., Afonin S., Strandberg E., Ulrich A. S. Concentration-dependent re-alignment of the peptide PGLa in lipid membranes observed by solid state <sup>19</sup>F-NMR // *Biophys. J.* - 2005. - Vol. 88. - P. 3392-3397.
- <sup>81</sup> Grage S. L., Suleymanova A. V., Afonin S., Wadhwani P., Ulrich A. S. Solid state NMR analysis of the dipolar couplings within and between distant CF<sub>3</sub>-groups in a membrane-bound peptide // *J. Magn. Reson.* - 2006. - Vol. 203. - P. 77-86.
- <sup>82</sup> Eisele A. Diploma Thesis. - 2007. - University of Karlsruhe.
- <sup>83</sup> Scheiner S., Kar T., Pattanayak J. Comparison of various types of hydrogen bonds involving aromatic amino acids // *J. Am. Chem. Soc.* - 2002. - Vol. 124. - P. 13257-13264.
- <sup>84</sup> Glaser R. W., Sachse C., Dürr U. H. N., Wadhwani P., Ulrich A. S. Orientation of the antimicrobial peptide PGLa in lipid membranes determined from <sup>19</sup>F-NMR dipolar couplings of 4-CF<sub>3</sub>-phenylglycine labels // *J. Magn. Reson.* - 2004. - Vol. 168. - P. 153-163.
- <sup>85</sup> Kollonitsch J., Marburg S., Perkins L. M. Fluorodehydroxylation, a novel method for synthesis of fluoroamines and fluoroamino acids // *J. Org. Chem.* - 1979. - Vol. 44. - P. 771-777.
- <sup>86</sup> Bravo P., Cavicchio G., Crucianelli M., Poggiali A., Zanda M. Stereoselective synthesis of the antibacterial 3-fluoro-*D*-alanine // *Tetrahedron: Asymmetry*. 1997. - Vol. 8. - P. 2811-2815.
- <sup>87</sup> Toke O., O'Connor R. D., Weldeghiorghis T. K., Maloy W. L., Glaser R. W., Ulrich A. S., Schaefer J. Structure of (KIAGKIA)<sub>3</sub> aggregates in phospholipid bilayers by solid state NMR // *Biophys. J.* - 2004. - Vol. 87. - P. 675-687.
- <sup>88</sup> Bargamov G. G., Rokhlin E. M., Galakhov M. V., Mysov E. I. Bis- $\alpha$ -hydrohexafluoroisobutyrate and bis-pentafluoromethacrylates // *Izvestiya Akademii Nauk SSSR, Seriya Khimicheskaya*. - 1989. - Vol. 7. - P. 1645-1616.

- <sup>89</sup> Itoh Y., Yamanaka M., Mikami K. Direct generation of Ti-enolate of  $\alpha$ -CF<sub>3</sub> ketone: theoretical study and high-yielding and diastereoselective aldol reaction // *J. Am. Chem. Soc.* - 2004. - Vol. 126. - P. 13174-13175.
- <sup>90</sup> Bargamov G. G., Rokhlin E. M., Galakhov M. V., Mysov E. I. Bis- $\alpha$ -hydrohexafluoroisobutyrate and bis-pentafluoromethacrylates // *Izvestiya Akademii Nauk SSSR, Seriya Khimicheskaya.* - 1989. - Vol. 7. - P. 1645-16.
- <sup>91</sup> Tremouihac P. PhD Thesis. - 2007. - University of Karlsruhe.
- <sup>92</sup> Fänghänel S. Diploma Thesis. - 2007. - University of Karlsruhe.
- <sup>93</sup> Maisch D. PhD Thesis. - 2008. - University of Karlsruhe.
- <sup>94</sup> Burger K., Mütze K., Hollweck W., Kokschi B. Incorporation of  $\alpha$ -trifluoromethyl substituted  $\alpha$ -amino acids into C- and N-terminal position of peptides and peptide mimetics using multicomponent reactions // *Tetrahedron.* - 1998. - Vol. 54. - P. 5915-5928.
- <sup>95</sup> Schlerlinger C., Burger K. Peptide modification by introduction of  $\alpha$ -trifluoromethyl  $\alpha$ -amino acids via 4-trifluoromethyl-1,3-oxazolidin-2,5-diones // *Tetrahedron Lett.* - 1992. - Vol. 33. - P. 193-194.
- <sup>96</sup> Jaeckel C., Seufert W., Thust S., Kokschi B. Evaluation of the molecular interactions of fluorinated amino acids with native polypeptides // *ChemBioChem.* - 2004. - Vol. 5. - P. 717-720.
- <sup>97</sup> Chiu H., Suzuki Y., Gullickson D., Ahmad R., Kokona B., Fairman R., Cheng R. P. Helix propensity of highly fluorinated amino acids // *J. Am. Chem. Soc.* - 2006. - Vol. 128. - P. 15556-15557.
- <sup>98</sup> Ojima I., Kato K., Nakahashi K., Fuchikami T., Fujita M. New and effective routes to fluoro analogs of aliphatic and aromatic amino acids // *J. Org. Chem.* - 1989. - Vol. 54. - P. 4511-4522.
- <sup>99</sup> Soloshonok V., Kukhar V., Pustovit Y., Nazaretyan V. A new and convenient synthesis of *S*-trifluoromethyl-containing amino acids // *Synlett.* - 1992. - Vol. 8. - P. 657-658.
- <sup>100</sup> Son S., Tanrikulu I. C., Tirrell D. A. Stabilization of bzip peptides through incorporation of fluorinated aliphatic residues // *ChemBioChem.* - 2006. - Vol. 7. - P. 1251-1257.
- <sup>101</sup> Bilgicer B., Fischera A., Kumar K. A coiled coil with a fluorinated core // *J. Am. Chem. Soc.* - 2001. - Vol. 123. - P. 4393-4399.
- <sup>102</sup> Xing X., Fischera A., Kumar K. A simple and efficient method for the resolution of all for diastereomers of 4,4,4-trifluorovaline and 5,5,5-trifluoroisoleucine // *J. Org. Chem.* - 2002. - Vol. 67. - P. 1722-1725.
- <sup>103</sup> Houston M. E., Honek J. F. Facile synthesis of fluorinated methionines // *Chem. Commun.* - 1989. - Vol. 12. - P. 761-762.
- <sup>104</sup> DesMarteau D. D., Montanari V. The novel iodonium salt (CF<sub>3</sub>SO<sub>2</sub>)<sub>2</sub>Ni(Ph)CH<sub>2</sub>CF<sub>3</sub> is a powerful alkylating reagent which can be utilized in water to trifluoroethylacetate amino acids and peptides // *Chem. Commun.* 1998. - P. 2241-2242.
- <sup>105</sup> Muller N. Synthesis of 5,5,5-trifluoro-*DL*-isoleucine and 5,5,5-trifluoro-*DL*-alloisoleucine // *J. Fluor. Chem.* - 1987. - Vol. 36. - P. 163-170.
- <sup>106</sup> Wang P., Tang Y., Tirrell D. A. Incorporation of trifluoroisoleucine into proteins in vivo // *J. Am. Chem. Soc.* - 2003. - Vol. 125. - P. 6900-6906.
- <sup>107</sup> Chen Q., Qui X. L., Qing F. L. Indium-mediated diastereoselective allylation of *D*- and *L*-glyceraldimines with 4-bromo-1,1,1-trifluoro-2-butene: highly stereoselective synthesis of 4,4,4-trifluoroisoleucines and 4,4,4-trifluorovaline // *J. Org. Chem.* - 2006. - Vol. 71. - P. 3762-3767.
- <sup>108</sup> Tang Y., Ghirlanda G., Vaidehi N., Kua J., Mainz D. T., Goddard W. A., DeGrado W. F., Tirrell D. A. Stabilization of leucine zipper coiled coils by introduction of trifluoroisoleucine // *Biochemistry.* - 2001. - Vol. 40. - P. 2790-2796.
- <sup>109</sup> Tang Y., Ghirlanda G., Petka W. A., Nakajima T., DeGrado W. F., Tirrell D. A. Fluorinated coiled-coil proteins prepared in vivo display enhanced thermal and chemical stability // *Angew. Chem. Int. Ed. Engl.* - 2001. - Vol. 40. P. 1494-1496.
- <sup>110</sup> Niemz A., Tirrell D. A. Self-association and membrane-binding behaviour of melittins containing trifluoroisoleucine // *J. Am. Chem. Soc.* - 2001. - Vol. 123. - P. 7407-7413.

- <sup>111</sup> *Tsushima T., Kawada K., Ishihara S., Uchida N., Shiratori O., Higaki J., Hirata M.* Fluorine containing amino acids and their derivatives. Synthesis and antitumor activity of  $\alpha$ - and  $\gamma$ -substituted methotrexate analogs // *Tetrahedron*. - 1988. - Vol. 44. - P. 5375-5387.
- <sup>112</sup> *Asensio A., Bravo P., Crucianelli M., Farina A., Fustero S., Soler J. G., Meille S. V., Panzeri W., Viani F., Volonterio A., Zanda M.* Synthesis of nonracemic  $\alpha$ -trifluoromethyl  $\alpha$ -amino acids from sulfinimines of trifluoropyruvate // *Eur. J. Org. Chem.* - 2001, Vol. 8. - P. 1449-1458.
- <sup>113</sup> *Bravo P., Crucianelli M., Vergani B., Zanda M.* Sulfinimines of trifluoropyruvate: novel intermediates for chiral non racemic  $\alpha$ -trifluoromethyl  $\alpha$ -amino acids. - *Tetrahedron Lett.* - 1998. - Vol. 39. - P. 7771-7774.
- <sup>114</sup> *Katagiri T., Irie M., Uneyama K.* Syntheses of optically active trifluoronorcoronamic acids // *Org. Lett.* - 2000. - Vol. 2. - P. 2423-2425.
- <sup>115</sup> *Chaume G., Van Severen M. C., Marinkovich S., Brigaud T.* Straightforward synthesis of (*S*)- and (*R*)- $\alpha$ -trifluoromethyl proline from chiral oxazolidinones derived from ethyl trifluoropyruvate // *Org. Lett.* - 2006. - Vol. 8. - P. 6123-6126.
- <sup>116</sup> *Qiu X., Qing F.* Practical synthesis of Boc-protected *cis*-4-trifluoromethyl and *cis*-4-difluoromethyl-*L*-prolines // *J. Org. Chem.* - 2002. - Vol. 67. - P. 7162-7164.
- <sup>117</sup> *Del Valle J. R., Goodman M.* Stereoselective synthesis of Boc-protected *cis*- and *trans*-4-trifluoromethylprolines by asymmetric hydrogenation reactions // *Angew. Chem. Int. Ed. Engl.* - 2002. - Vol. 41. - P. 1600-1602.
- <sup>118</sup> *Qiu X., Qing F.* Synthesis of Boc-protected *cis*- and *trans*-4-trifluoromethyl-*D*-prolines // *J. Chem. Perkin Trans. 1.* - 2002. - Vol. 34. - P. 2052-2057.
- <sup>119</sup> *Nadano R., Iwai Y., Mori T., Ichikawa J.* Divergent chemical synthesis of prolines bearing fluorinated one-carbon units at the 4-Position via nucleophilic 5-endo-trig cyclizations // *J. Org. Chem.* - 2006. - Vol. 71. - P. 8748-8754.
- <sup>120</sup> *Jiang J., Shah H., DeVita R. J.* Synthesis of 4-trifluoromethylated 2-alkyl- and 2,3-dialkyl-substituted azetidines dialkyl-substituted azetidines // *Org. Lett.* - 2003. - Vol. 5. - P. 4101-4103.
- <sup>121</sup> *Bretscher L. E., Jenkins C. L., Taylor K. M., DeRider M. L., Raines R.* Conformational stability of collagen relies on a stereoelectronic effect // *J. Am. Chem. Soc.* - 2001. - Vol. 123. - P. 777-778.
- <sup>122</sup> *Adcock W., Baran Y., Filippi A., Speranza M., Trout N. A.* Polar substituent effects in the bicyclo[1.1.1]pentane ring system: acidities of 3-substituted bicyclo[1.1.1]pentane-1-carboxylic acids // *J. Org. Chem.* - 2005. - Vol. 70. - P. 1029-1034.
- <sup>123</sup> All the values were calculated by QikProp (Schrödinger software) [www.schrodinger.com](http://www.schrodinger.com).
- <sup>124</sup> *Branden C., Tooze J.* Introduction to Protein Structure. - 1999. - Garland Publishing, New York.
- <sup>125</sup> *Costantino G., Maltoni K., Marinozzi M., Camaioni E., Prezeau L., Pin J., Pellicciari R.* Synthesis and biological evaluation of 2-(3'-(1H-tetrazol-5-yl)bicyclo[1.1.1]pent-1-yl)glycine (*S*-TBPG), a novel mGlu1 receptor antagonist // *Bioorg. Med. Chem.* - 2001. - Vol. 9. - P. 221-227.
- <sup>126</sup> *Pellicciari R., Raimondo M., Marinozzi M., Natalini B., Costantino G., Thomsen C.* (*S*)-(+)-2-(3'-Carboxybicyclo[1.1.1]pentyl)-glycine, a structurally new group I metabotropic glutamate receptor antagonist // *J. Med. Chem. Lett.* - 1996. - Vol. 39. - P. 2874-2876.
- <sup>127</sup> *Mondanaro K. M., Dailey W. P.* Improved preparations of 3-chloro-2-(chloromethyl)-1-propene and 1,1-dibromo-2,2-bis(chloromethyl)cyclopropane: intermediates in the synthesis of [1.1.1]propellane // *J. Org. Chem.* - 1995. - Vol. 60. - P. 4666-4668.
- <sup>128</sup> *Semmler K., Belzner J., Szeimes G.* Concerning the synthesis of [1.1.1]propellane // *Chem. Ber.* - 1989. - Vol. 122. - P. 397-398.
- <sup>129</sup> *Szeimes G., Semmler K.* Tetracyclo[5.1.0.0.1,6.0.2,7]octane, a [1.1.1]propellane derivative, and a new route to the parent hydrocarbon // *J. Am. Chem. Soc.* - 1985. - Vol. 107. - P. 6410-6411.
- <sup>130</sup> *Rehm J. D., Ziemer B., Szeimes G.* A facile route to bridgehead disubstituted bicyclo[1.1.1]pentanes involving palladium-catalyzed cross-coupling reactions // *Eur. J. Org. Chem.* - 1999. - Vol. 9. - P. 2079-2085.
- <sup>131</sup> *Rehm J. D., Ziemer B., Szeimes G.* A facile, palladium-catalyzed synthesis of 1,1'-bi(bicyclo[1.1.1]pentanes) // *Eur. J. Org. Chem.* - 2001. - Vol. 6. - P. 1049-1052.

- <sup>132</sup> *Wiberg K. B., Waddel S. T.* Reactions of [1.1.1]propellane // *J. Am. Chem. Soc.* - 1990. - Vol. 112. - P. 2194-2216.
- <sup>133</sup> *Adcock J. L., Gack A. A.* Nucleophilic substitution in 1-substituted 3-iodobicyclo[1.1.1]pentanes. A new synthetic route to functionalized bicyclo[1.1.1]pentane derivatives // *J. Org. Chem.* - 1992. - Vol. 57. - P. 6206-6210.
- <sup>134</sup> *Kostova K., Dimitrov V.* 1-Norbornyllithium as a precursor for the synthesis of novel organic 1-bicyclo[2.2.1]heptane derivatives and for the improved preparation of 1-chloro-bicyclo[2.2.2]octane // *Synthetic Commun.* - 1995. - Vol. 25. - P. 1575-1587.
- <sup>135</sup> *Clayden J., Greeves N., Warren S., Wothers P.* Organic chemistry. - 2001. - Oxford University Press Inc, New York. - P. 340-341.
- <sup>136</sup> *H. Hünther.* Introduction to NMR Spectroscopy. - 1980. - Mir, Moscow. - P. 130 [russ].
- <sup>137</sup> *H. Hünther.* Introduction to NMR Spectroscopy. - 1980. - Mir, Moscow. - P. 172 [russ].
- <sup>138</sup> *Dave R. H., Hosangadi B. D.* A simple and efficient diastereoselective Strecker synthesis of optically pure  $\alpha$ -aryl glycines // *Tetrahedron.* - 1999. - Vol. 55. - P. 11295-11308.
- <sup>139</sup> *Chakraborty T. K., Reddy G. V., Hussain K. A.* A simple and efficient diastereoselective Strecker synthesis of optically pure  $\alpha$ -aryl glycines // *Tetrahedron Lett.* - 1991. - Vol. 32. - P. 7597-7600.
- <sup>140</sup> *Chakraborty T. K., Reddy G. V., Hussain K. A.*  $\alpha$ -phenylglycinol as chiral auxiliary in diastereoselective strecker synthesis of  $\alpha$ -amino acids // *Tetrahedron Lett.* - 1995. - Vol. 51. - P. 9179-9190.
- <sup>141</sup> *Inaba T., Ogura K.* An efficient and practical synthesis of *L*- $\alpha$ -amino acids using (*R*)-phenylglycinol as a chiral auxiliary // *Bull. Chem. Soc. Jpn.* - 1992. - Vol. 65. - P. 2359-2365.
- <sup>142</sup> *Kobayashi S., Ishitani H., Ueno M.* Facile synthesis of  $\alpha$ -amino nitriles using lanthanide triflate as a Lewis acid catalyst // *Synlett.* - 1997. - Vol. - P. 115-116.
- <sup>143</sup> *Kobayashi S., Busujima T., Nagayama S.* Scandium triflate-catalyzed Strecker-type reactions of aldehydes, amines and tributyltin cyanide in both organic and aqueous solutions. Achievement of complete recovery of the tin compounds toward environmentally-friendly chemical processes // *Chem. Commun.* - 1998. - P. 981-982.
- <sup>144</sup> *Inaba T., Ogura K.* Thermodynamically controlled 1,3-asymmetric induction in an acyclic system: equilibration of  $\alpha$ -amino nitriles derived from  $\alpha$ -alkylbenzylamines and aldehydes // *J. Org. Chem.* - 1991. - Vol. 56. - P. 1274-1279.
- <sup>145</sup> *Gröger H.* Catalytic enantioselective strecker reactions and analogous syntheses // *Chem. Rev.* - 2003. - Vol. 103. - P. 2795-2827.
- <sup>146</sup> CCDC-293724 contains the crystallographic data for **30**. These data can be obtained free of charge from The Cambridge Crystallographic Data Centre via [deposit@ccdc.cam.ac.uk](mailto:deposit@ccdc.cam.ac.uk).
- <sup>147</sup> *Gershkovich A. A., Kibirev V. K.* Peptide synthesis. - 1987. - Naukova Dumka, Kyiv [russ].
- <sup>148</sup> *Parker D.* NMR determination of enantiomeric purity // *Chem. Rev.* - 1991. - Vol. 91. - P. 1441-1457.
- <sup>149</sup> *Li Y. H., Baek C. S., Jo B. W., Le W.* Direct chiral separation of *N*-fluorenylmethoxycarbonyl  $\alpha$ -amino acids by HPLC for determination of enantiomeric purity // *Bull. Korean Chem. Soc.* - 2005. - Vol. 26. - P. 998-1000.
- <sup>150</sup> *Morril T. C.* Lanthanide shift reagents in stereochemical analysis // *Methods in stereochemical analysis.* - 1985 VCH, Weinheim.
- <sup>151</sup> *MacArthur M., Thornton J.* Influence of proline residues on protein conformation // *J. Mol. Biol.* - 1991. - Vol. 218. - P. 397-412.
- <sup>152</sup> *Ball L., Kühne R., Schneider-Mergener J., Oschkinat H.* Recognition of proline-rich motifs by protein-protein-interaction domains // *Angew. Chem.* - 2005. - Vol. 117. - P. 2912-2930.
- <sup>153</sup> *Adzhubei A., Sternberg M.* Left-handed polyproline II helices commonly occur in globular proteins // *J. Mol. Biol.* - 1993. - Vol. 229. - P. 472-493.
- <sup>154</sup> *Bochicchio B., Tamburro A. M.* Polyproline II structure in proteins: identification by chiroptical spectroscopies, stability, and functions // *Chirality.* - 2002. - Vol. 14. - P. 782-792.

- <sup>155</sup> Rath A., Davidson A., Deber C. The structure of 'unstructured' regions in peptides and proteins: role of the polyproline II helix in protein folding and recognition // *Biopolymers*. - 2005. - Vol. 80. - P. 179-185.
- <sup>156</sup> Talluri S., Montellione G. T., Dwyne G., Piela L., Clardy J., Scheraga H. A. Conformational properties of 2,4-methanoproline (2-carboxy-2,4-methanopyrrolidine) in peptides: evidence for 2,4-methanopyrrolidine asymmetry based on solid state x-ray crystallography, proton NMR in aqueous solution, and CNDO/2 conformational energy calculations // *J. Am. Chem. Soc.* - 1987. - Vol. 109. - P. 4473-4477.
- <sup>157</sup> Piela L., Nemethy G., Scheraga H. A. Conformational properties of 2,4-methanoproline (2-carboxy-2,4-methanopyrrolidine) in peptides: theoretical conformational energy analysis of restrictions of the polypeptide chain conformation // *J. Am. Chem. Soc.* - 1987. - Vol. 109. - P. 4477-4485.
- <sup>158</sup> Campbell J. A., Rapoport H. Chiroselective syntheses of conformationally constrained 7-azabicycloheptane amino acids by transannular alkylation // *J. Org. Chem.* - 1996. - Vol. 61. - P. 6313-6325.
- <sup>159</sup> Avenozza A., Busto J. H., Peregrina J. M., Rodríguez F. Incorporation of AHC into model dipeptides as an inducer of a  $\beta$ -turn with a distorted amide bond. Conformational analysis // *J. Org. Chem.* - 2002. - Vol. 67. - P. 4241-4249.
- <sup>160</sup> Sewald N., Burger K. Synthesis of fluorine-containing amino acids. In "Kukhar V. P., Soloshonok V. A. Fluorine-containing amino acids synthesis and properties. - 1994. - John Wiley & Sons, New York."
- <sup>161</sup> Koksich B., Sewald N., Hofmann H., Burger K., Jakubke H. Proteolytically stable peptides by incorporation of  $\alpha$ -Tfm amino acids // *J. Pept. Sci.* - 1997. - Vol. 3. - P. 157-167.
- <sup>162</sup> Möhle K., Hofmann H. Conformational studies on peptides with unusual amino acid side-chains: The trifluoromethyl group // *Journal of Molecular Structure (Theochem)*. - 1995. - Vol. 339. P. 57-65.
- <sup>163</sup> Osipov S. N., Kolomiets A. F., Fokin A. V. Trifluoromethylhydroxyproline // *Izvestiya Akademii Nauk SSSR, Seriya Khimicheskaya*. - 1990. - Vol. 10. - P. 2456.
- <sup>164</sup> Koksich B., Ullmann D., Jakubke H., Burger K. Synthesis, structure and biological activity of  $\alpha$ -trifluoromethyl-substituted thyrotropin releasing hormone // *J. Fluor. Chem.* - 1996. - Vol. 80. - P. 53-57.
- <sup>165</sup> Osipov S. N., Kolomiets A. F., Bruneau C., Picquet M., Dixneuf P. H. Synthesis of fluorine-containing cyclic amino acid derivatives via ring closing olefin metathesis // *Chem. Commun.* - 1998. - Vol. 20. - P. 2053-2054.
- <sup>166</sup> Osipov S. N., Artyushin O. I., Kolomiets A. F., Bruneau C., Picquet M., Dixneuf P. H. Synthesis of fluorine-containing cyclic  $\alpha$ -amino acid and  $\alpha$ -amino phosphonate derivatives by alkene metathesis // *Eur. J. Org. Chem.* - 2001. - Vol. 20. - P. 3891-3897.
- <sup>167</sup> Kirij N. V., Babadzhanova L. A., Movchun V. N., Yagupolskii Y. L., Tyrro W., Naumann D., Fischer H. T. M., Scherer H. Trifluoromethylation of non-activated aldimines with trimethyl(trifluoromethyl)silane in the presence of tetramethylammonium fluoride: A closer look into the reaction route // *J. Fluor. Chem.* - 2008. - Vol. 129. - P. 14-21
- <sup>168</sup> Prakash G., Mogi R., Olah G. Preparation of tri- and difluoromethylated amines from aldimines using (trifluoromethyl)trimethylsilane // *Org. Lett.* - 2006. - Vol. 8. - P. 3589-3592.
- <sup>169</sup> Grygorenko O. O., Artamonov O. S., Palamarchuk G. V., Zubatyuk R. I., Shishkin O. V., Komarov I. V. Stereoselective synthesis of 2,4-methanoproline homologues // *Tetrahedron: Asymmetry*. - 2006. - Vol. 17. - P. 252-258.
- <sup>170</sup> Häusler J., Schmidt U. Synthese von *cis*- und *trans*-3-Phenoxyprolin // *Liebigs Ann. Chem.* - 1979. - Vol. 11. - P. 2081-2089.
- <sup>171</sup> Singh R. P., Shreeve J. M. Nucleophilic trifluoromethylation reactions of organic compounds with (trifluoromethyl)trimethylsilane // *Tetrahedron*. - 2000. - Vol. 56. - P. 7613-7632.
- <sup>172</sup> Marsilje T. H., Hedrick M. P., Desharnais J., Tavassoli A., Zhang Y., Wilson I. A., Benkovic S. J., Boger D. L. Design, synthesis, and biological evaluation of simplified  $\alpha$ -keto-heterocycle,



- trifluoromethyl ketone, and formyl substituted folate analogues as potential inhibitors of GAR transformylase and AICAR transformylase // *Bioorg. Med. Chem.* - 2003. - Vol. 11. - P. 4487-4501.
- <sup>173</sup> Doucet-Personeni C., Bentley P. D., Fletcher R. J., Kinkaid A., Kryger G., Pirard, B., Taylor A., Taylor R., Taylor J., Viner R., Silman I., Sussman J. L., Greenblatt H. M., Lewis T. A. Structure-based design approach to the development of novel, reversible AChE inhibitors // *J. Med. Chem.* - 2001. - Vol. 44. - P. 3203-3215.
- <sup>174</sup> Krishnamurti R., Donald R., Bellew G. K., Prakash S. Preparation of trifluoromethyl and other perfluoroalkyl compounds with (perfluoroalkyl)trimethylsilanes // *J. Org. Chem.* - 1991. - Vol. 56. - P. 984-989.
- <sup>175</sup> Zhang R., Mamai A., Madalengoitia J. S. Cyclopropanation reactions of pyroglutamic acid-derived synthons with alkylidene transfer reagents // *J. Org. Chem.* - 1999. - Vol. 64. - P. 547-555.
- <sup>176</sup> Marinozzi M., Natalini B., Ni M., Costantino G., Pellicciari R., Thomsen C. Synthesis and biological evaluation of 6-carboxy-3,4-methanoprolines, new rigid glutamate analogs // *Farmaco.* - 1995. - Vol. 50. - P. 327-331.
- <sup>177</sup> Marinozzi M., Natalini B., Ni M., Costantino G., Pellicciari R., Bruno V., Nicoletti F. Synthesis of 6,6-dicarboxy-3,4-methano-L-proline, a new constrained glutamate analog endowed with neuroprotective properties // *Farmaco.* - 1996. - Vol. 51. - P. 121-124.
- <sup>178</sup> Fujimoto Y., Irreverre F., Karle J. M., Witkop B. Synthesis and X-ray analysis of *cis*-3,4-methylene-L-proline, the new natural amino acid from horse chestnuts, and of its *trans* isomer // *J. Am. Chem. Soc.* - 1971. - Vol. 93. - P. 3471-3477.
- <sup>179</sup> Tverezovsky V. V., Baird M. S., Bolesov I. G. Synthesis of (2*S*,3*R*,4*S*)-3,4-methanoproline and analogues by cyclopropylidene insertion // *Tetrahedron.* - 1997. - Vol. 53. - P. 14773-14792.
- <sup>180</sup> Atherton J. H., Field R. Reaction of trifluoromethylcarbene with *cis*- and *trans*-but-2-enes // *J. Chem. Soc. C.* - 1967. - P. 1450-1454
- <sup>181</sup> Atherton J. H., Fields R. Cycloaddition reactions of 2,2,2-trifluorodiazethane // *J. Chem. Soc. C.* - 1968. - P. 1507-1513.
- <sup>182</sup> Fields R., Haszeldine R. N. Carbene chemistry. Part I. Reactions of fluoroalkyldiazo-compounds // *J. Chem. Soc.* - 1964. - P. 2081-2089.
- <sup>183</sup> Schumacher K. K., Jiang J., Joullie M. M. Synthetic studies toward astins A, B and C. Efficient syntheses of *cis*-3,4-dihydroxyprolines and (-)-(3*S*,4*R*)-dichloroproline esters // *Tetrahedron: Asymmetry.* - 1998. - Vol. 9. - P. 47-53.
- <sup>184</sup> Doyle M. Catalytic methods for metal carbene transformations // *Chem. Rev.* - 1986. - Vol. 66. - P. 919-939.
- <sup>185</sup> Donaldson W. Synthesis of cyclopropane containing natural products // *Tetrahedron.* - 2001. - Vol. 57. - P. 8589-8627.
- <sup>186</sup> Adams J., Spero D. M. Rhodium (II) catalyzed reactions of diazo-carbonyl compounds // *Tetrahedron.* - 1991. - Vol. 47. - P. 1765-2008.
- <sup>187</sup> Doyle M. P., Forbes D. C. Recent advances in asymmetric catalytic metal carbene transformations // *Chem. Rev.* - 1998. - Vol. 98. - P. 911-935.
- <sup>188</sup> Lebel H., Marcoux J. F., Molinaro C., Charette A. B. Stereoselective cyclopropanation reactions // *Chem. Rev.* - 2003. - Vol. 103. - P. 977-1050
- <sup>189</sup> O'Bannon P. E., Dailey W. P. Nitrocyclopropanes from nitrodiazomethanes. preparation and reactivity // *Tetrahedron.* - 1990. - Vol. 46. - P. 7341-7358.
- <sup>190</sup> Wang Y, Zhu S, Zhu G, Huang Q. An efficient synthesis of 3-trifluoromethylated 8-oxabicyclo[3.2.1]octa-2,6-dienes // *Tetrahedron.* - 2001. - Vol. 57. - P. 7337-7342.
- <sup>191</sup> Jiang B., Zhang X., Luo Z. High diastereoselectivity in intermolecular carbonyl ylide cycloaddition with aryl aldehyde using methyl diazo(trifluoromethyl)acetate // *Org. Lett.* - 2002. - Vol. 4. - P. 2453-2455.
- <sup>192</sup> Müller P., Grass S., Shahi S. P., Bernardinelli G. Rh(II)-Catalyzed asymmetric carbene transfer with ethyl 3,3,3-trifluoro-2-diazopropionate // *Tetrahedron.* - 2004. - Vol. 60. - P. 4755-4763.
- <sup>193</sup> Ghanem A., Lacrampe F., Aboul-Enein H., Schurig V. Diazo compounds and phenyliodonium ylides in inter- and intramolecular cyclopropanations catalyzed by dirhodium(II). Synthesis and

chiral resolution by GC versus HPLC // *Monatshefte für Chemie*. - 2005. - Vol. 136. - P. 1205-1219.

<sup>194</sup> Denton J. R., Sukumaran D., Davies H. M. L. Enantioselective synthesis of trifluoromethyl-substituted cyclopropanes // *Org. Lett.* - 2007. - Vol. 9. - P. 2625-2628.

<sup>195</sup> Altman L. J., Bramwell M. R., Vederas J. C. Synthesis and stereochemical assignments of some trifluoromethylphenylcyclopropanes // *Can. J. Chem.* - 1971. - Vol. 49. - P. 968-971.

<sup>196</sup> Salomon R. G., Kochi J. K. Copper(I) catalysis in cyclopropanations with diazo compounds. Role of olefin coordination // *J. Am. Chem. Soc.* - 1973. - Vol. 95. - P. 3300-3310.

<sup>197</sup> Salomon R. G., Salomon M. F., Heyne T. R. Vinylcyclopropanation of olefins with vinyl diazomethane // *J. Org. Chem.* - 1975. - Vol. 40. - P. 756-760.

<sup>198</sup> Mitchell R. E. Norcoronatine and N-coronafacoyl-L-valine, phytotoxic analogues of coronatine produced by a strain of *Pseudomonas syringae* pv. *glycinea* // *Phytochemistry*. - 1985. - Vol. 24. - P. 1485-1487.

<sup>199</sup> Gallow-Dagommer I., Gastaud P., RajanBabu T. V. Asymmetric synthesis of functionalized 1,2,3,4-tetrahydroquinolines // *Org. Lett.* - 2001. - Vol. 3. - P. 2053-2056.

<sup>200</sup> Katagiri T., Irie M., Uneyama K. Syntheses of optically active trifluoronorcoronamic acids // *Org. Lett.* - 2000. - Vol. 2. - P. 2423-2425.

<sup>201</sup> Arenare L., De Caprariis P., Marinozzi M., Natalini B., Pellicciari R. Synthesis of 2-azabicyclo[3.1.0]hexane tricarboxylate and its transformation into a new proline- $\gamma$ -acetic acid equivalent // *Tetrahedron Lett.* - 1994. - Vol. 35. - P. 1425-1426.

<sup>202</sup> Pellicciari R., Arenare L., De Caprariis P., Natalini B., Marinozzi M., Galli A. Synthesis of all four diastereoisomers of 4-(carboxymethyl)proline, a conformationally constrained analogue of 2-aminoadipic acid // *J. Chem. Soc., Perkin Trans. 1*. - 1995. - P. 1251.

<sup>203</sup> Hanessian S., Reinhold U., Saulnier M., Claridge S. Probing the importance of spatial and conformational domains in captopril analogs for angiotensin converting enzyme activity // *Bioorg. Med. Chem. Lett.* - 1998. - Vol. 8. - P. 2123-2128.

<sup>204</sup> Hanessian S., Reinhold U., Gentile G. The synthesis of enantiopure  $\omega$ -methanoprolines and  $\omega$ -methanopipicolinic acids by a novel cyclopropanation reaction: the „flattening“ of proline // *Angew. Chem. Int. Ed.* - 2006. - Vol. 45. - P. 5787-5789.

<sup>205</sup> CCDC-676507 contains the crystallographic data for **97b**. These data can be obtained free of charge from The Cambridge Crystallographic Data Centre via [deposit@ccdc.cam.ac.uk](mailto:deposit@ccdc.cam.ac.uk).

<sup>206</sup> CCDC-676508 contains the crystallographic data for **99b**. These data can be obtained free of charge from The Cambridge Crystallographic Data Centre via [deposit@ccdc.cam.ac.uk](mailto:deposit@ccdc.cam.ac.uk).

<sup>207</sup> Gause G. F., Brazhnikova M. G. Gramicidin S and its use in the treatment of infected wounds // *Nature*. - 1944. - Vol. 154. - P. 703.

<sup>208</sup> Tomino S., Yamada M., Itoh H., Kurahashik K. Cell-free synthesis of gramicidin S // *Biochemistry*. - 1967. - Vol. 6. - P. 2552-2560.

<sup>209</sup> Kondejewski L. H., Farmer S. W., Wishart D. S., Hancock R. E., Hodges R. S. Gramicidin S is active against both gram-positive and gram-negative bacteria // *Int. J. Pept. Protein Res.* - 1996. - Vol. 47. - P. 460-466.

<sup>210</sup> Kondejewski L. H., Farmer S. W., Wishart D. S., Kay C. M., Hancock R. E., Hodges R. S. Modulation of structure and antibacterial and hemolytic activity by ring size in cyclic gramicidin S analogues // *J. Biol. Chem.* - 1996. - Vol. 271. - P. 25261-25268.

<sup>211</sup> Krauss E. M., Chan S. I. Spectroscopic studies of intramolecular hydrogen bonding in gramicidin S // *J. Am. Chem. Soc.* - 1982. - Vol. 104. - P. 1824-1830.

<sup>212</sup> Hull S. E., Karlsson R., Main P., Woolfson M. M., Dodson E. J. Crystall structure of a hydrated gramicidin S-urea complex // *Nature*. - 1978. - Vol. 275. - P. 206-207.

<sup>213</sup> Ovchinnikov Y. A., Ivanov V. T. Conformational states and biological activity of cyclic peptides // *Tetrahedron*. - 1975. - Vol. 31. - P. 2177-2209.

<sup>214</sup> Carpino L. A., Han G. Y. The 9-fluorenylmethoxycarbonyl amino-protecting group // *J. Org. Chem.* - 1972. - Vol. 37. - P. 3404-3409.

- <sup>215</sup> Wadhvani P., Afonin S., Ieronimo M., Buerck J., Ulrich A. S. Optimized protocol for synthesis of cyclic Gramicidin S: starting amino acid is key to high yield // *J. Org. Chem.* - 2006. - Vol. 71. - P. 55-61.
- <sup>216</sup> Afonin S., Dürr U. H. N., Wadhvani P., Salgado J., Ulrich A. S. Solid state NMR structure analysis of the antimicrobial peptide gramicidin S in lipid membranes: concentration-dependent re-alignment and self-assembly as a barrel // *Top. Curr. Chem.* - DOI 10.1007/128\_2007\_20.
- <sup>217</sup> Hoffmann W., Richter K., Kreil G. A novel peptide designated PYLa and its precursor as predicted from cloned mRNA of *Xenopus Laevis* skin // *EMBO J.* - 1983. - Vol. 2. - P. 711-714.
- <sup>218</sup> Richter K., Aschauer H., Kreil G. Biosynthesis of peptides in skin of *Xenopus Laevis*: isolation of novel peptides predicted from the sequence of cloned cDNAs // *Peptides.* - 1985. - P. 17-21.
- <sup>219</sup> Soravia E., Martini G., Zasloff M. Antimicrobial properties of peptides from *Xenopus* granular gland secretions // *FEBS Lett.* - 1988. - Vol. 228. - P. 337-340.
- <sup>220</sup> Wade D., Boman A., Wahlin B., Drain C., Andreu D., Boman H. G., Merrifield R. B. All D-amino acid containing channel-forming antibiotic peptides // *Proc. Natl. Acad. Sci.* - 1990. - Vol. 87. - P. 4761-4765.
- <sup>221</sup> Bechinger B., Zasloff M., Opella S. J. Structure and dynamics of the antimicrobial peptide PGLa in biomembranes by solution and solid state nuclear resonance spectroscopy // *Biophys. J.* - 1998. - Vol. 74. - P. 981-987.
- <sup>222</sup> Afonin S., Mykhailiuk P., Komarov I., Ulrich A. Evaluating the amino acid CF<sub>3</sub>-bicyclopentylglycine as a new label for solid state <sup>19</sup>F-NMR structure analysis of membrane-bound peptides // *J. Pept. Sci.* - 2007. - Vol. 13. - P. 614-623.
- <sup>223</sup> Tremouilhac P., Strandberg E., Wadhvani P., Ulrich A. S. Synergistic transmembrane alignment of the antimicrobial heterodimer PGLa/magainin 2 // *J. Biol. Chem.* - 2006. - Vol. 281. - P. 32089-32094.
- <sup>224</sup> Tremouilhac P., Strandberg E., Wadhvani P., Ulrich A. S. Conditions affecting the re-alignment of the antimicrobial peptide PGLa in membranes as monitored by solid state <sup>2</sup>H NMR // *Biochim. Biophys. Acta.* - 2006. - Vol. - 1758. - P. 1330-1342.
- <sup>225</sup> Fernandes-Carneado J., Kogan M. J., Castel S., Giralt E. Potential peptide carriers: amphipathic proline-rich peptides derived from the N-terminal domain of  $\gamma$ -Zein // *Angew. Chem.* - 2004. - Vol. 116. - P. 2047-2050.
- <sup>226</sup> Sadler K., Eom K. D., Yang J.-L., Dimitrova Y., Tam J. P. Translocating proline-rich peptides from the antimicrobial peptide bactenecin // *Biochemistry.* - 2002. - Vol. 41. - P. 14150-14157.
- <sup>227</sup> Crespo L., Sanclimens G., Montaner B., Perez-Tomas R., Royo M., Pons M., Albericio F., Giralt E. Peptide dendrimers based on polyproline helices // *J. Am. Chem. Soc.* - 2002. - Vol. 124. - P. 8876-8883.
- <sup>228</sup> Kogan M. J., López O., Cocera M., López-Iglesias C., Mata A., Giralt E. Exploring the interaction of the surfactant N-terminal domain of gamma-zein with soybean phosphatidylcholine liposomes // *Biopolymers.* - 2004. - Vol. 73. - P. 258-268.
- <sup>229</sup> Kogan M., Dalcol I., Gorostiza P., López-Iglesias C., Pons R., Pons M., Sanz F., Giralt E. Supramolecular properties of the proline-rich gamma-zein N-terminal domain // *Biophys. J.* - 2002. - Vol. 83. - P. 1194-1204.
- <sup>230</sup> Pujals S., Fernández-Carneado J., López-Iglesias C., Kogan M. J., Giralt E. Mechanistic aspects of CPP-mediated intracellular drug delivery: relevance of CPP self-assembly // *BBA-Biomembranes.* - 2006. - Vol. 1758. - P. 264-279.
- <sup>231</sup> Foerg C., Ziegler U., Fernandez-Carneado J., Giralt E., Rennert R., Beck-Sickinger A. G., Merkle H. P. Decoding the entry of two novel cell-penetrating peptides in HeLa cells: lipid raft-mediated endocytosis and endosomal escape // *Biochemistry.* - 2005. - Vol. 44. - P. 72-81.
- <sup>232</sup> Pujals S., Sabidó E., Tarragó T., Giralt E. All-D proline-rich cell-penetrating peptides: a preliminary in vivo internalization study // *Biochem. Soc. Trans.* - 2007. - Vol. 35. - P. 794-796.
- <sup>233</sup> Pujals S., Fernandez-Carneado J., Kogan M. J., Martinez J., Cavalier F., Giralt E. Replacement of a proline with silaproline causes a 20-fold increase in the cellular uptake of a Pro-rich peptide // *J. Am. Chem. Soc.* - 2006. - Vol. 128. - P. 8479-8483.

<sup>234</sup> <http://www.avantilipids.com/Searchcode3.asp?search=DMPC>.

<sup>235</sup> *Armarego W. L. F., Chai C. L. L.* Purification of laboratory chemicals. - 2003. - Oxford, Elsevier. - P. 609.

<sup>236</sup> *Kaiser E., Colescot R. L., Bossinge C. D., Cook P. I.* Color test for detection of free terminal amino groups in the solid-phase synthesis of peptides // *Anal. Biochem.* - 1970. - Vol. 34. - P. 595.

<sup>237</sup> *De Angelis A. A., Jones D. H., Grant C. V., Park S. H., Mesleh M. F., Opella S. J.* NMR experiments on aligned samples of membrane proteins // *Methods Enzymol.* - 2005. - Vol. 394. - P. 350-382.

<sup>238</sup> *Strandberg E., Ulrich A. S.* NMR methods for studying membraneactive antimicrobial peptides // *Conc. Magn. Reson. A.* - 2004. - Vol. 23. - P. 89-120.

## ABBREVIATIONS

acac	acetylacetonate
Aib	aminoisobutyric acid
AMPs	antimicrobial peptides
B <sub>0</sub>	static magnetic field
9-BBN	9-borabicyclo[3.3.1]nonane
Boc	<i>tert</i> -butyloxy-carbonyl
b.p.	boiling point
bs	broad singlet
CD	circular dichroism
CF <sub>3</sub> -MePro	trifluoromethyl-4,5-methanoproline
CF <sub>3</sub> -Bpg	3-trifluoromethyl-bicyclopent[1.1.1]-1-ylglycine
4CF <sub>3</sub> -Phg	4-trifluoromethyl-phenylglycine
6Cl-HOBt	6-chloro-N-hydroxybenzotriazole
CPPs	cell-penetrating peptides
CSA	chemical shift anisotropy
d	doublet
DBU	1,8-diazobicyclo[5,4,0]undec-7-ene
DCM	dichloromethane
DIC	diisopropylcarbodiimide
DIEA	diisopropylamine
DMF	dimethylformamide
DMPC	1,2-dimyristoyl-glycero-3-phosphocholine
DMPG	1,2-dimyristoyl-glycero-3-phospho-1-glycerol
Dowex-50	cation-exchanging resin
EI	electronic ionization
EM	electron microscopy
F <sub>3</sub> -Aib	2,2,2-trifluoro-aminoisobutyric acid
4F-Phg	4-fluoro-phenylglycine
FA	fluorine-labelled amino acid
Fmoc	9-fluorenylmethoxy-carbonyl
GC	gas chromatography
GC-MS	gas chromatography with mass detection
GS	gramicidin S (antimicrobial peptide)
HCTU	5-chloro-1-[bis(dimethylamino)methylene]-1H-benzotriazolium 3-oxide hexafluorophosphate
HPLC	high performance liquid chromatography
IR	infrared (spectroscopy)
ivDde	1-(4,4-dimethyl-2,6-dioxocyclohex-1-ylilide)-3-methylbutyl
LSR	lanthanoid shifting reagent
m	multiplet

MALDI-TOF	matrix assisted laser-induced desorption/ionization with time-of-flight detection
MIC	minimal inhibitory concentration
m.p.	melting point
NMR	nuclear magnetic resonance
P/L	peptide/lipid
PGLa	peptidyl-glycylleucine-carboxamide (antimicrobial peptide)
Pbf	2,3,4,6,7-pentamethyldihydro-benzofuran-5-sulfonyl
PP I	poly- <i>L</i> -proline helix of the type 1
PP II	poly- <i>L</i> -proline helix of the type 2
PyBop	(benzotriazol-1-yloxy)tripyrrolidino-phosphonium hexafluorophosphate
PPTS	pyridine p-toluene sulfonate
PTSA	p-toluene sulfonic acid
RMSD	root mean square deviation
ppm	parts per million
PRPs	proline rich peptides
q	quartet
py	pyridine
s	singlet
SAP	Sweet Arrow Peptide (cell-penetrating peptide)
SPPS	solid phase peptide synthesis
t	triplet
TLC	thin layer chromatography
TIS	triisopropylsilane
TBTU	O-benzotriazol-1-yl-N,N,N',N'-tetramethyl-uronium tetrafluoroborate
TFA	trifluoroacetic acid

## LIST OF PUBLICATIONS

- 1) *Mykhailiuk P. K., Afonin S., Chernega A. N., Rusanov E. B., Platonov M., Dubinina G., Berditsch M., Ulrich, Komarov I. V.* Conformationally rigid trifluoromethyl-substituted  $\alpha$ -amino acid designed for peptide structure analysis by solid state  $^{19}\text{F}$ -NMR spectroscopy // *Angew. Chem.* - 2006. - Vol. 118. - P. 5787-5789; *Angew. Chem. Int. Ed.* - 2006. - Vol. 45. - P. 5659-5661.
- 2) *Afonin S., Mykhailiuk P. K., Komarov I. V., Ulrich A. S.* Evaluating the use of  $\text{CF}_3$ -bicyclopentylglycine as a label for  $^{19}\text{F}$ -NMR structure analysis of membrane-bound peptides // *J. Pept. Sci.* - 2007. - Vol. 13 - P. 614-623.
- 3) *Kubyshkin V. S., Mykhailiuk P. K., Komarov I. V.* Synthesis of 7-azabicyclo[2.2.1]heptane-1,4-dicarboxylic acid, a rigid non-chiral analogue of 2-aminoadipic acid // *Tetrahedron Lett.* - 2007. - Vol. 48. - P. 4061-4063.
- 4) *Grygorenko O. O., Kopylova N. A., Mykhailiuk P. K., Meißner A., Komarov I. V.* An approach to 2-cyanopyrrolidines bearing a chiral auxiliary // *Tetrahedron: Asymmetry.* - 2007. - Vol. 18. - P. 290-297.
- 5) *Grage S. L., Dürr U. H. N., Afonin S., Mykhailiuk P. K., Komarov I. V., Ulrich A. S.* Solid state  $^{19}\text{F}$  NMR parameters of fluorine-labeled amino acids. Part II: Aliphatic substituents // *J. Magn. Res.* - 2008. - Vol. 191. - P. 16-23.
- 6) *Mykhailiuk P. K., Afonin S., Ulrich A. S., Komarov I. V.* A convenient route to trifluoromethyl-substituted cyclopropane derivatives // *Synthesis.* - 2008. - in press.
- 7) *Mykhailiuk P. K., Afonin S., Palamarchuk G. V., Shishkin O. V., Ulrich A. S., Komarov I. V.* Synthesis of trifluoromethyl-substituted proline analogues - new  $^{19}\text{F}$ -NMR labels for peptides in polyproline II conformation // *Angew. Chem.* - 2008. - in press.

## CONFERENCE REPORTS

- 1) *Mykhailiuk P. K., Komarov I. V.* Synthesis of a conformationally rigid trifluoromethyl-substituted  $\alpha$ -amino acid for peptide studies by  $^{19}\text{F}$ -NMR // The third joint scientific conference in chemistry Kyiv national Taras Shevchenko university and Paul Sabatier university (Toulouse). - Kyiv, Ukraine. - 2005. - P. 65.
- 2) *Mykhailiuk P. K., Afonin S., Ulrich A. S., Komarov I. V.* Synthesis of a conformationally rigid trifluoromethyl-substituted  $\alpha$ -amino acid for peptide studies by  $^{19}\text{F}$ -NMR // 6<sup>th</sup> Tetrahedron symposium "Challenges in organic chemistry". - Bordeaux, France, - 2005. - P. 176.

- 3) *Mykhailiuk P. K., Komarov I. V.* Synthesis of a conformationally rigid trifluoromethyl-substituted  $\alpha$ -amino acid for peptide studies by  $^{19}\text{F}$ -NMR // 6<sup>th</sup> Ukrainian Conference of Young Scientists "Modern challenges in chemistry". - Kyiv, Ukraine. - 2005. - P. 93.
- 4) *Mykhailiuk P. K., Gvozдовska N. P., Tolmachev A. A., Komarov I. V.* Addition of carbenes as a route to 3,4- and 4,5-methanoprolines - building blocks for drug design // XIX International Symposium on Medical Chemistry. - Istanbul, Turkey. - 2006. - P. 119.
- 5) *Mykhailiuk P. K., Afonin S., Gvozдовska N., Ulrich A. S., Komarov I. V.* Synthesis of  $^{19}\text{F}$ -NMR labels for structural studies of peptides - novel trifluoromethyl-substituted amino acids // 8<sup>th</sup> Tetrahedron symposium "Challenges in organic chemistry". - Berlin, Germany. - 2007. - P. 2.29.
- 6) *Afonin S., Grage S. L., Ieronimo M., Berditsch M., Wadhwani P., Mykhailiuk P. K., Komarov I. V., Ulrich A. S.* Protein crowding effects on the alignment states of PGLa in lipid membranes // 8<sup>th</sup> German Peptide Society Meeting. - Heidelberg, Germany. - 2007. - P. 127.
- 7) *Afonin S., Grage S. L., Wadhwani P., Ieronimo M., Berditsch M., Mykhailiuk P. K., Komarov I. V., Ulrich A. S.* Distinct alignment states of the antimicrobial peptide PGLa in phospholipid bilayers. - 2<sup>nd</sup> workshop on biophysics of membrane-active peptides. - Lisbon, Portugal. - 2007. - P. 95.
- 8) *Afonin S., Grage S. L., Ieronimo M., Wadhwani P., Bürck J., Tremouilhac P., Strandberg E., Mykhailiuk P. K., Komarov I. V., Ulrich A. S.* The antimicrobial peptide PGLa can adopt three distinct alignment states in lipid bilayers // 6<sup>th</sup> European Biophysics Congress. - London, UK. - 2007. - P. S114.
- 9) *Afonin S., Mykhailiuk P. K., Grage S. L., Bürck J., Sternberg U., Wadhwani P., Komarov I. V., Ulrich A. S.* Structural investigations of the cell-penetrating peptide SAP in lipid membranes // 52<sup>th</sup> Annual Meeting, Biophysical society/16<sup>th</sup> IUPAB Congress. - Long Beach, CA. - 2008. - P. 948.
- 10) *Mykhailiuk P.* Use of fluorine-substituted amino acids  $\text{CF}_3\text{Bpg}$  and  $\text{CF}_3\text{MePro}$  as labels in NMR study of membrane-active peptides // The Workshop on "Supramolecular chemistry and chemical biology of polypeptides: synergy towards bio-nanotechnology". - Kiev, Ukraine. - 2008 (oral talk).
- 11) *Mykhailiuk P.* New fluorine-labelled amino acids as  $^{19}\text{F}$ -NMR reporters for structural peptide studies // 11<sup>th</sup> Naples Workshop on bioactive peptides. - Naples, Italy. - 2008 (oral talk).



## CURRICULUM VITAE

Mykhailiuk Pavlo

Date of birth: 05.04.1984  
Place of birth: Kerch, Ukraine  
Nationality: Ukrainian  
Marital status: single, no children

Education:

1991-2000 School № 4, Kerch, Ukraine

2000-2004 Kyiv National Taras Shevchenko University, Kyiv, Ukraine  
Department of chemistry, chair of organic chemistry  
bachelor's degree

2004-2005 Kyiv National Taras Shevchenko University, Kyiv, Ukraine  
Department of chemistry, chair of organic chemistry  
master's degree, grade „excellent“

07.2005-08.2005 Visiting scientist in the group of Prof. Anne S. Ulrich  
01.2007-11.2007 at University of Karlsruhe

11.2007 Ph.D. student in the group of Prof. Anne S. Ulrich  
at University of Karlsruhe

Awards:

2001-2002 Grant of the President of Ukraine

2006-2008 Grant of the Alexander von Humboldt Foundation